UNIVERSITÉ DE MONTRÉAL

EFFET DE LA LIBÉRATION MINÉRALE ET DES OXY-HYDROXYDES DE FER SUR LE COMPORTEMENT GÉOCHIMIQUE DES REJETS MINIERS SULFUREUX

ABDELLATIF ELGHALI

DÉPARTEMENT DE GENIES CIVIL, GÉOLOGIQUE ET DES MINES

ÉCOLE POLYTECHNIQUE DE MONTRÉAL

THÈSE PRÉSENTÉE EN VUE DE L'OBTENTION

DU DIPLÔME DE PHILOSOPHIAE DOCTOR

(GÉNIE MINÉRAL)

Octobre 2018

UNIVERSITÉ DE MONTRÉAL

ÉCOLE POLYTECHNIQUE DE MONTRÉAL

UNIVERSITÉ DU QUÉBEC EN ABITIBI-TÉMISCAMINGUE

Cette thèse intitulée :

EFFET DE LA LIBÉRATION MINÉRALE ET DES OXY-HYDROXYDES DE FER SUR LE COMPORTEMENT GÉOCHIMIQUE DES REJETS MINIERS SULFUREUX

présentée par : ELGHALI Abdellatif

en vue de l'obtention du diplôme de : Philosophiae Doctor

a été dûment acceptée par le jury d'examen constitué de :

M. PLANTE Benoit, Ph. D., président

M. BENZAAZOUA Mostafa, Ph. D., membre et directeur de recherche

M. BUSSIERE Bruno, Ph. D., membre et codirecteur de recherche

M. OUELLET Serge, Ph. D., membre

M. AL Tom, Ph. D., membre externe

DÉDICACE

À la mémoire de mon père, ma mère, mon frère et mes sœurs.

REMERCIEMENTS

Je tiens à remercier toute personne qui m'a aidé, motivé et soutenu tout au long de mes études. Un grand merci mes parents, mon frère et mes sœurs qui étaient présents à mes côtés lors des étapes clés de ce doctorat.

Mes remerciements vont à mon directeur de thèse Mostafa Benzaazoua et mon co-directeur Bruno Bussière de m'avoir donné l'opportunité de réaliser mon projet de recherche dans les meilleures conditions possibles. Je tiens à les remercier pour leurs encouragements, implications et disponibilités lors des étapes clés de ce projet de recherche. Sans leur précieuse aide, ce travail n'aurait pas abouti. Je tiens à remercier également la chaire CRSNG sur la restauration des sites miniers d'avoir financé ce projet de recherche, ainsi que Mitacs d'avoir accepté de financer 4 stages Mitacs chez Agnico Eagle Mines ltd.

Je tiens à remercier chaleureusement mon grand frère Hassan Bouzahzah qui m'a appris, dès mon arrivée ici à l'UQAT, les bases de la minéralogie appliquée et qui m'a transmis ses connaissances et surtout ses valeurs. J'adresse mes remerciements au staff de la restauration régionale et de la division d'environnement au CSD des Mines Agnico-Eagle ltd de m'avoir donné la chance d'effectuer 2 ans de stage Mitacs au sein des mines Agnico Eagle Limitées, je pense particulièrement à Josée Noel, Thomas Genty, Jean Cayouette, et Chris Kennedy. Mon épanouissement professionnel tient à ces personnes. J'adresse mes remerciements à toute l'équipe de l'IRME/URSTM et spécialement : Louise, Tikou, Mamert, Nancy et Benoit ainsi que tous mes professeurs. Les travaux de laboratoire et de terrain ont été réalisé dans les meilleures conditions grâce à la collaboration du personnel de l'URSTM : je remercie chaleureusement mon partner de terrain Joel pour son aide et ses jokes durant l'échantillonnage des cellules pendant 2 ans de suivi, Patrick 'le génie' qui était toujours présent pour résoudre mes problèmes techniques et aussi de m'avoir intégré à la ligue de billard de rouyn, Alain 'the master' pour son aide et disponibilité et surtout sa bonne humour durant la réalisation de tous mes essais cinétiques, Yvan de m'avoir aidé durant construction des cellules de terrain même s'il faisait 'frette'. Merci également à toute l'équipe: Marc, Mélinda, Mathieu, Mélanie, Pierre-Alain, Tony, Janie, Sylvette et Véronique. Je remercie également tous mes amis (es) et collègues que j'ai côtoyés durant ce doctorat, particulièrement Yassine, Aurélie, Chloé, Babacar, Koly, Jalil, Marie-Pier, Hamza, Hicham, Nathalie,, Houssem, Takoua, Rayen, Marouen, Gwendoline, Emma, Andrée, Alex, Bini, Ibrahima,

Simon, WiWi, Faneiva et Patrick. Un merci à Gary d'avoir pris le temps pour corriger mon 'franglais'. Je m'excuse d'avance auprès de ceux et celles que je n'ai pas cités, mais je n'oublie pas dans mes pensées. Je remercie spécialement Karim Samra, étudiant en master à l'université de Lille d'avoir participé à la réalisation de ce projet dans le cadre de son stage.

RÉSUMÉ

L'industrie minière, lorsqu'elle mène des exploitations de gisements pour produire des minerais devant subir un traitement, est confrontée à différents défis et enjeux liés à la gestion des rejets miniers. Le drainage minier acide et la mise en solution des contaminants constituent les principaux problèmes environnementaux dus à l'exposition des rejets miniers sulfureux à l'eau et à l'oxygène atmosphérique. Les réglementations environnementales obligent les compagnies minières à réhabiliter les sites et en particulier les aires d'entreposage des rejets avant la fermeture de la mine. La gestion des rejets miniers diffère selon le type de l'exploitation et la géologie du gisement exploité. En effet, lors d'une exploitation à ciel ouvert, les stériles miniers sont produits en quantité considérables et sont ensuite déposés dans des haldes à stériles non-saturés en eau et caractérisés par une hétérogénéité de la distribution granulométrique. En revanche, lors des exploitations souterraines, moins de stériles sont générés et se sont les résidus finement broyés qui représentent le plus gros des rejets, qui sont déposés dans des parcs à résidus. Dans un climat humide comme celui du Canada, ces derniers sont le plus souvent saturés en eau avec juste une partie au-dessus de nappe phréatique en perpétuel changement de la saturation vers la désaturation. Dans les deux cas (stériles et résidus), la prédiction du comportement géochimique des rejets miniers est un paramètre important qui influence grandement la faisabilité d'un projet minier. Durant ce doctorat, les deux types de rejets miniers ont été étudiés au vu de deux objectifs différents sachant la différence de leurs propriétés mais cependant pour la même finalité qui est de mieux prédire et gérer le rejet minier en question. Pour ce qui est des stériles, une nouvelle méthode de gestion est proposée en amont lors de leur extraction et avant leur entreposage. Quant aux résidus étudiés, des formulations d'amendements alcalins et cimentaires ont été testées en cellules de terrain comme technique de stabilisation/solidification des résidus miniers oxydés générateurs d'acide après avoir démontré l'effet des oxy-hydroxydes de fer sur le comportement géochimique des résidus miniers.

Trois lithologies de stériles ont été échantillonnées à la mine Canadian Malartic juste après dynamitage pour respecter la représentativité du paramètre 'distribution granulométrique'; souvent mal considéré par les études de nos jours. Les trois lithologies CPO (lithologie A), AGR (lithologie B) et CGR (lithologie C) ont été séparées en sept fractions granulométriques (-53µm, +53µm/-300µm, +300µm/-850µm, +850µm/-2.4mm, +2.4mm/-5mm, +5mm/-1.5cm, +1.5cm/-5cm). La caractérisation chimique et minéralogique a montré que les trois lithologies et leurs fractions

contiennent plus de carbonates (≥2.5%) par rapport aux sulfures (≤1.5%). Les carbonates sont majoritairement représentés par la calcite et les sulfures sont principalement constitués de pyrite. Le contenu en sulfures varie en fonction de la fraction granulométrique. En effet, les fractions fines sont plus enrichies en sulfures par rapport aux fractions grossières. En terme textural, l'analyse minéralogique a montré que les sulfures sont libres au niveau des fractions fines (95%) et inclus au niveau des fractions grossières et idem pour les carbonates. Par ailleurs, le degré de libération de sulfures devient presque négligeable (5%) à partir de 2.4 mm comme diamètre des grains pour les trois lithologies par comparaison au degré de libération des carbonates qui reste non-négligeable (10%) à 2.4mm offrant une sécurité. En conséquence, 2.4mm a été défini comme le diamètre limite d'encapsulation physique de sulfures (DPLS) pour ces trois échantillons. Le DPLS est défini comme un seuil qui sépare un stérile minier en deux fractions granulométriques dépendamment de leurs réactivités : i) la fraction fine (-DPLS) qui constitue être la fraction réactive et probablement problématique et ii) la fraction grossière (+DPLS) qui constitue être la fraction non réactive et ne présenterait pas un risque lié à l'oxydation des sulfures. La fraction -DPLS représente une proportion faible de l'échantillon total (moins de 23% considérant 1m comme Dmax pour la lithologie A) par rapport à la fraction +DPLS qui représente la majorité de l'échantillon total. En plus de la caractérisation chimico-minéralogique et les tests statiques, des essais cinétiques en colonnes ont été monitorés sur une période 543 jours pour confirmer cette conclusion. Les trois lithologies ont été séparées en deux fractions granulométriques à savoir -2.4mm et +2.4mm tout en testant l'échantillon total aussi. Les résultats du suivi géochimique ont montré qu'effectivement la fraction -2.4mm est beaucoup plus réactive que la fraction +2.4mm et l'échantillon total. La lithologie B était la lithologie la plus réactive; le taux d'oxydation de la pyrite au niveau de sa fraction -2.4mm était de 12.5 µmol/kg/jour, au niveau de sa fraction +2.4mm était de l'ordre de 0.27 µmol/kg/jour et le taux d'oxydation au niveau de l'échantillon total était de l'ordre 2.45 µmol/kg/jour. La même tendance a été remarquée pour les deux autres lithologies. L'intérêt du calcul du DPLS se situe au niveau des éventuels gains économiques qui peuvent avoir lieu s'il est intégré en amont de la gestion des stériles miniers. En effet, au lieu de gérer les stériles comme une seule entité, il est maintenant suggéré de les séparer en deux fractions; une fraction réactive (-DPLS) et une fraction non réactive (+DPLS) sachant que la fraction réactive présente une faible proportion de l'échantillon total et qu'elle puisse être soit déposé avec les résidus minier soit encore traités métallurgiquement et économiquement elle devenait intéressante.

Par ailleurs, la problématique de prédiction du comportement géochimique des résidus miniers est différente de celle liée aux stériles miniers. Les résidus miniers, par comparaison aux stériles miniers, sont caractérisés par une granulométrie fine; ce qui favorise et accélère même les taux de réactions dans des conditions non saturées (oxydation des sulfures, dissolution des carbonates). Le comportement géochimique des résidus miniers est généralement évalué en utilisant des essais cinétiques au laboratoire. Ces essais sont conçus pour simuler l'oxydation naturelle des résidus miniers et ont démontré leurs capacités à prédire adéquatement le comportement géochimique des rejets miniers. Cependant, le cas des résidus miniers de Joutel témoigne de l'importance de considérer la composante du terrain pour bien comprendre le comportement géochimique des résidus miniers. Le parc à résidus de Joutel qui s'étend sur une superficie de 120 ha est fermé depuis environ 25 ans. L'exposition des résidus aux agents atmosphériques a causé l'apparition d'un horizon oxydé à la surface du parc à résidus avec une formation localisée du hardpan tendant à se généraliser sur tout le site. Ce dernier est défini comme une couche cimentaire qui se forme à l'interface entre l'horizon oxydé et l'horizon des résidus frais par précipitation des oxy-hydroxydes de fer. La caractérisation minéralogique et chimique a montré un épuisement des sulfures et des carbonates en allant du résidu frais vers le résidu oxydé avec un changement de texture assez remarquable au niveau du hardpan. Les essais cinétiques réalisés sur les résidus frais ont montré qu'il s'agit d'un comportement non-générateur d'acide à long terme. Cependant, sur le parc à résidus de Joutel, une acidité a été générée à travers de la couche oxydée. Ce constat a été confirmé moyennant des essais cinétiques sur des résidus oxydés. Étant donné que le résidu oxydé est le résultat de l'oxydation du résidu frais sur environ 25 ans et que la prédiction du comportement géochimique du résidu frais était non-générateur d'acide mais le résidu oxydé a montré un comportement acidogène, ceci prouve l'incapacité des essais cinétiques à prédire correctement le comportement géochimique des résidus miniers de Joutel. Après une investigation sur le terrain et au laboratoire, le rôle essentiel du hardpan sur le comportement géochimique global des résidus miniers de Joutel est démontré. En effet, l'occurrence du hardpan constitue un écran aux les écoulements verticaux des eaux. La formation du hardpan, caractérisé par sa faible perméabilité estimée par analyse tomographique, favorise les écoulements latéraux (ruissellement de surface) au dépend des écoulements verticaux des eaux de surface. C'est pour cette raison que la géochimie globale du parc à résidus de Joutel est influencée grandement par la réactivité des résidus oxydés en surface. Ces derniers sont caractérisés par un épuisement plus ou moins important des sulfures,

constat confirmé par les essais de consommation d'oxygène. Dans les zones oxydées, les flux d'oxygène ne dépassent pas 30 mole/m^2/année. En plus de leurs réactivités faibles, les résidus oxydés sont caractérisés par l'abondance des minéraux secondaires à l'exemple du gypse et des oxy-hydroxydes de fer. Ces oxy-hydroxydes de fer, qui étaient responsables de l'atténuation des réponses géochimiques de l'oxydation des résidus frais, peuvent réagir différemment en générant de l'acidité. La répartition spatiale de l'acidité au niveau du parc à résidus de Joutel n'était pas systématique. En effet, l'échantillonnage systématique réalisé à Joutel a permis de cartographier la variabilité spatiale des propriétés géochimiques des résidus oxydés. L'utilisation des SIG a permis de délimiter les zones les plus problématiques et qui étaient localisées à l'ouest du parc Sud et au nord du parc Nord, ce qui a permis de proposer un schéma conceptuel illustrant le comportement des résidus à Joutel. Par la suite, les amendements alcalins et cimentaires ont été proposés et testés comme technique de stabilisation/solidification sur le site Joutel. L'utilisation du calcaire à 5 et 10 wt.% a permis une neutralisation immédiate du pH des lixiviats et la plupart des éléments chimiques ont été immobilisés grâce à la précipitation des phases secondaires dans des conditions proches de la neutralité. Cependant, les concentrations en Zn et en As étaient parfois plus grandes dans les lixiviats provenant des résidus amendés par rapport à la cellule témoin. Les amendements cimentaires ont été testés en utilisant le ciment portland et les cendres volantes de la combustion de la biomasse produites en région à un dosage total de 5%. La première formulation qui contenait 50% ciment et 50% cendres volantes a montré des résultats prometteurs concernant la stabilisation des contaminants. L'efficacité de ces amendements à court terme a été démontré, mais il reste à étudier leurs efficacités à long terme ainsi que les coûts économiques liés à cette alternative.

Mots clés : rejets miniers, le degré de libération minérale, séparation des stériles, hardpan, minéraux secondaires, amendements miniers.

ABSTRACT

During ore extraction and processing, mining industries generate high quantities of solid mine wastes. Their management during all mine life cycle is a serious challenge facing these industries. Acid mine drainage and contaminants mobilization constitute the most known problems related to exposition of sulphidic mine wastes to atmospheric oxygen and water. Conformity to current environmental regulations and standards requires mine sites reclamation and especially waste storage facilities before the final closure of mine sites. Mine waste management depends on the extraction method and the geological properties of the deposit. Hereafter, mine waste will refer to waste produced mostly during open pits extraction (compared to underground exploitation) and which didn't go through ore processing steps, mine tailings refer to finely grinded tailings and produced during ore processing. Waste rocks are mostly deposited in large surface unsaturated waste rock piles, and mine tailings are deposited in slurry state in tailings storage facilities. In Canada, the environmental behavior of waste rocks and tailings is one of the parameter which is considered during mine project feasibility studies. This is why, prediction of environmental behavior of waste rocks and mine tailings becomes a serious concern of mining industries all around the world. During this study, waste rocks and tailings were studied in order to improve understanding of geochemical reactions within waste rocks and mine tailings which will be used for a better prediction of their environmental behavior. Concerning waste rocks, a novel methodology was suggested to consider mineral textures (mineral liberation and mineralogical associations) during characterization steps. As demonstrated in this study, a new method of waste management is suggested, and it consisted on waste rock sorting considering the diameter of physical locking of sulphides. Concerning mine tailings, it is demonstrated in this study that iron-oxyhydroxides is very common phenomenon occurring during sulfides oxidation and carbonates dissolution and it could influence the prediction of the geochemical behavior of mine tailings which may require in some cases to consider the field conditions. Finally, four amendment formulations (cementitious and alkaline) were tested in the field conditions and showed promising results to stabilize/solidify oxidized acid generating tailings.

Three waste rock (WR) lithologies was collected from Canadian Malartic mine immediately after in-situ WR blasting to consider the actual particle distribution which is rarely considered during nowadays studies. The three lithologies CPO (lithology A), AGR (lithology B) and CGR (lithology C) were divided into seven fractions (-53µm, +53µm/-300µm, +300µm/-850µm, +850µm/-2.4mm,

+2.4mm/-5mm, +5mm/-1.5cm, +1.5cm/-5cm). the chemical and mineralogical characterization showed that the three total samples and their fractions contained more carbonates mainly as calcite ($\geq 2.5\%$) than sulphides mostly as pyrite ($\leq 1.5\%$). Sulphides content depended on the particle size, fine particle sizes were more enriched in sulphides compared to coarse fractions. Moreover, automated mineralogy characterization performed on the concerned fractions showed that sulphides are mostly liberated (95%) within fine fractions compared to coarser fractions where sulphides are mostly encapsulated within non-sulphide gangue (NSG) and their liberation is almost negligible (5%). Based on mineral textures analysis within the studied lithologies, 2.4mm was defined as the diameter of physical locking of sulphides (DPLS). The DPLS defines a critical particle size that could be used to divide a waste rock into two fractions with extremely different reactivities: the fraction -DPLS is the most reactive one and it consists on only a low proportion of total samples ($\leq 23\%$) and the fraction +DPLS which is characterized by a low sulphide oxidation. This diameter was also confirmed using kinetic tests monitored for 543 days. The three lithologies were divided into two fractions which are the sample -2.4mm and +2.4mm and the total sample was tested separately. Results of geochemical monitoring showed that the fraction -2.4mm of the three lithologies was the most reactive fraction compared to total sample and the fraction +2.4mm. The lithology B was the most reactive one, pyrite oxidation rates of fraction -2.4mm, total sample and fraction +2.4mm were about 12.5 μmol/kg/day, 2.45 μmol/kg/day and 0.27 μmol/kg/day respectively. Tendency of pyrite oxidation rates between the different fractions of the lithology B was the same for the two other lithologies A and C. Calculation and determination of DPLS will allow to challenge waste management. Indeed, the use of this parameter will allow depositing waste rocks into two waste rock piles instead of one. A pile which will contain only particles -DPLS and another one containing particles +DPLS. Consequently, the volume of the reactive part of the waste rocks will be minimized considerably and so economic cost related to waste rocks management.

Otherwise, the challenge related to prediction of the geochemical behavior of mine tailings is different to that related to waste rocks. Mine tailings, compared to waste rocks, are characterized by fine and homogeneous particle size distribution; which accelerates reactions rates in unsaturated conditions (sulphides oxidation and carbonates dissolution). The geochemical behavior of mine tailings is usually studied using laboratory kinetic testing. This kinetic testing is deigned to simulate the natural oxidation of tailings. However, Joutel's tailings are an example of the importance of considering the field conditions to understand correctly the actual geochemical behavior of mine

tailings. Joutel is a closed tailing storage facility (TSF) of about 120 ha for 25 years. Tailings exposition to water and oxygen lead to apparition of an oxidized horizon and local formation of hardpans which may be a generalized phenomenon in the TSF. The hardpan is defined as cementitious layers that occur at the interface between the oxidized horizon and the unweathered tailings due to iron oxy-hydroxides precipitation. The chemical and mineralogical characterization showed that carbonates and sulphides depletion increases from the unweathered tailings to the oxidized horizon with a spectacular change regarding the minerals texture. Knowing that the oxidized horizon is the result of oxidation of the unweathered tailings for 25 years and the geochemical behavior of the unweathered tailings was predicted as non-acid generating, however the oxidized tailings were acidic in some location in the TSF; this shows the incapacity of kinetic testing in this case to predict correctly the geochemical behavior of Joutel's unweathered tailings. Laboratory and field investigations showed the effect of hardpans on the geochemical behavior of Joutel's TSF. Indeed, hardpan constitutes a screen against vertical water flows due its low porosity as analyzed using computed tomography. Consequently, hardpans occurrence deflects water vertical infiltration and enhances surface and sub-surface runoff. This why the reactivity of the TSF is almost controlled by the reactivity of upper oxidized tailings. These oxidized tailings are characterized by high sulphides depletion as demonstrated using oxygen consumption tests. Oxygen consumption within oxidized tailings didn't exceed 30 mole/m^2/year. Furthermore, oxidized tailings are mainly formed by secondary minerals such as gypsum and iron oxy-hydroxides. These iron oxy-hydroxides which were responsible for metals/metalloids attenuation may react again and release the sorbed elements and generate acidity. The spatial mapping of the acidity and the geochemical properties of Joutel's TSF showed that they were spatially dependent. The use of GIS allowed delimiting the zones of acidity which were spatially located at the west of the south zone and at the north of the north zone. Consequently, a conceptual model was proposed to explain the geochemistry of Joutel's tailings. Then, alkaline and cementitious amendments were tested as mitigation scenario to stabilize oxidized tailings. Thus, the use of 5% and 10% limestone allowed an immediate pH buffering and immobilization of the most chemical species. The chemical species were stabilized within limestone dissolution by iron-oxyhydroxides precipitation at neutral conditions. However, zinc and arsenic were sometimes more released within the amended tailings. The cementitious amendments were tested using ordinary cement and fly ash with 5% dosage. The first formulation consisted on 50:50 cement and fly ash showed promising results concerning the

chemical species stabilization. The efficiency and the cost of these amendments must be studied at the long-term scale.

Key words: Tailings, waste rocks, mineral liberation degree, waste rock sorting, hardpan, secondary minerals, mining amendments.

TABLE DES MATIÈRES

LISTE DES TABLEAUX

LISTE DES FIGURES

LISTE DES SIGLES ET ABRÉVIATIONS

ABA	Acid base accounting
ACP (PCA)	Analyse en composantes principales
AEV	Air entry value (valeur d'entrée d'air)
ASTM	American society for testing and materials
CRSNG	Conseil de recherche en sciences naturelles et en génie
CT	Computed tomography
DMA (AMD)	Drainage minier acide
DRA (ARD)	Drainage rocheux acide
DNC (CND)	Drainage neutre contaminé
DPLS	Diameter of physical locking of sulfides
DRX (XRD)	Diffraction des rayons X
EPA	Environmental protection agency
FRX (XRF)	Fluorescence X
GRG	Generalized reduced gradient
Gs	Densité relative
ICP-AES	Inductively Coupled Plasma Atomic Emission Spectroscopy
K_{sat}	Conductivité hydraulique saturée
MEB (SEM)	Microscope électronique à balayage
MNT (DEM)	Modèle numérique de terrain
MO	Microscope optique
NAG	Net acidity generation
NSG	Non-sulfide gangue

PA (AP)	Potentiel de génération d'acidité
PMA	Particle mineralogy analysis
PN (NP)	Potentiel de neutralisation
PNN (NNP)	Potentiel net de neutralisation
QEMSCAN	Quantitative Evaluation of Minerals by scanning electron microscopy
S/C	Soufre/carbone
SIG (GIS)	Systèmes d'informations géographiques
SS (SSA)	Surface spécifique
TLM (TLT)	Test de lixiviation monolithe
TSF	Tailings storage facility

LISTE DES ANNEXES

CHAPITRE 1   INTRODUCTION

L'industrie minière est un secteur qui constitue un pilier important pour de nombreux pays à travers le monde, le Canada en faisant partie. La première opération du cycle de vie d'une mine consiste en l'étape de prospection géologique et d'exploration pour la localisation et la définition plus ou moins précises des zones minéralisées et des réserves en valeur. Le projet minier fait ensuite l'objet d'une étude de faisabilité technico-économique, sociale et environnementale pour déterminer la viabilité du projet. La construction des infrastructures minières et ensuite le démarrage de l'exploitation minière permettent l'entrée en production. Au Canada, l'opération minière intègre, de nos jours, la composante environnementale incluant un plan de gestion des différents rejets générés et un plan de fermeture (réhabilitation) bien définis à l'avance avec une garantie financière assurée dès les premières années d'exploitation. Dépendamment du type et de la cadence d'exploitation ainsi que les réserves minières, la durée de vie d'un gisement peut varier de quelques années à des dizaines d'années. L'exploitation génère une quantité plus ou moins importante de stériles miniers qui ne présentent pas une valeur économique obéissant à ce qu'on nomme la teneur de coupure.   Cette dernière est définie selon des facteurs d'ordre techniques, économique et d'autres intrinsèques aux minerais (exemple des minerais d'or réfractaires). Le minerai extrait est ensuite concassé, broyé et traité dans les usines de traitements pour fins de concentration et de valorisation. Les éléments de valeur sont généralement présents dans le minerai à une faible à très faible concentration disséminée dans une gangue stérile (comme le cas de l'or et de l'argent). De ce fait, le processus de traitement de minerais génère des quantités importantes de résidus de concentration. La dernière étape du cycle de vie d'une mine est l'étape de la fermeture; cette dernière comprend le démantèlement des infrastructures et la restauration minière qui consiste à la réhabilitation en particulier des sites d'entreposage, et parfois, le reprofilage des paysages.

Les stériles miniers et les résidus sont donc les principaux rejets solides produits lors d'une opération minière. Les deux types de rejets contiennent des éléments de valeur résiduelles, mais surtout peuvent contenir des contaminants instables géo-chimiquement lorsque soumis à une altération atmosphérique. Les résidus miniers sont caractérisés par une granulométrie fine à cause du broyage et sont considérés un matériau homogène. Cependant, les stériles miniers sont des matériaux à granulométrie hétérogène, souvent très étalée et présentent des caractéristiques différentes des résidus miniers de point de vue hydrogéologique et géochimique. Leurs modes de

gestion respectifs sont en conséquence différentes. Ils peuvent être réutilisés pour le remblayage de la mine souterraine et même en surface avec ou sans ciment. Le remblayage souterrain permet, en plus de débarrasser la surface du site d'une quantité importante de rejets potentiellement nuisibles, de contribuer au support des terrains et faciliter l'exploitation du gisement. En surface, les résidus miniers sont généralement entreposés dans des aires de stockage ce qu'on appelle parc à résidu. Quant aux stériles miniers, ils sont entreposés sous forme de haldes à stériles. Les deux catégories de rejets miniers sont généralement caractérisées par la présence d'une large gamme de minéraux de différentes réactivités vis-à-vis les conditions météorologiques. Les sulfures de fer (pyrite et pyrrhotite) sont la famille minérale qui présente un impact négatif potentiel pour l'environnement avoisinant (eaux souterraines, faune, flore…). En effet, l'exposition des sulfures à l'eau et à l'oxygène atmosphérique peut générer le phénomène de drainage minier acide (DMA) ou de drainage rocheux acide (DRA). La génération d'acide est l'un des principaux défis de l'industrie minière à l'échelle de la planète, à cause de ses impact nuisible sur l'environnement. Le DMA/DRA est un phénomène qui résulte de l'oxydation des sulfures en absence d'une quantité suffisante de minéraux neutralisants capables de neutraliser l'acidité produite. Les eaux du drainage minier acide sont caractérisées par des pH faibles, des concentrations élevées en sulfates et fer, et des concentrations plus ou moins importantes en contaminants (As, Sb, Co, Ni, Hg, Se, etc.). Dans le cas où le rejet minier contient une quantité suffisante de minéraux neutralisants, les eaux de drainage minier sont caractérisées par des pH proches de la neutralité, et ne pouvant induire qu'une contamination plus ou moins prononcée appelée drainage neutre contaminé (DNC). Les coûts associés à la restauration des sites miniers sont proportionnels à la qualité des eaux du drainage minier. De ce fait, les compagnies minières s'investissent à bien prédire le comportement géochimique des rejets miniers dès les premières étapes du cycle de vie de l'opération minière et, de plus en plus dès l'étape d'exploration.

La prédiction du comportement géochimique des rejets miniers peut être effectuée avec l'aide des essais statiques et/ou des essais cinétiques. Dans tous les cas, une caractérisation physique, chimique et minéralogique approfondie des rejets en question est capitale. Les essais statiques nommés ABA (Acid Base Accounting) consistent à faire le bilan instantané entre le pouvoir d'acidification (PA) et celui de neutralisation (PN) du rejet sans considérer la cinétique des réactions et en se basant sur des hypothèses discutables; considérer tout le soufre d'un échantillon comme réactif et comme étant de la pyrite constitue l'une des faiblesses de ce genre de tests

(Bouzahzah *et al.*, 2015a; Sobek *et al.*, 1978b). En revanche, les essais cinétiques sont désignés pour simuler l'oxydation des rejets en fonction du temps. Ils permettent de quantifier la cinétique et les taux des réactions des phases en présence. Ces essais cinétiques peuvent se réaliser à différentes échelles; les minicellules d'altération , les cellules humides (Bouzahzah *et al.*, 2015b; Lapakko, 2003; Sapsford *et al.*, 2009), les colonnes (Benzaazoua *et al.*, 2004c; Morin & Hutt, 1998) et les cellules de terrain (Bussière *et al.*, 2007). Les difficultés liées à la prédiction du comportement géochimique des stériles miniers diffèrent de celles des résidus miniers. En effet, les caractéristiques physiques, géotechniques et minéralogiques (compositionnelles et texturales) des résidus miniers sont différentes de celles des stériles miniers. En effet, les résidus saturés en eau sont peu ou pas réactifs, l'oxygène diffusant très peu dans l'eau faisant que l'oxydation des sulfures demeure inhibée (Ouangrawa *et al.*, 2009). Les stériles sont, quant à eux, caractérisés par une granulométrie étalée faisant qu'en général seulement une proportion faible du stérile est réactive et donc responsable du comportement global du stérile.

Les stériles miniers, caractérisés par une taille de particule qui peut aller de quelques microns à des blocs métriques, sont souvent entièrement gérés dans des haldes à stériles sans se soucier des aspects hydro-géotechniques. Or, la réactivité des rejets miniers dépend de plusieurs propriétés dont la granulométrie. La taille des particules est un paramètre qui peut définir partiellement le degré d'exposition des minéraux ou autrement le degré de libération minérale. Le degré de libération d'un minéral est défini comme la proportion du minéral disponible aux réactions. Ce paramètre peut être quantifié à l'aide de diverses techniques minéralogiques, et de plus en plus par des systèmes de minéralogie automatisés. L'objectif ultime est de définir une granulométrie du stérile issu de d'exploitation en roche dure au-dessus de laquelle les sulfures sont presque entièrement encapsulés dans une matrice rocheuse imperméable. Basé sur ce paramètre, la quantité de stériles réactifs à gérer sera réduite considérablement pour minimiser les coûts associés à la gestion des haldes à stériles. Un principe similaire utilisé *in situ* en mines à ciel ouvert a été développé pour la récupération du minerai par l'australien CRCore et appelé *grade engineering* (Carrasco *et al.*, 2016).

Après dépôt des résidus miniers dans des parcs à résidus de surface et dépendamment des conditions du site, le niveau de la nappe peut baisser induisant, ainsi, une désaturation des résidus. Par conséquent, l'oxydation aérobique des sulfures commence et peut être accélérée considérablement par l'activité bactérienne (Nordstrom *et al.*, 2015). Ensuite, le profil d'oxydation

peut atteindre une dizaine de centimètres dépendamment de la réactivité des ces résidus. Ceci a été remarqué dans plusieurs sites miniers inactifs fermés ou abandonnés non restaurés. L'état d'oxydation avancé des parcs à résidus fermés rend la tâche de restauration et de compréhension des phénomènes géochimiques spécifiques et différentes de celles d'un parc à résidus actif. De ce fait, les eaux interstitielles sont préalablement acides et chargées en espèces chimiques.

Dans des conditions spécifiques, les résidus miniers incertains en termes de potentiel de génération d'acidité et contenant des carbonates de Fe-Mn présentent des difficultés pour bien prédire leur comportement géochimique à long terme sur la base des essais de laboratoire avec des modèles physiques simulant des phénomènes unidimensionnels (1D) (Bouzahzah *et al.*, 2015a; Plante *et al.*, 2012). En effet, durant les processus d'oxydation/neutralisation et d'hydrolyse, une large gamme de minéraux secondaires précipitent et peuvent s'accumulent en formant même dans certaines conditions un horizon induré appelé *hardpan* (Blowes *et al.*, 1991; DeSisto *et al.*, 2011; McGregor & Blowes, 2002). L'occurrence du hardpan et des minéraux secondaires modifie considérablement la réactivité des minéraux et, encore plus, le bilan hydrique sur les parcs à résidus. En outre, la formation des minéraux secondaires comme les oxy-hydroxydes de fer permet de diminuer la mobilité des métaux par le biais de différents mécanismes regroupés dans les phénomènes de sorption sauf que ce phénomène est réversible sous certaines conditions physico-chimiques (Eh, pH). Ils peuvent aussi affecter la réactivité des sulfures par le phénomène de passivation par enrobage appelé *coating*. L'interface entre la zone oxydée et la zone non-oxydée des résidus miniers dans des sites fermés surtout constitue une zone d'interface et de contraste géochimique. Ce contraste géochimique favorise la précipitation et l'accumulation des minéraux secondaires ce qui forme un horizon à perméabilité et porosité faible, d'où la formation d'une barrière contre les écoulements verticaux d'eau et la diffusion de l'oxygène (Graupner *et al.*, 2007; Holmström & Öhlander, 2001; Meima *et al.*, 2007; Rammlmair, 2002). Pour cette catégorie de résidus, une technique de stabilisation/solidification est testée en conditions de terrain pour diminuer la mobilité des contaminants et neutraliser l'acidité produite. Les amendements alcalins et cimentaires sont une technique qui a été utilisé avec succès pour la stabilisation des sols contaminés. Les amendements alcalins ont pour objectif, simplement, un ajout de la neutralisation aux résidus miniers ce qui réduit les concentrations en métaux et métalloïdes suite de l'augmentation du pH des eaux (Doye & Duchesne, 2003; Hakkou *et al.*, 2009; Yi *et al.*, 2017). Par ailleurs, les amendements cimentaires ne visent pas simplement un ajout de la neutralisation mais aussi une

fixation physique des contaminants en réduisant la surface disponible aux réactions (Benzaazoua *et al.*, 2004b; Falciglia *et al.*, 2017; Fatahi & Khabbaz, 2015; Kim & Jung, 2011; Moon *et al.*, 2016; Pesonen *et al.*, 2016; Wang *et al.*, 2015b).

Le sujet de ce doctorat vise l'amélioration des connaissances en lien avec la prédiction du potentiel de drainage minier des deux types de rejets miniers; des résidus de concentrateur et des stériles d'exploitation en visant une gestion intégrée. Le travail de thèse peut être divisé en deux principale parties. La première partie traitera l'effet de la libération minérale sur le comportement géochimique des stériles miniers. La deuxième partie focalisera sur les résidus du site fermé de Joutel. La thèse contient huit chapitres dont la présente introduction, un chapitre de revue de littérature pertinente au sujet et débouchant sur les défis scientifiques. Cinq chapitres suivent présentés sous forme de papiers de revues; un chapitre discussion et une conclusion permettent de boucler la thèse.

Le chapitre revue de littérature soulignera dans un premier temps les principales réactions et phénomènes étudiés lors des processus du drainage minier, ensuite mettra en évidence les principales caractéristiques des résidus miniers et des stériles miniers pour ressortir les défis liés à la prédiction du comportement géochimique de ces deux types de rejets miniers. La deuxième partie de la revue de littérature portera sur l'effet de la granulométrie et de la libération minérale sur la réactivité des stériles miniers et, ensuite, le mode de formation du hardpan, son rôle ainsi que les mécanismes réactionnels liés aux oxy-hydroxydes de fer seront soulignés. Ce chapitre décrira aussi brièvement les outils particuliers utilisés pour l'analyse minéralogique et texturale des stériles miniers et les techniques dédiées pour la caractérisation des oxy-hydroxydes de fer comme phases minières dans les rejets miniers. À la fin de cette section, les hypothèses de recherche ainsi que les objectifs du doctorat seront définis.

Il est judicieux de mentionner ici le choix qui a été fait par rapport à la non nécessité de présenter un chapitre Matériels et méthodes en sachant que tout ce qu'impliquerait ce chapitre se retrouve en détails dans les cinq chapitres (articles de revue) et les annexes afférents.

Les cinq autres chapitres, le corps de cette thèse, vont contenir les principaux résultats de ce doctorat. Le premier papier présentera la méthodologie proposée pour la caractérisation des stériles miniers de la mine d'or à ciel ouvert Canadian Malartic afin de mieux calculer leurs PA et PN. C'est une méthodologie basée sur une caractérisation pluridisciplinaire combinant des outils

conventionnels et d'autres techniques pour la première fois utilisées pour un objectif d'évaluation environnementale. Le principal résultat de ce papier réside dans la suggestion d'un paramètre appelé diamètre d'encapsulation physique des sulfures (DPLS) qui sépare le stérile minier en deux fractions avec une réactivité différente. Le deuxième papier présente les résultats de l'approche cinétique qui a été utilisée pour la validation du DPLS. À la lumière des résultats de ces deux papiers, une nouvelle méthodologie de la gestion de stérile est proposée. Les deux papiers suivants s'articulent autour de la géochimie des résidus miniers du site minier Joutel. Ainsi, le 3ème papier traitera l'effet du hardpan sur la géochimie des résidus miniers de Joutel. L'effet du hardpan est mis en évidence via une caractérisation pluridisciplinaire des résidus oxydés, frais et du hardpan des points de vues chimique, minéralogique et hydrogéologique et des essais cinétiques en colonnes. Le 4ème papier propose une nouvelle méthodologie pour l'étude des parcs à résidus fermés ou abandonnés ayant fait l'objet d'une altération météorique. Cette méthodologie propose l'utilisation d'une approche sous les systèmes d'information géographique (SIG). Cette approche combine différentes composantes de point de vue spatiale pour mieux comprendre les processus géochimiques d'une façon intégrale d'une part et, d'autre part, orienter le scénario de restauration des sites inactifs en considérant la variabilité spatiale des propriétés géochimiques des résidus oxydés et un papier issu d'une conférence internationale, présenté en annexe, détaillera les caractéristiques des *hardpans* à Joutel. Le dernier papier présentera les principaux résultats du suivi des cellules de terrain qui ont été mises en place pour tester l'efficacité des amendements miniers à stabiliser les résidus miniers oxydés de Joutel. Les deux derniers chapitres (discussion et conclusions) vont ressortir les principales retombées scientifiques et économiques de ces travaux de recherche.

CHAPITRE 2   REVUE DE LITTÉRATURE

2.1 Généralités sur la géochimie du drainage minier

La revue de littérature développée dans ce chapitre porte sur les plus importants aspects scientifiques développés dans ce doctorat. Il s'agit essentiellement de la géochimie du drainage minier, l'effet de la libération des sulfures sur la réactivité minérale et de la présence des oxy-hydroxydes de fer sur le comportement géochimique des rejets miniers sulfureux. En premier lieu, l'oxydation des sulfures et la dissolution des minéraux neutralisants seront discutées. Ensuite, l'effet de la libération minérale ou encore le taux d'exposition des minéraux sulfurés sur la réactivité des rejets miniers. Finalement, l'effet de la précipitation des minéraux secondaires sur le comportement géochimique des résidus miniers incertains par rapport à leur potentiel de génération d'acidité; il sera question d'abord d'évoquer la formation du hardpan basé sur des études bibliographiques antérieures et ensuite quelques mécanismes réactionnels liés aux oxy-hydroxydes de fer seront présentés car pouvant remettre en jeu la qualité de la prédiction environnementale basée sur des essais au laboratoire.

2.1.1 Le drainage minier, l'oxydation des sulfures et la dissolution des minéraux neutralisants

2.1.1.1   Le drainage minier et le rôle de l'oxydation des sulfures

L'oxydation des sulfures par l'eau et l'oxygène est une réaction naturelle. L'exposition des rejets miniers aux conditions atmosphériques accélère cette oxydation. La pyrite et la pyrrhotite sont les principaux sulfures de fer rencontrés dans les rejets miniers. L'oxydation des sulfures de fer génère de l'acidité et augmente la solubilité des métaux (Benzaazoua *et al.*, 2004c; Bussière *et al.*, 2005). L'oxydation typique de la pyrite dans un milieu aqueux peut se faire directement par l'oxygène ou encore par le fer ferrique. L'oxydation de la pyrite par l'oxygène atmosphérique peut s'exprimer par la réaction suivante (Eq 1) :

$$FeS_2 + 7/2\ O_2 + H_2O \rightarrow Fe^{2+} + 2SO_4^{2-} + 2H^+ \hspace{3cm} \textit{(Eq 1)}$$

Durant cette réaction d'oxydation, le fer est libéré sous sa forme ferreuse (Fe^{2+} ou FeII) et le soufre sulfure est oxydé en sulfates (Lowson, 1982). Le fer ferreux libéré s'oxyde à son tour en fer ferrique (Fe^{3+} ou FeIII), ce dernier prends le relais de l'oxygène et oxyde la pyrite dans des conditions acides. Cette réaction d'oxydation de la pyrite par le fer ferrique génère plus d'acidité que l'oxydation par l'eau et l'oxygène (Nordstrom, 1982). La cinétique d'oxydation de la pyrite par le fer ferrique en absence de l'oxygène est rapide. Ce processus d'oxydation se fait selon la stœchiométrie suivante (Evangelou & Zhang, 1995a; Nordstrom, 2009; Rimstidt & Vaughan, 2003) (Eq 2) :

$$FeS_2 + 14Fe^{3+} + 8H_2O \rightarrow 15Fe^{2+} + 2SO_4^{2-} + 16H^+ \hspace{3cm} \textit{(Eq 2)}$$

L'oxydation du fer ferreux en fer ferrique conduit par la suite à la précipitation du fer ferrique sous forme d'oxy-hydroxyde de fer. Cette oxydation se fait sous l'action de l'oxygène mais fortement accélérée par l'activité bactérienne, en particulier les bactéries ferro-oxydantes et thiooxydantes. Des auteurs ont statué que la présence bactérienne est obligatoire pour atteindre des valeurs de pH très basses (1-2) parce qu'en absence des bactéries ferro-oxydantes, la cinétique de précipitation du fer ferrique est beaucoup plus rapide que la cinétique d'oxydation du fer ferreux en fer ferrique (Rohwerder *et al.*, 2003). Ces auteurs pensent que l'acidité ne sera pas maintenue en absence des bactéries. D'autres auteurs pensent que l'intervention bactérienne est indispensable pour la génération d'acidité lors du processus d'oxydation des sulfures (Ledin & Pedersen, 1996). Ce mécanisme d'oxydation de la pyrite avec l'intervention bactérienne est connu sous le nom d'oxydation biologique de la pyrite par métabolisme indirect (Tributsch, 2001).

L'intervention de l'activité bactérienne est aussi supposée oxyder directement les sulfures. Les microorganismes peuvent oxyder directement les sulfures ; ce mécanisme est décrit comme l'oxydation des sulfures par métabolisme direct. Cette voie d'oxydation implique un contact direct entre les bactéries et la pyrite, il s'agit d'une dissolution oxydative de la pyrite en présence de l'oxygène selon la réaction suivante (Eq 3) (Edwards *et al.*, 1998; Evangelou *et al.*, 1995a) :

$$FeS_2 + O_2 \text{ (bactéries)} \rightarrow Fe^{2+} + 2SO_4^{2-} + H^+ \hspace{3cm} \textit{(Eq 3)}$$

La réaction globale d'oxydation biologique directe de la pyrite consiste au début en une dissolution de la pyrite ce qui relargue des ions Fe^{2+} et S_2^{2-}. Par la suite, les ions S_2^{2-} sont immédiatement oxydés par l'action enzymatique des bactéries pour donner naissance aux ions sulfates. Cette réaction continue jusqu'à épuisement des sulfures. Le taux d'oxydation de la pyrite dans ce cas, dépend de plusieurs paramètres, tels que les caractéristiques cristallographiques et morphologiques du minéral comme l'abondance de fractures et la dislocation. Konishi *et al.*, 1990 ont démontré que le taux d'oxydation de la pyrite est positivement corrélé à la multiplication des bactéries. Les bactéries peuvent se développer au niveau du solide comme elles peuvent se multiplier au niveau de la phase liquide. L'oxydation de la pyrite n'est pas instantanée dans ce cas et un *lag time* est remarqué. Par la suite, le processus d'oxydation est accéléré. Lors de l'oxydation bactérienne de la pyrite, il est très difficile de quantifier la participation des trois voies discutés (métabolisme direct et indirect, de l'action chimique).

En plus de l'oxydation chimique et biologique des sulfures, l'oxydation galvanique est un processus non-négligeable (Chopard *et al.*, 2017b). Elle consiste en un contact physique entre deux sulfures dans un milieu qui facilite le transfert des charges électriques (Holmes & Crundwell, 1995). L'effet galvanique a lieu entre deux minéraux, un minéral conducteur et un autre semi-conducteur. Les effets galvaniques changent les taux des demi-réactions anodiques et cathodiques sur la surface des deux minéraux en contact. Les effets galvaniques ont été observés durant les processus de flottation et la biolixiviation (Majima & Peter, 1968; Mehta & Murr, 1983; Tributsch, 2001).

Le couple galène-pyrite a été étudié pour mettre en évidence l'oxydation galvanique dans un milieu qui contient des nitrates de fer (Holmes *et al.*, 1995). Le contact galène-pyrite a permis d'accélérer le taux de dissolution de la galène. La raison pour laquelle la dissolution de la galène augmente est la suivante : lorsque la galène est en contact avec la pyrite, sa dissolution est couplée à la réduction du fer ferrique sur la surface de la pyrite. Lorsqu'elle n'est pas en contact avec la pyrite, sa dissolution est liée la réduction du fer ferrique qui se produit sur la surface de la galène. Il est conclu par Holmes *et al.*, 1995 que la réduction du fer ferrique sur la surface de la pyrite est beaucoup plus rapide que sur la surface de la galène, le taux de dissolution de la galène est important lorsqu'elle est en contact avec la pyrite. Mais dans le cas de rejets uniquement pyriteux, ce phénomène est moins propice (Holmes *et al.*, 1995).

En résumé, la pyrite est de loin le minéral le plus étudié dans la littérature vu son abondance dans les rejets miniers (Blowes *et al.*, 2014; Blowes *et al.*, 1994; Blowes *et al.*, 2013; Chopard *et al.*, 2015; Elberling *et al.*, 1994; Elberling & Nicholson, 1996; Evangelou *et al.*, 1995a; Lapakko, 2002; Nicholson *et al.*, 1988; Nordstrom, 1982; Nordstrom, 2000; Nordstrom *et al.*, 2015; Nordstrom & Southam, 1997; Paktunc & Davé, 2000a; Rimstidt *et al.*, 2003; Silverman, 1967). Le Tableau 2.1 présente un résumé des réactions d'oxydation des sulfures les plus communs (Dold, 2017). Ces résultats montrent clairement que l'apport en H^+ de l'oxydation des sulfures par le fer ferrique est beaucoup plus important par comparaison à l'oxydation des mêmes sulfures par l'oxygène.

Tableau 2.1: Réactions d'oxydations des sulfures communs (tiré de (Dold, 2017))

Minéral	Réaction	Moles de H^+/mole de sulfates
Oxydation par oxygène et hydrolyse de Fe^{3+}		
Pyrite	$FeS_2 + 3,75O_2 + 3,5H_2O \rightarrow Fe(OH)_3 + 2\ SO_4^{2-} + 4H^+$	4
Arsénopyrite	$FeAsS + 2O_2 + 3H_2O \rightarrow Fe(OH)_3 + SO_4^{2-} + HAsO_4^{2-} + 3H^+$	3
Chalcopyrite	$CuFeS_2 + 4O_2 + 3H_2O \rightarrow Cu^{2+} + Fe(OH)_3 + 2SO_4^{2-} + 2H^+$	2
Pyrrhotite	$Fe_{0.9}S + 2,157O_2 + 2,35H_2O \rightarrow 0,9Fe(OH)_3 + SO_4^{2-} + 2H^+$	2
Enargite	$Cu_3AsS_4 + 8,75O_2 + 2.5H_2O \rightarrow 3Cu^{2+} + HAsO_4^{2-} + 4SO_4^{2-} + 4H^+$	4
Oxydation par le fer ferrique		
Pyrite	$FeS_2 + 14Fe^{3+} + 8H_2O \rightarrow 15Fe^{2+} + 2SO_4^{2-} + 16H^+$	16
Arsénopyrite	$FeAsS + 13Fe^{3+} + 8H_2O \rightarrow 14Fe^{2+} + SO_4^{2-} + HAsO_4^{2-} + 15H^+$	15
Chalcopyrite	$CuFeS_2 + 16Fe^{3+} + 8H_2O \rightarrow Cu^{2+} + 17Fe^{2+} + 2SO_4^{2-} + 16H^+$	16
Pyrrhotite	$Fe_{0.9}S + 7.8Fe^{3+} + 4H_2O \rightarrow 8.7Fe^{2+} + SO_4^{2-} + 8H^+$	8
Enargite	$Cu_3AsS_4 + 35Fe^{3+} + 20H_2O \rightarrow 3Cu^{2+} + HAsO_4^{2-} + 35\ Fe^{2+} + 4SO_4^{2-} + 39H^+$	39

Quant à la réactivité des sulfures, elle diffère selon le minéral, sa stœchiométrie, et sa cristallinité. Chopard *et al.* (2015) ont évalué les taux d'oxydation d'une large gamme de sulfures de fer, sulfosels et les sulfures des métaux de base en utilisant des essais en minicellules d'altération. Le calcul des taux d'oxydations expérimentaux des différents minéraux testés sont présentés dans le Tableau 2.2.

Tableau 2.2: Taux d'oxydation expérimentaux des sulfures (tiré de Chopard et al. (2014))

Taux d'oxydation (mg de S/kg/jour)					
Sulfures de fer		Sulfures de métaux de base		Sulfures (contenant As/Sb)	
Pyrrhotite 1	8.2	Bornite	0.23	Arsénopyrite	6.9
Pyrrhotite 2	2.6	Chalcocite	0.28	Gersdorffite	93.6
Pyrite 1	2.4	Chalcopyrite 1	2	Fehlore	3.2
Pyrite 2	4.8	Chalcopyrite 2	1	Stibnite	0.49
Pyrite 3	4.6	Covellite	2.7		
		Galène	0.53		
		Sphalérite	2.3		
		Sphalérite-Fe	3.2		

2.1.1.2   Dissolution des minéraux neutralisants

L'oxydation des sulfures libère des protons H^+ en augmentant ainsi l'acidité du milieu. En conséquence, des minéraux neutralisants, quand ils sont présents, se dissolvent pour neutraliser totalement ou partiellement l'acidité produite ; ce sont les réactions de neutralisation (Benzaazoua *et al.*, 2004c; Blowes *et al.*, 2003; Blowes *et al.*, 2014; Blowes *et al.*, 2013; Brown & Glynn, 2003; Dold, 2017; Kwong, 1993; Lawrence & Wang, 1997b; Nordstrom, 2000; Nordstrom, 2009; Nordstrom *et al.*, 2015; Paktunc, 1999a; Plante *et al.*, 2012). Les carbonates de calcium (calcite) et de calcium-magnésium (dolomite) sont connus comme les principaux neutralisants du drainage minier acide. Dans une moindre mesure, les minéraux silicatés peuvent contribuer plus ou moins timidement aux réactions de neutralisation.

Les carbonates les plus rencontrés dans les rejets miniers sont : la calcite ($CaCO_3$), la dolomite ($CaMg(CO_3)_2$, la magnésite ($MgCO_3$), la sidérite ($FeCO_3$) et l'ankérite ($Ca(Fe, Mg, Mn)(CO_3)_2$).

La dissolution de la calcite et/ou la dolomite permet de maintenir le pH à des valeurs proches de la neutralité grâce à leurs cinétiques de dissolution rapides et augmentent ainsi l'alcalinité des eaux de drainage. Dans le cas d'un système fermé et dans des conditions proches de la neutralité, la dissolution de la calcite neutralise un proton H^+ selon la réaction suivante (Eq 4) :

$$CaCO_3 + H^+ \rightarrow HCO_3^- + Ca^{2+} \qquad \qquad (Eq\ 4)$$

Par ailleurs, dans le cas d'un système ouvert, la dissolution de la calcite est réalisée en présence du dioxyde de carbone selon la réaction suivante (Eq 5) :

$$CaCO_3 + CO_2 + H_2O \rightarrow Ca^{2+} + 2HCO_3^- \qquad \qquad (Eq\ 5)$$

Lorsque le pH du milieu est inférieur à 6.3, la dissolution de la calcite neutralise deux protons H^+ selon la réaction suivante *(Eq 6)*:

$$CaCO_3 + 2H+ \rightarrow Ca^{2+} + H_2CO_3^- \qquad \qquad (Eq\ 6)$$

Les silicates, à l'exemple de la biotite, de la chlorite, du plagioclase, de la muscovite et des amphiboles, possèdent une capacité non négligeable à neutraliser l'acidité (Blowes *et al.*, 2003; Blowes *et al.*, 2014; Miller *et al.*, 2010; Sherlock *et al.*, 1995). La dissolution des silicates, à l'exception du quartz qui est considéré comme inerte, consomme les protons H^+ du système et libère H_4SiO_4. La dissolution des silicates peut être congruente ou incongruente (Sherlock *et al.*, 1995). Plusieurs auteurs considèrent que les silicates fournissent un potentiel de neutralisation important pour les résidus miniers (Paktunc, 1999a). Cependant, d'autres auteurs suggèrent de ne pas prendre en considération les silicates lors du calcul et mesure du NP des rejets miniers pour la raison de la faible cinétique de réaction de ces minéraux (Jambor *et al.*, 2002a). Jambor *et al.* (2002) ont mesuré le NP de plusieurs minéraux silicatés et argileux. Leurs résultats ont montré que le NP de la plupart des silicates est faible par rapport à celui de la calcite. Leurs PN était inférieur à 20 kg $CaCO_3$/t à l'exception de l'olivine et la wollastonite qui ont présenté un PN supérieur à 20 kg $CaCO_3$/t. Les minéraux silicatés qui ont démontré un PN important, selon Jambor et al. (2002), contenaient des impuretés de carbonates.

Tout comme les sulfures, les minéraux neutralisants ont des réactivités différentes. Le taux de dissolution d'un minéral neutralisant dépend de plusieurs paramètres comme le pH, la température,

et la pression du CO_2. La réactivité relative des différents carbonates et minéraux silicatés à pH 5 est présentée dans le Tableau 2.3.

Tableau 2.3: réactivité relative de quelques minéraux communs (Kwong, 1993; Sverdrup, 1990)

Groupe	Minéraux	Réactivité relative (à pH=5)
Soluble	Calcite, dolomite, magnésite, aragonite, brucite,	1
Dissolution rapide	Anorthite, olivine, diopside, wollastonite, nepheline, jadeite, leucite,	0.6
Dissolution intermédiaire	Augite, hornblende, actinolite, biotite, chlorite, serpentine, épidote	0.4
Dissolution lente	Plagioclase sodique, kaolinite, vermiculite	0.02
Dissolution très lente	Muscovite, feldspaths potassiques	0.01
Inerte	Quartz, zircon, rutile	0.004

Les oxyhydroxydes de Fe et Al sont aussi considérés comme des minéraux neutralisants parce que leurs dissolutions impliquent la consommation des protons H^+ (Blowes *et al.*, 2014), sauf que la dissolution de ces oxyhydroxydes tamponne le pH à des valeurs de 4-4.5 (Moncur *et al.*, 2005).

2.2 Tests de prédiction du comportement environnemental des rejets miniers

Auparavant, l'étude de faisabilité des projets miniers contenait majoritairement l'aspect économique et technique pour trancher de l'exploitabilité ou non d'un gisement minier. Récemment, l'aspect environnemental est devenu un facteur clé pour déterminer la faisabilité d'un gisement minier avec la nécessité de mener des études d'impact sur l'environnement, d'où la nécessité de prédire le comportement environnemental des rejets avant même le début des opérations minières sur les bases des échantillons qui servent à la définition des réserves du gisement. Plusieurs méthodes ont été développées pour prédire le comportement géochimique des rejets miniers. Les techniques les plus utilisés sont les tests statiques et les essais cinétiques

(Aubertin *et al.*, 2002; Benzaazoua *et al.*, 2004c; Bouzahzah, 2013; Bouzahzah *et al.*, 2010; Dold, 2017; Maest & Nordstrom, 2017; Morin & Hutt, 1994, 2001; Price, 2009; Price *et al.*, 1997b). La principale différence entre les deux tests est la composante temporelle. En effet, les tests statiques sont conçus pour évaluer le bilan entre le pouvoir de neutralisation et celui d'acidification d'un rejet minier donné, alors que les essais cinétiques permettent d'incorporer le facteur temps pendant l'altération des rejets, permettant d'avoir une idée sur les taux de relargage des éléments chimiques, les cinétiques des réactions et le temps nécessaire pour l'épuisement des minéraux concernés.

2.2.1 Tests statiques

Les tests statiques largement utilisés dans l'industrie minière sont les tests statiques chimiques, les tests statiques minéralogiques et les tests NAG (Net acidity generation). Les tests statiques sont désignés pour évaluer le pouvoir de neutralisation (PN) et le pouvoir d'acidité (PA) d'un échantillon solide à un instant donné. Plusieurs tests ont été développés à cet effet comme les tests ABA (acid base accounting) qui renferment eux-mêmes plusieurs tests. Le test de Sobek et al (1978) est l'un des tests les plus connus qui a ensuite été amélioré pour différentes raisons comme la prise en considération des carbonates de Fe-Mn et l'hydrolyse de fer ferreux (Bouzahzah *et al.*, 2015a; Chopard *et al.*, 2017a; Frostad *et al.*, 2002; Kwong & Ferguson, 1997; Lawrence & Scheske, 1997a; Lawrence *et al.*, 1997b; Paktunc, 1999a). Les tests ABA se basent sur une analyse chimique et/ou une digestion acide du rejet. Les détails sur le mode opératoire des différents tests statiques sont disponibles dans différents documents (Bouzahzah, 2013; Bouzahzah *et al.*, 2014b; Price, 2009). L'objectif ultime des tests ABA est d'évaluer tout d'abord le PN de l'échantillon et ensuite déterminer son PA pour pouvoir évaluer le bilan entre les deux et statuer sur son potentiel de génération d'acide. L'interprétation des essais ABA se fait à l'aide des critères PNN (PN-PA) et RPN (PN/PA). Les critères de classification sont illustrés à la Figure 2.1. Cette interprétation se base sur l'utilisation du soufre et carbone. Ceci posera un problème lorsqu'il s'agira des rejets miniers ayant une granulométrie étalée comme le cas des stériles. Durant ces tests, les analyses du carbones et soufres se font à l'aide des échantillons pulvérisés. De ce fait, le PA et le PN d'un échantillon sont considérés totaux (absolus) indépendamment de sa granulométrie et texture initiale. Par contre, dépendamment de la libération des sulfures et des carbonates le PN et le PN peuvent être partiellement disponibles.
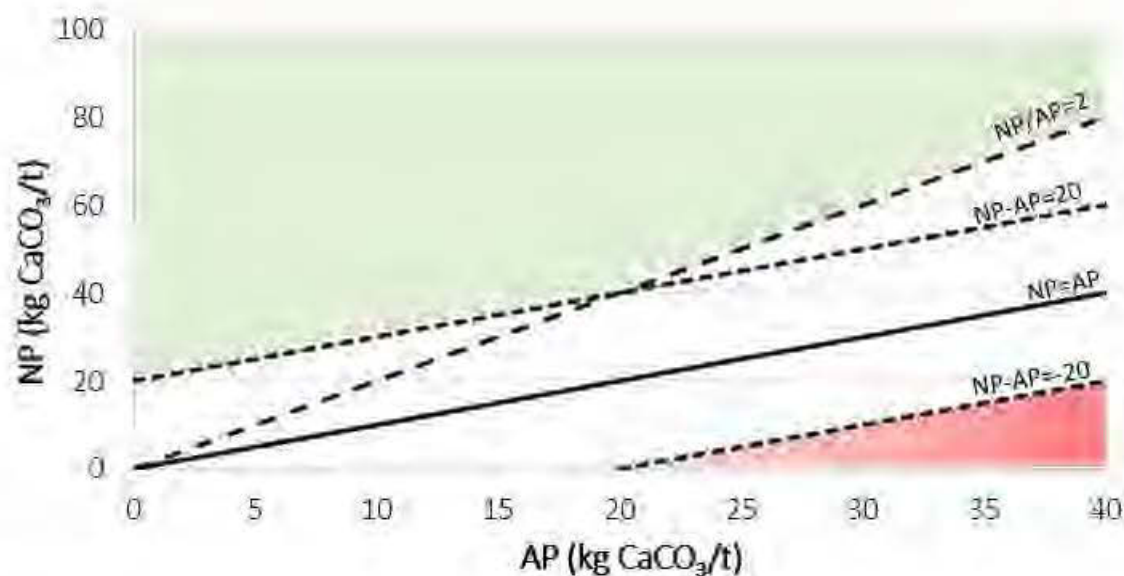
Figure 2.1 : Critères de classification pour les tests ABA. La zone rouge correspond à la zone de génération d'acidité, la zone verte correspond à la zone de non-génération d'acidité et la zone blanche correspond à la zone d'incertitude

Par ailleurs, les tests NAG permettent seulement de quantifier le bilan entre le PN et le PA d'un échantillon solide sans pouvoir quantifier son PA et son PN. Il existe trois variantes des tests NAG à savoir : le NAG simple, le NAG cinétique et le NAG séquentiel (Price, 2009; Smart *et al.*, 2002; Stewart *et al.*, 2006). L'utilisation de l'un ou l'autre des tests NAG dépend du contenu en sulfures de l'échantillon et l'objectif du test; le NAG cinétique est utilisé lorsque l'objectif du test est d'estimer le lag time et connaitre la vitesse relative des neutralisants grâce à l'utilisation d'une sonde de température. L'interprétation des tests statiques dépend du type de l'essai. L'interprétation des tests NAG se fait à l'aide du NAGpH qui est le pH final du lixiviat du test. L'échantillon est considéré générateur d'acide si son NAGpH est inférieur à 4.5, sinon il est considéré non générateur d'acide (Parbhakar-Fox *et al.*, 2017b; Smart *et al.*, 2002). Dans des cas, les tests NAG peuvent être combinés à l'analyse du pH de la pâte pour avoir une idée sur le comportement environnemental à long terme d'un échantillon mais cette approche n'est pas encore validée par des essais cinétiques pour confirmer ce critère (Parbhakar-Fox *et al.*, 2017b; Weber *et al.*, 2006). Ce critère est illustré à la Figure 2.2.
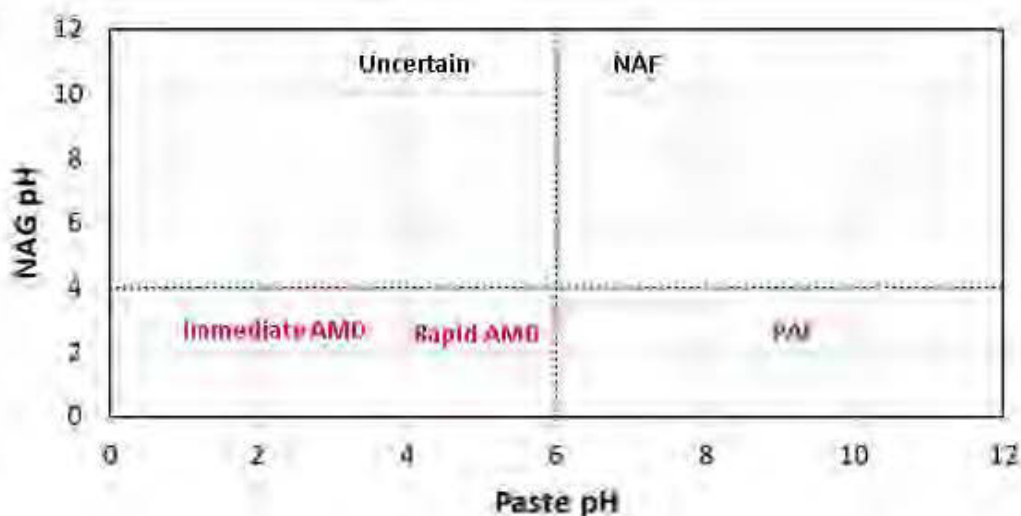
Figure 2.2 : Critère de classification des échantillons selon le NAG pH vs pH de pâte. Immediate AMD : génération instantanée du drainage minier acide, Rapid AMD : génération rapide du drainage minier acide, PAF : génération potentielle du drainage minier acide, NAF : non générateur d'acide, Uncertain : incertain

2.2.2 Essais cinétiques

Les essais cinétiques sont des tests qui simulent au laboratoire et au terrain l'oxydation naturelle d'un rejet minier. Ils permettent de calculer le taux de lixiviation des espèces chimiques, l'épuisement des minéraux neutralisants et acidifiants, ce qu'on appelle le *lag time* s'il existe. Ce dernier est défini comme le temps nécessaire avant la génération d'acidité. Au laboratoire, un rejet minier peut être testé en utilisant des minicellules d'altération, des cellules d'humidité ou encore des colonnes. En général, les essais cinétiques sont recommandés après avoir réalisé les tests statiques (Bouzahzah, 2013; Chopard, 2017; Lapakko, 2002; Price & Kwong, 1997a; Price *et al.*, 1997b). Les trois tests diffèrent selon la quantité d'échantillon testée, la durée du test, la fréquence des rinçages, le ratio liquide/solide (L/S) et les dimensions de l'essai.

Les tests en minicellules d'altération sont les plus rapides et nécessitent seulement 67 g. L'échantillon est rincé deux fois par semaine en utilisant 50 ml d'eau déionisée (Cruz *et al.*, 2001). C'est un test qui permet d'avoir des résultats assez rapidement et sa mise en place est facile et moins couteuse par rapport aux autres tests. Cependant, ce test présente l'inconvénient du séchage de l'échantillon qui peut mener à des fausses conclusions et remédié par Bouzahzah *et al* (2014). Les essais en cellules humide est le seul essai cinétique normé par la norme ASTM D-5744-96

(ASTM-D5744-96, 2007). Ce test consiste à mettre 1 kg d'échantillon sec dans une cellule en plexiglas et le rincer une fois par semaine avec 500 ml ou 1 L d'eau déionisée. Ce test nécessite plus d'interventions de l'opérateur. La durée d'essai est de 20 à 40 semaines. Les essais en colonnes sont des essais qui nécessitent une quantité d'échantillon plus élevée par rapport aux minicellules et aux cellules humides. La mise en place des essais en colonnes est coûteuse par rapport aux autres tests (Bouzahzah, 2013; Villeneuve, 2006). L'échantillon est rincé une fois par mois en utilisant une quantité d'eau déionisée définie par l'opérateur. Les essais en colonnes offrent la possibilité d'installer des instruments de mesure (e.g. sondes de teneur en eau) (Bussière *et al.*, 2004). Les colonnes présentent l'avantage de simuler mieux les conditions hydrogéologiques du terrain (positionnement de la nappe) et permettent de tester des scénarios de restauration. Les lixiviats des trois essais cinétiques sont généralement analysés pour les mêmes paramètres : concentrations chimiques élémentaires, pH, Eh, conductivité électrique et acidité/alcalinité.

2.2.3 Limites et enjeux des essais de prédiction environnementale

Les essais statiques sont généralement réalisés sur des échantillons pulvérisés ou au moins concassés pour répondre aux exigences expérimentales (Bouzahzah *et al.*, 2015b; Bouzahzah *et al.*, 2015a; Chotpantarat, 2011; Jambor *et al.*, 2002a; Lapakko, 2003; Lapakko & Lawrence, 2009; Miller *et al.*, 1997; NEDEM, 1995, 2008; Plante *et al.*, 2012). La pulvérisation des échantillons se fait indépendamment de sa granulométrie initiale. Même, le calcul du PN à la base des carbonates et le PA à la base des sulfures se fait automatiquement pour des échantillons pulvérisés. De ce fait, deux échantillons ayant initialement deux granulométries totalement différentes vont se retrouver aux mêmes conditions de granulométrie pour pouvoir passer les tests statiques. Par ailleurs, la granulométrie est corrélée à la surface spécifique et, par conséquent, à la réactivité de l'échantillon (Blowes *et al.*, 2014). En effet, la pulvérisation de l'échantillon augmente sa surface spécifique et, plus précisément, libère les minéraux qui constitue l'échantillon et finalement détruit les textures originales de l'échantillon. De ce fait, le PN et le PA de l'échantillon seront surestimés à cause de la libération non réaliste des sulfures et des carbonates qui constituent l'échantillon. En effet, un sulfure inclut dans du quartz ne réagira jamais à moins qu'on le libère. Par conséquent, le bilan entre le PA et le PN de l'échantillon peut être biaisé parce que la pulvérisation peut libérer différemment les sulfures et les carbonates, d'où la nécessité d'introduire un facteur correctif qui

va prendre en considération la texture initiale de l'échantillon ou encore le degré de libération des minéraux réactifs.

Les essais cinétiques présentent l'avantage de quantifier des paramètres importants pour la prédiction du comportant environnemental des rejets miniers comme le *lag time* et le taux de lixiviation des espèces chimiques (Benzaazoua *et al.*, 2004c; Plante *et al.*, 2014; Price, 2009; Price *et al.*, 1997b). Cependant, les ratios L/S qui sont utilisés restent différents des ratios L/S du terrain. Par ailleurs, les essais cinétiques du laboratoire sont désignés pour simuler seulement un écoulement d'eau vertical (1D). En revanche, sur le terrain, et dépendamment la topographie des sites, la composante des ruissellements de surface et subsurface est, de loin, la composante dominante du bilan hydrique. Par conséquent, les conditions climatiques et biologiques du terrain ne peuvent pas être reproduites au laboratoire. Pour ces raisons, plusieurs auteurs ont remarqué des différences de réponses géochimiques pour le même échantillon testé au laboratoire et sur le terrain (Banwart *et al.*, 2002; Malmström *et al.*, 2000; Miller *et al.*, 2003; Plante *et al.*, 2014; Strömberg & Banwart, 1999).

2.3 Effet de la libération minérale sur la réactivité des rejets miniers

2.3.1 Particularités des stériles miniers

Le terme stérile minier signifie, dans cette thèse, la roche fragmentée et extraite pour atteindre le gisement et dont la teneur en élément de valeur est inférieure à la teneur de coupure. Les stériles miniers sont souvent produits en grandes quantités lors des exploitations minières à ciel ouvert. Les stériles miniers sont caractérisés par une granulométrie étalée par comparaison avec les résidus miniers classifiés comme relativement homogène d'un point de vue granulométrique (Amos *et al.*, 2015; Bussière *et al.*, 2007; Bussière *et al.*, 2004). Les stériles sont aussi produits lors des travaux d'accès pour le cas des mines souterraines. La production journalière des stériles au Canada est estimée à plus de 1 000 000 tonnes (Blowes *et al.*, 2014). Quand ils ne sont pas réutilisés en remblais sous terre (remblais rocheux), ils sont généralement déposés en surface sous forme de grandes haldes à stériles. L'hétérogénéité des propriétés physiques de ces matériaux génère d'autres anisotropies des propriétés hydrogéologiques, minéralogiques et thermiques (Amos *et al.*, 2015).

2.3.2 Effet de la granulométrie sur le comportement géochimique des rejets miniers

La taille des stériles miniers varie de quelques microns à des blocs de taille métrique dépendamment du schéma du tir utilisé (Amos *et al.*, 2015). La granulométrie d'un matériel influence grandement sa surface spécifique (MbonimpaA *et al.*, 2009). En effet, la surface spécifique est parmi les paramètres qui influencent la réactivité d'un matériel (Blowes *et al.*, 2003; Blowes *et al.*, 2014; Blowes *et al.*, 2013; Chopard *et al.*, 2015; Langmuir, 1971; Lapakko *et al.*, 2006). Par ailleurs, la surface spécifique décrit la finesse du matériel ou encore le degré d'exposition des particules qu'il renferme; plus une fraction granulométrique est fine, plus sa réactivité est importante, ayant une surface spécifique importante. Mais dans le cas des rejets miniers (oxydation de leurs sulfures), la surface spécifique seule ne peut pas décrire la réactivité du rejet. Étant donné que la réactivité du rejet minier est aussi liée à la réactivité des minéraux qui le constituent, la granulo-minéralogie pourrait mieux décrire la réactivité de ce dernier. En général, dans le contexte minier, les minéraux acidifiants (sulfures) et les minéraux neutralisants (carbonates) sont les minéraux qui contrôlent cette réactivité et ont des cinétiques de réaction rapides par rapport à la réactivité des autres minéraux comme les silicates, par exemple (Bouzahzah *et al.*, 2014a; Bouzahzah *et al.*, 2015a; Chopard *et al.*, 2015; Jambor, 1994; Jambor *et al.*, 2002b; Kwong *et al.*, 1997; Sverdrup, 1990). Récemment, avec le développement des systèmes de minéralogie automatisés, des paramètres texturaux ont été développés pour décrire l'exposition des minéraux (Ayling *et al.*, 2012; Butcher *et al.*, 2000; Goodall *et al.*, 2005; Gu, 2003; Lastra & Paktunc, 2016; Lastra *et al.*, 1998; Petruk, 2000; Petruk & Lastra, 1993; Pirrie *et al.*, 2004). Il s'agit du degré de libération minérale, qui a été développé initialement pour quantifier la proportion du minerai qui va être récupérée durant les processus minéralurgique comme la flottation et la gravimétrie (Sutherland & Gottlieb, 1991). Récemment, ce paramètre textural, en plus d'autres comme la distribution élémentaire des contaminants, est utilisé pour des objectifs environnementaux (Benzaazoua *et al.*, 2017a). En effet, le degré de libération minérale décrit la proportion surfacique du minéral qui n'est pas partagé avec aucun autre minéral. Les proportions surfaciques sont converties en volume. Un minéral est libre si son contour n'est pas partagé avec aucun autre minéral et il est inclus si la totalité de son contour est partagé avec un ou plusieurs minéraux. Le degré de libération minérale ou encore le degré d'exposition du minéral est un paramètre textural intrinsèque qui dépend de la taille du minéral et la taille des particules. Par

conséquent, ce paramètre va inclure l'effet de la granulométrie de l'échantillon (surface spécifique) et la granulométrie du minéral lui-même dans le matériau en question.

Plusieurs études antérieures ont étudié l'effet de la granulométrie de l'échantillon sur sa réactivité (Erguler & Kalyoncu Erguler, 2015; Lapakko *et al.*, 2006; Paktunc *et al.*, 2000a). En effet, Erguler et Kalyoncu (2015) ont étudié le comportement géochimique d'un rejet minier à différentes granulométries. Les résultats de ces travaux ont montré que la géochimie des lixiviats était différente dépendamment de la granulométrie de l'échantillon. Par ailleurs, le *lag time*, défini comme le temps nécessaire avant le début de la génération d'acidité après l'épuisement du PN, était positivement corrélé à la granulométrie de l'échantillon. La Figure 2.3 présente les résultats du calcul du *lag time* des échantillons testés. En effet, la réactivité de l'échantillon est liée à sa granulométrie. Plus la taille des particules est fine pus la réactivité est importante. Ceci peut être expliqué par la grande proportion des sulfures exposés aux réactions d'oxydation dans l'échantillon fin par rapport à un échantillon grossier. Par conséquence, les concentrations en espèces chimiques vont être inversement proportionnelles à la granulométrie de l'échantillon. Les lixiviats d'un échantillon fin vont être plus chargés en éléments chimiques par rapport aux lixiviats du même échantillon mais grossier.
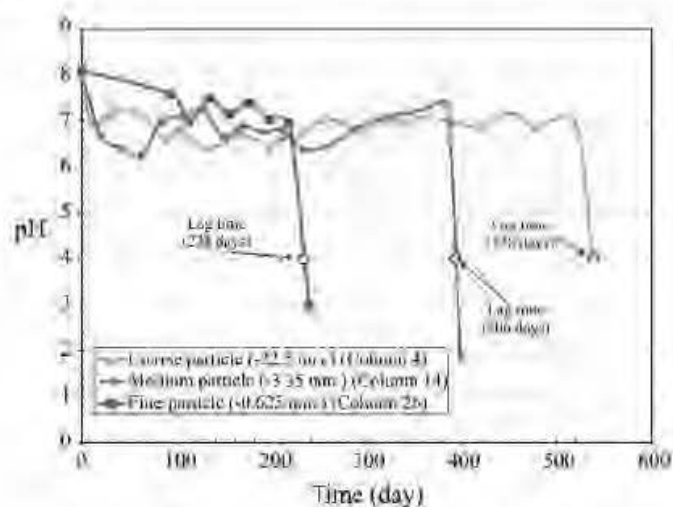
Figure 2.3: Résultats de suivi du pH d'un échantillon à différentes granulométries (tiré de Erguler & Kalyoncu Erguler, 2015)

Le degré de libération désigne la partie libérée du minéral par rapport à sa totalité. Le sujet de l'analyse du degré de libération est beaucoup discuté au niveau de la minéralogie appliquée et les

processus métallurgiques du minerai (Gu, 2003). Dans un échantillon un minéral cible peut être complètement libéré, inclus ou encore partiellement libre (Figure 2.4).
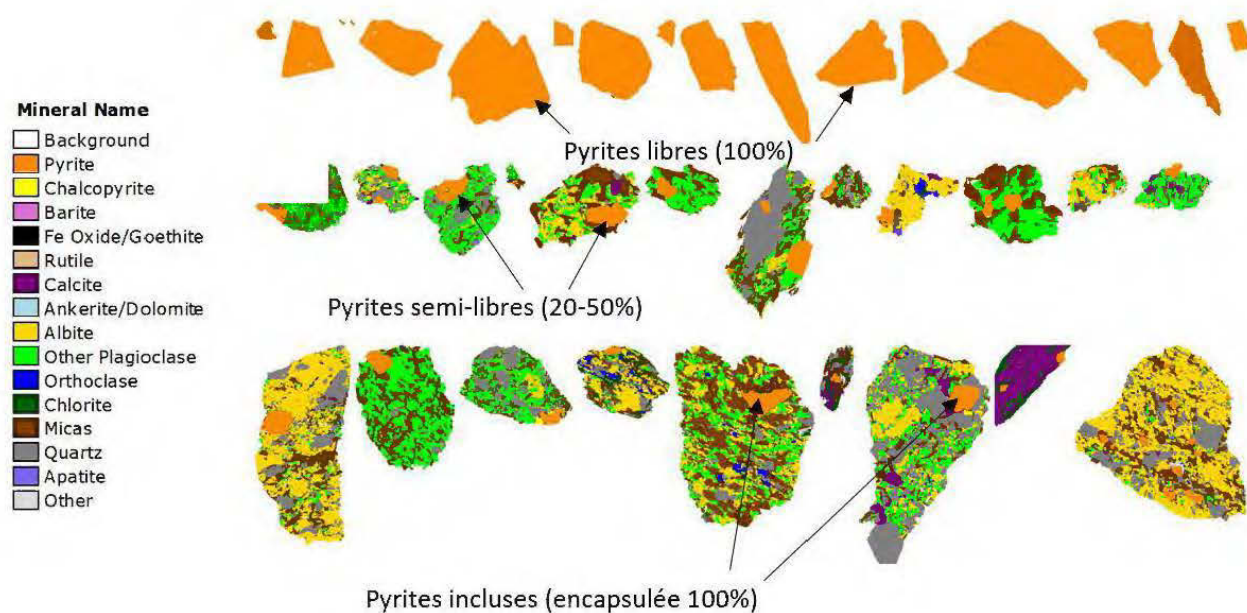
Figure 2.4: Extraits de cartographie minérales illustrant différents états de libération de la pyrite

Il existe plusieurs techniques pour quantifier et estimer le degré de libération des minéraux. Les systèmes de minéralogie automatisé basés sur la spectrométrie EDS sont les plus utilisés actuellement à l'exemple du QEMSCAN (Quantitative Evaluation of Minerals by SCANning electron microscopy), MLA (Mineral Liberation Analyser), Mineralogic Mining de Zeiss et TIMA de TESCAN. Ces techniques nécessitent un microscope électronique à balayage et une composante logicielle de traitement des données et d'analyse d'image.

2.4 Effet des oxy-hydroxydes de fer sur le comportement géochimique des rejets miniers

2.4.1 Généralités sur les oxy-hydroxydes de fer

Lors des réactions d'oxydation/neutralisation et d'hydrolyse d'un rejet minier, différentes phase secondaires sont précipitées groupées sous le nom de phases secondaires. Le terme phases ou minéraux secondaire, ici, signifie les minéraux qui sont formés après le traitement du minerai ou la déposition des résidus. Par conséquent, l'assemblage minéralogique d'un rejet minier va contenir ses minéraux primaires et les minéraux secondaires qui sont formés après les différents

processus impliqués lors de l'oxydation des sulfures (Bligh & Waite, 2010; Blowes *et al.*, 2003; Blowes *et al.*, 1991; Nordstrom *et al.*, 2015). Différentes phases secondaires ont été identifiées dans le contexte du drainage minier à savoir les sulfates de fer, sulfates de calcium, les oxy-hydroxydes de fer, hydroxydes d'aluminium et de manganèse (Acero *et al.*, 2006; Appelo *et al.*, 2002; Bigham *et al.*, 1978; Blesa & Matijević, 1989; Blowes *et al.*, 2003; Blowes *et al.*, 2014; Brown, 1971; Burke & Banwart, 2002; Cornell & Schwertmann, 2004a; Cravotta III, 1994; Cravotta III, 2008a; Davranche & Bollinger, 2000; Egal *et al.*, 2008; Jones *et al.*, 2014; Manceau, 1995; McGregor *et al.*, 2002; McGregor *et al.*, 1998a, 1998b; Moncur *et al.*, 2009; Moncur *et al.*, 2005; Murad *et al.*, 1994; Schwertmann & Cornell, 2007; Sheoran & Sheoran, 2006; Sherman & Randall, 2003; Waychunas *et al.*, 1993; Webster *et al.*, 1998). Les minéraux secondaires qui éraient identifiés dans un contexte d'oxydation des rejets miniers sont : la goethite, l'hématite, la lépidocrocite, les oxy-hydroxydes de fer amorphes, la schwertmannite, la jarosite, la mélantérite et le gypse. Dans les deux sections qui suivent, les oxy-hydroxydes de fer seront discutés lorsqu'ils forment le hardpan en premier lieu et ensuite seront discutés de point de vue mécanismes réactionnels qui peuvent affecter la géochimie du drainage minier.

2.4.2 Mode et effet de formation du hardpan sur le comportement des rejets miniers

2.4.2.1 Formation et minéralogie du hardpan

L'oxydation des sulfures en présence de l'eau et l'oxygène génère de l'acidité qui catalyse la dissolution des carbonates (Blowes *et al.*, 2003). Durant ce processus, d'autres réactions peuvent avoir lieu comme l'hydrolyse et la précipitation dépendamment des conditions géochimiques du milieu (pH, Eh, concentrations en espèces chimiques, etc.). De ce fait, différents minéraux secondaires précipitent et les plus communs sont les oxy-hydroxydes de fer, les sulfates de fer et calcium (Evangelou *et al.*, 1995a; Lapakko, 2002; Maest *et al.*, 2017; Nordstrom *et al.*, 2015). Dans des conditions spécifiques, la précipitation et l'accumulation des minéraux secondaires mènent à un changement de la texture des résidus. En effet, la précipitation des minéraux secondaires diminue la porosité des résidus et change complètement l'assemblage minéralogique. Ce phénomène a été observé au niveau des parcs à résidus inactifs qui renferment des résidus réactifs exposés aux agents météorologiques (McGregor *et al.*, 2002; Meima *et al.*, 2007; Pérez-López *et*

al., 2007; Rammlmair, 2002). La couche formée est appelée hardpan ou horizon induré. La composition minéralogique du hardpan est formée essentiellement de minéraux primaires (sulfures, carbonates) et de minéraux secondaires qui jouent le rôle du ciment pour agglomérer les grains entre eux (Graupner *et al.*, 2007; Holmström *et al.*, 2001; McGregor *et al.*, 2002; Meima *et al.*, 2007; Quispe *et al.*, 2013). Le Tableau 2.4 illustre la composition minéralogique des hardpans étudiés dans la littérature.

Tableau 2.4: Composition minéralogique des hardpans étudiés dans la littérature

Minéralogie du hardpan	Référence
Gypse, jarosite, oxy-hydroxysulfates de fer	Quispe *et al.*, 2013
Jarosite, gypse, oxy-hydroxydes de fer	Graupner *et al.*, 2007
Thermonatrite, calcite,sulfates de sodium, aragonite, gel Si-O, phases amorphes Si-O, burkeite, glasérite, hydroxydes d'aluminium, hématite, magnétite	Meima *et al.*, 2007
Gypse, goethite, Jarosite, sulfures	McGregor *et al.*, 2002
Oxy-hydroxydes de Fe-Mn	Holmström *et al.*, 2001
Ferrihydrite, goethite, lépidocrocite, jarosite, mélantérie, gypse, anglésite	Blowes *et al.*, 1991

2.4.2.2   Effet de la formation du hardpan sur l'infiltration d'eau et la migration d'oxygène

L'occurrence du hardpan au niveau des parcs à résidus peut affecter le comportement géochimique globale des résidus. L'effet du hardpan peut se présenter de différentes manières : i) changer le bilan hydrique, ii) limiter la migration de l'oxygène et diminuer la mobilité des contaminants.

La précipitation et l'accumulation des minéraux secondaires lors de la formation du hardpan réduit la porosité des résidus. De ce fait, la conductivité hydraulique du hardpan est considérée très faible malgré l'absence de mesures quantitatives de sa porosité et/ou de la sa conductivité hydraulique (Blowes *et al.*, 1991; Graupner *et al.*, 2007; McGregor *et al.*, 2002). L'hypothèse de l'imperméabilité du hardpan est basée sur sa micro-texture. En effet, son occurrence comme une couche dure et compacte par comparaison aux résidus miniers, le hardpan semble être très

faiblement perméable. Le hardpan se forme à l'interface de neutralisation ou autrement à la zone de mixage des eaux provenant des résidus oxydés et les eaux interstitielles des résidus frais (saturés en eau). Par conséquence, les lixiviats provenant de la couche de surface ne subissent pas de mélange avec l'eau interstitielle des résidus frais. En général, l'infiltration verticale d'eau est limitée au dépend des ruissellements de surface et de subsurface. Dans le cas où les résidus oxydés présentent un comportement acide, le hardpan empêche la neutralisation de ces lixiviats en profondeur. D'autre part, le hardpan participe à la conservation du potentiel de neutralisation des résidus en profondeur. Alors, la réactivité des parcs à résidus contenant un hardpan est strictement influencée et déterminée par la réactivité des résidus oxydés de surface.

La précipitation des minéraux secondaires (oxy-hydroxydes de fer) à la surface des sulfures mènent à leur passivation (Figure 2.5). La passivation protège les sulfures de l'action de l'oxygène et l'eau (Belzile *et al.*, 1997; Cai *et al.*, 2005; Kang *et al.*, 2016). Ce mécanisme empêche la diffusion de l'oxygène au noyau réactif des sulfures d'une part et d'autre part, la formation du hardpan constitue un écran physique contre la migration de l'oxygène vers les résidus frais en profondeur (Blowes *et al.*, 1991). En effet, Blowes et al. (1991) ont simulé l'effet de la présence du hardpan sur la diffusion de l'oxygène en profondeur à travers des résidus oxydés. Ils ont démontré que la présence du hardpan n'affecte pas seulement les cinétiques de réactions mais aussi le développement du profil d'oxydation. La Figure 2.6 montre que la présence du hardpan empêche la diffusion de l'oxygène en profondeur ce qui limite le profil d'oxydation. Le coefficient de diffusion de l'oxygène à travers le hardpan est estimé être 100 fois plus petit que celui des résidus (Blowes *et al.*, 1991).
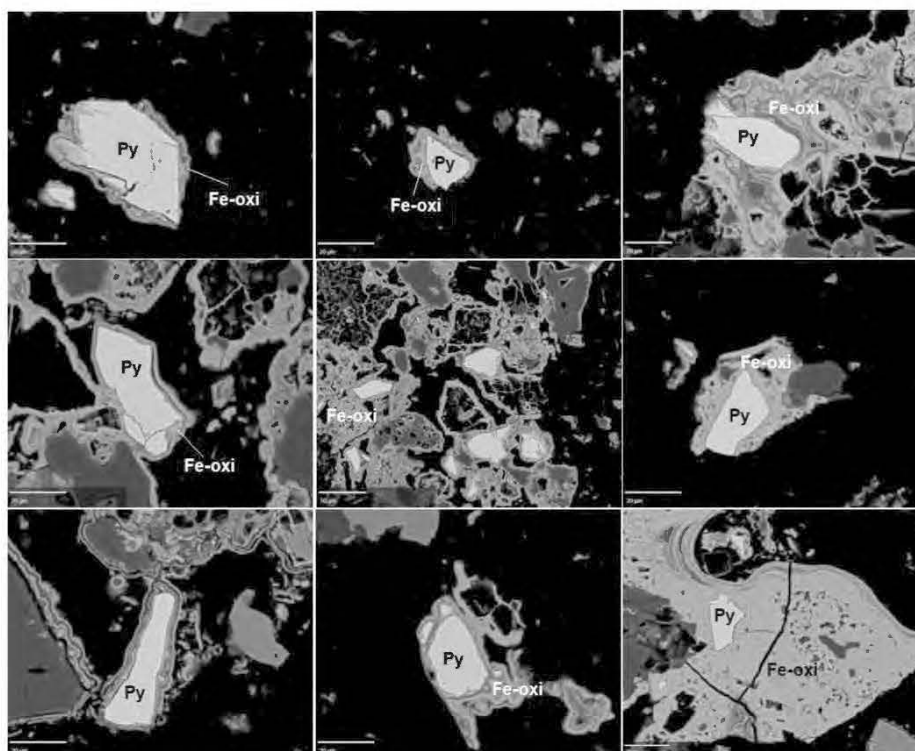
Figure 2.5: Précipitation des oxy-hydroxydes de fer sur les grains de sulfures observés à Joutel
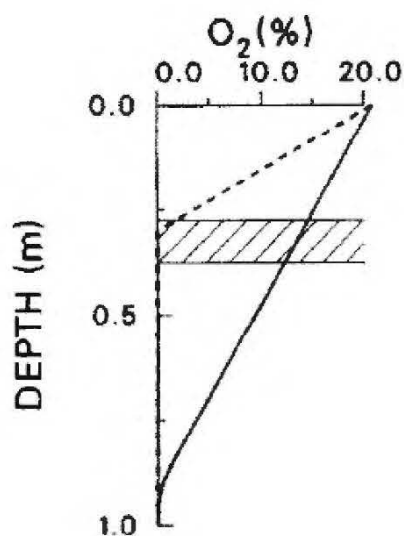
Figure 2.6 : Concentrations d'oxygène vs profondeur prédites utilisant le coefficient d'oxygène (trait continu) et incorporant la présence du hardpan (trait discontinu) (tiré de Blowes et al.,1991)

En plus de l'effet des mécanismes de limiter la migration de l'eau et l'oxygène, le hardpan peut influencer la mobilité des contaminants grâce à aux différents mécanismes liés aux phases

secondaires qui le constituent surtout les oxy-hydroxydes de fer. Les mécanismes réactionnels liés aux oxy-hydroxydes de fer seront discutés à la section suivante.

2.4.3 Mécanismes réactionnels des oxy-hydroxydes de fer

Les oxy-hydroxydes de fer sont les phases secondaires les plus étudiées à cause de leur implication dans la géochimie des eaux du drainage minier. En effet, les oxy-hydroxydes de fer permettent d'atténuer et diminuer la mobilité des métaux lourds lors du processus d'oxydation des rejets miniers. Ces phases secondaires, qui se présentent généralement sous forme d'une matrice ou d'un assemblage de minéraux mal cristallisés, ont une capacité à adsorber, substituer, précipiter et co-précipiter des métaux lors ou après leurs formations. Les différents mécanismes d'atténuation de la mobilité des contaminants sont regroupés sous le nom de la 'sorption' (Plante *et al.*, 2011a). Cependant, les mécanismes réactionnels liés aux oxydes et hydroxydes de fer sont généralement étudiés sur des phases primaires ou synthétiques. Or, dans le contexte du drainage minier les phases secondaires formées sont généralement mal cristallisées, amorphes ou parfois finement cristallisées. Mais, d'une manière générale, ces phases secondaires seront régies par les mêmes lois que les phases primaires ou synthétiques avec des variations au niveau des taux de réactions par exemple. Les mécanismes réactionnels qui seront discutés sont la dissolution et l'adsorption (anionique, cationique et mixte) sachant que plusieurs réactions ont été étudiés mais elles ne feront pas l'objet de cette revue de littérature.

2.4.3.1 Généralités sur les oxydes et hydroxydes de fer

Tout minéral qui consiste en un atome central de Fe entouré d'atomes de O et/ou OH désigne un oxy-hydroxydes de fer. Il existe 15 oxy-hydroxydes connus et décrits dans la en addition des oxy-hydroxydes comme $Fe(OH)_2$, FeO (wustite), $\beta-Fe_2O_3$, $\varepsilon-Fe_2O_3$ et FeOOH de haute pression. Selon leurs abondances, les oxy-hydroxydes majeurs sont présentés dans le

Tableau 2.5. La structure cristalline des oxy-hydroxydes et de toutes les espèces minérales influencent grandement leurs mécanismes réactionnels. Les oxy-hydroxydes de fer diffèrent selon la valence de l'atome de Fe ainsi que la structure cristalline. Tous les oxy-hydroxydes de fer communs contiennent un atome de fer avec une valence +3 à l'exception de la magnétite qui contient les deux valences de fer +2 et +3.

Tableau 2.5: Les oxy-hydroxydes de fer majeurs (tiré de Schwertmann et al., 2007b)

Minéral	Formule chimique	Minéral	Formule chimique
Goethite	$\alpha-FeOOH$	Ferrihydrite	$Fe_5HO_8.4H_2O$
Akaganeite	$\beta-FeOOH$	Hématite	$\alpha-Fe_2O_3$
Lepidocrocite	$\gamma-FeOOH$	Maghemite	$\gamma-Fe_2O_3$
Feroxyhyte	$\sigma'-FeOOH$	Magnétite	Fe_3O_4
Schwertmannite	$Fe_{16}O_{16}(OH)_{12}(SO_4)_2$		

Dans le cas d'une substitution isomère, l'ion central Fe^{3+} peut être substitué par un autre métal sans changement et modification de la structure cristalline de la phase minérale. Le métal substituent doit avoir un rayon atomique proche de celui de l'élément substitué (Fe^{3+}) (Cornell & Schwertmann, 2004b). Dans ce cas de substitution, les solutions solides sont formées entre le pôle du minéral pure et le minéral formé par l'élément substituant. Dans le Tableau 2.6 sont résumés les métaux qui ont été incorporés par succès dans différents oxy-hydroxydes de fer avec leurs rayons ioniques (Cornell *et al.*, 2004b).

Tableau 2.6: Métaux substituants le Fe^{3+} et leurs rayons ioniques (tiré de Cornell et al., 2004b)

Ion	Fe^{2+}	Al^{3+}	Cr^{3+}	Mn^{3+}	V^{3+}	Co^{3+}	Cu^{2+}	Zn^{2+}	Pb^{4+}	Cd^{2+}
Rayon ionique (nm)	0.077	0.053	0.061	0.065	0.064	0.053	0.073	0.075	0.078	0.095

Dans le contexte de l'oxydation des rejets miniers, les oxy-hydroxydes de fer peuvent se précipiter sous forme de goethite ou schwertmannite selon les réactions suivantes (Eq 7, (Eq *8*) :

$$8FeS_2 + 30O_2 + 18H_2O \rightarrow Fe_8O_8(OH)_6SO_4 + 15SO_4^{2-}+ + 30\ H^+ \text{ (schwertmannite)} \qquad (Eq\ 7)$$

$$FeS_2 + 3.75O_2 + 2.5H_2O \rightarrow FeOOH + 2SO_4^{2-}+ + 4H^+ \text{ (goethite)} \qquad (Eq\ 8)$$
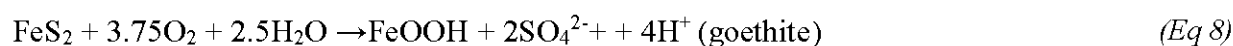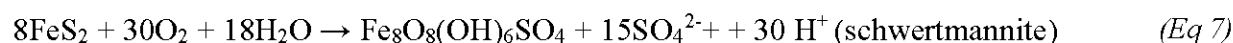
2.4.3.2 Dissolution

Les oxy-hydroxydes de fer sont généralement formés par du fer ferrique, cette forme de fer est stable et immobile (Cornell & Schwertmann, 2004c). De ce fait, les oxy-hydroxydes de fer dans les systèmes naturels sont caractérisés par une faible solubilité. Dans l'industrie minière, les oxy-hydroxydes de fer sont dissouts par une lixiviation à voie acide. (Bloom & Nater, 1991; Casey, 1995) ont étudié la cinétique de dissolution des oxydes et des silicates primaires. La force motrice de la dissolution est l'indice de saturation du milieu vis-à-vis l'oxy-hydroxyde. Les paramètres qui influencent la dissolution des oxy-hydroxydes de fer sont : i) les caractéristiques du milieu (température, pH), ii) les propriétés du solide (surface spécifique, chimie, degré d'altération, cristallinité...) et iii) les propriétés de la phase liquide (pH, Eh, acidité, présence/absence d'agents réducteurs et complexants, etc.). Il n'existe pas de modèle de dissolution des oxy-hydroxydes de fer qui combine tous ces paramètres vu la complexité du système (Blesa & Maroto, 1986; Cornell *et al.*, 2004c). Dans la plupart des cas, seulement l'effet de la surface spécifique du solide et de la composition de la solution sont considérés lors de la dissolution. La réaction de dissolution est difficile à modéliser; lors de ce mécanisme autres réactions peuvent avoir lieu comme l'adsorption. Blesa *et al* (1986) ont conclu que même pour le même oxy-hydroxyde, il n'y a pas de réactivité unique. En effet, la réactivité d'un oxy-hydroxyde de fer peut changer selon les faces du cristal. Ce problème structural est lié à la différence du taux de croissement du cristal selon la face du minéral. En résumé, le pH a une grande influence sur la dissolution des oxy-hydroxydes de fer (Evangelou & Zhang, 1995b). Pour un oxy-hydroxyde de fer bien cristallisé, sa dissolution nécessite une solution avec un pH inférieur à 1 et à une température de 70°C (Cornell *et al.*, 2004c). La solubilité des oxy-hydroxydes de fer est largement influencée par le pH; le minimum de solubilité est observé dans une gamme de pH variant de 7 à 8 (Cornell & Schwertmann, 2004e; Cravotta III, 2008b; Regenspurg *et al.*, 2004). Cette gamme de pH se situe autour du pH de zéro charge (pH$_{pzc}$), alors la solubilité des oxy-hydroxydes de fer va augmenter si le pH s'éloigne du pH$_{pzc}$. Cependant, la solubilité des oxy-hydroxydes de fer dans des pH entre 6 et 9 est incertaine (Cornell *et al.*, 2004e, 2004c). Comme les oxy-hydroxydes sont considérés comme des amphotères, les produits de solubilité changent s'il s'agit d'un milieu acide ou alcalin. Dans des milieux acides, la solubilité des oxy-hydroxydes de fer produit des formes cationiques et des espèces hydroxo. Lors d'une dissolution dans des milieux alcalins, il y a formation des formes anioniques et des espèces hydroxo. La solubilité des oxydes de fer et des hydroxydes métalliques en général est semblable.

la tendance de la solubilité est typique, elle est maximale à des pH acides et basiques et faible à des pH proche de la neutralité (Cravotta III, 2008b). La zone de solubilité minimale peut être déplacée en fonction du métal (Figure 2.7).
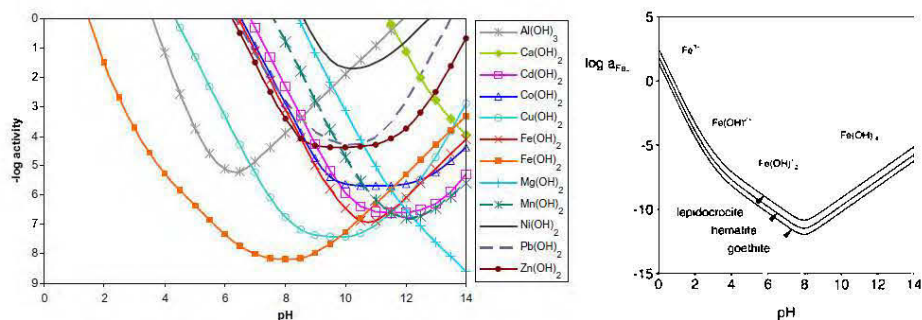
Figure 2.7: Solubilité des hydroxydes métalliques (à gauche) et des oxydes de fer (à droite) (tiré de Cravotta III, 2008 et Regenspurg et al., 2004)

La dissolution des oxy-hydroxydes de fer est une réaction qui produit de l'alcalinité en consommant des protons H^+. Elle peut être assurée par le biais de trois mécanismes à savoir : la protonation, la complexation et la réduction. La protonation consiste à la dissolution du minéral sous action des protons H^+ (Cornell & Schindler, 1987; Cornell *et al.*, 2004c), la complexation consiste à la dissolution du minéral suite à la présence d'un ligand de charge négative qui se complexe avec l'ion Fe pour libérer des ions OH⁻ dans le système (Cornell *et al.*, 2004e; Gledhill & van den Berg, 1994; Rue & Bruland, 1995) et la réduction consiste en la réduction du fer ferrique en fer ferreux.

2.4.3.3 Adsorption des anions et cations

L'adsorption des molécules et des ions par les oxy-hydroxydes de fer influence la mobilité des espèces adsorbées. Le processus d'adsorption implique l'interaction de l'espèce adsorbée (molécules, ions) avec le groupe hydroxyle des oxy-hydroxydes de fer. L'atome donneur d'électrons du groupe hydroxyle peut réagir avec les protons (Cornell & Schwertmann, 2004f), tandis que l'ion métallique sous-jacent agit comme l'acide de Lewis et échange le groupe OH avec d'autres ligands pour former des complexes de surface.

<u>Adsorption des anions</u>

L'adsorption des anions inorganiques, organiques et oxy-anions par les oxy-hydroxydes de fer a été extensivement étudiée. Les anions possèdent un ou plusieurs atomes avec au moins une paire d'électrons libres et peuvent fonctionner comme le donneur dans une liaison de coordination.

L'adsorption des anions sur les oxy-hydroxydes de fer peut être spécifique ou non spécifique. L'adsorption spécifique implique le remplacement du groupe hydroxyle par le ligand adsorbé (Eq 9, (Eq 10) :

$$\equiv FeOH + L^- \leftrightarrow \equiv FeL + OH^- \hspace{4cm} (Eq\ 9)$$

$$\equiv (FeOH)_2 + L^- \leftrightarrow \equiv Fe_2L^+ + 2OH^- \hspace{3cm} (Eq\ 10)$$

L'adsorption spécifique implique une coordination directe de l'anion adsorbé sur la surface de l'oxy-hydroxyde de fer. Il n'existe pas de molécule intermédiaire entre l'anion et la surface d'adsorption; cette relation a un caractère covalent. L'adsorption des anions est majoritairement influencée par le pH et la concentration de l'anion dans le milieu. Pour un pH donné, l'adsorption augmente avec l'augmentation de la concentration des anions dans le milieu. L'adsorption est faible à nulle pour un pH supérieur au pH_{pzc} des oxy-hydroxydes de fer qui varie entre 8 et 9 selon la phase minérale.

Adsorption des cations

L'adsorption des cations peut être aussi spécifique ou non spécifique. Les deux types d'adsorption des cations se diffèrent selon le mode de coordination entre l'espèce adsorbée et la surface des oxy-hydroxyde fer. L'adsorption non spécifique implique la présence d'une molécule d'eau entre l'espèce adsorbée et la surface fonctionnelle de la phase minérale (Schwertmann *et al.*, 2007b). En revanche, l'adsorption spécifique implique une coordination directe entre l'espèce adsorbée et la surface fonctionnelle de l'oxy-hydroxyde de fer. L'adsorption spécifique consiste en une déprotonation du groupe hydroxyle. Le mécanisme d'adsorption spécifique est expliqué par les réactions suivantes (Eq 11, (Eq 12) :

$$\equiv FeOH + Me^{z+} \leftrightarrow \equiv FeOM^{(z-1)+} + H^+ \hspace{3cm} (Eq\ 11)$$

$$\equiv (FeOH)_2 + Me^{z+} \leftrightarrow \equiv (Fe-O)_2M^{(z-2)+} + 2H^+ \hspace{2cm} (Eq\ 12)$$

Plusieurs études expérimentales ont porté sur l'adsorption de différents cations sur différents oxy-hydroxydes de fer (Asta *et al.*, 2009; Cornell *et al.*, 2004f; España *et al.*, 2006; Fukushi *et al.*, 2003; McKenzie, 1980; Schroth & Parnell Jr, 2005). Il est démontré que la goethite est le minéral dans cette catégorie qui est capable d'adsorber la plus large gamme de cations (Ag, Al, Au, Cd, Co, Cr,

Cu, Hg, Mg, Mn, Ni, Np, Pb, Sr, U, Zn). En comparaison, la schwertmannite n'est capable d'adsorber que 3 éléments chimiques (Cd, Cu, Pb). La capacité des oxy-hydroxydes de fer à adsorber les cations est influencée par le domaine de stabilité de chaque minéral ainsi que par leur réseau cristallin. Par exemple, la schwertmannite est métastable vis-à-vis la goethite.

L'adsorption cationique, contrairement à l'adsorption anionique, est accompagnée par une déprotonation du groupe hydroxyle ce qui implique un relargage des protons H^+. Ce mécanisme réactionnel est acidogène. L'adsorption cationique est aussi influencée par la force ionique du milieu et le pH. Une forte activité anionique peut supprimer l'adsorption des cations. La courbe qui décrit l'adsorption d'un métal en fonction du pH est une fonction sigmoïdale. On définit pH_{50} comme la valeur de pH qui correspond à l'adsorption de 50% d'un cation donné. L'adsorption des cations diffère selon l'espèce et l'oxy-hydroxyde adsorbant. Il n'existe pas d'ordre unique de l'adsorption des cations (Cornell *et al.*, 2004f; Kooner, 1993).

<ins>Adsorption dans un système mixte</ins>

L'adsorption anionique ou cationique a été testée par différents auteurs pour des systèmes simples qui contiennent un seul anion/cation. Dans un système qui contient plus d'un cation, il existe une adsorption compétitive entre les cations dépendamment du cation et de son affinité au minéral. Cette compétition est observée lorsque la concentration totale des cations est plus élevée que le nombre de sites vacants sur la surface de l'oxy-hydroxyde de fer. Le Zn supprime l'adsorption du Cd sur la ferrihydrite (Benjamin & Leckie, 1981b). Pour des concentrations égales de Ni et Zn, les deux s'adsorbent indépendamment l'un de l'autre sur la ferrihydrite, mais la présence de Cr^{3+} augmente l'adsorption des deux (Cornell *et al.*, 2004f). Il a été démontré que, dans ce cas, le Cr^{3+} altère les propriétés de surface de l'oxy-hydroxyde de fer.

L'adsorption des anions est aussi compétitive lors de la présence de plusieurs anions dans le système. Les phosphates empêchent l'adsorption des arséniates et des sélénites sur la goethite (Cornell *et al.*, 2004f; Hingston *et al.*, 1971). Ceci est significatif lorsque les phosphates sont présents en grandes concentrations dans le système. Les phosphates favorisent aussi la désorption des sulfates adsorbés (Liu & Millero, 1999). Les anions de phosphates sont aussi désorbés en présence d'acide citrique. Les ions OH^- sont connus comme des anions qui participent à l'adsorption compétitive à cause de leurs positions dans la couche intérieure de Helmholtz. Par ailleurs, dans un système qui contient des anions et des cations, l'adsorption est compétitive entre

les deux espèces. La présence des ions OH⁻ en concentrations élevées empêche l'adsorption d'Al. Dans ce cas, l'Al se trouve sous forme d'un complexe dans le système. De même, l'adsorption de l'arsenic sur la ferrihydrite est réduite par la présence des carbonates et des silicates dans le système (Appelo et al., 2002). Par contre, la présence des anions augmente parfois l'adsorption des cations suite à la formation complexes de surface selon les réactions suivantes (Eq 13(Eq 14) (Cornell *et al.*, 2004f) :

$$\equiv FeOH + L^- + M^{z+} \leftrightarrow \equiv FeOML^{(z-2)+} + H^+ \qquad (Eq\ 13)$$

$$\equiv FeOH + M^{z+} + L^- \leftrightarrow \equiv FeLM^{z+} + OH^- \qquad (Eq\ 14)$$

Lors d'une adsorption simultanée d'un cation et d'un anion, il existe deux modes de coordination : i) coordination du métal sur la surface de l'oxy-hydroxyde de fer et ii) coordination indirecte du cation sur la surface d'un pont polydenté formé par l'adsorption de l'anion sur la surface de l'oxy-hydroxyde de fer. Davis & Leckie (1978) ont étudié l'effet de différentes concentrations des thiosulfates sur l'adsorption de l'Ag en fonction du pH. Pour des pH inférieurs à 6, l'adsorption de l'Ag sur la ferrihydrite est augmentée avec l'augmentation de la concentration des thiosulfates. Cependant pour des pH plus basiques (supérieur à 7), l'augmentation des concentrations des thiosulfates empêchent l'adsorption de l'Ag (Davis & Leckie, 1978). En conclusion, la présence des anions change le comportement et les conditions d'adsorption des cations. L'adsorption dans un système mixte est le cas le plus proche du contexte minier. En effet lors de l'oxydation des rejets miniers, plusieurs anions (sulfates) et cations (calcium) sont libérés dans le système.

2.5 Stabilisation des résidus miniers générateurs d'acide par amendements alcalins et cimentaires

2.5.1 Introduction

L'oxydation des sulfures contenus dans les rejets miniers peut générer du drainage minier acide et des concentrations non-négligeables en contaminants. La prévention de la génération d'acide peut se faire en agissant au niveau de l'une des composantes de l'oxydation des sulfures (sulfures, eau, oxygène). Les techniques de stabilisation/solidification (S/S) sont souvent utilisées avec succès pour la décontamination et la stabilisation des sols pollués ainsi que les déchets industriels

(Kogbara & Al-Tabbaa, 2011a; Kogbara *et al.*, 2011b; Wang *et al.*, 2018; Wang *et al.*, 2015b). Dans le domaine minier, cette technique est souvent restée au stade expérimental malgré l'engouement grandissant envers cette pratique. L'objectif principal des techniques de S/S est de fixer les contaminants dans une matrice monolithique ce qui entraine la réduction de la lixiviation des contaminants et la neutralisation de l'éventuelle acidité produite. Les mécanismes impliqués durant les techniques de stabilisation et solidification diffèrent selon la technique utilisée ce qui en engendre plusieurs variantes au niveau pratique. Ci-dessous, on en citera deux catégories.

2.5.2 Amendements alcalins

Les amendements alcalins consistent en l'ajout d'un ou plusieurs additifs neutralisants à des résidus miniers générateurs d'acide pour augmenter leur pouvoir de neutralisation ce qui permet de contrer l'acidité produite par l'oxydation des sulfures. Ce procédé est très souvent appliqué pour des sites miniers avant de procéder à une réhabilitation. Différents matériaux et sous-produits industriels ont été utilisés avec succès pour stabiliser des sols contaminés et aussi des résidus miniers générateurs d'acide (Alkattan *et al.*, 1998; Doye *et al.*, 2003; Duchesne & Reardon, 1998; Holmström *et al.*, 1999; Komnitsas *et al.*, 2004; Mylona *et al.*, 2000; Rodríguez *et al.*, 2018). La chaux et les calcaires sont parmi les additifs les plus utilisés dans la catégorie des amendements alcalins. Un amendement alcalin peut être appliqué de deux manières : i) par mélange qui consiste à mélanger les ajouts alcalins avec les résidus problématiques à des dosages prédéfinis, ii) ou par épandage, qui consiste à l'ajout des amendements comme une couche au-dessus des résidus miniers. La formule proposée pour le calcul de l'ajout d'un amendement alcalin est présentée dans le chapitre 8 et dépend du PN et du PA du résidu et de l'amendement. Dans le cas des résidus miniers générateurs d'acide, l'ajout d'un agent neutralisant permit de tamponner l'acidité produite et diminuer la mobilité des contaminants suite à des mécanismes chimiques (Alkattan *et al.*, 1998; Deschamps *et al.*, 2009; Doye *et al.*, 2003; Fatahi *et al.*, 2015; Forján *et al.*, 2014; Holmström *et al.*, 1999). En effet, la dissolution des neutralisants dans des conditions acides permet d'augmenter l'alcalinité du milieu et tamponne le pH. En général, dans des conditions proches de la neutralité, la mobilité de nombreux éléments chimiques (incluant la plupart des métaux) devient faible et leur solubilité est minimale (Cravotta III, 2008a, 2008b; Doye *et al.*, 2003; Fleri & Whetstone, 2007). De plus, dans ces conditions, plusieurs phases secondaires sont précipitées, ce qui permet de réduire la mobilité des espèces chimiques. Les processus chimiques impliqués après ajout d'amendements alcalins

sont :i) la précipitation (co-précipitation, adsorption, etc.) des oxy-hydroxydes de fer qui permet d'atténuer les concentrations des métaux et métalloïdes comme le plomb et l'arsenic (Cornell *et al.*, 2004a; Coston *et al.*, 1995; España *et al.*, 2006; Fendorf & Fendorf, 1996; Fukushi *et al.*, 2003; Giménez *et al.*, 2007; Jönsson *et al.*, 2005) et ii) la passivation des sulfures : la précipitation des phases secondaires à leur surface réduit leurs disponibilités à réagir avec l'eau et l'oxygène, ce qui entraine une diminution des taux d'oxydation des sulfures, et enfin iii) diminuer l'activité bactérienne (bactéries acidophiles) dans des conditions proches de la neutralité (Evangelou *et al.*, 1995a; NEDEM, 1997; Nordstrom *et al.*, 1997).

2.5.3 Amendements cimentaires

Par comparaison aux amendements alcalins, les amendements cimentaires consistent en l'ajout d'additifs cimentaires (ciments conventionnels ou alternatifs à base de sous-produits industriels). Ils permettent de modifier la texture du résidu minier en question en une matrice monolithique. Ils permettent aussi d'augmenter le pouvoir de neutralisation des résidus comme les amendements alcalins en plus de modifier la cohésion et la perméabilité du composite final. Ils sont généralement utilisés comme méthode efficace pour la solidification et la stabilisation *in-situ* des sols et déchets industriels contaminés (Duchesne & Laforest, 2006; Ichrak *et al.*, 2016; Nehdi & Tariq, 2007; Wang *et al.*, 2015b). Le ciment Portland est l'additif le plus utilisé à cet effet mais, parfois, il a été substitué par des sous-produits industriels à caractère hydraulique et/ou pozzolanique comme les cendres volantes de la combustion du charbon et de la biomasse dans les centrales thermiques (Benzaazoua *et al.*, 2008; Benzaazoua *et al.*, 1999; Criado *et al.*, 2007; Kogbara *et al.*, 2011a; Kogbara *et al.*, 2011b; Nehdi *et al.*, 2007; Rodríguez *et al.*, 2018; Tariq & Yanful, 2013; Wang *et al.*, 2018; Wang *et al.*, 2015b). Ceci permet de réduire le coût lié à l'utilisation du ciment et valoriser les déchets d'autres industries. Les contaminants sont stabilisés lors de ce processus grâce à différents mécanismes : i) le piégeage physique des contaminants lors de l'hydratation du liant, ii) la réduction de la surface réactive du résidu, iii) l'augmentation de la cohésion et de la résistance du résidu ce qui permet de développer une imperméabilité à long terme et enfin iv) la sorption des contaminants lors de la précipitation des minéraux secondaires (Benzaazoua *et al.*, 2004b; Deschamps *et al.*, 2009; Nehdi *et al.*, 2007; Tariq *et al.*, 2013; Wang *et al.*, 2018; Wang *et al.*, 2015b).

2.6 Besoins en recherche, hypothèses et objectifs de recherche

Ce doctorat a pour objectif de pousser la recherche en ce qui concerne l'effet de la libération minérale sur la réactivité des rejets miniers. Au lieu de tester l'effet de la granulométrie (Erguler *et al.*, 2015), ce doctorat vise à quantifier l'effet de la libération minérale. Par ailleurs, la prédiction du comportement environnemental des résidus miniers incertains est basée sur des essais cinétiques au laboratoire qui peuvent parfaitement prédire le type du comportement environnemental des résidus miniers *in-situ*. Cependant, dans des conditions spécifiques, les essais de laboratoire peuvent complètement rater la prédiction environnementale; il s'agit de la précipitation et l'accumulation des oxy-hydroxydes comme phases minérales ou encore comme hardpan. Par conséquent, l'effet de libération minérale est testé au niveau des stériles miniers et l'effet des oxy-hydroxydes de fer est étudié au niveau des résidus miniers.

Actuellement, la gestion des stériles miniers produit en grandes quantités lors des exploitations à ciel ouvert est assez complexe à cause du coût lié à la gestion des haldes à stériles. Dans ces haldes, les stériles, dont la taille varie de quelques microns à des blocs métriques, sont entreposés ensemble. En général, dans tels matériaux, la fraction fine est celle responsable de la réactivité globale de la halde à stériles. La première réflexion de ce travail était de se poser de question sur la possibilité de séparer les stériles en deux fractions distinctes en termes de leurs réactivités pour diminuer les coûts liés à la gestion de la fraction problématique. Par conséquent, l'objectif principal de cette première partie de thèse est de définir une taille des particules pour laquelle la réactivité des sulfures devienne négligeable. En effet, un nouveau paramètre sera défini et appelé diamètre d'encapsulation physique des sulfures (DPLS). Ce diamètre correspond à une granulométrie des stériles au-dessus de laquelle les sulfures sont presque entièrement encapsulés dans une matrice de gangue silicatée. Alors, comme hypothèse, on admit que le degré de libération des sulfures et des carbonates sera inversement corrélé à la taille des particules. De plus, si les sulfures sont encapsulés dans une matrice silicatée, ils vont être protégés contre l'action de l'eau et de l'oxygène (oxydation). Ces hypothèses seront vérifiées moyennant une étude minéralogique et géochimique détaillée réalisée au niveau de trois lithologies de stériles miniers. À la lumière de résultats de cette partie, un protocole de caractérisation des stériles sera proposé. Il s'agit d'une méthodologie de caractérisation valable pour tout type de stériles et lithologies. Ce guide de caractérisation va

essentiellement différencier entre le PN et le PA totaux d'un échantillon et le PA et PN disponibles du même échantillon.

Les résidus miniers qui contiennent des sulfures et des carbonates disponibles vont réagir sous l'action de l'eau et de l'oxygène atmosphérique. Ces réactions d'oxydation/neutralisation mènent à d'autres réactions de précipitation de minéraux secondaires. Le taux de précipitation de ces minéraux secondaires dépend essentiellement de la quantité initiale des sulfures et des carbonates, de leurs réactivités et des mouvements d'eau. Les essais cinétiques sont utilisés pour prédire le comportement des rejets miniers pour bien se préparer lors de la planification et du design du scénario de restauration. Sous certaines conditions, les essais cinétiques ne réussissent pas la prédiction du comportement environnemental des rejets miniers. La formation du hardpan et des oxy-hydroxydes de fer est l'un des phénomènes qui peut influencer complètement la prédiction environnementale basée sur des essais cinétiques de laboratoire. L'hypothèse à ce niveau se base sur l'imperméabilité du hardpan, donc son occurrence dans les parcs à résidus change le bilan d'eau et, ensuite, le comportement géochimique global des résidus miniers *in-situ*. De plus, à l'état oxydé des résidus miniers, une acidité résiduelle et une acidité liée à la dissolution des oxy-hydroxydes de fer pourra être générée, même après épuisement des sulfures. Ces hypothèses seront vérifiées à l'aide d'essais cinétiques et des caractérisations pluridisciplinaires sur des résidus miniers oxydés, frais et des échantillons de hardpan. Finalement, les amendements alcalins par ajout de calcaire (5 et 10 wt.%) et les amendements cimentaires (5 wt.% liant) seront testés comme techniques de stabilisation des résidus oxydés générateurs d'acide. L'efficacité de ces amendements sera testée moyennant des cellules de terrain qui permettent de tester un scénario en conditions réelles (température, ratio L/S, humidité, gel-dégel, conditions biologiques, etc.).

CHAPITRE 3   ARTICLE 1: DETERMINATION OF THE AVAILABLE ACID GENERATING POTENTIAL OF WASTE ROCKS, PART I: MINERALOGICAL APPROACH

A. Elghali[1], M. Benzaazoua[1], H. Bouzahzah[2], B. Bussière[1], H. Villarraga-Gómez[3]

[1] Université du Québec en Abitibi Témiscamingue, 445 Boul. Université, Rouyn-Noranda, Qc, J9X 5E4, Canada

[2] Université de Liège, Génie minéral, matériaux et environnement. Allée de la découverte, 13/A. Bât. B52/3 Sart-Tilman, 4000 Liège, Belgique

[3] Nikon Metrology, 12701 Grand River Ave., Brighton, MI 48116, USA

3.1 Abstract

Significant volumes of waste rock are produced in mining operations, particularly in open pit operations. Waste rock is characterized by a high heterogeneity in their mineralogical, hydrogeological, and physical properties, especially in comparison to tailings. The purpose of this study was to develop an improved method to quantify the net acid-generating potential of waste rock by incorporating the degree of liberation of acid-generating and neutralizing minerals. Three lithologies were sampled immediately after waste rock blasting. Each lithology was separated into seven fractions: D < 0.053 mm, 0.053 mm < D < 0.3 mm, 0.3 mm < D < 0.85 mm, 0.85 mm < D < 2.4 mm, 2.4 mm < D < 5 mm, 5 mm < D < 15 mm, 15 mm < D < 50 mm; particles > 5 cm were not considered. Mineralogical and chemical characterizations showed that sulphides, mainly pyrite, were enriched in the fine to mid-sized fractions (between 0.053 mm and 0.85 mm), and carbonates, mainly calcite, decreased as the particle size increased. Sulphides were more liberated within the fine fractions and their liberation was considered negligible at sizes > 2.4 mm. For coarser fractions (> 5 mm), sulphides were associated with non-sulphide gangue minerals which was confirmed by micro-computed tomography. The waste rock samples were submitted to both acid base accounting (ABA) and net acid generation (NAG) tests to evaluate their acid-generating potentials. Sixteen size fractions were non-acid generating and five were classified as uncertain. However, standard ABA and NAG tests are based on pulverized samples that don't consider the initial textures of

samples. Therefore, ABA results (acid-generating potentials and neutralization potentials) were corrected using the degrees of sulphide and carbonate liberation. The corrected classifications reduced the acid-generating potential of most of the uncertain samples due to the high carbonates content in relation to sulphides. This study also defines a parameter, the diameter of physical locking of sulphides, that can be used to separate waste rock into a reactive and non-reactive fraction based on the relationship between sulphide liberation and particle-size fraction. The reactive fraction refers to waste rock likely to require active acid rock drainage (ARD) management, whereas non-reactive fraction refers to waste rock likely not require active management.

Keywords: waste rocks, acid mine drainage, mineral liberation, diameter of physical locking of sulphides, computed tomography, QEMSCAN®.

3.2 Introduction

Mining operations around the world generate significant volumes of waste rock and tailings. Tailings, which are the solid waste product of ore processing, are characterized by relatively homogeneous particle-size distributions (Bussière, 2007). However, waste rock, which is the non-economic rocks that are extracted to access to an ore body, are more physically, chemically, and hydrogeologically heterogeneous (Amos et al., 2015; Aubertin et al., 2002; Blowes et al., 2003; Erguler & Kalyoncu Erguler, 2015; Lahmira et al., 2015). Waste rock often contain sulphide minerals that, when exposed to water and atmospheric oxygen, can oxidize and release acid, metals, and sulphate. This process can lead to the formation of acid mine drainage (AMD) if the material does not contain enough neutralizing minerals to buffer acidic drainages (Benzaazoua et al., 2004).

The generation of AMD depends on the types of sulphide and carbonate minerals present, as well as the dissolution rates of these minerals, which can be highly variable (Blowes et al., 2003; Blowes et al., 2014; Blowes et al., 1994; Blowes et al., 2013; Paktunc, 1999a; Paktunc & Davé, 2000a; Paktunc, 1999b; Paktunc & Dave, 2000b). The rate of acid generation in waste rock is controlled by their intrinsic physical and mineralogical properties, as well as by other external factors (Blowes et al., 2003; Parbhakar-Fox & Lottermoser, 2015). Sulphide oxidation rates are influenced by factors including: i) mineralogy, ii) temperature, iii) dissolved oxygen concentrations, iv) pH, v) chemical activity of ferrous iron, and vi) bacterial activity (Blowes et al., 2003; Bouzahzah et al., 2013; Evangelou & Zhang, 1995; Nordstrom, 2000; Nordstrom et al., 2015; Nordstrom &

Southam, 1997; Olson, 1991; Rimstidt & Vaughan, 2003). Carbonate dissolution rates are primarily influenced by the mineral reactivity and pH. Several studies also suggest that specific surface area and the degree of liberation are highly important factors controlling the rates of sulphide oxidation and carbonate dissolution (Barazzoul et al., 2012; Benzaazoua et al., 2017; Blowes et al., 2003; Brough et al., 2017; Buckwalter-Davis et al.; Erguler et al., 2015; Lapakko et al., 2006; Parbhakar-Fox et al., 2011). The degree of mineral liberation is commonly used in ore grinding and processing (especially in flotation) to quantify the proportion of a mineral that could be recovered (Benzaazoua et al., 2017; Petruk, 2000; Petruk & Lastra, 1993), however, it is currently not as commonly used in assessments of the environmental behavior of mine wastes.

The environmental behavior of waste rock is usually assessed before and/or during mining operations through static and kinetic tests (Plante et al., 2011; Price et al., 1997; Sapsford et al., 2009; Villeneuve, 2006; White III et al., 1999). The primary objective of these tests is to predict the onset of AMD and determine the contaminant leaching potential of a material so that appropriate waste management plans can be developed. Static tests, or acid-base accounting, are designed to determine the acid-generating potential (AP) and neutralization potential (NP) of finely pulverized samples (Bouzahzah et al., 2014; Bouzahzah et al., 2015; Chotpantarat, 2011; Kwong & Ferguson, 1997; Lapakko & Lawrence, 2009; Miller et al., 1997). In contrast, kinetic tests are used to assess metal leaching potential and estimate the time before AMD generation (Benzaazoua et al., 2004; Maest & Nordstrom, 2017).

Sampling is the first step in static and kinetic testing, but it can be challenging due to the large particle-size distributions of waste rock. In fact, waste rock particles often vary from a few millimeters to several meters in the case of hard rock mines. Different particle sizes are recommended depending on the test being performed. For static tests, Smart et al. (2002) suggest that the particle size of the sample must be less than 4 mm, while Lapakko (2003) suggests that the sample must be less than 6.3 mm, and Smith et al. (2000) recommends considering only particles less than 2 mm because these grains are more available for reactions. This may make it necessary to pulverize samples or to choose a specific particle-size fraction in order to achieve a representative sample and satisfy the requirements of static (Bouzahzah et al., 2015; Lawrence & Wang, 1997; Paktunc, 1999a; Sobek et al., 1978) and kinetics tests (Lapakko, 2003). However, reducing a sample's particle-size distribution by pulverization increases its specific surface area and increases the degree of liberation of the sulphides and carbonates. Therefore, the NP of

pulverized samples will be overestimated due to sample fragmentation if sulphides are not subject to the same degree of fragmentation, as would the case if carbonates or sulphides were preferentially distributed in the size fractions represented by the pulps.

This study investigates the influence of particle size of waste rock and degree of sulphide and carbonate liberation on the geochemistry of mine drainages. Three lithologies were sampled from an open pit mine in Abitibi, Western Québec, Canada, and separated into seven particle-size fractions to carefully identify variations in the chemical, mineralogical, and textural properties of each fraction. Based on these data, a new parameter is suggested to describe sulphide reactivity in freshly blasted waste rock: the diameter of physical locking of sulphides (DPLS). Initially introduced by Smith et al. (2000) for use in a waste rock sampling strategy, the DPLS refers to a particle size above which sulphides are locked by non-sulphide gangue (NSG) minerals and are unreactive for AMD assessment purposes. The DPLS is site- and lithology-specific, and its determination must be confirmed using kinetic tests (e.g. column tests); this will be discussed in a companion paper.

3.3 Materials and methods

This section describes the methods used during field sampling, material preparation, material characterization, and static testing in order to determine the AP and NP of the three studied waste rock lithologies. The methods used in this study are summarized in Figure 3.1.
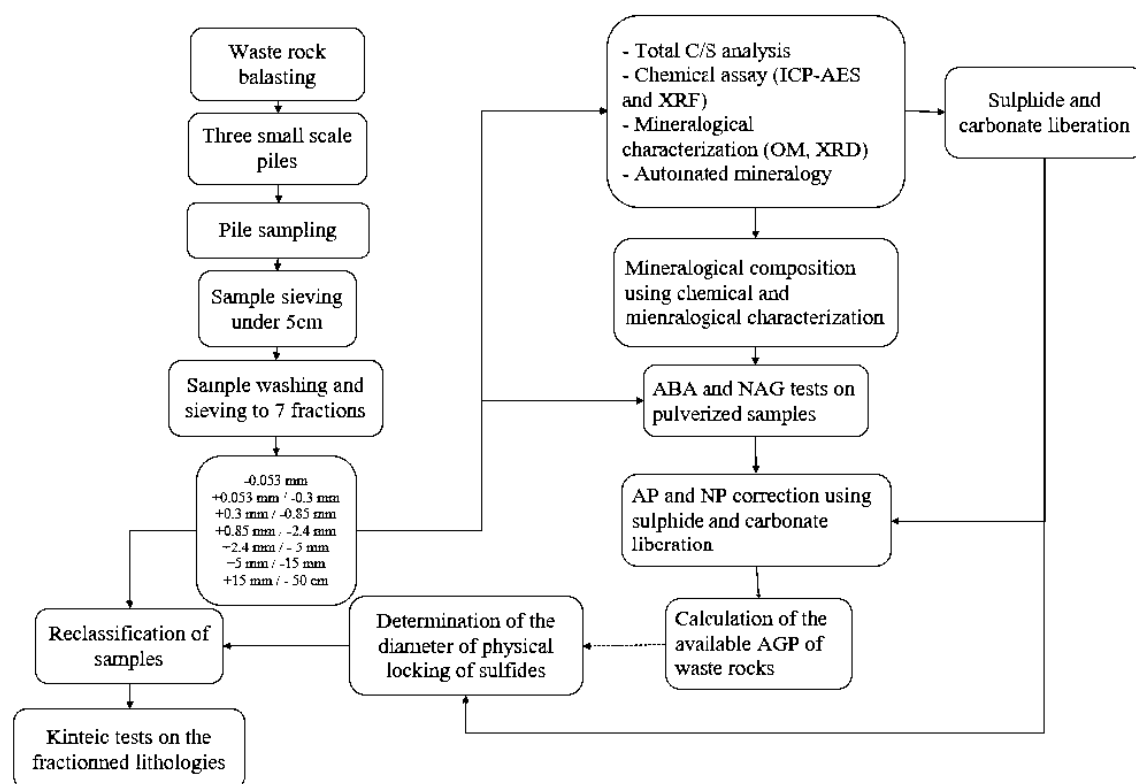
Figure 3.1: Waste rock characterization for better AP determination.

3.3.1 Field site, sampling, and material preparation

The deposit from which the three lithologies used in this study were sampled is an Archean gold porphyry system consisting of an extended area of disseminated gold and pyrite mineralization within a dioritic porphyry and altered metasediments. The geology of the deposit is largely defined by the metasedimentary units. These units are intersected by several epizonal to mesozonal felsic porphyry intrusions defined as syenites, quartzic syenites, quartzic monzonites, and granodiorites. The geometry of the felsic intrusions is highly variable. The mineralization forms a continuous envelope of 1 to 5% pyrite, disseminated with fine native gold (less than 20 microns) and traces of chalcopyrite and sphalerite (Helt *et al.*, 2014). The mineralization is mainly hosted by altered clastic sediments (greywacke, mudstone, and some siltstone) found over an epizonal porphyry diorite intrusion. The waste rocks lithologies within the mineralization are represented as greywackes and porphyry. For this study, the three most common lithologies, which comprise more than 50% of the ore body, were sampled. These were: carbonated porphyry, altered greywackes,

and carbonated greywackes. These lithologies have undergone potassic, silicic, and carbonate alteration (Helt *et al.*, 2014).

Small-scale piles of each lithology (> 100 tonnes) were built immediately after blasting. This allowed for obtaining realistic particle sizes during sampling, whereas other widely used approaches, such as core sampling or local sampling in the waste rocks dump, can alter particle-size distributions. Samples collected from the small-scale piles in October 2015 were sieved onsite (D < 5 cm) and shipped to the lab for further preparation and characterization. In this study 50 mm was the maximum particle size considered.

In the laboratory, the three waste rocks lithologies samples were homogenized separately using a quartage method. The manual quarting was repeated several times to ensure homogenity and representativeness of samples. Each lithology was then divided into seven particle-size fractions:

- Fraction 1 (F1): D < 0.053 mm

- Fraction 2 (F2): 0.053 mm < D < 0.3 mm

- Fraction 3 (F3): 0.3 mm < D < 0.85 mm

- Fraction 4 (F4): 0.85 mm < D < 2.4 mm

- Fraction 5 (F5): 2.4 mm < D < 5 mm

- Fraction 6 (F6): 5 mm < D < 15 mm

- Fraction 7 (F7): 15 mm < D < 50 mm

The coarse fractions were washed to remove fine particles that were attached to the particles' surfaces.

3.3.2 Material characterization

3.3.2.1 Physical and chemical analyses

The particle-size distribution of each lithology was determined by sieving at the following sizes: 0.053 mm, 0.3 mm, 0.85 mm, 2.4 mm, 5 mm, 15 mm and 50 mm (ASTM, 2014). Field particle size determinations were performed using a mechanical screener equipped with a conveyor and a screen (Figure 2S).

Samples were homogenized and pulverized prior to performing all chemical analyses. The bulk chemical composition of samples was determined by ICP-AES (Perkin Elmer Optima 3100 RL) following a complete digestion with $HNO_3/Br_2/HF/HCl$. Detection limits for each analyte by ICP-AES are presented in Table 1S. Total sulfur and inorganic carbon content were analyzed by induction furnace (ELTRA CS-2000; detection limit = 0.09%).

3.3.2.2   Mineralogical analyses

The mineralogical composition of the waste rocks was studied by XRD using a Bruker AXS D8 Advance X-ray diffractometer equipped with a copper anticathode, scanning over a diffraction angle (2θ) ranging from 5° to 70°. Scan settings were 0.005° 2θ step size and 4-s counting time per step. The DiffracPlus EVA software (v.9.0 rel. 2003) was used to identify mineral species and the TOPAS software (v 2.2) implementing Rietveld refinement was used to quantify the abundance of all identified mineral species. The detection limit of this quantification method depends on samples properties; it generally ranges from 1-5%. Approximately 2 g of pulverized solid sample were micronized with isopropanol for 10 to 15 min to achieve a particle size < 10 μm. The samples were dried under ambient temperature; then the samples were carefully packed in sample holders.

Each sample (size fraction < 5 mm) corresponding to the three sample lithologies was sized by wet screening to produce particle-size F1-F5. The number of polished sections prepared for each particle size fraction was determined such that there would be good statistical representation; more than 10000 grains were analyzed in fine fractions. The number of polished sections analyzed were 4, 3, 2, 2, and 1 for fractions F5, F4, F3, F2, and F1, respectively. Polished sections for each waste rock lithology were prepared and observed using optical microscopy in reflected light mode. Mineralogy was investigated using QEMSCAN (Mackay *et al.*, 2016). A total of twelve polished sections for each waste rock sample were analyzed using QEMSCAN, which is an automated, quantitative SEM-based tool specifically designed to rapidly analyze the mineralogical composition of samples based on their chemical composition at the micrometer-scale. The corresponding data enabled quantification of the modal mineralogy, mineral textures, grain size, elemental deportment, and mineral liberation of the analyzed samples (Benzaazoua *et al.*, 2017b; Butcher *et al.*, 2000; Pirrie *et al.*, 2004). The polished sections were also analyzed by PMA mode

(particle mineralogy analysis). The measurement resolution varied from 2.5 μm to 6 μm depending on the sample's particle size fraction.

Mineralogical reconciliation consisted of changing mineralogical compositions in order to overlay the results of the chemical assays with the theoretical chemical compositions of the identified minerals. The identification of major and minor phases was achieved using the results of XRD, QEMSCAN, and optical microscope analyses. The average chemical composition was calculated based on data from ICP-AES and XRF analyses. Then, the theoretical chemical composition was calculated based on the stoichiometries of the identified minerals. The theoretical chemical composition was compared to the analyzed chemical composition (ICP-AES for metals, XRF for minor and major elements and induction furnace for total S/C). If the relative difference between the theoretical and observed chemical compositions was greater than 5%, iterations were performed using an excel solver that essentially changed the percentages of the minerals (using a nonlinear generalized reduced gradient; GRG) until the relative difference between the theoretical and observed chemical compositions was less than 5% (Lasdon et al., 1974; Yeniay, 2005). The nonlinear GRG method consisted of solving the matrix presented in supplementary materials.

3.3.2.3 Micro computed tomography

For the composite fraction F6 and F7 for each lithology type, samples were scanned by X-ray computed tomography (X-ray CT) using an XTH 225 ST system (Nikon Metrology). X-ray CT is a non-destructive technique with wide applications in geological disciplines and materials science (Cnudde et al., 2006; Maire & Withers, 2014; Mees et al., 2003a; Stock, 2008a). Figure 3S shows the full X-ray CT process, which consists of scanning a specimen using X-rays, then using the contrast in the projected images, which is generated by differences in X-ray attenuation that arise principally from differences in density within the sample, to produce a 3D reconstruction. After generating a reconstruction, the data can be used to produce qualitative or quantitative analyses of both the interior and exterior of the specimen. Quantitative analysis can be obtained as well as localization of structural material inclusions and identification of pores that are not usually visible through traditional non-destructive methods. The > 5 mm fraction was selected for each lithology using rotary rifle divider. Each sample was filled in a cylindrical polystyrene mold (100 mm × 200 mm). The number of projections taken per CT scan was 2880 radiographs over a

full 360° rotation, which means that each radiograph was taken at step of 0.125°. All 2880 radiographs were used for the 3D reconstruction. The exposure time for each radiograph was about 0.708 seconds and the voxel size resolution was 70 μm. The number of analyzed particles was 34764, 37764, and 71752 for the carbonated porphyry, altered greywacke and carbonated greywacke lithologies, respectively.

3.3.2.4 Acid generation potential assessment

The acid generation potential (AGP) was determined for each sample using the Sobek *et al* (1978a) ABA test modified by Bouzahzah *et al* (2015), and the single-addition NAG test (Stewart *et al.*, 2006). The net neutralization potential (NNP) was calculated by subtracting the AP from the NP (with values expressed in kilograms of $CaCO_3$ equivalent per tonne of sample) (Miller *et al.*, 1991a; Weber *et al.*, 2004). When the NNP value was higher than 20 kg $CaCO_3$/t, the sample was considered non-acid-generating; when the NNP was lower than -20 kg $CaCO_3$/t, the sample was considered acid-generating; and when the NNP was between -20 kg and 20 kg $CaCO_3$/t, the AGP was considered to be uncertain (Bouzahzah *et al.*, 2015a; Miller *et al.*, 1991b; Morin *et al.*, 1994). The AGP of each sample was also classified using the neutralization potential ratio (NPR), in which the NP of a sample is divided by the AP. Samples were considered acid-generating when the NPR was less than 1, non-acid-generating when the NPR was greater than 2, and uncertain when the NPR was between 1 and 2. The three lithologies were analyzed in duplicate with the NAG tests. The relative percent difference between the two pH values obtained by these tests was 1.04%, 1.60%, and 3.24% for the three lithologies carbonated porphyry, altered greywacke and carbonated greywacke, respectively.

Only the results of the ABA tests were corrected using the degree of carbonate and sulphide liberation, which considered the initial texture of the studied materials. To perform these corrections, the NP values were multiplied by the degree of carbonate liberation, and the AP values were multiplied by the degree of sulphide liberation, as shown in the following equations:

$$NP = 83.3 \times C \text{ (wt.\%)} \times L_c \text{ (kg CaCO3/t)}$$

$$AP = 31.25 \times S_{sulphides} \text{ (wt.\%)} \times L_s \text{ (kg CaCO3/t)}$$

where: L_c and L_s are the degree of liberation for carbonates and sulphides, respectively; and C and $S_{sulphides}$ are the wt. % of carbonates and sulphides, respectively. Values of L_c and L_s were obtained using QEMSCAN.

3.4 Results and discussion

3.4.1 Physical and chemical characteristics

The specific surface area is related to the particle-size distribution and determines the reactivity of a sample (Erguler *et al.*, 2015; Kalyoncu Erguler *et al.*, 2014). Ergüler *et al.* (2015) evaluated the time until acid generation (i.e., the lag time) for samples with different particle-size distributions. Their results showed that, for potentially acid-generating samples, the coarser the sample, the longer the lag time. This means that, considering chemicaly identical samples, the environmental behavior will depend on the particle-size distribution. As shown in Table 3.1, the particle-size distributions of the three lithologies used in this study are relatively similar. The fine particles represent a low proportion of the total sample mass. Considering 1 m as the maximum grain size, particle sizes less than 10 cm comprised 23, 42, and 50 wt.% of the carbonated porphyry, carbonated greywacke, and altered greywacke samples, respectively. Considering 5 cm as the maximum particle size, the D_{90} was 42 mm, 40 mm, and 40 mm for the carbonated porphyry, altered greywacke, and carbonated greywacke lithologies, respectively (Table 3.1).

Table 3.1: Particle-size distribution of the three lithologies.

	Grain size distribution					
	Laboratory grain size distribution to 5cm				Field grain size distribution up to 1m	
					% mass	
Sample	D_{10} (mm)	D_{30} (mm)	D_{50} (mm)	D_{90} (mm)	- 10 cm	+ 10 cm
Carbonated porphyry	0.07	6	18	42	23.04	76.96
Altered greywacke	0.05	4	16	40	42.19	57.81
Carbonated greywacke	0.03	3	15	40	49.91	50.09

Chemical assays of the total samples and their corresponding fractions showed compositions dominated primarily by Al, Ca, Fe, K, Mg, and Na (Table 1S), which are related to NSG minerals. Titanium and manganese contents in all samples did not exceed 0.3 and 0.01 wt.%, respectively.

The total S and C contents did not exceed 1.1 and 1 wt.%, respectively. Average Cu concentrations were approximately < 10 ppm, 32 ppm, and 38 ppm for the carbonated porphyry, altered greywacke, and carbonated greywacke lithologies, respectively. Average Zn concentrations were approximately 60 ppm, 84 ppm, and 78 ppm for the carbonated porphyry, altered greywacke, and carbonated greywacke, respectively. Iron-, zinc-, and copper-bearing minerals were primarily sulfides but occurred in small quantities. Concentrations of Pb, Ni, Co, Cd, and As were below the detection limits of the ICP-AES for all samples. Sulphide phases were enriched in the F2 and F3 particle-size fractions of all samples. Carbon distribution, which occurred mainly as carbonates, showed a different trend as compared to S; it decreased when particle sizes increases. The average concentrations of C were 0.51%, 0.26%, and 0.29% for the carbonated porphyry, altered greywacke, and carbonated greywacke, respectively. The carbonated porphyry was the most carbonate-rich lithology and the carbonated greywacke lithology was the most enriched in sulphides.

3.4.2 Mineralogical characteristics

All particle-size fractions were analyzed using XRD and optical microscopy. Samples $\leq$ 5 mm were also analyzed using QEMSCAN and samples > 5 mm were characterized using computed tomography to estimate the degree of sulphide liberation.

3.4.2.1 Bulk mineralogy

Optical microscopy observations showed that the main sulphide in all three lithologies was pyrite, with trace amounts of pyrrhotite and chalcopyrite also present (Figure 3.2). Sulphides displayed different textures that could be classified as three exposure states: i) free sulphides not in contact with other NSG minerals (Figure 3.2A-B), ii) moderately liberated sulphides with boundaries partially shared with NSG minerals (Figure 3.2C), and iii) locked sulphides that are entirely enclosed within NSG minerals. Optical microscopy observations qualitatively showed that the degree of sulphide liberation depended on the size fraction of the sample. Sulphides within fine fractions (< 0.85 mm) were more liberated than those in coarser fractions ($\geq$ 0.85 mm) (Figure 3.2A-B). Liberated pyrites have no edges shared with other minerals. However, for coarse fractions (> 2.4 mm) sulphides became more locked and their boundaries were completely or partially shared with NSG minerals (Figure 3.2C, D).
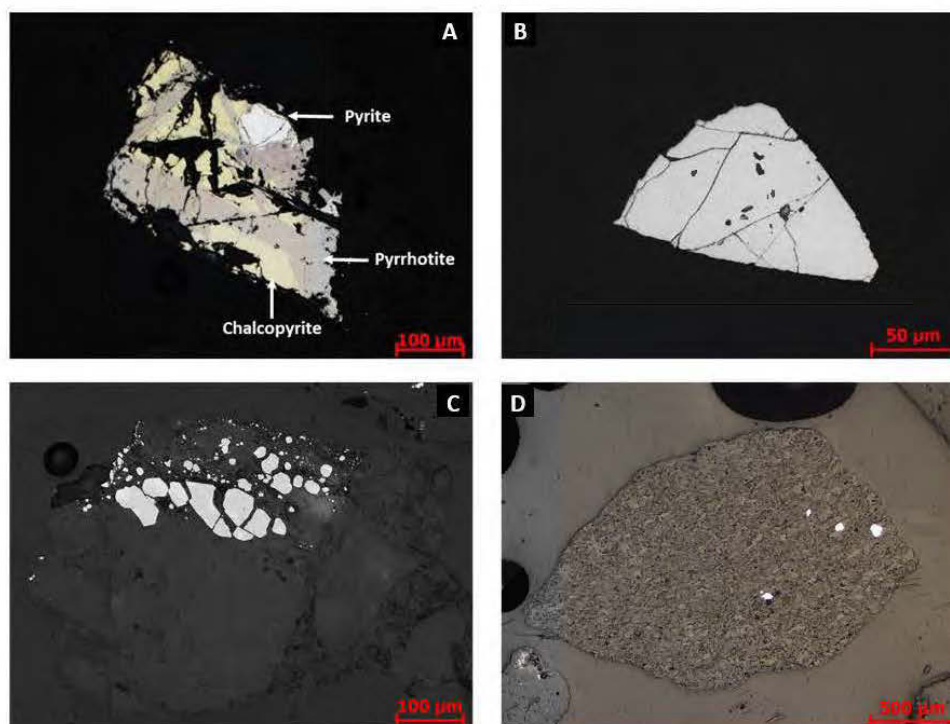
Figure 3.2: Optical microscope images showing sulphides and their liberation states (A, B: liberated pyrite, C and D: pyrite encapsulated within NSG minerals).

The mineralogical reconciliation consisted of calculating a mineralogical composition, which is in respect with the chemical assay (ICP-AES, XRF and induction furnace S/C). This was achieved by setting minerals wt.% until achieving the minimal difference between the solid chemical assay and the chemical composition calculated by the minerals stoichiometry. The chemical assay and the calculated chemical composition are plotted for total waste rocks samples and the 21 corresponding fractions. The coefficient of correlation between the two chemical compositions was around 1 for the studied waste rocks samples (Figure 3.3). The three lithologies contain mainly NSG minerals; aluminosilicates (Figure 3.4) and small occurrences of sulphides and carbonates. Fractions between 0.053 mm and 0.850 mm are the most sulphidic.

The results of QEMSCAN modal analyses agreed with the XRD results except for trace minerals that were not detected by XRD. The reconciled mineralogical composition showed that silicates constituted approximately 89 to 94 wt.% of the carbonated porphyry lithology, and 90 to 96 wt.% of the altered greywacke and carbonated greywacke lithologies (Figure 3.4). The abundance of aluminosilicate minerals explains the high Al, Si, Ca, Fe, K, Mg, and Na contents of the samples

(Table 2S). The silicates detected within the studied samples were quartz, albite, bytownite, orthoclase, muscovite, phlogopite, and chamosite. More than 90% of carbonates occurred as calcite with the remainder occurring as rhodochrosite and dolomite. The carbonated porphyry lithology was the richest in carbonates, with proportions varying from 4 to 8 wt.%. Carbonates ranged from 1 to 4.8 wt.% in the altered greywacke and carbonate greywacke samples. Pyrite contents ranged from 0.3 to 0.5 wt.% within the carbonated porphyry and from 0.5 to 2 wt.% within the greywacke lithologies. Chalcopyrite occurred as a trace mineral (< 0.1 wt.%), while sphalerite, which was identified only by QEMSCAN, did not exceed 0.04 wt.% (values were calculated based on the Zn content analyzed by ICP-AES in each sample and considering that sphalerite contains 64.06% Zn). All fractions and total samples contained more carbonates than sulphides.
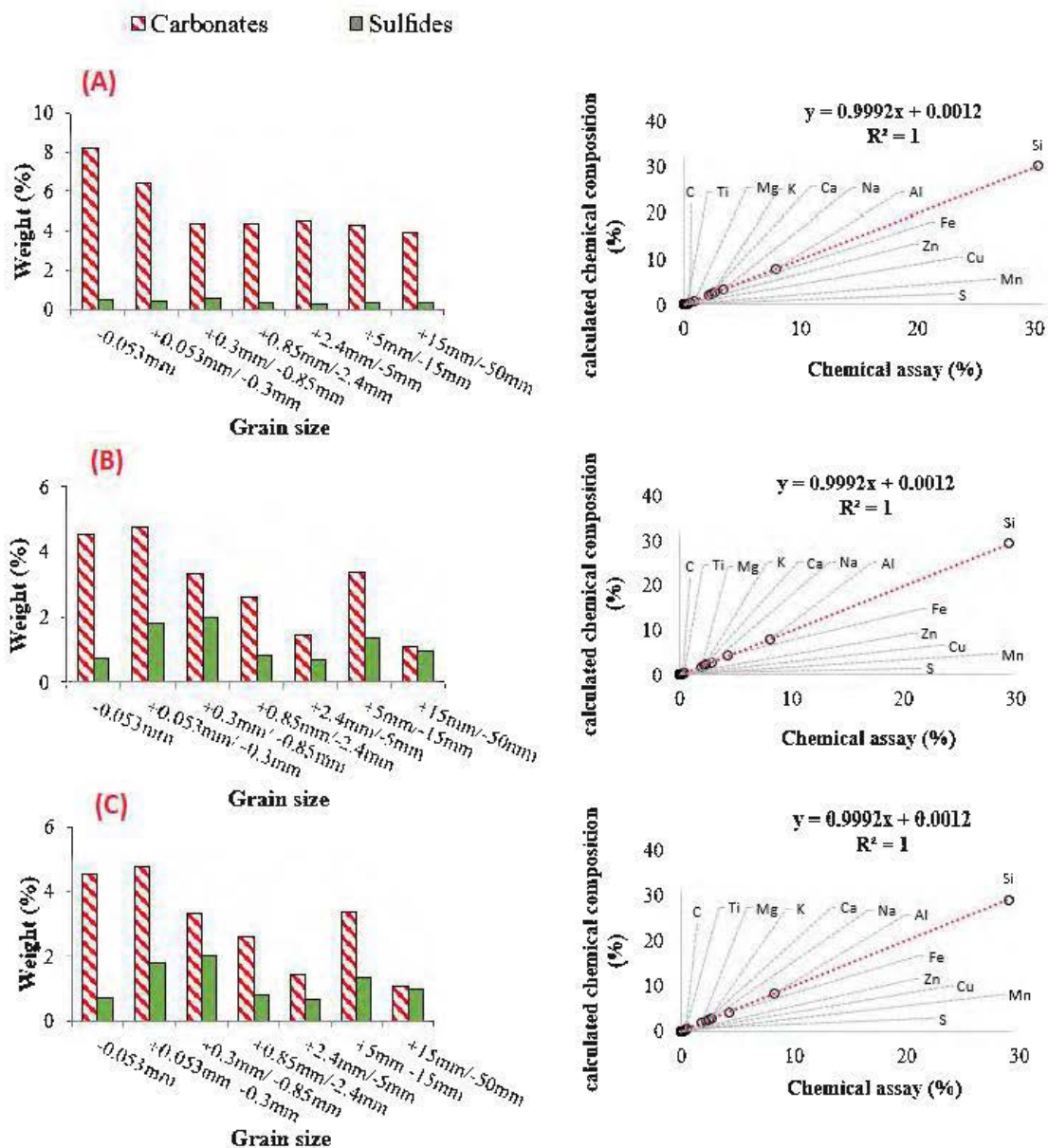
Figure 3.3: Sulphide and carbonate distributions within the three sample lithologies (left) and correlation of chemical assay results versus calculated chemical compositions (right). The red line represents the correlation between the chemical assays and the calculated chemical compositions based on minerals stoichiometries.
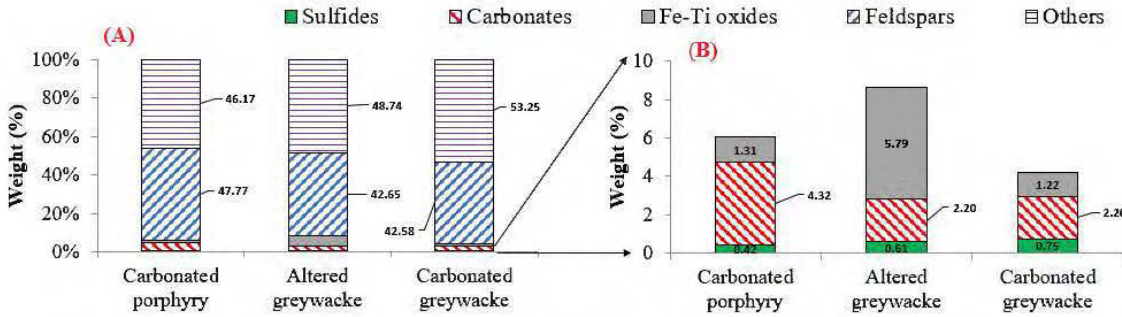
Figure 3.4: Reconciled mineralogical compositions of the carbonated porphyry, altered greywacke, and carbonated greywacke lithologies. A: total mineralogical composition, B: minor phases.

3.4.2.2 Textural and mineral liberation analyses

The degree of liberation of sulphides and carbonates, which are the main acid-generating and neutralizing minerals, respectively, describes the level to which these minerals are exposed in a sample (Blowes *et al.*, 2003; Paktunc & Dave, 2000b; Petruk, 2000). QEMSCAN analyses were used to quantify this parameter as function of particle size. Once determined, the degree of liberation was used to suggest corrections to apply to the results of static tests for samples under 5 mm. For coarser fractions, the degree of sulphide liberation was considered to be negligible based on the results of CT analyses. The number of particles measured for the all lithologies was approximately 18000, 21000, 9000, 1000, and 400 for fractions F1, F2, F3, F4 and F5, respectively. The degrees of sulphide and carbonate liberation degree (% L) were recalculated to account for all the liberation classes using the formula presented below:

$$\%L = \sum_{c=0}^{100} C_i * A_i/100$$

where C_i is the average liberation class as provided by QEMSCAN, and A_i is the average frequency of class C_i.

The overall calculated liberation of minerals considered all classes of liberation depending on their proportion within the whole particle distribution. Results for the calculated sulphide and carbonate liberations are presented in Figure 3.5. The degree of sulphide liberation decreases as grain size

increases (Figure 3.5A). The maximum sulphide liberation was approximately 96.5% for carbonated greywacke lithology within the finest fraction (F1). The highest liberation was recorded for carbonated greywacke lithology. At 2.4 mm, sulphide liberation was negligible (<5%). The degree of carbonate liberation also decreased with increasing grain size. Overall, carbonates within the carbonated porphyry lithology were more liberated than in the other lithologies. In contrast to the sulphides, at 2.4 mm carbonate liberation was still significant; i.e., 30%, 8.5%, and 13.5% for the carbonated porphyry, altered greywacke, and carbonated greywacke lithologies, respectively (Figure 3.5B).

The mineralogical associations of sulphides and carbonates are illustrated in Figure 3.5C-D. Sulphides were mostly linked with silicates (71%, 55%, and 39% for the carbonated porphyry, altered greywacke and carbonated greywacke lithologies, respectively), and less frequently present as free pyrite particles (Figure 3.5C). Carbonates were associated mostly with NSG minerals (82%, 73%, and 73% for the carbonated porphyry, altered greywacke and carbonated greywacke lithologies, respectively).
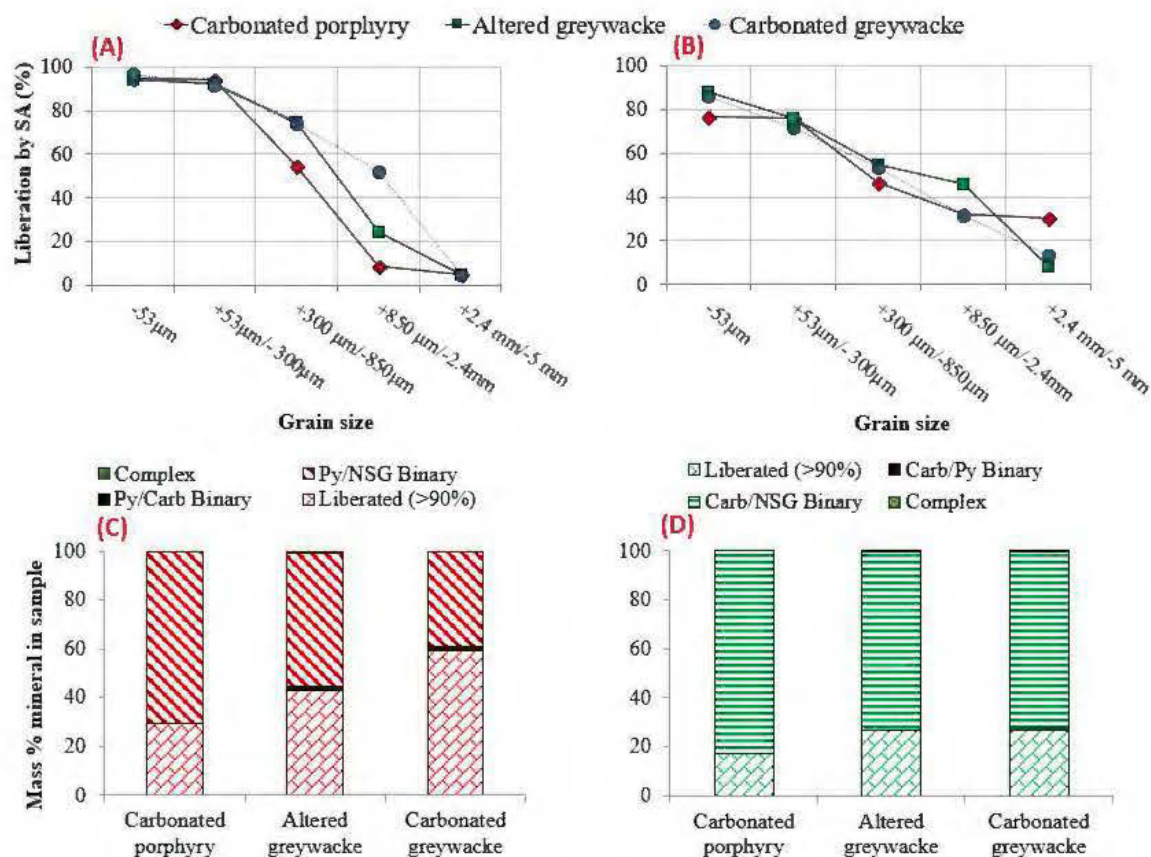
Figure 3.5: Degree of liberation and mineralogical associations for carbonates and sulphides within the three waste rock samples. A: degree of sulphide liberation, B: degree of carbonate liberation, C: sulphide mineralogical associations, D: carbonate mineralogical associations.

The reactivity of waste rocks is influenced by the degree of liberation of the acid-generating and neutralizing minerals (Erguler *et al.*, 2015; Smith & Huyck, 1999) and also by the particle sizes (specific surface area) of these minerals (Cornell *et al.*, 2004e; Lapakko *et al.*, 2006). Particle-size distributions for carbonate and pyrite particles within the three lithologies, determined using QEMSCAN, are illustrated in Figure 3.6. Carbonates were present as finer grains than pyrite. The D_{50} of pyrite was 105 µm, 165 µm, and 125 µm for the carbonated porphyry, altered greywacke, and carbonated greywacke lithologies, respectively. The D_{50} of carbonates was 55 µm, 50 µm, and 57 µm for the carbonated porphyry, altered greywacke, and carbonated greywacke lithologies, respectively.
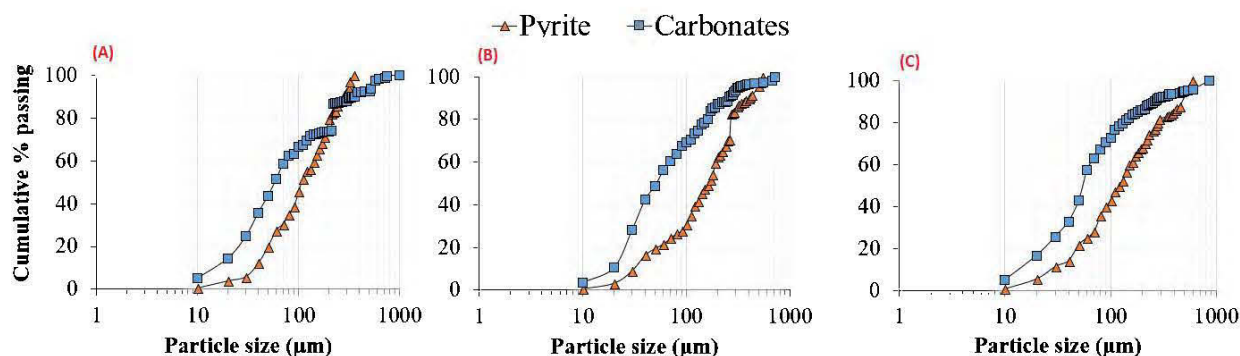
Figure 3.6: Pyrite and carbonate particle-size distributions within the three lithologies (A: carbonated porphyry, B: altered greywacke, and C: carbonated greywacke).

Because of the limitations of sample preparation, fractions coarser than 5 mm could not be mounted into polished sections for automated mineralogy analyses. The diameter of the polished sections mold was ~ 3 cm, which would require a significant number of polished sections to be analyzed to have statistically acceptable results for coarser fractions. Consequently, the coarse fractions were analyzed using CT to estimate the degree of sulphide liberation, sulphide volume distribution, and sulphide contents within the three lithologies. Micro-CT allowed for mapping of sulphides based on their density contrast with NSG minerals. Figure 3.7 illustrates the spatial distribution of sulphides within the three lithologies (> 5 mm). Micro-CT data showed that the percentages of sulphides appearing at the surfaces of grains were negligible compared to that of sulphides encapsulated within grains. The degree of sulphide in this case was defined as the ratio between the pyrite mass appearing at the grain surface and the total pyrite mass within the whole grain. Consequently, sulphide liberation could be considered negligible for the coarse fraction of these studied samples. These results were expected considering that QEMSCAN results showed that the degree of sulphide liberation decreased with increasing grain size (Figure 3.5A). Within coarse fractions, sulphides were more encapsulated within NSG minerals. This technique allowed for the calculation of sulphide volume in every lithology (fractions F6 and F7) (Figure 3.8). The volumes analyzed were 360005 mm^3, 357559 mm^3, and 347318 mm^3 for the carbonated porphyry, altered greywacke, and carbonated greywacke lithologies, respectively. The volume distribution of sulphides was 1.60%, 0.79%, and 0.57% for the carbonated porphyry, altered greywacke, and carbonated greywacke lithologies, respectively. The sulphide volume distribution (Figure 3.8) showed that more than 99% of sulphides had a volume less than 1 mm^3. A small amount of sulphide

had larger volumes. Sulphide liberation within fractions F6 and F7 was estimated using CT to be approximately 5% for the three lithologies.
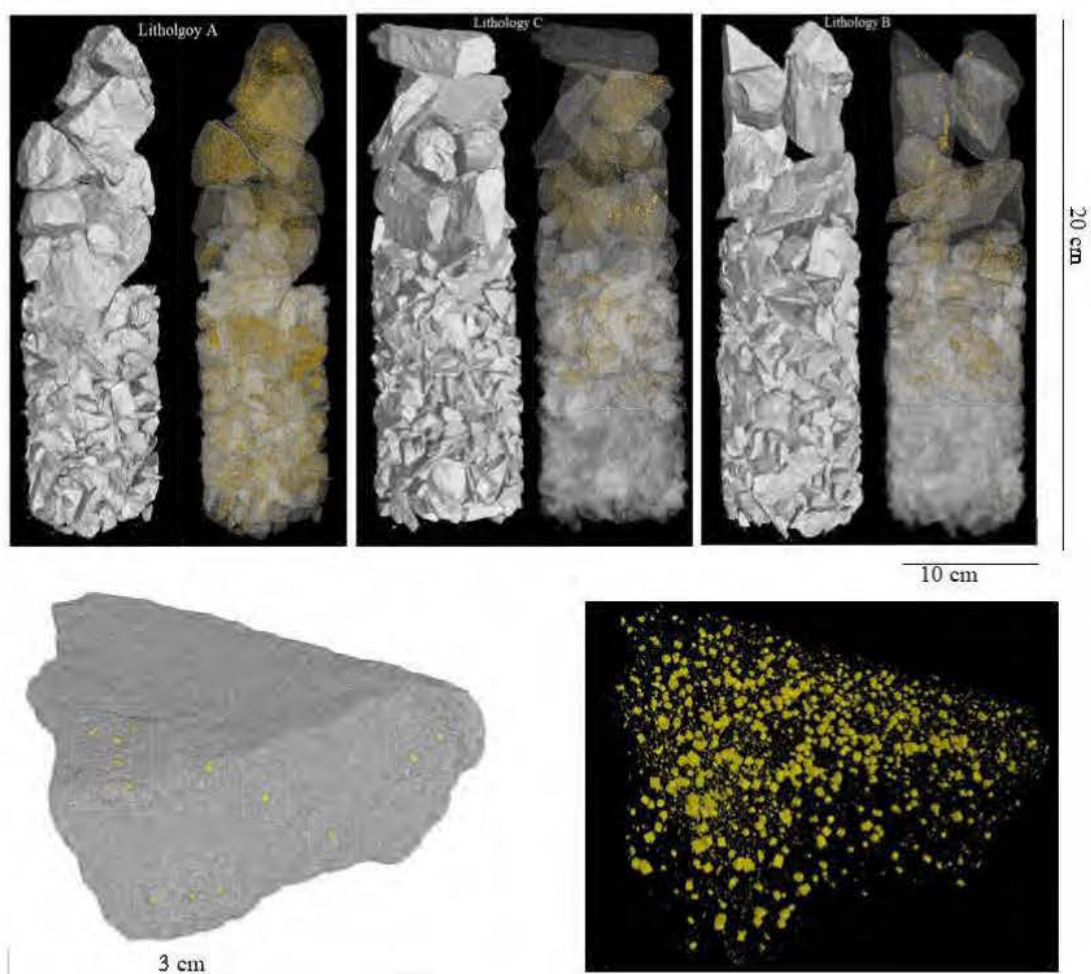
Figure 3.7: Sulphide mapping within the three lithologies using computed tomography. The yellow pixels represent sulphides and the grey pixels are NSG minerals.
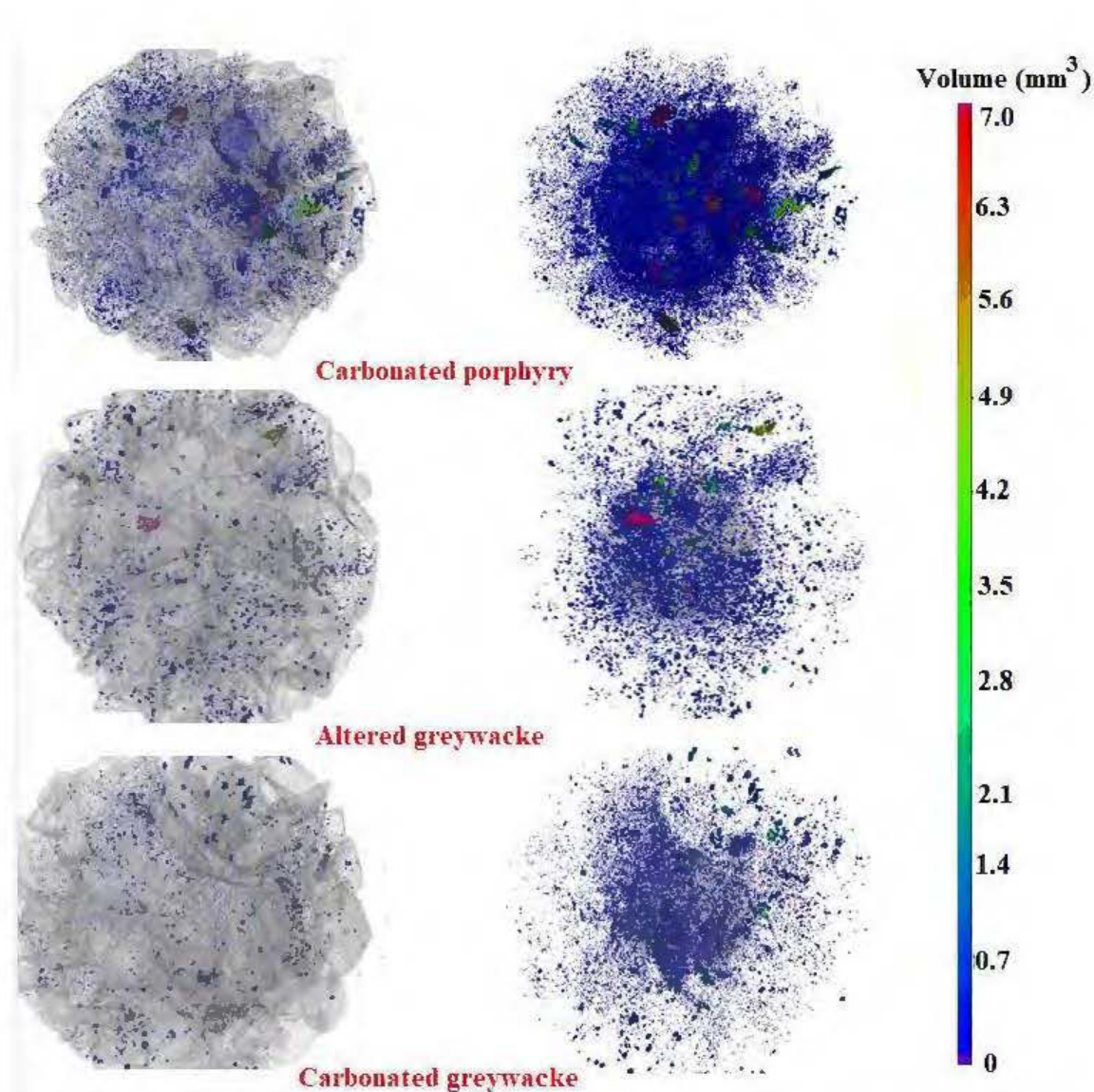
Figure 3.8: Sulphide volume distribution within the three lithologies.

3.4.3 Acid base accounting and NAG tests

Prediction of the AGP for the 21 fractions and the total samples was performed using the Sobek, as modified by (Bouzahzah *et al.*, 2015a), and the NAG test (Stewart *et al.*, 2006). NPs were also calculated based on the total carbon of the samples without accounting for the potential for hydrolysis of iron and manganese from carbonates such as siderite and rhodochrosite. NAG and modified Sobek test results are presented in Figure 3.9. The pH values for all samples were greater than 4.5, varying between 5.8 and 6.8 for the carbonated porphyry lithology, between 5.1 and 6.15 for the altered greywacke lithology, and between 5.19 and 6.07 for carbonated greywacke lithology. Therefore, based on the NAG test, all samples could be considered non-acid-generating

(Miller *et al.*, 1997). The electrical conductivity (EC) measured on post-NAG solutions did not exceed 1 mS/cm, and the maximum EC was recorded in fractions F2 and F3. Moreover, the acidity of NAG solutions was also analyzed using titration and results agreed with EC values. The, acidity of all samples did not exceed 5 mg $CaCO_3$/L. The low acidity (produced by oxidation of pyrite under H_2O_2 action) of post-NAG solution is explained by neutralization by calcite dissolution.

The results of ABA tests showed that most samples were non-acid-generating, except for a few samples that were uncertain: fractions F2, F3, F6, and F7 of the altered greywacke porphyry, and fractions F2, F3, F4, F6, and F7 of the carbonated greywacke. The NNP values of most waste rock samples corresponding to the three lithologies were greater than 20 kg $CaCO_3$/t and considered to be non-acid-generating (Figure 3.9B). Only three fractions of the altered greywacke and one fraction of the carbonated greywacke were considered uncertain according to the NNP classification (Bouzahzah *et al.*, 2015a). The NPR of most particle-size fractions was > 2 and, thus, non-acid-generating. However, four fractions of the altered greywacke were uncertain according to their NPR (Figure 3.9). The fine fractions had the highest NP values. The carbonated porphyry had the highest NP values and the lowest AP values, and all samples of the carbonated were non-acid-generating.
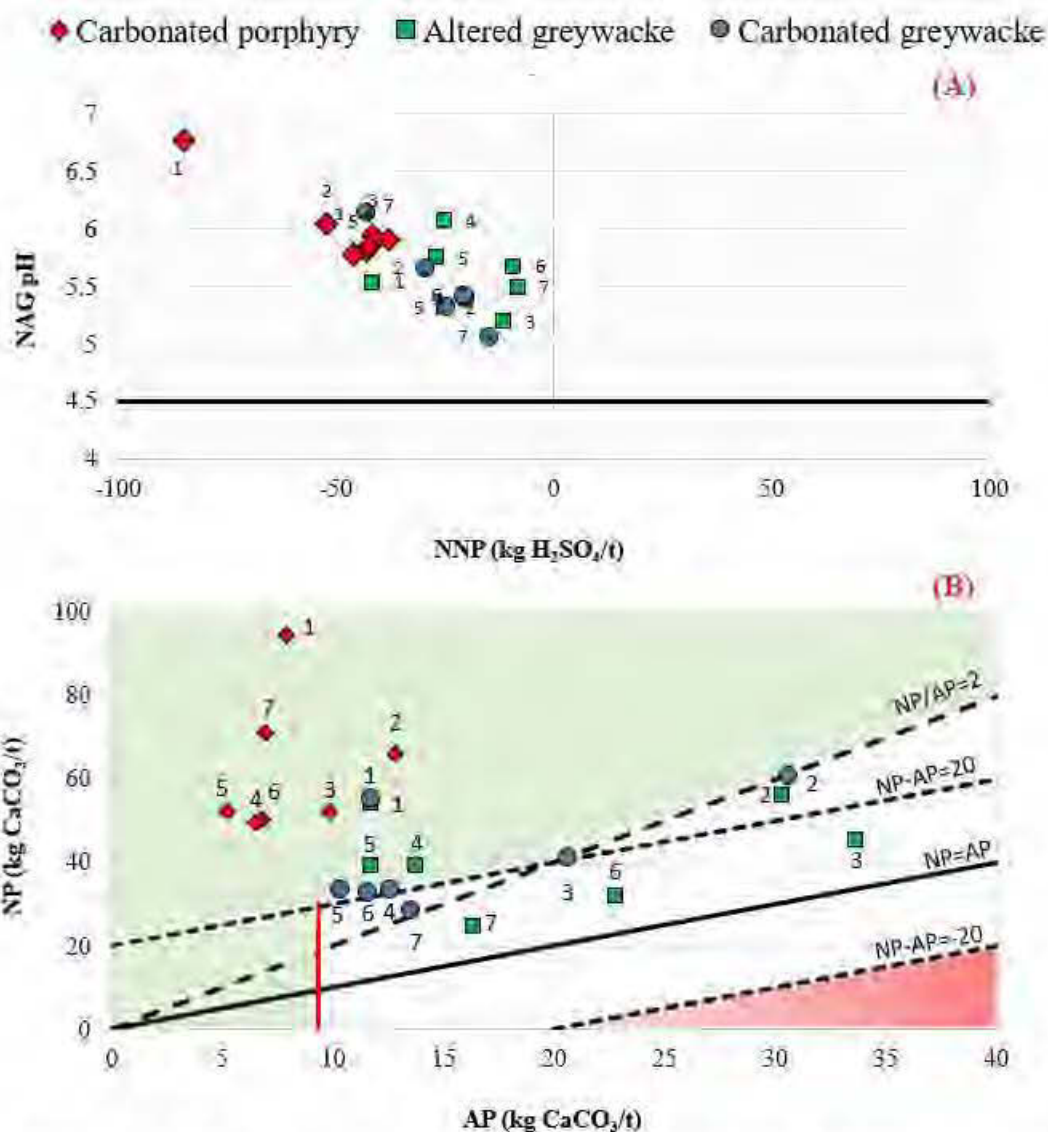
Figure 3.9: Results of the (A) NAG tests and (B) ABA tests. Red zone is potentially acid-generating, green zone is non-acid-generating, and white is uncertain. Numbers refer to the particle-size fractions (1=F1, 2=F2, 3=F3, 4=F4, 5=F5, 6=F6 and 7=F7).

3.5 Discussion

NAG and ABA tests were performed on pulverized samples as recommended by Bouzahzah et al (2015), Lapakko (1994), Miller et al (1997), Smart et al (2002) and Sobek et al (1978). Results of the NAG and ABA tests showed that all fractions were non-acid-generating, and some are in the uncertainty zone. Carbonate contents were higher than sulphide contents in all samples, which explains the results obtained with the NAG and ABA tests. During the NAG test, the liquor acidity

of all fractions did not exceed 9 mg CaCO3/L due to acidity buffering by carbonate dissolution. Sample pulverization required for these tests significantly modified the initial texture of each sample. Sulphides and carbonates were more liberated and thus their mineralogical associations were greatly modified during the pulverization process. As stated in Blowes et al. (2003), the determination of NP and AP based on pulverized samples assumes that the sulphides and carbonates are completely liberated, which is not the case for waste rock (large particle size distribution), especially in comparison with tailings. Consequently, the degrees of liberation sulphides and carbonates are important features to consider during the assessment of the environmental behavior of waste rock. This was highlighted also using kinetic leaching tests on locked and liberated calcite and pyrite by Paktunc and Davé (2000).

Fractions with a particle size > 5 mm were not considered during this correction due to their low sulphide liberation as shown by QEMSCAN and CT results (Figure 5, Figure 7). The calculation of the new AP and NP based on sulfide and carbonate liberation degrees showed a new classification of the three studied lithologies with respect to their potential for acid generation (Figure 3.10). Depending on the difference between carbonate and sulphide liberation, the samples were placed in different spots in the static tests diagram. For example, the fraction F4 of the altered greywacke and carbonated greywacke were initially categorized as non-acid-generating, but became uncertain after corrections. NP and AP values determined on pulverized samples should represent the maximum potentials that can be achieved by samples when all sulphides and carbonates have reacted completely.

QEMSCAN analyses showed that the degree of liberation of carbonates and sulphides decreased as the particle size increased. Corrections applied to the NP and AP using the degrees of liberation allowed for a determination of the effective NP and AP, meaning that only the exposed part of sulphides and carbonates are taken into account (Blowes et al., 2003; Erguler et al., 2015; Paktunc et al., 2000a). The difference between the available and absolute NP and AP depends on the particle sizes and mineralogical textures. For fine fractions, the difference between the available and absolute NP and AP was not very significant; for example, F1 of the carbonated porphyry compared to F4 of the carbonated greywacke (Figure 3.10). For the coarse fractions, sulphide liberation is only determined by the sulphide outcrop on the grain surface.
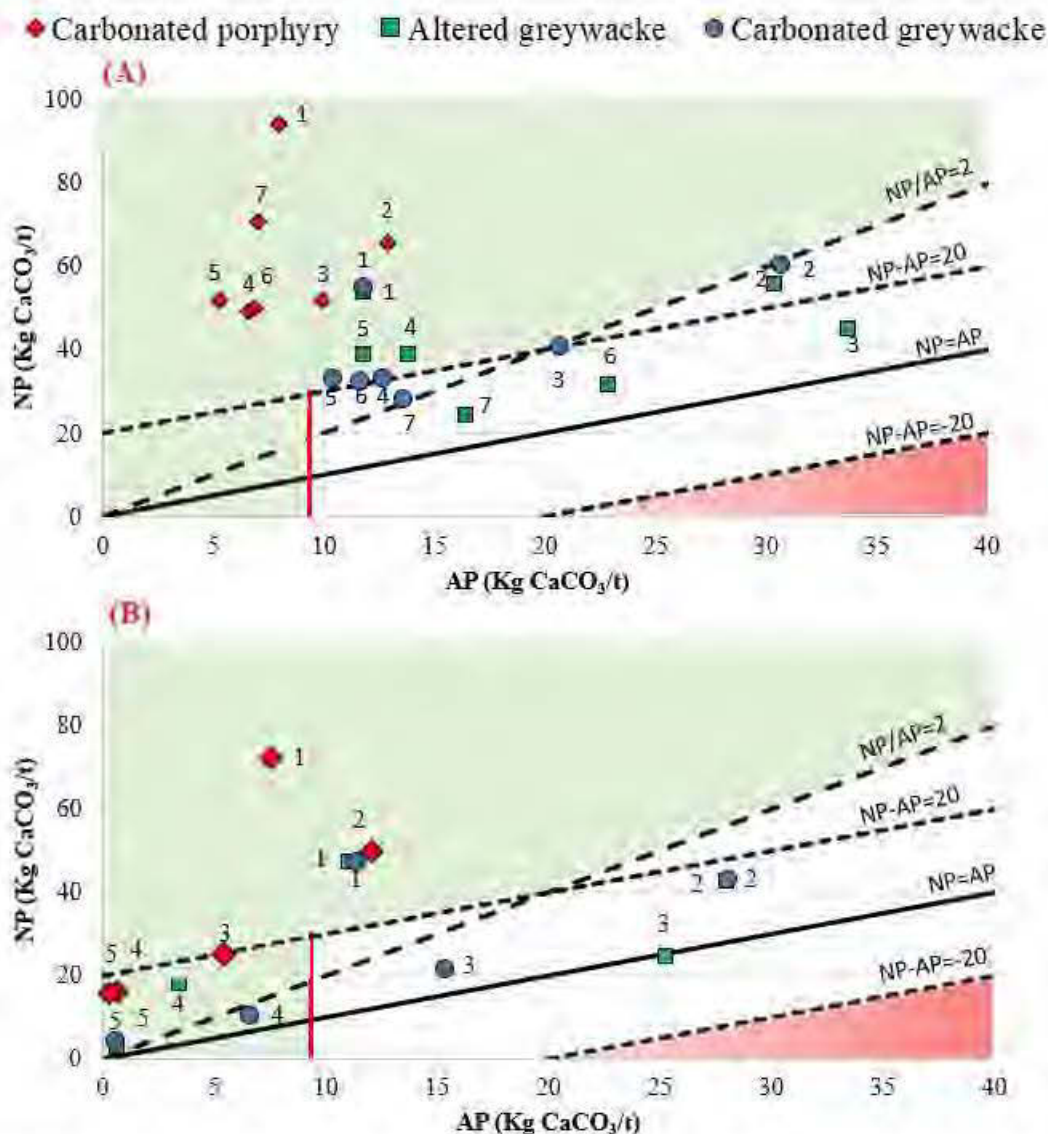
Figure 3.10: Results of ABA tests with (A) the overall NP and AP, and (B) the effective NP and AP corrected with sulphide and carbonate liberation. Red line (NP = 9.4 kg CaCO₃/t) corresponds to 0.3% S, which is considered as a non-acid-generating sample in Directive 019. Numbers refer to the particle-size fractions (1=F1, 2=F2, 3=F3, 4=F4, 5=F5, 6=F6 and 7=F7).

The diameter of physical locking of sulphides is a particle size at which liberation degree of sulphides is almost zero. The DPLS separates waste rocks into two fractions: a finer, reactive fraction and a coarser, nearly non-reactive fraction. This diameter is defined in this article using a

mineralogical approach, but it must be confirmed using continued geochemical and physical weathering of the rock must be further examined, for example, through kinetic tests. Considering the results of mineralogical analyses on the samples in this study and data on the degree of sulphide liberation, the three lithologies can be separated into two fractions at a DPLS of 2.4 mm (Figure 3.5A). Three column leaching tests for each lithology are ongoing and will be the topic of a follow-up paper. These columns are comprised of the total sample, a < 2.4 mm fraction, and a > 2.4 mm fraction for each lithology. Considering the particle-size distribution (Table 3.1), the < 2.4 mm fraction represents a low percentage of each sample; i.e., 7 wt.%, 10 wt.%, and 12 wt.% of the carbonated porphyry, altered greywacke, and carbonated greywacke lithologies, respectively (considering 1 m as the maximum particle size). Although the < 2.4 mm fraction represents a low proportion of the total waste rock, it is the most reactive fraction and can control the overall drainage chemistry at the dump scale. The use of the DPLS of waste rocks should consider its persistence with continued geochemical and physical weathering of the rock.

3.6 Conclusion

The main conclusions of this work are:

- Waste rock size fractions should be better characterized for a more accurate determination of the AGP. It is more appropriate to collect samples after waste rock blasting to consider the actual particle distribution.

- Carbonate contents are higher than sulphide contents in the three waste rocks lithologies used in this study. AGP were determined by both ABA and NAG tests and showed that most samples were non-acid-generating.

- Fractions between 0.053 mm and 0.85 mm were the most problematic because of their sulphide contents were high (relative to the other fractions).

- During NAG and ABA tests samples are pulverized. This destroys the initial texture of samples, which is an essential quality for waste rocks which are characterized by wide and heterogeneous particle-size distributions. The authors suggest that ABA and NAG tests

results on waste rocks must be corrected using the degrees of carbonate and sulphide liberation.

- For the samples in this study, sulphide and carbonate liberation decreased with increasing particle sizes.

- Based on QEMSCAN results, at 2.4 mm, sulphide liberation was less than 10% and fractions coarser than 2.4 mm could be considered insignificant with respect to their AGP.

- The diameter of physical locking of sulphides (DPLS) for the samples in this study is suggested to be 2.4 mm.

Acknowledgements

References

Amos, R. T., Blowes, D. W., Bailey, B. L., Sego, D. C., Smith, L., & Ritchie, A. I. M. (2015). Waste-rock hydrogeology and geochemistry. *Applied Geochemistry, 57,* 140-156. doi:10.1016/j.apgeochem.2014.06.020

ASTM, A. (2014). C136/C136M–14, Standard Test Method for Sieve Analysis of Fine and Coarse Aggregates, ASTM International, West Conshohocken, PA, 2014.

Aubertin, M., Bussière, B., & Bernier, L. (2002). Environnement et gestion des résidus miniers [CD-ROM]. *Les Presses Internationales Polytechnique de Montréal, Québec.*

Barazzoul, L., Sexsmith, K., Buckham, C., & Lopex, D. (2012). *Application of an advanced mineralogical technique: Sulphide mineral availability and humidity cell interpretations based on MLA analysis.* Paper presented at the 9th International Conference on Acid Rock Drainage.

Benzaazoua, M., Bussière, B., Dagenais, A.-M., & Archambault, M. (2004). Kinetic tests comparison and interpretation for prediction of the Joutel tailings acid generation potential. *Environmental Geology, 46*(8), 1086-1101. doi:10.1007/s00254-004-1113-1

Benzaazoua, M., Bouzahzah, H., Taha, Y., Kormos, L., Kabombo, D., Lessard, F., Bussière, B., Demers, I., & Kongolo, M. (2017). Integrated environmental management of pyrrhotite

tailings at Raglan Mine: Part 1 challenges of desulphurization process and reactivity prediction. *Journal of Cleaner Production*.

Blowes, D., Ptacek, C., Jambor, J., & Weisener, C. (2003). The geochemistry of acid mine drainage. *Treatise on geochemistry, 9*, 612.

Blowes, D., Ptacek, C., Jambor, J., Weisener, C., Paktunc, D., Gould, W., & Johnson, D. (2014). The geochemistry of acid mine drainage.

Blowes, D. W., Jambor, J. L., & Alpers, C. N. (1994). *The environmental geochemistry of sulfide mine-wastes* (Vol. 22): Mineralogical Association of Canada.

Blowes, D. W., Ptacek, C. J., & Jambor, J. (2013). Mineralogy of mine wastes and strategies for remediation. *Environmental Mineralogy II: Vaughan, Wogelius (Eds), Europ. Mineral. Union Notes in Mineral, 13*, 295-338.

Bouzahzah, H., Benzaazoua, M., Bussière, B., & Plante, B. (2013). Acid-generating potential calculation using mineralogical static test: Modification of Paktunc equation. *Mise en garde*, 65.

Bouzahzah, H., Benzaazoua, M., Bussiere, B., & Plante, B. (2014). Prediction of Acid Mine Drainage: Importance of Mineralogy and the Test Protocols for Static and Kinetic Tests. *Mine Water and the Environment, 33*(1), 54-65. doi:10.1007/s10230-013-0249-1

Bouzahzah, H., Benzaazoua, M., Plante, B., & Bussiere, B. (2015). A quantitative approach for the estimation of the "fizz rating" parameter in the acid-base accounting tests: A new adaptations of the Sobek test. *Journal of Geochemical Exploration, 153*, 53-65. doi:http://dx.doi.org/10.1016/j.gexplo.2015.03.003

Brough, C., Strongman, J., Bowell, R., Warrender, R., Prestia, A., Barnes, A., & Fletcher, J. (2017). Automated environmental mineralogy; the use of liberation analysis in humidity cell testwork. *Minerals Engineering, 107*, 112-122.

Buckwalter-Davis, M., Lussier-Purdy, C., & Jamieson, H. Mineralogically-Based Determinations of Neutralization and Acid Potential Using Automated Mineralogy.

Bussière, B. (2007). Hydro-geotechnical properties of hard rock tailing from metal mines and emerging geo-environmental disposal approaches. *Canadian Geotechnical Journal, 44*(9), 1019-1052.

Butcher, A., Helms, T., Gottlieb, P., Bateman, R., Ellis, S., & Johnson, N. (2000). *Advances in the quantification of gold deportment by QemSCAN*. Paper presented at the Seventh Mill Operators Conference, Kalgoorlie, WA, AusIMM.

Chotpantarat, S. (2011). A review of static tests and recent studies. *American Journal of Applied Sciences, 8*(4), 400.

Cnudde, V., Masschaele, B., Dierick, M., Vlassenbroeck, J., Van Hoorebeke, L., & Jacobs, P. (2006). Recent progress in X-ray CT as a geosciences tool. *Applied Geochemistry, 21*(5), 826-832. Retrieved from http://ac.els-cdn.com/S0883292706000503/1-s2.0-S0883292706000503-main.pdf?_tid=d7fb19ce-8288-11e7-bc58-00000aacb362&acdnat=1502891171_a2fab75a5ca25a85e33eb507cc2367fc

Cornell, R. M., & Schwertmann, U. (2004). Solubility *The Iron Oxides* (pp. 201-220): Wiley-VCH Verlag GmbH & Co. KGaA.

Erguler, Z. A., & Kalyoncu Erguler, G. (2015). The effect of particle size on acid mine drainage generation: Kinetic column tests. *Minerals Engineering, 76*, 154-167. doi:10.1016/j.mineng.2014.10.002

Evangelou, V. P., & Zhang, Y. L. (1995). A review: Pyrite oxidation mechanisms and acid mine drainage prevention. *Critical Reviews in Environmental Science and Technology, 25*(2), 141-199. doi:10.1080/10643389509388477

Helt, K. M., Williams-Jones, A. E., Clark, J. R., Wing, B. A., & Wares, R. P. (2014). Constraints on the genesis of the Archean oxidized, intrusion-related Canadian Malartic gold deposit, Quebec, Canada. *Economic Geology, 109*(3), 713-735.

Kalyoncu Erguler, G., Erguler, Z. A., Akcakoca, H., & Ucar, A. (2014). The effect of column dimensions and particle size on the results of kinetic column test used for acid mine drainage (AMD) prediction. *Minerals Engineering, 55*, 18-29. doi:10.1016/j.mineng.2013.09.008

Kwong, Y. J., & Ferguson, K. D. (1997). *Mineralogical changes during NP determinations and their implications.* Paper presented at the Proc. 4th International Conference on Acid Rock Drainage, Vancouver, BC.

Lahmira, B., Lefebvre, R., Aubertin, M., & Bussiere, B. (2015). Effect of heterogeneity and anisotropy related to the construction method on transfer processes in waste rock piles. *J Contam Hydrol, 184*, 35-49. doi:10.1016/j.jconhyd.2015.12.002

Lapakko, K. (2003). Developments in humidity-cell tests and their application. *Environmental Aspects of Mine Wastes. Mineralogical Assoc. Canada, Short Course, 31*, 147-164.

Lapakko, K., & Lawrence, R. W. (2009). Modification of the net acid production (NAP) test.

Lapakko, K. A., Engstrom, J. N., & Antonson, D. A. (2006). *Effects of particle size on drainage quality from three lithologies.* Paper presented at the Poster paper presented at the 7th International Conference on Acid Rock Drainage (ICARD).

Lasdon, L. S., Fox, R. L., & Ratner, M. W. (1974). Nonlinear optimization using the generalized reduced gradient method. *Revue française d'automatique, informatique, recherche opérationnelle. Recherche opérationnelle, 8*(V3), 73-103.

Lawrence, R. W., & Wang, Y. (1997). *Determination of neutralization potential in the prediction of acid rock drainage.* Paper presented at the Proceedings of the fourth international conference on acid rock drainage.

Mackay, D., Simandl, G., Ma, W., Redfearn, M., & Gravel, J. (2016). Indicator mineral-based exploration for carbonatites and related specialty metal deposits—A QEMSCAN® orientation survey, British Columbia, Canada. *Journal of Geochemical Exploration, 165*, 159-173.

Maest, A., & Nordstrom, D. K. (2017). A geochemical examination of humidity cell tests. *Applied Geochemistry.*

Maire, E., & Withers, P. J. (2014). Quantitative X-ray tomography. *International Materials Reviews, 59*(1), 1-43.

Mees, F., Swennen, R., Van Geet, M., & Jacobs, P. (2003). Applications of X-ray computed tomography in the geosciences. *Geological Society, London, Special Publications, 215*(1), 1-6.

Miller, S., Jeffery, J., & Wong, J. (1991a). *In-pit identification and management of acid forming waste rock at the Golden Cross Gold Mine, New Zealand.* Paper presented at the Proceedings of the Second International Conference on the Abatement of Acidic Drainage Montreal, Quebec September.

Miller, S., Jeffery, J., & Wong, J. (1991b). *Use and misuse of the acid base account for "AMD" prediction.* Paper presented at the Proceedings of the 2nd International Conference on the Abatement of Acidic Drainage, Montréal, Que.

Miller, S., Robertson, A., & Donahue, T. (1997). *Advances in acid drainage prediction using the net acid generation (NAG) test.* Paper presented at the Proc. 4th International Conference on Acid Rock Drainage, Vancouver, BC.

Morin, K. A., & Hutt, N. M. (1994). *Observed preferential depletion of neutralization potential over sulfide minerals in kinetic tests: site-specific criteria for safe NP/AP ratios.* Paper presented at the Proceedings of the Third International Conference on the Abatement of Acidic Drainage, Pittsburgh, USA.

Nordstrom, D. K. (2000). Advances in the hydrogeochemistry and microbiology of acid mine waters. *International Geology Review, 42*(6), 499-515.

Nordstrom, D. K., & Southam, G. (1997). Geomicrobiology of sulfide mineral oxidation. *Reviews in mineralogy, 35,* 361-390.

Nordstrom, D. K., Blowes, D. W., & Ptacek, C. J. (2015). Hydrogeochemistry and microbiology of mine drainage: An update. *Applied Geochemistry, 57,* 3-16.

Olson, G. J. (1991). Rate of pyrite bioleaching by Thiobacillus ferrooxidans: results of an interlaboratory comparison. *Applied and environmental microbiology, 57*(3), 642-644.

Paktunc, A. (1999a). Mineralogical constraints on the determination of neutralization potential and prediction of acid mine drainage. *Environmental Geology, 39*(2), 103-112.

Paktunc, A., & Davé, N. (2000a). *Mineralogy of pyritic waste rock leached by column experiments and prediction of acid mine drainage.* Paper presented at the In: Rammlmair D (ed.) Applied Mineralogy, pp. 621–623. Balkema.

Paktunc, A. D. (1999b). Characterization of mine wastes for prediction of acid mine drainage *Environmental impacts of mining activities* (pp. 19-40): Springer.

Paktunc, A. D., & Dave, N. K. (2000b). *Prediction of Acidic Drainage and Accompanying Metal Releases from Unsegregated Pyritic Uranium Mill Tailings Based on Effluent Chemistry and Post Leaching Sample Mineralogy.* Paper presented at the Proceedings of the Fifth International Conference on Acid Rock Drainage. Society for Mining, Metallurgy, and Exploration, Inc.(SME), Denver.

Parbhakar-Fox, A., & Lottermoser, B. G. (2015). A critical review of acid rock drainage prediction methods and practices. *Minerals Engineering, 82,* 107-124. doi:10.1016/j.mineng.2015.03.015

Parbhakar-Fox, A. K., Edraki, M., Walters, S., & Bradshaw, D. (2011). Development of a textural index for the prediction of acid rock drainage. *Minerals Engineering, 24*(12), 1277-1287.

Petruk, W. (2000). Applied mineralogy to tailings and waste rock pile-sulfide oxidation reactions and remediation of acidic water drainage. *Applied mineralogy in the mining industry,* 201-225.

Petruk, W., & Lastra, R. (1993). Evaluation of the recovery of liberated and unliberated chalcopyrite by flotation columns in a copper cleaner circuit. *International Journal of Mineral Processing, 40*(1), 137-149. doi:https://doi.org/10.1016/0301-7516(93)90046-D

Pirrie, D., Butcher, A. R., Power, M. R., Gottlieb, P., & Miller, G. L. (2004). Rapid quantitative mineral and phase analysis using automated scanning electron microscopy (QemSCAN); potential applications in forensic geoscience. *Geological Society, London, Special Publications, 232*(1), 123-136.

Plante, B., Benzaazoua, M., & Bussière, B. (2011). Predicting geochemical behaviour of waste rock with low acid generating potential using laboratory kinetic tests. *Mine Water and the Environment, 30*(1), 2-21.

Price, W. A., Morin, K., & Hutt, N. (1997). *Guidelines for the prediction of acid rock drainage and metal leaching for mines in British Columbia: Part II. Recommended procedures for static and kinetic testing.* Paper presented at the Proceedings of the Fourth International Conference on Acid Rock Drainage.

Rimstidt, J. D., & Vaughan, D. J. (2003). Pyrite oxidation: a state-of-the-art assessment of the reaction mechanism. *Geochimica et Cosmochimica Acta, 67*(5), 873-880. doi:http://dx.doi.org/10.1016/S0016-7037(02)01165-1

Sapsford, D. J., Bowell, R., Dey, M., & Williams, K. P. (2009). Humidity cell tests for the prediction of acid rock drainage. *Minerals Engineering, 22*(1), 25-36.

Smith, K., & Huyck, H. (1999). The Environmental Geochemistry of Mineral Deposits, Part A. Processes, Techniques, and Health Issues.

Sobek, A. A., Schuller, W. A., & Freeman, J. R. (1978). Field and laboratory methods applicable to overburdens and minesoils *Field and laboratory methods applicable to overburdens and minesoils*: EPA.

Stewart, W. A., Miller, S. D., & Smart, R. (2006). *Advances in acid rock drainage (ARD) characterisation of mine wastes.* Asmr.

Stock, S. (2008). Recent advances in X-ray microtomography applied to materials. *International Materials Reviews, 53*(3), 129-181.

Villeneuve, M. (2006). *Évaluation du comportement géochimique à long terme de rejets miniers à faible potentiel de génération d'acide à l'aide d'essais cinétiques.*

Weber, P. A., Thomas, J. E., Skinner, W. M., & Smart, R. S. C. (2004). Improved acid neutralisation capacity assessment of iron carbonates by titration and theoretical calculation. *Applied Geochemistry, 19*(5), 687-694. doi:http://dx.doi.org/10.1016/j.apgeochem.2003.09.002

White III, W., Lapakko, K., & Cox, R. (1999). Static-test methods most commonly used to predict acid-mine drainage: practical guidelines for use and interpretation. *Reviews in Economic Geology, 6*, 325-338.

Yeniay, O. (2005). A comparative study on optimization methods for the constrained nonlinear programming problems. *Mathematical Problems in Engineering, 2005*(2), 165-173.

CHAPITRE 4 ARTICLE 2: DETERMINATION OF THE AVAILABLE ACID GENERATION POTENTIAL OF WASTE ROCKS, PART II: WASTE MANAGEMENT INVOLVEMENT

A. Elghali[1], M. Benzaazoua[1], B. Bussière[1], H. Bouzahzah[1,2]

1 Université du Québec en Abitibi Témiscamingue, 445 Boul. Université, Rouyn-Noranda, QC, J9X 5E4, Canada

2 Université de Liège, Génie minéral, matériaux et environnement. Allée de la découverte, 13/A. Bât. B52/3 Sart-Tilman, 4000 Liège, Belgique

4.1 Abstract

Open pit mining operations often produce large amounts of waste rock that are characterized by large particle size distributions (PSD). Waste rock are normally deposited in surface piles that contain grains varying from a few microns to meters in size. Furthermore, the mineralogical and textural properties of the waste rock are influenced by their PSD. The diameter of physical locking of sulfides (DPLS) is a newly suggested parameter that was defined using an automated mineralogy system to separate waste rock according to their geochemical reactivity. Three lithologies (A, B, and C) were extracted from an open-pit gold mine and their geochemical behaviors, with respect to degree of sulfide liberation, were evaluated using column kinetic tests. The main results of this study showed that fine fractions of the studied waste rock were more sulfidic compared to coarse fractions. Moreover, sulfide liberation was negligible for fractions > 2.4 mm. Consequently, 2.4 mm was defined as the critical diameter of sulfide reactivity for the three studied waste rock. Column kinetic tests were used to confirm this hypothesis and to assess the geochemical behavior of the three lithologies. Geochemical analyses of leachates from the column tests showed that pH values remained between 7 and 8 and the instantaneous concentrations of metals such as iron (Fe) and zinc (Zn) were below environmental limits over the entire test duration (543 days). Considering sample reactivity, the data showed that the fine fractions primarily control the geochemical behavior of total samples. Sulfide oxidation rates were high for fractions < 2.4 mm, whereas they were negligible for fractions > 2.4 mm; total samples showed intermediate rates. For example, in lithology B, pyrite oxidation rates were 12.46 µmol/kg/day, 2.43 µmol/kg/day, and 0.27

µmol/kg/day for the fine fraction (< 2.4 mm), total sample (< 5 cm), and coarse fraction (> 2.4 mm) respectively. Sulfide and carbonate contents and their liberation were defined as key factors controlling the geochemical behavior of the studied waste rock, which was confirmed by the correlation factor between calcium leaching vs. carbonate liberation and between sulfur leaching vs. sulfide liberation. The coarse, unreactive fraction (> 2.4 mm) comprised a high proportion of the total sample weight (up to 90 wt. %). Screening waste rock, after blasting, according to the critical diameter of sulfide reactivity could be an efficient technique for global waste rock management that will reduce the economic costs related to waste rock pile reclamation.

Key words: Waste rock, Waste rock sorting, Mineral liberation, Kinetic tests, oxidation rate, Diameter of physical locking of sulfides.

4.2 Introduction

Over the last few decades, ore exploitation methods have evolved. Increasing metal prices and the availability of new equipment and technologies have allowed for the exploitation, usually by open-pit methods, of high-tonnage/low-grade ores. This type of exploitation generates large volumes of blasted and non-economic material called waste rock. Waste rock is part of the ore body that must be mined but is not treated because its metal content is lower than the operation-cutting grade. In general, waste rocks are deposited in unsaturated piles that can be hundreds of meters in height and cover thousands of hectares (Aubertin *et al.*, 2008; Bailey *et al.*, 2016; Blowes *et al.*, 2003) . Interactions between atmospheric oxygen, water, and sulfide minerals (mainly pyrite and pyrrhotite) in the waste rock could lead to the release of metals/metalloids, sulfates, and acidity in drainage waters (Blowes *et al.*, 1994; Bussière *et al.*, 2005; Caldeira *et al.*, 2003; Egiebor & Oni, 2007). In some cases, the neutralization potential of a waste rock is sufficient to neutralize the acidity produced by sulfide oxidation, but if the chemical quality of drainage waters is still above regulatory criteria it could cause environmental issues (Amos *et al.*, 2015; Plante *et al.*, 2011). Because of the way the material is deposited, waste rock piles are characterized by high chemical, physical, mineralogical, and hydrogeological anisotropies (Aubertin *et al.*, 2008; Bussière *et al.*, 2011; Jamieson *et al.*, 2015; Lefebvre *et al.*, 2001; Smith *et al.*, 2013). In general, waste rock piles are characterized by high heterogeneity of their internal structure, particularly regarding PSD (Poisson *et al.*, 2009). These heterogeneities result from the methods used to construct the piles as well as particle segregation that could occur inside the piles due to water infiltration (McLemore

et al., 2006). Generally, end- and push-dumping are the most used techniques for waste rock pile construction, both of which cause high internal structural heterogeneity in piles (Amos *et al.*, 2015).

The environmental behavior of waste rocks is controlled by their chemical, biological, mineralogical, and physical parameters (Aubertin *et al.*, 2008; Blowes *et al.*, 2003; Jambor, 1994; Jamieson *et al.*, 2015; Lindsay *et al.*, 2009; Lindsay *et al.*, 2015; Nordstrom, 2000; Nordstrom, 2009; Nordstrom *et al.*, 2015; Nordstrom & Southam, 1997; Paktunc, 1999a; Paktunc & Davé, 2000; Paktunc, 1999b). Particle size is recognized as one of the most important factors controlling the reactivity of waste rocks (Erguler & Kalyoncu Erguler, 2015; Lefebvre *et al.*, 2006). Indeed, PSD determines waste rock reactivity by influencing the degree of liberation of acid-generating and neutralizing minerals (Elghali *et al.*, 2018). The PSD of waste rocks ranges from a few microns to meters in size (Bailey *et al.*, 2016; Blowes *et al.*, 2006; Blowes *et al.*, 2003; Elghali *et al.*, 2018) and will depend on the blasting technique and the type of lithology. The mineral exposure rate is correlated to the PSD and is defined as the degree of mineral liberation (Petruk & Lastra, 1993). This parameter is commonly used for mineral recovery during the flotation process and has been recently used as a key factor for environmental issues (Blowes *et al.*, 2014; Brough *et al.*, 2017; Erguler *et al.*, 2015; Lapakko *et al.*, 2006; Paktunc *et al.*, 2000; Paktunc, 1999b; Parbhakar-Fox *et al.*, 2011; Petruk *et al.*, 1993). According to Elghali *et al.*, (2018), waste rocks could be separated into two fractions with highly different reactivities using automated mineralogical characterization. A new parameter, the diameter of physical locking of sulfides (DPLS), was defined that corresponds to the critical particle size where the degree of sulfide liberation becomes negligible (Elghali *et al.*, 2018). This parameter should be integrated during waste rock management in order to reduce the costs associated with waste rock pile construction and reclamation.

Three lithologies from an existing mine were sampled and characterized using a multi-disciplinary approach (Elghali *et al.*, 2018). The main results of these characterizations showed that not all fractions are acid-generating, and at 2.4 mm, the degree of sulfide liberation becomes negligible except for sulfides appearing at the surfaces of grains. This means that for coarse fractions (> 2.4 mm), negligible sulfide reactivity, and thus low acid production and metal release, could be expected. The main objectives of this companion paper are: i) to confirm that 2.4 mm is the DPLS, as is stated in Elghali *et al.*, (2018), using column kinetic tests, and ii) to predict the oxidation/neutralization rates of waste rocks considering sulfide and carbonate mineral liberation.

4.3 Materials and methods

4.3.1 Field site and material preparation

The three studied lithologies were sampled in an open pit mine in Québec (Canada). The deposit constitutes a part of the Cadillac-Larder Lake tectonic zone (Helt et al., 2014). The deposit is an Archean gold porphyry consisting of ≤ 20 µm of disseminated gold (Helt et al., 2014). The mineralization is mainly related to altered clastic sediments such as greywacke, mudstone and some siltstone. The metasediments have undergone carbonate, silicic and potassic alteration. The three lithologies samples in this study were: carbonated porphyry (lithology A), altered greywacke (lithology B) and carbonated greywacke (lithology C).

The three lithologies were sampled from three sub-piles constructed in the field immediately after waste rock blasting. The three lithologies (A, B, and C) were homogenized using a quartering technique and a part of each lithology was sampled. The remaining samples were sieved with an aperture of 2.4 mm following the conclusions of the study by Elghali et al. (2018). Additional details about sampling, sample preparation, and characterizations can be found in Elghali et al. (2018). The particle diameter of 2.4 mm was defined as the DPLS for the three lithologies. Humid sieving was used to avoid fine particles attached at the surface of coarse particles (> 2.4 mm). At the end of this step, for each lithology, three samples were ready to be used in column leaching tests: i) samples with all grains < 5 cm, hereafter called total sample; ii) fractions between 5 cm and 2.4 mm, called coarse fraction sample; and iii) fractions < 2.4 mm, hereafter called fine fraction sample.

4.3.2 Methods

A total of nine columns was set up and run for 543 days: three columns for lithology A (total, fine, and coarse samples), three for lithology B (total, fine, and coarse samples), and three for lithology C (total, fine, and coarse samples). Columns were constructed from Plexiglas with a 28-cm inner diameter and 1-m height for the total samples and coarse fraction samples. For the fine fraction samples, a 14-cm inner diameter was used. Due to the PSD and column size, the masses of samples used in column tests were 64 kg for total samples and coarse fraction samples, and 10.25 kg for fine fraction samples. The columns with coarse and total samples were flushed monthly with 18 L of deionized water and columns with fine samples were flushed monthly with 2.7 L of deionized

water. The water volume was chosen so as to keep the same liquid/solid ratio (L/S) for all columns. Samples were allowed to dry in ambient air between flushes. The leachates were collected and analyzed after four hours of contact with samples (Plante et al., 2011).

At the end of the test, only columns with fine fractions were dismantled by collecting samples at depths of 1, 3, 5, 10, 15, 20, 25, and 38 cm. The solid samples were homogenized and analyzed for total sulfur and carbon content (wt.%) using an induction furnace (ELTRA CS-2000) with a detection limit of 0.009% and a precision of ±5%. Soluble sulfates were analyzed using acid extraction with 40% HCl. Chemical composition for the first depth (1 cm) was analyzed using inductively coupled plasma atomic emission spectroscopy (ICP-AES). Samples collected at 1 cm depth were also analyzed using QEMSCAN® automated mineralogy to evaluate the degree of sulfide and carbonate liberation as well as probable sulfide coating. Solid chemical composition was analyzed by ICP-AES after the total digestion of samples using HNO3/Br2/HF/HCl. Some samples were analyzed using an aqua regia digestion, which yields a partial digestion of soluble minerals.

Leachate waters from the columns were analyzed for pH, Eh, electrical conductivity (EC), acidity, alkalinity, and chemical composition. The pH, Eh, and EC were analyzed using pH-Eh-conductivity meters. The acidity and alkalinity were analyzed using automated titration. The chemical composition of the leachates was analyzed using ICP-AES after sample acidification and filtration to 0.45μm with 2% HNO3. The soluble sulfates within the different leachates were analyzed using ionic chromatography with a precision of ±5%. For each analysis, a blank is analyzed, and randomly selected samples were analyzed as duplicates. Results of duplicate analysis showed a reproducibility of more than 95%.

The mineralogy of initial samples and the 1 cm depth dismantled fine fractions was studied using Quantitative Evaluation of Minerals by Scanning Electron Microscopy (QEMSCAN®). QEMSCAN is an automated mineralogy system allowing detailed investigation of the mineralogical composition of samples mounted in polished sections. This system allows for the quantification of mineralogical parameters such as modal mineralogy, mineral liberation, and mineralogical association. Initial samples (≤5 mm) were sized by wet screening to produce five particle size fractions as described in Elghali et al., (2018). Several polished sections were analyzed by particle size fraction to produce enough data for good statistical representation. A total of more

than 10000 grains were analyzed in fine fractions. The particle size fractions ≥5 mm were analyzed only using XRD. Furthermore, the computed tomography was used to determine the sulfide liberation for fractions ≥5 mm (Elghali et al., 2018).

Samples post kinetic tests were sized by wet screening and Ro-Tap sieve shaking to produce two fractions: < 300 µm and > 300 µm to evaluate sulfide coating in these two fractions. This was used to identify if there was any preferential oxidation of sulfides dependent on the PSD. The polished sections for each fraction were analyzed by particle mineralogy analysis (PMA) mode. Measurement resolution varied from 2.5 µm to 6 µm depending on the particle size.

4.4 Results and discussion

4.4.1 Results

4.4.1.1 Chemical and mineralogical characteristics of total, fine, and coarse fractions

<u>Chemical characterization</u>

Results of the chemical analyses of samples are summarized in Table 4.1. The chemical composition of studied samples is mainly composed by Si, Al, Fe, Na, Ca and K. Other elements such and C, S and Zn are marginally present. Silicon concentrations were > 28 wt. % for all nine samples (Table 1). Sulfur (totally as sulfide-sulfur) and carbon (totally as carbonate -carbon) concentrations were low compared to other elements. This is explained by the mineralogical composition of the tested lithologies which were mostly comprised of silicate minerals as is shown later. The only metals occurring in non-negligible concentrations within the samples were Fe, Al and Zn with concentrations around 2.5%, 8%, and 60 ppm, respectively. Additional details about the chemistry and distribution of elements can be found in Elghali et al. (2018).

Table 4.1 : ICP-AES and induction furnace chemical analyses of total, fine, and coarse fractions

		Concentrations (%)												
		C	Al	Ba	Ca	Fe	K	Mg	Mn	Na	S	Si*	Ti	Zn (ppm)
	Detection limit (ppm)	90	60	5	60	10	1	15	5	1	90	-	25	55
Lithology A	Total sample (< 5cm)	0.51	8.13	0.11	2.05	2.56	2.3	0.82	0.03	3.33	0.24	30.4	0.17	60.18
	Coarse fraction (> 2.4mm)	0.5	8.23	0.13	1.86	2.58	2.34	0.73	0.03	3.62	0.22	30.15	0.17	63.54
	Fine fraction (< 2.4mm)	0.68	7.95	0.15	2.82	3.04	2.54	0.93	0.04	2.92	0.29	29.31	0.2	78.04
Lithology B	Total sample (< 5cm)	0.26	8.3	0.06	2.27	4.41	2.17	1.81	0.05	2.78	0.48	29.4	0.32	84.06
	Coarse fraction (> 2.4mm)	0.35	8.42	0.07	1.99	4.32	2.18	1.69	0.05	2.86	0.47	29.17	0.3	84.09
	Fine fraction (< 2.4mm)	0.43	7.84	0.08	2.57	4.63	2.3	1.96	0.06	2.44	0.59	28.74	0.32	98.02
Lithology C	Total sample (< 5cm)	0.29	8.32	0.06	2.04	4.12	2.33	1.63	0.05	2.6	0.49	28.98	0.3	78.01
	Coarse fraction (> 2.4mm)	0.28	8.26	0.05	1.91	4.08	2.13	1.42	0.06	2.86	0.46	29.64	0.27	76.74
	Fine fraction (< 2.4mm)	0.49	8.17	0.07	2.47	4.5	2.5	1.57	0.07	2.47	0.56	28.37	0.29	86.04

Si: was analyzed using XRF whole rock analysis*

Mineralogical characteristics

The mineralogical composition of the studied samples was determined using QEMSCAN (Elghali et al., 2018). Figure 4.1 shows a summary of the mineralogical composition of the three lithologies. Sulfides consisted primarily of pyrite, as well as chalcopyrite, pyrrhotite, and sphalerite in trace amounts. Carbonate content was more significant within fine fractions (< 2.4 mm) for the three lithologies. Carbonates mainly occurred as calcite, but small concentrations of ankerite, dolomite, and rhodochrosite were found. The bulk mineralogical composition was dominated by non-sulfide gangue minerals, particularly quartz, albite, and muscovite.

Quantitatively, the 3 lithologies contained low sulfide contents (< 1 wt. %) and higher carbonate contents (>2.2 wt. %). The sulfide minerals are enriched in fine to mid-size fraction (+53 μm/-300 μm) (Figure 1). Carbonate contents decreased with the increase of the PSD. Sulfide contents were ~ 0.60 wt. %, 0.99 wt. %, and 1.04 wt. % for the lithologies A, B and C, respectively. Carbonate contents ranged from 3.2 wt. % to 5 wt. % for lithology A (Figure 4.1), from 2.2 wt. % to 4.30 wt. % for lithology B (Figure 4.1), and from 1.4 wt. % to 4.4 wt. % for lithology C (Figure 1). Furthermore, quartz and albite contents were > 20 wt. % and > 10 wt. %, respectively, for all studied samples. Micas contents varied between 11 wt.% and 28 wt. % for lithology A, 15 wt. % and 32 wt. % for lithology B, and 23 wt. % and 35 wt. % for lithology C. Other identified minerals, with content lower than 5 wt. %, included: orthoclase, rutile, barite, apatite, Fe-oxide/Goethite and ankerite/dolomite.
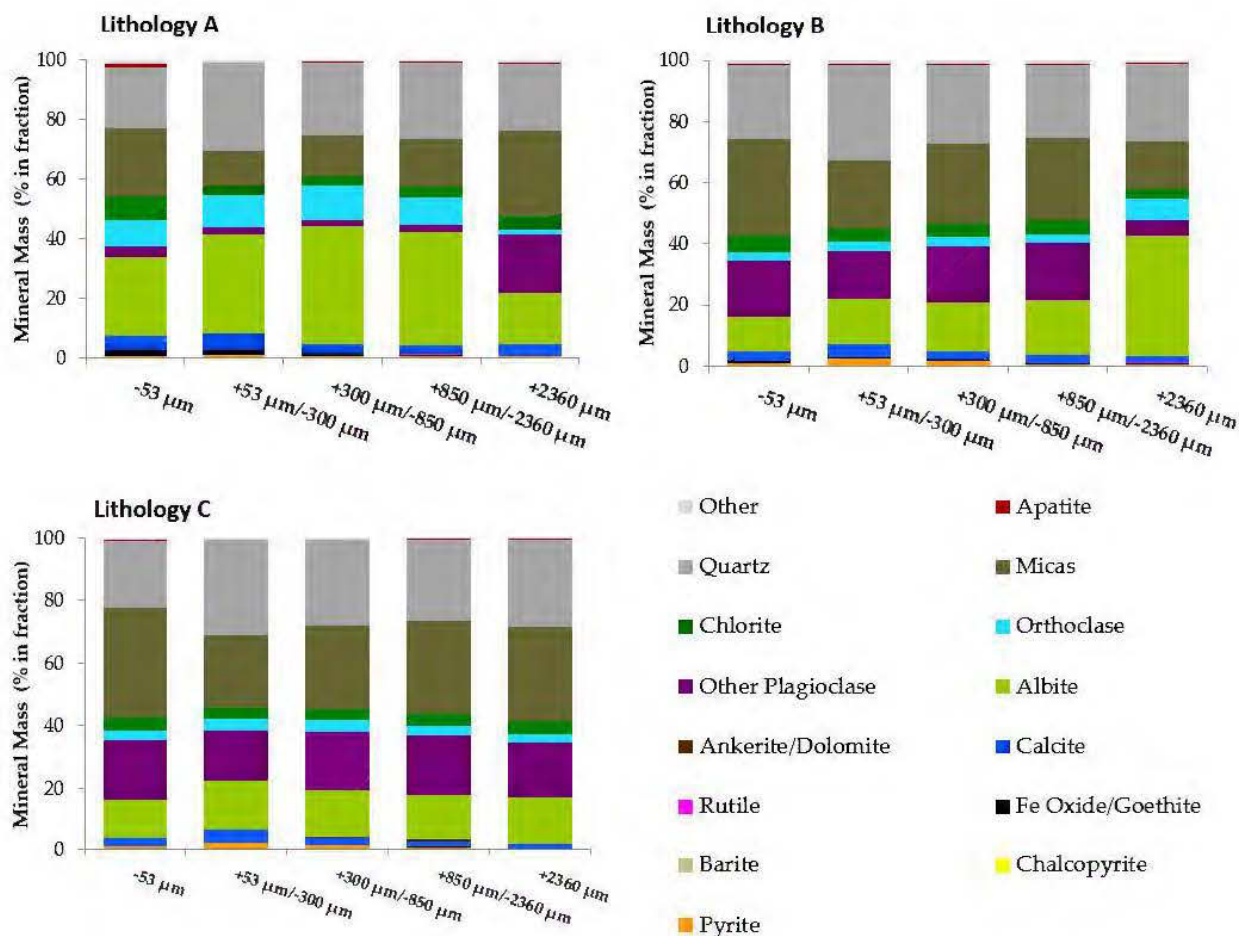
Figure 4.1: Mineralogical composition of the three lithologies

Calcium deportment

The mineralogical composition of the studied samples shows Ca occurring in four minerals: calcite ($CaCO_3$), albite ($(Na,Ca)AlSi_3O_8$), and apatite ($Ca_5(PO_4)_3F$). Figure 1S illustrates Ca deportment within the three waste rock lithologies. In lithology A (Figure 1S-A), Ca mainly occurs within carbonates (calcite); about 64% for the total sample, 78% for the finer sample, and 71% for the coarse sample. In lithology B (Figure 1S-B), only 36% of Ca comes from carbonates within the total sample, 51% for the finer sample, and 40% for the coarse sample. For lithology C (Figure 1S-C), 44% of Ca is associated with carbonates in the total sample, 71% in the fine sample, and 45% in the coarse sample.

Sulfur deportment

Sulfur within the studied waste rock was associated with pyrite and barite. The two minerals differ in their involvement in mine drainage processes. Figure 2S shows S deportment within the studied samples. For lithology A (Figure 2S-A), 88% of S mainly occurs within pyrite in the total sample, 81% within the fine sample, and 80% within the coarse sample. For lithology B (Figure 2S-B), approximately 97%, 93%, and 95% of S is associated with pyrite for the total, fine, and coarse samples, respectively. In lithology C (Figure 2S-C), 97.5%, 98%, and 97.8% of S is associated with pyrite for the total, fine, and coarse samples, respectively.

Mineral liberation degree

In terms of mineral distributions/associations and textures, carbonates and sulfides within the studied lithologies displayed different degrees of liberation with respect to the particle size fractions (Figure 4.2). The main conclusions drawn in the companion paper (Elghali *et al.*, 2018) were that the sulfide liberation degree became negligible for particle sizes above 2.4 mm; however, carbonate liberation was higher than that of sulfides for the same particle size. Furthermore, static tests (acid base accounting and net acid generation tests) performed on the three lithologies showed that they could mostly be classified as non-acid-generating, although some fractions were classified as uncertain with respect to their acid generation potential (Elghali *et al.*, 2018a). To confirm these static test predictions, column kinetic tests were performed.
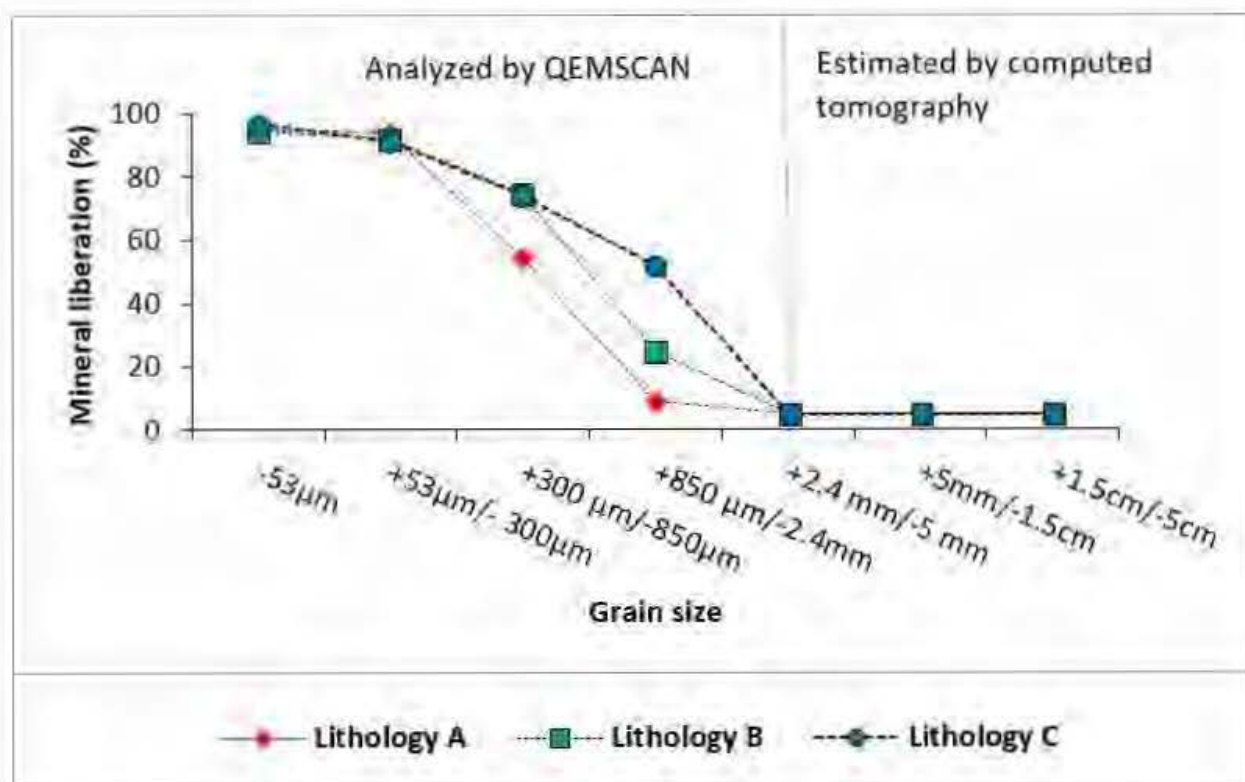
Figure 4.2 : Pyrite liberation degree within the three studied lithologies (adapted from Elghali et al., 2018)

4.4.1.2 Kinetic leaching tests

Chemical results from the column kinetic tests (543 days) in terms of leachate quality are illustrated in Figure 4.3, Figure 4.4 and Figure 4.5. Concentrations are presented as cumulative, mass-normalized releases (mg/kg) to allow for comparison of chemical release rates in the different samples (due to different sample weights in the column tests). Evolution of pH values (A) showed the same behavior for all nine samples, with circumneutral values (between 7.5 and 8.5). Lithology A samples showed higher pH values than lithologies B and C. For each lithology, fine fraction samples showed lower pH values than total samples and coarse samples. Electric conductivity (Figure 4.3B) varied considerably depending on sample particle size and lithology. The coarse samples showed the lowest EC values, while total samples showed medium values and fine samples showed the highest values. Average EC values were around 1000 µS/cm for fine samples, 60 µS/cm for coarse samples, and 220 µS/cm for total samples. Redox potential (Figure 4.3C) was higher than 200 mV for all samples, suggesting oxidizing conditions. Alkalinity results (Figure 4.3D) showed the same tendancy as EC; alkalinity was the highest for leachates from fine samples. The average alkalinity was smiliar for coarse and total samples at around 19 mg CaCO$_3$/L.

However, for fine samples, the average alkalinity was variable depending on the lithology and equal to 49 mg CaCO₃/L for lithology A, 57 mg CaCO₃/L for lithology B, and 83 mg CaCO₃/L for lithology C.
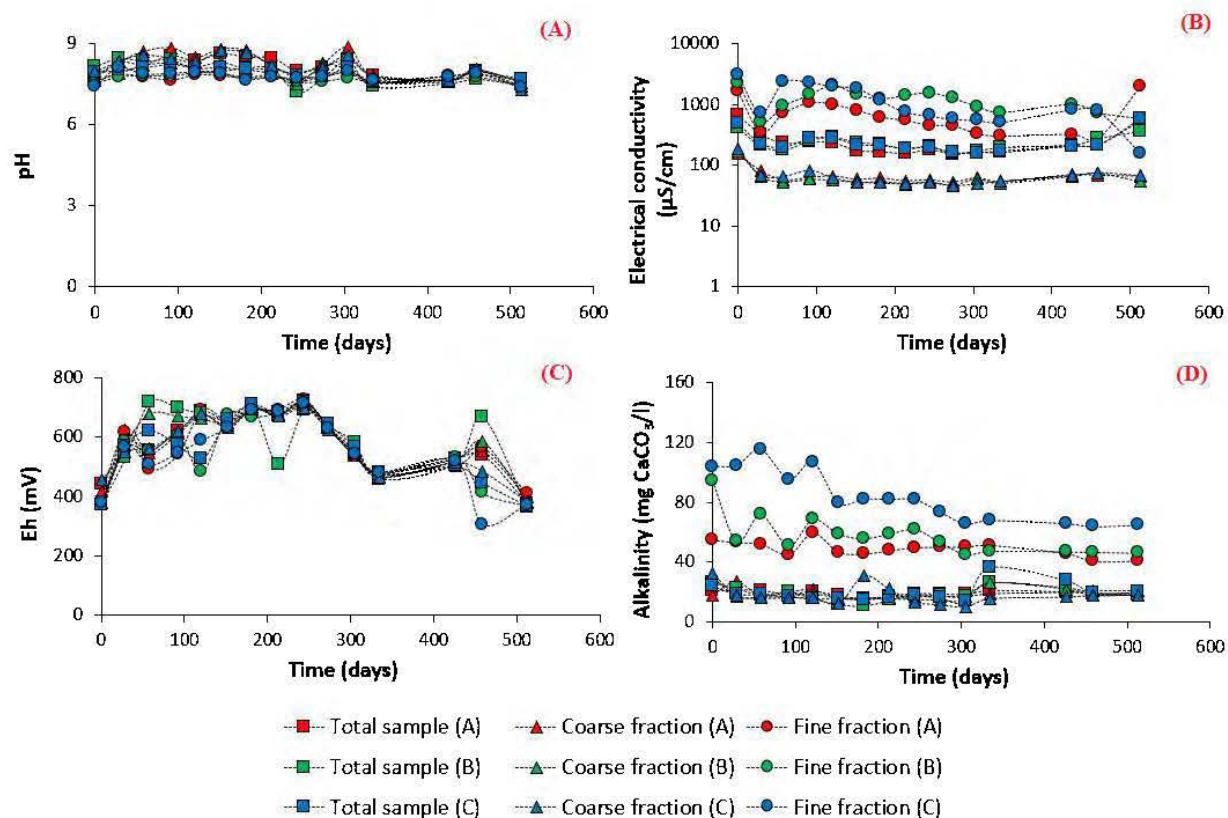
Figure 4.3: Evolution of pH, EC, Eh and alkalinity within the different columns

Calcium, magnesium, and manganese were chosen to indicate carbonate dissolution (Benzaazoua *et al.*, 2004c), while silicon was assumed to be indicative of alumino-silicate mineral dissolution. Calcium, which occurs mainly as calcite, is the most leachable element as compared to Mg, Mn, and Si within the different samples, and Mn concentrations (occurring within ankerite) were the lowest. After 543 days of leaching tests, cumulative Ca concentrations were (Figure 4.4A): 120 mg/kg for the total sample of lithology A, 66 mg/kg for the coarse fraction of lithology A, 238 mg/kg for the fine fraction of lithology A, 122 mg/kg for the total sample of lithology B, 33 mg/kg for the coarse fraction of lithology B, 529 mg/kg for the fine fraction of lithology B, 123 mg/kg for the total sample of lithology C, 37 mg/kg for the coarse fraction of lithology C and 461 mg/kg for the fine fraction of lithology C. Magnesium and manganese showed the same behavior as Ca, but at lower concentrations according to their initial concentrations in the solid samples. Silicon

leaching was low compared to Ca leaching (Figure 4.4D) in agreement with findings in the literature; Si leaching was less than 8.5 mg/kg for total samples and coarse fraction samples, and less than 23 mg/kg for fine fraction samples.
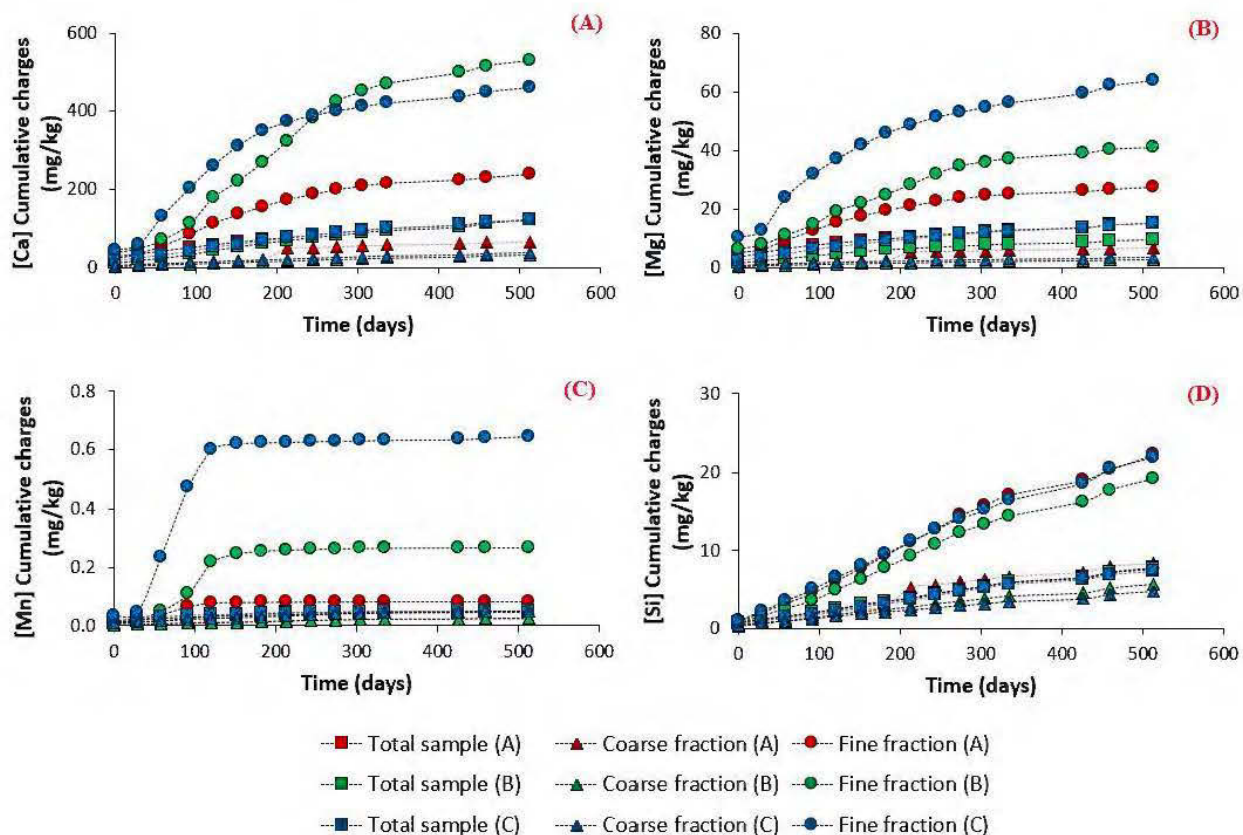
Figure 4.4: Calcium, magnesium, manganese and silicon load in the studied samples

Sulfate, iron, and zinc leaching from the column tests is illustrated in Figure 4.5. Sulfates, iron, and zinc (from sulfide oxidation) were leached in high concentrations from the fine samples relative to the coarse samples and total samples. After 543 days of leaching tests, total sulfates released (Figure 4.5A) were about 262 mg/kg for the total sample of lithology A, 28 mg/kg for the coarse sample of lithology A, 493 mg/kg for the fine sample of lithology A, 2 mg/kg for the total sample of lithology B, 29 mg/kg for the coarse sample of lithology B, 1277 mg/kg for the fine sample of lithology B, 257 mg/kg for the total sample of lithology C, 32 mg/kg for the coarse sample of lithology C and 959 mg/kg for the fine sample of lithology C. Iron was leached in small concentrations (Figure 4.5B). Iron was leached more in the fine samples (maximum of 0.16 mg/kg

cumulative concentration). As expected, Zn was leached more in the fine samples (Figure 4.5C); the maximum cumulative concentration was 0.5 mg/kg for the fine sample of lithology C.
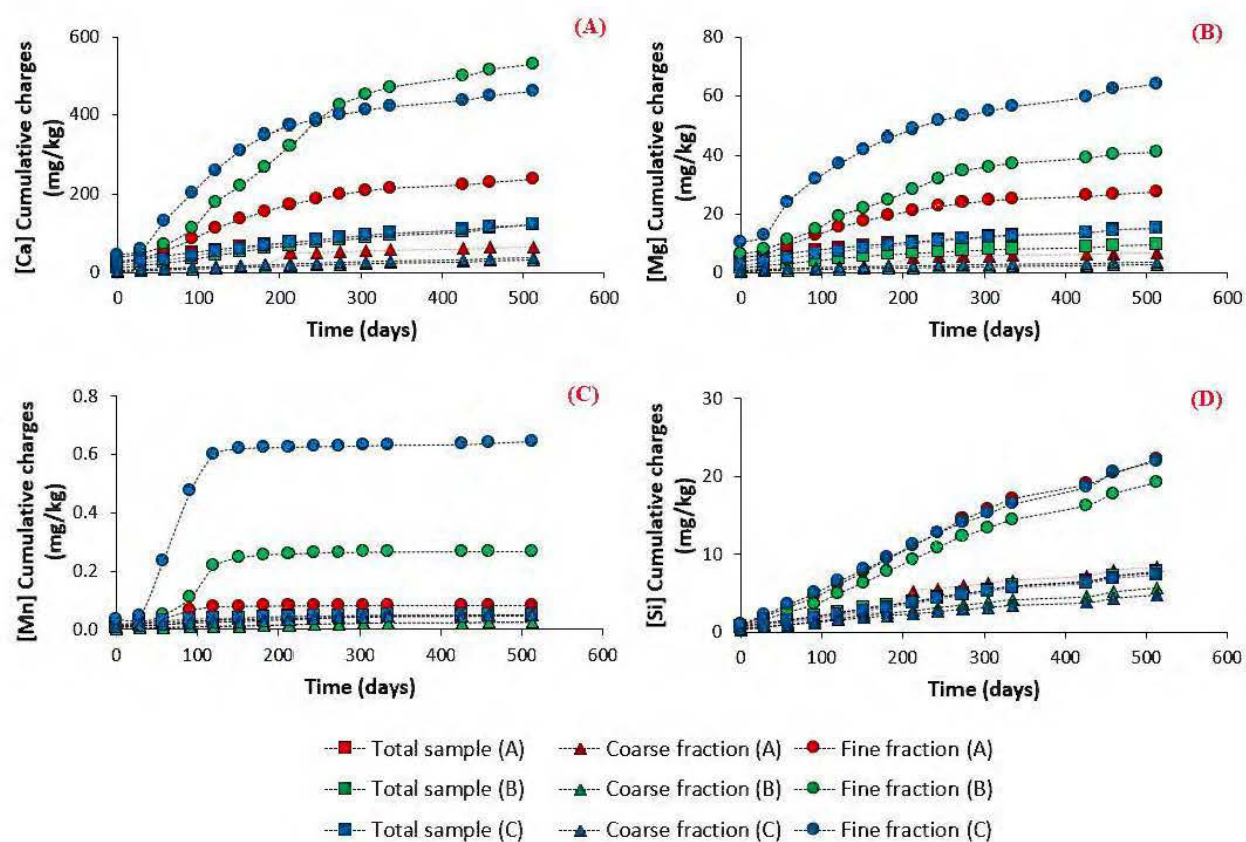
Figure 4.5: Sulfates, iron, and zinc load within the studied samples

4.4.1.3   Columns dismantlement results

Characterization of post-testing samples allowed for interpretation of the geochemical behavior and confirmation of assumptions. Only columns containing the fine samples for each lithology were dismantled and analyzed for total S, inorganic C, and sulfates. Results of the dismantlement are illustrated in Figure 3S. The vertical profile of inorganic C concentrations showed a small variation between the top and bottom of the columns. Carbon concentrations ranged between 0.69% and 0.75% for lithology A, 0.40% and 0.44% for lithology B, and 0.46% and 0.50% for lithology C (Figure 3S-A). The total S profiles (Figure 3S-B) showed small variations. Total S concentrations ranged from 0.18 wt. % to 0.23 wt. % for lithology A, from 0.53 wt. % to 0.64 wt. % for lithology B, and from 0.49 wt. % to 0.56 wt. % for lithology C. Since initial sulfate concentrations within solid samples were below the limit of detection, sulfate analyses indicated

sulfide oxidation and, more specifically, secondary mineral precipitation. The results of sulfate analyses for the three columns showed low concentrations, which indicate a low sulfide oxidation rate at the short time scale (cf Section 2). Sulfate concentrations were less than 0.023 wt. % for the three lithologies (Figure 3S-C).

Automated mineralogical characterization was performed on dismantled samples to evaluate sulfide coating. Automated mineralogical characterization (QEMSCAN) of fine samples confirmed that carbonate and pyrite liberation degree depended on particle size (Figure 4.6). In general, pyrite liberation was low within fractions > 300 μm, but carbonate liberation was higher for the same particle size. This means that there is more available neutralization potential than available acid generation potential within the three lithologies, which leads to the characterization of the long-term geochemical behavior of these lithologies as non-acid-generating. Furthermore, the alkalinity generated by fine fractions was greater than that generated by the total or coarse fraction samples during kinetic testing. Carbonates were less encapsulated (more reactive) when compared to sulfides for the coarse fractions (> 300 μm). Their encapsulation degrees (0–10% liberated) were about 52%, 26%, and 41% for lithologies A, B, and C, respectively. For fractions < 300 μm, carbonate encapsulation was about 2.50%, 4.40%, and 4.10% for lithologies A, B, and C, respectively. Sulfides were more encapsulated for fractions > 300 μm, and more liberated for fractions < 300 μm. For fractions > 300 μm, pyrite encapsulation was about 81%, 94%, and 77% for samples A, B, and C, respectively. However, for fractions < 300 μm, pyrite encapsulation was about 2.3%, 3.2%, and 0.8% for samples A, B, and C, respectively. Particle maps produced by QEMSCAN and backscattered-electron images showed that pyrite was encapsulated within non-sulfide gangue minerals for particle sizes > 300 μm. However, in fine fractions (< 300 μm), some pyrite grains were coated with a fine layer of iron oxides. The coating width was about 2–10 μm (Figure 4.7) and pyrite had a particle size of about 20–60μm. The proportion of coated pyrite was estimated to be between 5% and 22% depending on the lithology (using QEMSCAN data). This coating was not observed within the initial unweathered samples.
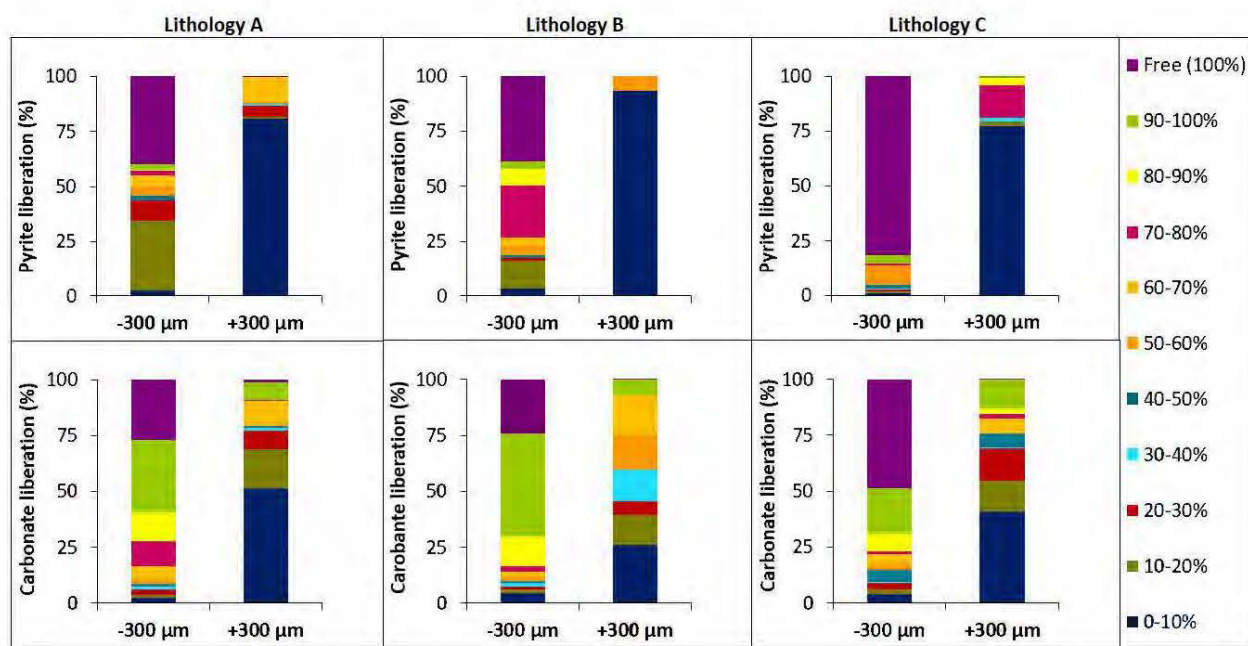
Figure 4.6: Liberation degree of carbonate and pyrite in fine (< 2.4 mm) samples post-dismantlement
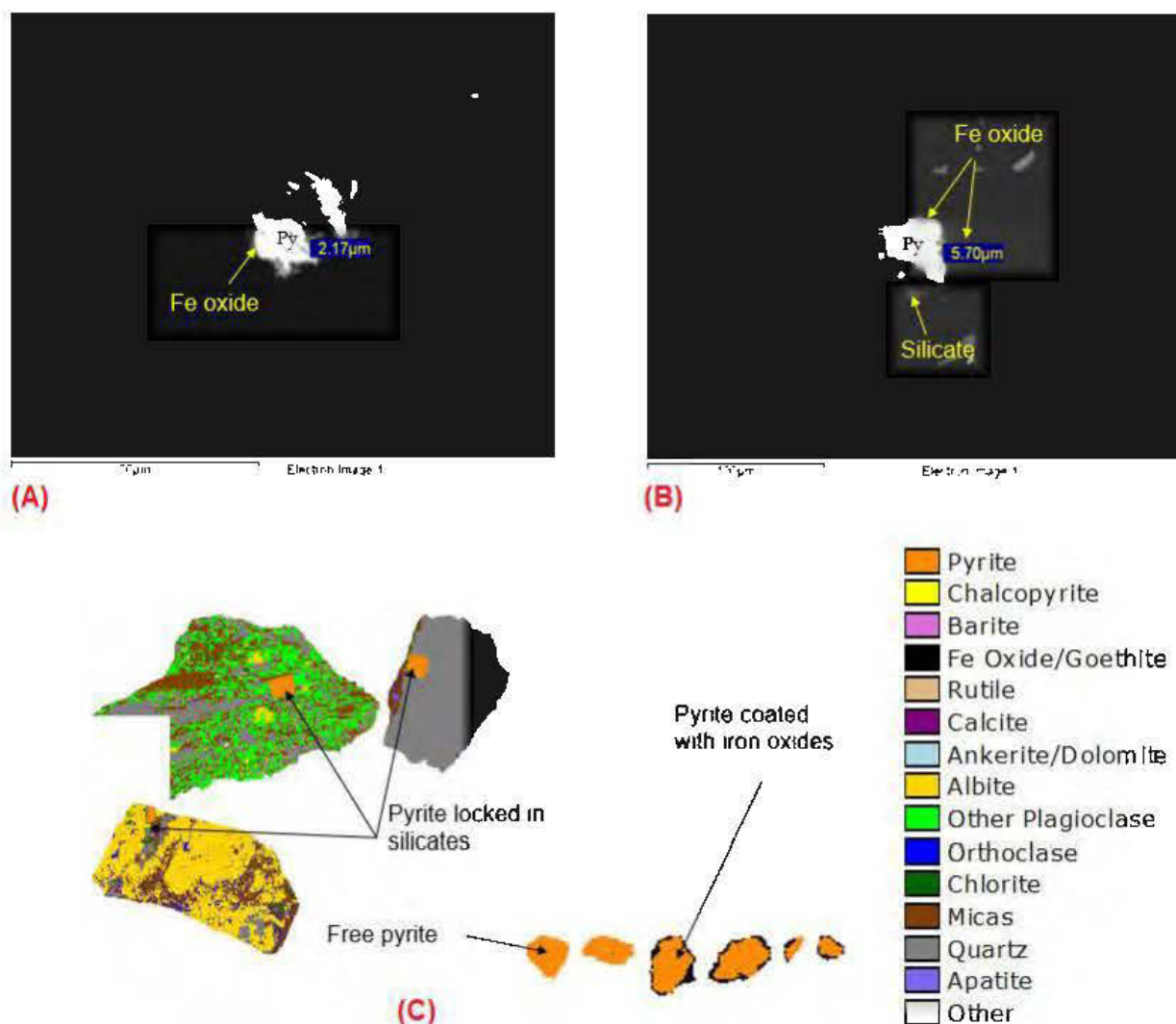
Figure 4.7: A, B: backscattered-electron images for fine (< 2.4 mm) samples of lithology A; and C: false particle map showing an example of pyrite coating with iron oxides and free pyrite for lithology A

4.4.2 Discussion

Waste rock samples B and C could be considered to have similar lithologies, as they presented comparable mineralogical and chemical properties. Lithology A was slightly different in terms of sulfide and carbonate contents. In fact, lithology A was characterized by the highest carbonate content and the lowest sulfide content. These mineralogical and chemical differences influenced the geochemical responses in the kinetic tests performed on the three samples of each lithology. In general, these three lithologies are considered as non-acid-generating in the short-term since the leachate pH values were between 7 and 8 for the duration of the column tests. Additionally,

concentrations of Fe and Zn (Figure 4.8) collected immediately after each leaching cycle never exceeded environmental criteria (Directive 019 in Québec). With respect to the reactivity of these samples, the kinetic tests showed that the fine fractions of each lithology were the most reactive and mainly responsible for the overall geochemical behavior of the total sample. Table 4.2 summarizes the oxidation rates calculated for each sample over a period of 543 days. These results clearly show that the reactivity of the fine fractions is greater than that of the total samples and coarse fractions, regardless of the type of lithology. Based on the pyrite oxidation rates presented in table 2, the fine fraction was two times more reactive than the total sample for lithology A, five times more reactive for lithology B, and four times more reactive for lithology C. This explains the high EC and alkalinity values observed within fine fractions as compared to total samples and coarse fractions for all of the lithologies.

Moreover, calculated pyrite oxidation rates for the nine studied samples were: 4.8 µmol/kg/day, 2.5 µmol/kg/day, and 0.3 µmol/kg/day for the fine, total, and coarse samples, respectively of lithology A; 12.5 µmol/kg/day, 2.4 µmol/kg/day, and 0.27 µmol/kg/day for the fine, total, and coarse samples, respectively of lithology B; and 9.4 µmol/kg/day, 2.5 µmol/kg/day, and 0.3 µmol/kg/day for the fine, total, and coarse samples, respectively of lithology C. These results confirmed the conclusions drawn from the study by Erguler *et al.*, (2015), who tested the overall effect of PSD on waste rock reactivity. Furthermore, calculated depletion times (

Table 4.2) were approximately three times longer for carbonates than for sulfides.

Long-term predictions of geochemical behavior for the nine samples were performed using the oxidation/neutralization curves proposed by Benzaazoua et al., (2004), which use Ca+Mg+Mn releases as a tracer of neutralizing minerals dissolution, and sulphate releases as a tracer of sulfide oxidation. In this method, the initial concentrations in the solid samples are projected onto the graph Ca+Mg+Mn vs SO42- and the sample is classified as acid-generating if it is located on the side of sulphates and non-acid-generating if it is located on the side of Ca+Mg+Mn (Villeneuve et al., 2009). However, manganese was not used in this study as a neutralizing element because of its capacity to be hydrolyzed (Bouzahzah et al., 2015; Jambor et al., 2002; Lapakko, 1994). Therefore, only calcium and magnesium were used for the long-term prediction. Another issue related to the initial composition of solid samples consists of the use of total digestion analysis for projection. This assumes that the reactive minerals (sulfides and carbonates) will react completely on a long-term scale. However, only soluble minerals and exposed parts of the sulfides and carbonates will be able to react. In this study, two ways are suggested to solve this issue: i) use results of an aqua regia digestion, which gives a partial digestion of solid samples, and/or ii) correction of the total digestion results with mineral liberation data. Oxidation/neutralization curves for the nine samples are shown in Figure 4S. The three types of projections (total digestion, aqua regia digestion, and chemistry corrected by mineral liberation) showed that the different studied samples are classified as non-acid-generating regardless of the type of projection used. This is explained by the high NP of the studied samples compared to their AP.

Since the three fine fraction samples of each lithology are characterized by a different liberation degree of sulfides and carbonates, Ca and S leaching rates were different for each sample. Calcium and sulfur concentrations were normalized to the initial mass of Ca and S for each sample to avoid the effect of initial chemical/mineralogical differences. Calcium and sulfur concentrations were recorded over the kinetic test period and plotted against the liberation degree of carbonates and sulfides, respectively. The linear regressions for both elements are displayed in Figure 4.9 and show a high correlation coefficient between S leaching and pyrite liberation degree on one side and between Ca leaching and carbonate liberation degree on the other side. Indeed, the correlation coefficient between S leaching and sulfide liberation was 0.95; the correlation coefficient between Ca leaching and carbonate liberation was 0.93. These results confirm and complement previous conclusions of other studies which demonstrated that sample particle size greatly influences

reactivity (Amos et al., 2015; Brough et al., 2017; Erguler et al., 2015; Lapakko et al., 2006; Smith et al., 2000), but in this study, the quantitative aspect of the effect of mineral liberation on the geochemical behavior of mine waste rock is highlighted as an important factor controlling mineral reactivity.
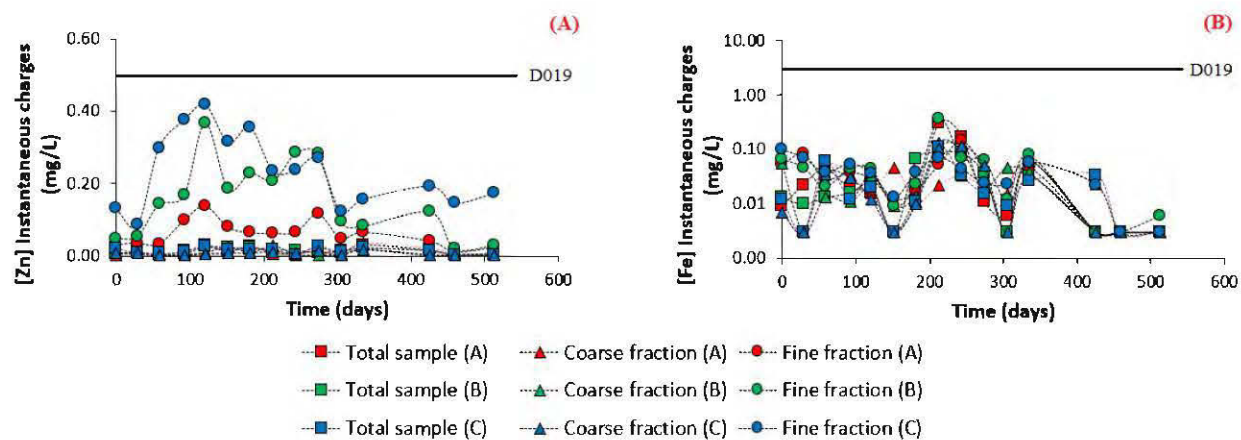
Figure 4.8: Instantaneous Zn and Fe concentrations within the studied samples

Table 4.2 : Results of sulfide oxidation rate, oxidation/neutralization curves and S/Ca depletion

Lithology	Sample	Sulfide oxidation rate (µmol/kg/day)	Oxidation/neutralization curves		Sulfur depletion curves			Calcium depletion curves		
			R^2	Slope	R^2	Slope	Depletion (year)	R^2	Slope	Depletion (year)
A	< 2.4 mm	**4.84**	0.998	0.55	0.88	-1E-04	2739	0.89	-2E-05	13698
	< 5 cm	2.50	0.999	0.56	0.96	< 5E-05	5479	0.97	-9E-06	30441
	> 2.4 mm	0.26	0.913	3.26	0.97	-3E-06	91324	0.87	-7E-06	39139
B	< 2.4 mm	**12.46**	0.996	0.445	0.92	-1E-04	2740	0.93	-4E-05	6849
	< 5 cm	2.43	0.977	0.539	0.96	-3E-05	9132	0.98	-1E-05	27397
	> 2.4 mm	0.27	0.995	1.298	0.96	-3E-06	91324	0.99	-3E-06	91324
C	< 2.4 mm	**9.41**	0.993	0.585	0.85	-9E-05	3044	0.81	-3E-05	9132
	< 5 cm	2.45	0.999	0.530	0.96	-3E-05	9132	0.97	-1E-05	27397
	> 2.4 mm	0.30	0.988	1.120	0.96	-4E-07	684932	0.99	-3E-07	913242
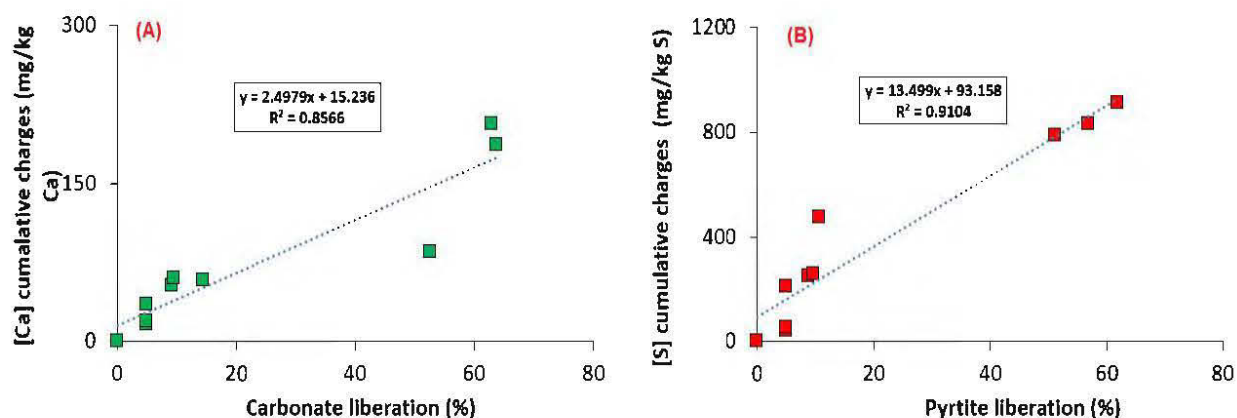
Figure 4.9: Projection of Ca leached vs carbonate liberation (A) and S leached vs. pyrite liberation (B)

4.4.3 Methodological guide for waste rock characterization and management

Considering these results, which confirm the conclusions of Elghali et al., (2018), a new method for waste rock management is suggested in which waste rock could be separated into two fractions with extremely different reactivities. This could be accomplished by defining the DPLS of a waste rock, which is a critical particle size that delimits the reactive fraction of a given sulfide-bearing waste rock (Elghali et al., 2018). For this parameter, fractions smaller than the DPLS are largely responsible for the reactivity of the total sample, while the larger fraction has a minimal effect. Therefore, this parameter could be used to separate waste rock prior to the construction of conventional waste rock piles. This technique could considerably reduce the costs associated with waste rock pile reclamation and management in cases where the waste rock contains a higher sulfur content.

The proposed methodology for waste rock management is illustrated in Figure 4.10. This proposed methodology consists of sampling materials in the field (< 5 cm) after blasting operations to consider the particle size distribution. The collected samples should be separated into several fractions; then submitted to chemical assays and static tests to evaluate the acid-generating potential of these fractions. Acid base accounting and net acid generation tests are two of the most used tests for these purposes. Next, the fine fractions (< 5 mm) should be characterized using an

automated mineralogy system, while the coarse fractions (> 5 mm) should be characterized using computed tomography to evaluate sulfide liberation. Subsequently, the DPLS can be defined (Elghali et al., 2018). Using this diameter and based on the results of static tests, kinetic tests could be performed to evaluate the reactivity of samples under the defined DPLS, above the defined DPLS, and for the total sample. Thus, the results from automated mineralogical analyses and computed tomography could be confirmed.
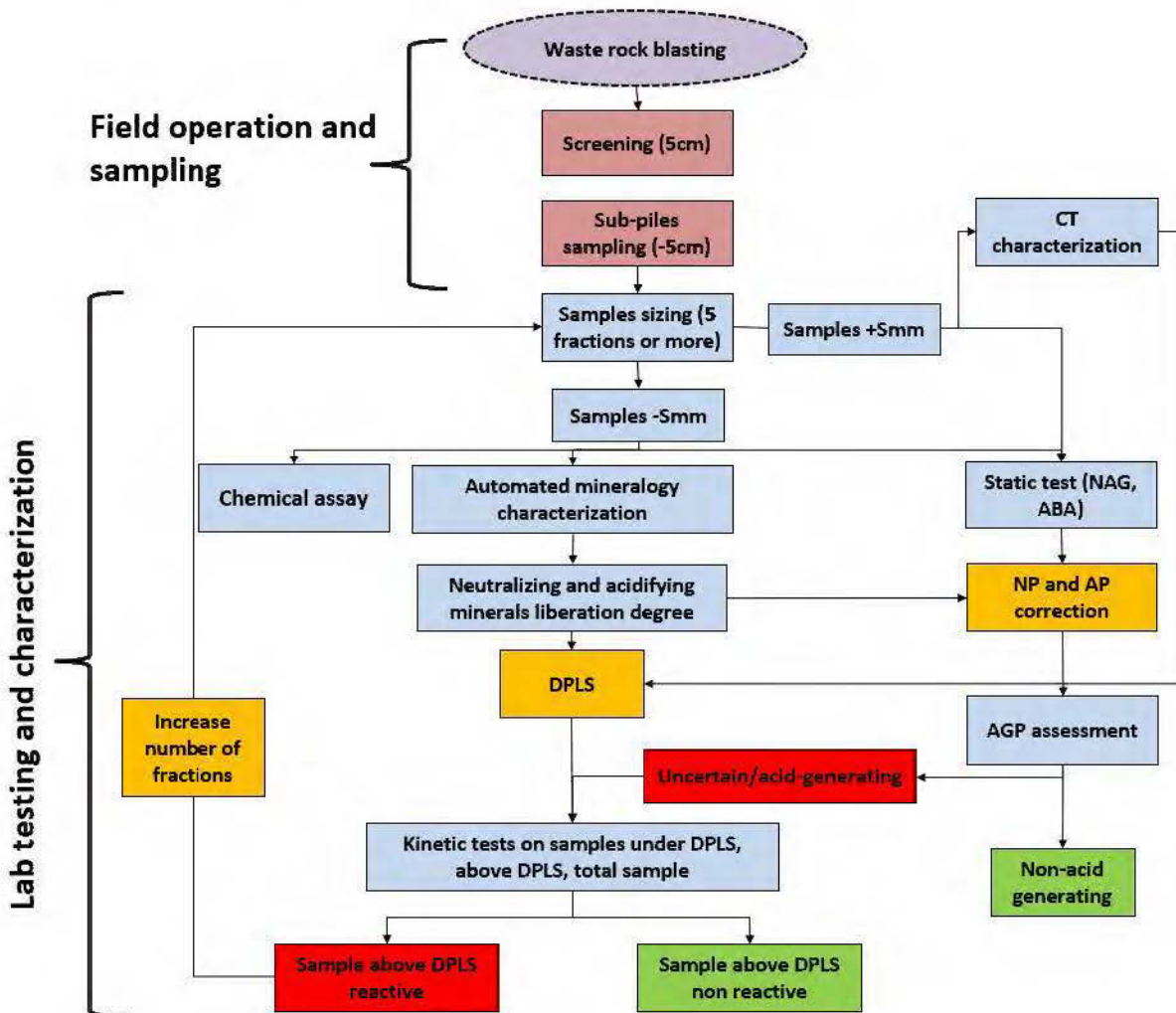
Figure 4.10: Proposed methodology for waste rock characterization for environmental purposes

4.5 Conclusion

The main objectives of this study were to confirm that 2.4 mm is the diameter of physical locking of sulfides within the three studied lithologies and to evaluate the geochemical behavior of these

lithologies through kinetic testing. The results showed that fine fractions are the most sulfidic and where mineral liberation is higher relative to coarser fractions. The three studied lithologies showed similar geochemical behaviors. Within the three studied samples, carbonate contents were higher than sulfide contents, which explains the neutral behavior observed during the 534-day kinetic test. However, sulfide oxidation rates and species release rates were completely different depending on the sample (< 2.4 mm, > 2.4 mm, < 5 cm). The sulfide oxidation rate was higher for lithologies B and C than for lithology A due to their initial sulfide contents. Sulfide content was significant within lithologies B and C, which are considered to have the same petrogenesis (greywackes).

With respect to the effect of particle size distribution, fine fractions (< 2.4 mm) showed high oxidation rates compared to coarse fractions (> 2.4 mm) and to total samples (< 5 cm) due to different degrees of sulfide mineral liberation. Fine fractions were characterized by high sulfide mineral liberation compared to total samples. The samples containing only fractions > 2.4 mm showed very low oxidation rates and low species release rates due to their low sulfide mineral liberation. Linear regressions of sulfate releases vs sulfide mineral liberation and Ca release vs carbonate mineral liberation showed correlation coefficients; about 0.95 for sulfates and 0.93 for calcium. The two equations established for mineral liberation (sulfides and carbonates) and species release (Ca and S) could be used as a tool for predicting species leaching for samples with known carbonate and sulfide mineral liberation.

Acknowledgements

References

Amos, R. T., Blowes, D. W., Bailey, B. L., Sego, D. C., Smith, L., & Ritchie, A. I. M. (2015). Waste-rock hydrogeology and geochemistry. *Applied Geochemistry, 57,* 140-156.

Aubertin, M., Fala, O., Molson, J., Chouteau, M., Anterrieu, O., Hernandez, M. A., Chapuis, R. P., Bussière, B., Lahmira, B., & Lefebvre, R. (2008). *Caractérisation du comportement hydrogéologique et géochimique des haldes à stériles.* Paper presented at the Proceedings: Symposium.

Bailey, B. L., Blowes, D. W., Smith, L., & Sego, D. C. (2016). The Diavik Waste Rock Project: Geochemical and microbiological characterization of low sulfide content large-scale waste

rock test piles. *Applied Geochemistry, 65,* 54-72. doi:http://dx.doi.org/10.1016/j.apgeochem.2015.10.010

Benzaazoua, M., Bussière, B., Dagenais, A.-M., & Archambault, M. (2004). Kinetic tests comparison and interpretation for prediction of the Joutel tailings acid generation potential. *Environmental Geology, 46*(8), 1086-1101. doi:10.1007/s00254-004-1113-1

Blowes, D., Ptacek, C., Jambor, J., & Weisener, C. (2003). The geochemistry of acid mine drainage. *Treatise on geochemistry, 9,* 612.

Blowes, D., Ptacek, C., Jambor, J., Weisener, C., Paktunc, D., Gould, W., & Johnson, D. (2014). The geochemistry of acid mine drainage.

Blowes, D., Moncur, M., Smith, L., Sego, D., Bennet, J., Garvie, A., Linklater, C., Gould, D., & Reinson, J. (2006). *Construction of two large-scale waste rock piles in a continuous permafrost region.* Paper presented at the Proceedings-7th International Conference on Acid Rock Drainage (ICARD). St Louis. Mo. US.

Blowes, D. W., Jambor, J. L., & Alpers, C. N. (1994). *The environmental geochemistry of sulfide mine-wastes* (Vol. 22): Mineralogical Association of Canada.

Bouzahzah, H., Benzaazoua, M., Plante, B., & Bussiere, B. (2015). A quantitative approach for the estimation of the "fizz rating" parameter in the acid-base accounting tests: A new adaptations of the Sobek test. *Journal of Geochemical Exploration, 153,* 53-65. doi:http://dx.doi.org/10.1016/j.gexplo.2015.03.003

Brough, C., Strongman, J., Bowell, R., Warrender, R., Prestia, A., Barnes, A., & Fletcher, J. (2017). Automated environmental mineralogy; the use of liberation analysis in humidity cell testwork. *Minerals Engineering, 107,* 112-122.

Bussière, B., Aubertin, M., Zagury, G. J., Potvin, R., & Benzaazoua, M. (2005). *Principaux défis et pistes de solution pour la restauration des aires d'entreposage de rejets miniers abandonnées.* Paper presented at the Symposium 2005 sur l'environnement et les mines.

Bussière, B., Demers, I., Dawood, I., Plante, B., Aubertin, M., Peregoedova, A., Pepin, G., Lessard, G., Intissar, R., & Benzaazoua, M. (2011). *Comportement géochimique et hydrogéologique des stériles de la mine Lac Tio.* Paper presented at the Proceedings of the Symposium sur l'Environnement et les Mines, Rouyn-Noranda, CD-Rom, CIM, Montreal.

Caldeira, C. L., Ciminelli, V. S. T., Dias, A., & Osseo-Asare, K. (2003). Pyrite oxidation in alkaline solutions: nature of the product layer. *International Journal of Mineral Processing, 72*(1–4), 373-386. doi:http://dx.doi.org/10.1016/S0301-7516(03)00112-1

Egiebor, N. O., & Oni, B. (2007). Acid rock drainage formation and treatment: a review. *Asia-Pacific Journal of Chemical Engineering, 2*(1), 47-62.

Elghali, A., Benzaazoua, M., Bouzahzah, H., Bussière, B., & Villarraga-Gómez, H. (2018). Determination of the available acid-generating potential of waste rock, part I: Mineralogical approach. *Applied Geochemistry, 99,* 31-41. doi:https://doi.org/10.1016/j.apgeochem.2018.10.021

Elghali, A., Benzaazoua, M., Bussière, B., Kennedy, C., Parwani, R., & Graham, S. (2019). The role of hardpan formation on the reactivity of sulfidic mine tailings: A case study at Joutel

mine (Québec). *Science of The Total Environment, 654*, 118-128. doi:https://doi.org/10.1016/j.scitotenv.2018.11.066

Erguler, Z. A., & Kalyoncu Erguler, G. (2015). The effect of particle size on acid mine drainage generation: Kinetic column tests. *Minerals Engineering, 76*, 154-167. doi:10.1016/j.mineng.2014.10.002

Helt, K. M., Williams-Jones, A. E., Clark, J. R., Wing, B. A., & Wares, R. P. (2014). Constraints on the genesis of the Archean oxidized, intrusion-related Canadian Malartic gold deposit, Quebec, Canada. *Economic Geology, 109*(3), 713-735.

Jambor, J. (1994). Mineralogy of sulfide-rich tailings and their oxidation products. *Environmental geochemistry of sulfide mine-wastes, 22*, 59-102.

Jambor, J., Dutrizac, J., Groat, L., & Raudsepp, M. (2002). Static tests of neutralization potentials of silicate and aluminosilicate minerals. *Environmental Geology, 43*(1-2), 1-17.

Jamieson, H. E., Walker, S. R., & Parsons, M. B. (2015). Mineralogical characterization of mine waste. *Applied Geochemistry, 57*, 85-105. doi:10.1016/j.apgeochem.2014.12.014

Lapakko, K. A. (1994). *Evaluation of neutralization potential determinations for metal mine waste and a proposed alternative.* Paper presented at the Proceeding: of the Third International Conference on the Abatement of Acidic Drainage, April.

Lapakko, K. A., Engstrom, J. N., & Antonson, D. A. (2006). *Effects of particle size on drainage quality from three lithologies.* Paper presented at the Poster paper presented at the 7th International Conference on Acid Rock Drainage (ICARD).

Lefebvre, R., Hockley, D., Smolensky, J., & Gélinas, P. (2001). Multiphase transfer processes in waste rock piles producing acid mine drainage: 1: Conceptual model and system characterization. *Journal of Contaminant Hydrology, 52*(1–4), 137-164. doi:http://dx.doi.org/10.1016/S0169-7722(01)00156-5

Lindsay, M. B. J., Condon, P. D., Jambor, J. L., Lear, K. G., Blowes, D. W., & Ptacek, C. J. (2009). Mineralogical, geochemical, and microbial investigation of a sulfide-rich tailings deposit characterized by neutral drainage. *Applied Geochemistry, 24*(12), 2212-2221. doi:https://doi.org/10.1016/j.apgeochem.2009.09.012

Lindsay, M. B. J., Moncur, M. C., Bain, J. G., Jambor, J. L., Ptacek, C. J., & Blowes, D. W. (2015). Geochemical and mineralogical aspects of sulfide mine tailings. *Applied Geochemistry, 57*, 157-177. doi:10.1016/j.apgeochem.2015.01.009

McLemore, V. T., Donahue, K. M., Phillips, E., Dunbar, N., Walsh, P., Gutierrez, L. A., Tachie-Menson, S., Shannon, H. R., Lueth, V. W., & Campbell, A. R. (2006). *Characterization of Goathill North Mine Rock Pile, Questa Molybdenum Mine, Questa, New Mexico.* Paper presented at the International Conference of Acid Rock Drainage (ICARD). ASMR, St. Louis.

Nordstrom, D. K. (2000). Advances in the hydrogeochemistry and microbiology of acid mine waters. *International Geology Review, 42*(6), 499-515.

Nordstrom, D. K. (2009). Acid rock drainage and climate change. *Journal of Geochemical Exploration, 100*(2–3), 97-104. doi:http://dx.doi.org/10.1016/j.gexplo.2008.08.002

Nordstrom, D. K., & Southam, G. (1997). Geomicrobiology of sulfide mineral oxidation. *Reviews in mineralogy, 35,* 361-390.

Nordstrom, D. K., Blowes, D. W., & Ptacek, C. J. (2015). Hydrogeochemistry and microbiology of mine drainage: An update. *Applied Geochemistry, 57,* 3-16.

Paktunc, A. (1999a). Mineralogical constraints on the determination of neutralization potential and prediction of acid mine drainage. *Environmental Geology, 39*(2), 103-112.

Paktunc, A., & Davé, N. (2000). *Mineralogy of pyritic waste rock leached by column experiments and prediction of acid mine drainage.* Paper presented at the In: Rammlmair D (ed.) Applied Mineralogy, pp. 621–623. Balkema.

Paktunc, A. D. (1999b). Characterization of mine wastes for prediction of acid mine drainage *Environmental impacts of mining activities* (pp. 19-40): Springer.

Parbhakar-Fox, A., Lottermoser, B., Hartner, R., Berry, R. F., & Noble, T. L. (2017). Prediction of Acid Rock Drainage from Automated Mineralogy *Environmental Indicators in Metal Mining* (pp. 139-156): Springer.

Petruk, W., & Lastra, R. (1993). Evaluation of the recovery of liberated and unliberated chalcopyrite by flotation columns in a copper cleaner circuit. *International Journal of Mineral Processing, 40*(1), 137-149. doi:https://doi.org/10.1016/0301-7516(93)90046-D

Poisson, J., Chouteau, M., Aubertin, M., & Campos, D. (2009). Geophysical experiments to image the shallow internal structure and the moisture distribution of a mine waste rock pile. *Journal of Applied Geophysics, 67*(2), 179-192.

Smith, K. S., Ramsey, C. A., & Hageman, P. L. (2000). *Sampling strategy for the rapid screening of mine-waste dumps on abandoned mine lands*: US Department of the Interior, US Geological Survey.

Smith, L. J., Bailey, B. L., Blowes, D. W., Jambor, J. L., Smith, L., & Sego, D. C. (2013). The Diavik Waste Rock Project: Initial geochemical response from a low sulfide waste rock pile. *Applied Geochemistry, 36,* 210-221.

Villeneuve, M., Bussière, B., Benzaazoua, M., & Aubertin, M. (2009). Assessment of interpretation methods for kinetic tests performed on tailings having a low acid generating potential. *Proceedings, Securing the Future and 8th ICARD, Skelleftea, Sweden.*

CHAPITRE 5   ARTICLE 3: THE ROLE OF HARDPAN FORMATION ON THE REACTIVITY OF SULFIDIC MINE TAILINGS: A CASE STUDY AT JOUTEL MINE (QUÉBEC)

A. Elghali[1], M. Benzaazoua[1], B. Bussière[1], C. Kennedy[2], R. Parwani[3], S. Graham[4]

[1] Université du Québec en Abitibi Témiscamingue, 445 Boul. Université, Rouyn-Noranda, Québec, J9X 5E4, Canada

[2] Agnico Eagle Mines Ltd. 145 King St. East, Suite 400 - Toronto, ON, Canada M5C 2Y7

[3] Carl Zeiss Microscopy, LLC One Zeiss Drive Thornwood, NY 10594,

[4] Carl Zeiss Microscopy Limited, 509 Coldhams Lane Cambridge, CB1 3JS, United Kingdom

5.1 Abstract

The former Eagle and Telbel mine site (hereafter referred to as Joutel mine), located near the town of Joutel in the Nord-du-Québec (Canada) houses a tailings storage facility (TSF) that has been inactive since 1996. Fresh, unweathered tailings (beneath 10−30 cm of oxidized horizon) are characterized by an average sulfide content of 6 - 7 wt.% and an average Fe-Mn-carbonate content of 20−40 wt.%. The oxidation of Joutel's tailings under atmospheric conditions resulted in the precipitation of secondary phases such as ferric oxyhydroxides and gypsum. Accumulation of these secondary phases throughout the TSF caused cementation and agglomeration of grains, which decreased the porosity of the material in a horizon below the surface. This horizon, which is referred to as hardpan, is frequently encountered within fine, reactive tailings. Characterizations showed that hardpans have a highly compact texture. The formation of hardpans limits vertical water infiltration and oxygen diffusion and these layers greatly affect the global geochemical behavior of underlying tailings in the Joutel TSF by protecting the unweathered material from oxidation. As a result, the water quality of the TSF is largely controlled by the reactivity of the upper oxidized tailings horizon.

Joutel's oxidized tailings showed an acidic behavior early during laboratory kinetic leaching tests despite the near absence of sulfides and neutralizing minerals. However, when unweathered tailings were added under oxidized tailings, the water became neutral and metal leaching rates were reduced. After over a year of laboratory leaching tests, hardpans formed within the columns and the natural phenomenon was reproduced under laboratory conditions.

Key words: Hardpan, oxidized tailings, kinetic tests, secondary phases, acid mine drainage, Joutel mine site.

5.2 Introduction

Mining operations generate large volumes of finely crushed rock, commonly referred to as tailings. The reactivity of tailings can result in acidic, highly charged drainage waters (Blowes et al., 2014; Paktunc, 1999). Acid mine drainage (AMD) is essentially caused by the oxidation of sulfide minerals (in the presence of oxygen and water) when there is an insufficient neutralization potential to buffer acid produced. The neutralization potential of tailings is mainly determined by their carbonate content (e.g., calcite, dolomite) (Blowes et al., 2003).

During oxidation, neutralization, and hydrolysis reactions, various secondary minerals may precipitate (Evangelou & Zhang, 1995; Lapakko, 2002; Maest & Nordstrom, 2017; Nordstrom et al., 2015), with the most common being ferric oxyhydroxides, gypsum, and iron sulfates (e.g., jarosite) (Holmström & Öhlander, 2001; Quispe et al., 2013). The mineralogical composition of the secondary minerals in oxidized tailings depends on the pH, dissolved metal concentrations, and complexing ligands (Jönsson et al., 2006; Nordstrom, 1982). Numerous studies focused on the role of secondary phases in the natural attenuation of contaminants in mine drainages (e.g., Bowell, 1994; Coston et al., 1995; Gilbert et al., 2003b; McGregor et al., 1998; Schroth & Parnell Jr, 2005; Webster et al., 1998). These attenuation phenomenon are largely attributable to mechanisms including: sorption, co-precipitation, substitution, and other processes (DeSisto et al., 2011).

Under certain specific conditions, the accumulation of secondary precipitates can lead to the formation of cemented layers, or hardpans. Hardpans are formed naturally within exposed, reactive sulfidic tailings and to a lesser extent within waste rocks that contain fine particles (Hakkou et al.,

2008; Meima et al., 2007). Currently, hardpan formation in reactive tailings is thought to occur due to the oxidation of sulfides, which encourages carbonate dissolution and, in turn, favors the precipitation of ferric oxyhydroxides, gypsum, and sulfate phases (Benzaazoua et al., 2004; Blowes et al., 1991; Carbone et al., 2013; DeSisto et al., 2011; Graupner et al., 2007; Sracek et al., 2010). The accumulation of secondary phases is enhanced by evaporation cycles and by seasonal fluctuations in the water table. These reactions play an important role in mineral agglomeration and cementation (Meima et al., 2007). The mineralogical composition of hardpans varies from one site to another and depends on the initial physical, chemical, and mineralogical properties of the reactive tailings. The different mineralogical compositions of hardpans studied in the literature are presented in Table 5.1. Normally, hardpans are naturally formed beneath the surface of reactive tailings and their depths depend on the water table level (Blowes et al., 1991). In tailings storage facilities (TSFs), hardpans may occur as continuous or discontinuous layers depending on the topography of the site (Blowes et al., 1991). Hardpan thickness varies from a few millimetres to several centimetres, and varies by location (Alakangas & Öhlander, 2006; DeSisto et al., 2011; Graupner et al., 2007).

Table 5.1 : Mineralogical composition of hardpans

Mineralogical composition	Site	Country	Reference
Gypsum, ferric oxyhydroxides, primary minerals (sulphides, quartz, carbonates)	Joutel	Canada	Elghali et al. (2017)
Gypsum, jarosite, ferric oxyhydroxy-sulphates	Monto Romero	Spain	Quispe et al. (2013)
Hematite, gypsum	Chambishi and Mindolo	Zambia	Sracek et al. (2010)
Jarosite, gypsum, ferric oxyhydroxides	Muenzbachtal	Germany	Graupner et al. (2007)
Thermonatrite, calcite, Na-sulphates, aragonite, Si-O gels, amorphous phases, burkeite, glaserite, Al-hydroxydes, hematite, magnetite	Not indicated	Not indicated	Meima et al. (2007)
Gypsum, goethite, jarosite, sulphides	Nickel rim, Fault lake, East mine	Canada	McGregor and Blowes (2002)
Fe-Mn-oxyhydroxides	Stekenjokk	Sweden	Holmström and Öhlander (2001)
Ferrihydrite, goethite, lepidocrocite, jarosite, melanterite, gypsum, anglesite	Waite Amulet, Heath Steele	Canada	Blowes et al. (1991)

The mobility of contaminants can be reduced considerably as a result of hardpan formation. Ferric oxyhydroxides are known for their capacity to adsorb and co-precipitate a large amount of heavy metals such as Al, Cu, Zn, and As (Acero et al., 2006; Appleton Jr et al., 1989; Benjamin & Leckie, 1981a, 1981b; Zhang et al., 1992). Therefore, hardpans generally have higher heavy metal concentrations than fresh tailings (Elghali et al., 2017; Lottermoser & Ashley, 2006; McGregor & Blowes, 2002).

Due to the precipitation of novel secondary phases, the physical characteristics of hardpans differ from those of their parent material, particularly in terms of porosity, hydraulic conductivity, and specific gravity (McGregor et al., 2002). Hardpans are characterized by low porosities and hydraulic conductivities compared to the initial tailings due to the cementation of grains (Ahn et al., 2011). Consequently, hardpan formation in TSFs may influence the geochemical behavior of wastes in several ways:

i. Reducing oxygen fluxes: hardpans can act as a barrier to oxygen ingress due to their low porosity and higher saturations (Blowes et al., 1991; DeSisto et al., 2011; Gilbert et al., 2003a).

ii. Inhibiting or minimizing water infiltration: due to the low hydraulic conductivity of hardpans, they can minimize infiltration of water into underlying unweathered tailings (Blowes et al., 1991; McGregor et al., 2002). When hardpans form, the hydrological balance is modified. In general, vertical infiltration is reduced and (sub-)surface runoff is enhanced.

iii. Reducing the reactivity of sulfides within hardpans: during hardpan formation, novel secondary phases precipitate and cover the surfaces of sulfide minerals (Kang et al., 2016; V. Nicholson et al., 1990). These secondary phases decrease the rate of oxygen diffusion to the mineral's reactive core.

The main objective of this study was to highlight the effect of hardpan formation on the reactivity of tailings, considering the mineralogical, hydrogeological, and chemical variability between oxidized and unweathered tailings. Understanding hardpan formation may help to explain why, in some cases, laboratory kinetic tests do not accurately predict geochemical behaviors observed under field conditions.

5.3 Site description and conceptual model

5.3.1 Joutel mine

Joutel mine is a closed gold mine located approximately 195 km north of Val d'Or in the Nord-du-Québec (Québec, Canada, Figure 1S). The mine was in operation from 1974 to 1994 and the gold

was contained in a sulfide deposit of mainly pyrite and pyrrhotite (Barnett et al., 1982; Blowes et al., 1998). The ore was provided from the Eagle and Telbel mines and gold was extracted by bulk sulfide flotation followed by concentrate regrinding-cyanidization (Blowes et al., 1998). The tailings were deposited in a 120-ha TSF that was divided into two zones. The northern zone (Zone 2) was used from 1974 to 1986 and the southern zone (Zone 1) was used from 1986 to 1993. The northern zone has a relative elevated topography compared to the southern zone (Agnico-Eagle Mines Ltd).

The geochemistry of the Joutel tailings was first studied by Blowes et al. (1998) and Benzaazoua et al. (2004). Initial tests in these studies suggested that the net acid-generating potential of the tailings was uncertain. Kinetic tests (humidity cells) on unweathered and oxidized tailings confirmed that, in the long-term, most of the tailings samples would be non-acid-generating, with acid-generating occurring only in localized areas (Benzaazoua et al., 2004). The results also identified a high spatial variability in the tailings' chemical and mineralogical characteristics. Recently, paste pH was measured in the field using the supernatant waters in several important areas of the impoundment (Elghali et al., 2017).

5.3.2 Hypothesis and conceptual model

The main hypothesis of this study is that hardpans may act as a barrier against vertical water infiltration and oxygen diffusion. Therefore, leachates form oxidized tailings are not mixed with the neutral pore water of the unweathered tailings below. Acidity is produced at the upper tailings layer due to iron secondary phases, some residual sulphides and potentially with bacterial activity. Blowes et al (1998) demonstrated the presence of *T. thiooxidans* and *T. ferrooxidans* and neutrophilic sulphur-oxidizing bacteria at Joutel mine site.

The conceptual model that could explain hardpan formation and acidity generation in some localized zone in the TSF of Joutel mine is presented in the Figure 5.1. The global geochemistry of Joutel tailings can be explained by four stages:

- Stage 1 consists of tailings freshly deposited at the TSF where the water table was elevated, and fresh tailings were immersed or protected from oxygen by their elevated water

saturation. At this stage, sulphides oxidation was very low or absent due to the elevated water table.

- During stage 2, the water table dropped, and the previously saturated tailings became partially desaturated and consequently exposed to atmospheric conditions (water and oxygen). Sulphide oxidation started, with subsequent carbonate dissolution. During these reactions of oxidation/neutralization, secondary minerals were precipitated, like gypsum and ferric oxyhydroxides (Cravotta III, 2008b). At the beginning of this process of sulphides oxidation/carbonate neutralization, only the upper surface of TSF was oxidized. Then, the chemical oxidation of sulphides was considerably accelerated by bacterial activity (Baker & Banfield, 2003; Blowes *et al.*, 2003; Dold, 2017; Nordstrom *et al.*, 1997; Silverman, 1967). At this stage, water table fluctuation delimited the vadose zone and vertical water infiltration took place. During the first years of sulphides oxidation, the global geochemical behavior of tailings was neutral due to presence of sufficient carbonate content compared to sulphide content.

- During stage 3, oxygen migrated to deeper tailings and thus the oxidized horizon became thicker. More sulphide oxidation favors more secondary phase precipitation which accumulate locally over time. Water cycles led to hardpan formation, in some specific conditions regarding water table position and geochemical profile. Within hardpan samples, secondary phases were cementing grains. This cementation reduces the available porosity and protect residual sulphide minerals from oxygen diffusion (McGregor *et al.*, 2002). The textural and mineralogical properties of mature hardpan considerably influence its hydrogeological properties and could be considered as low hydraulic conductivity layer as assumed in previous studies (Blowes *et al.*, 1991; DeSisto *et al.*, 2011; McGregor *et al.*, 2002). Therefore, hardpan occurrence influences the water balance on Joutel TSF. Indeed, the vertical infiltration of water is inhibited or at least limited by hardpan presence, and so deviated to surface and sub-surface runoff. Furthermore, hardpan could limit the oxygen diffusion to the unweathered tailings (Kohfahl *et al.*, 2011). This stage corresponds to the present geochemical situation of Joutel mine site.

- During stage 4, hardpan formation will be almost formed at the entire TSF. At this stage, sulphides and carbonates will be completely depleted and the acidity could be generated for

years due to residual acidity from secondary phases like the ferric oxyhydroxides and Fe-sulphates (Cravotta III, 1994) and the high hydraulic residence time of water.
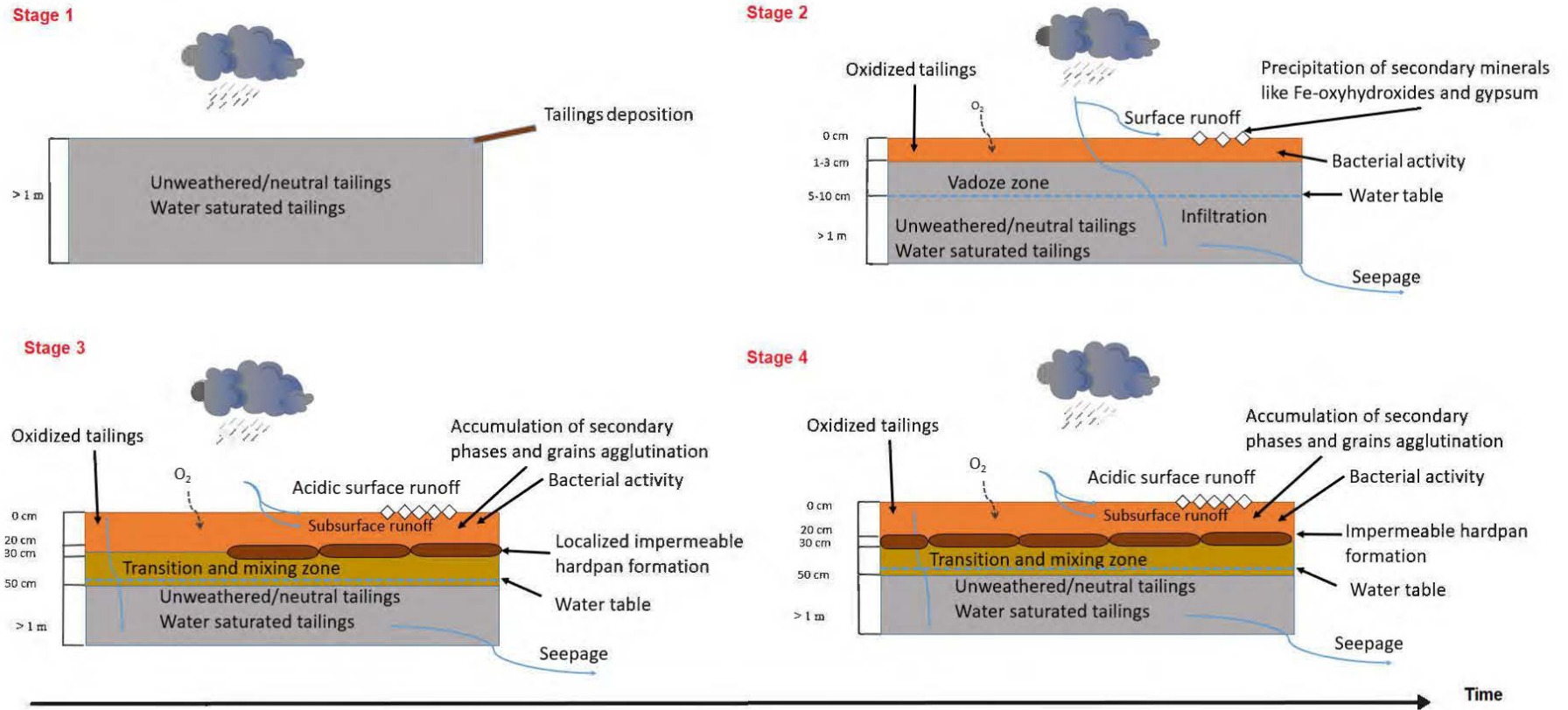
Figure 5.1 : Conceptual model illustrating the reactivity of Joutel's tailings

5.4 Materials and methods

5.4.1 Tailings sampling and preparation

The tailings samples used in this study were collected in acidic zones of the TSF (based on the paste pH of the upper layer tailings). Using trenches (figure 2S), samples from oxidized, hardpan, and unweathered layers were collected at different depths and locations. Distinctions between the different tailings horizons were made using visual indicators (such as color). The vertical profile of the tailings was heterogeneous, and hardpans occurred as discontinuous layers throughout the TSF, except a few locations. In certain locations, hardpan thickness exceeded 80 cm and it occurred as stratified layers. All samples were homogenized in the laboratory and composite samples were prepared for each tailings horizon.

The unweathered (non-oxidized) samples from the south zone are named J1-NO and those from the north zone are named J2-NO. While the oxidized samples from the south zone are named J1-Oxy and those from the north zone are named J2-Oxy, and the hardpan sample from the south and north zone hardpans are named respectively Hardpan 1 and Hardpan 2.

5.4.2 Physical, chemical, mineralogical and hydrogeological characterization

Tailings particle size was analyzed using a Malvern Mastersizer S laser analyzer. The specific gravity (Gs) was evaluated using micromeritics Helium Pycnometer (Astm, 2000), and the specific surface area (SSA) was analyzed with a micromeritics analyzer using the B.E.T. method (Nelsen & Eggertsen, 1958).

Solid chemical composition was analyzed by inductively coupled plasma (ICP-AES) after a total digestion of samples using $HNO_3/Br_2/HF/HCl$. Total sulphur and inorganic carbon were analyzed using induction furnace (ELTRA CS-2000) (CEAEQ, 2006). Chemical composition of columns leachates was analyzed using ICP-AES on acidified samples with 2% HNO_3. Acidity and alkalinity were evaluated using automatic titrator. pH, Eh and electrical conductivity of leachates from columns and tank leaching tests (TLT) were analyzed using pH/Eh/conductivity meters.

Mineralogical composition of studied samples was studied by X-ray diffraction using a Bruker AXS D8 Advance X-ray diffractometer equipped with a Cu anticathode, scanning over a diffraction angle (2θ) range from 5° to 70°. Scan settings were a 0.005° 2θ step size and a four-second counting

time per step. The DiffracPlus EVA software (v.9.0 rel. 2003) was used to identify mineral species and the TOPAS software (v 2.2) implementing was used to quantify the abundance of all identified mineral species (Rietveld, 1969). The absolute precision of this quantification method is ±0.5–1% per cent.

Saturated hydraulic conductivity (k_{sat}) of the oxidized and unweathered tailings was evaluated using a rigid-wall compaction-mold permeameter (ASTM-D5856-95, 2002). It was predicted as well using the particle size properties of samples and their specific gravity (Gs) (Mbonimpa *et al.*, 2002). The water retention curves of the oxidized and unweathered tailings were also evaluated using a pressure extractor (ASTM-D-6836-02, 2008) and the experimental curves were fitted using van Genuchten model (Van Genuchten, 1980). The air entry value (AEV) was estimated using the graphical method (Fredlund & Xing, 1994).

5.4.3 Porosity analysis

There are several methods that allow measuring or evaluating the porosity (qualitatively and quantitatively) of porous media. In this study, an innovative technique based on X-ray tomography was preferred due to the compact texture of the hardpan samples. The hardpan samples were imaged non-destructively using the ZEISS Xradia 520 Versa X-ray Microscope at Carl Zeiss X-Ray Microscopy in Pleasanton, CA. The resulting 2D projections were back-projected into a 3D volume using the manufacturer's software with a Gaussian filter (0.7 strength). A cropped volume of the resulting 3D dataset was segmented to estimate connected and internal porosity using grayscale intensity-based segmentation implemented in DragonFly Pro V3.1 software (ORS, Montreal, Canada).

5.4.4 Static Tests

Acid potential (AP) of oxidized and unweathered samples were calculated using sulphur sulphides which is the difference between total sulphur and sulphates. Neutralization potential (NP) was analyzed using the titration method as described in Bouzahzah et al. (2015) and calculated based on carbonates content (Lawrence & Wang, 1996; Sobek *et al.*, 1978a). The net neutralization potential (NNP) is defined as the difference between the NP and AP of the sample; the neutralization potential ratio (NPR) is defined as the ratio between the NP and the AP of the sample. The sample is considered as acid-generating if its NNP is lower than -20 Kg $CaCO_3$/t, non-acid-

generating if its NNP is higher than 20 Kg $CaCO_3$/t, and uncertain if its NNP is between -20 and 20 Kg $CaCO_3$/t (Bouzahzah *et al.*, 2015a). Using NPR criteria, the sample is considered as acid-generating if its NPR is under 1, non-acid-generating if its NPR is higher than 2 and uncertain if its NPR is between 1 and 2 (Bouzahzah *et al.*, 2015a).

5.4.4.1 Column and tank leaching tests

Two kinetic column tests were performed for each TSF zone. The first scenario consisted of using only oxidized tailings to simulate surface and sub-surface water runoff due to the presence of hardpan (C1 for the southern zone and C3 for the northern zone). The second scenario consisted of using oxidized tailings above unweathered tailings to simulate vertical infiltration in the absence of hardpans (C2 for the southern zone and C4 for the northern zone). The samples were placed into Plexiglas columns with a 14 cm inner diameter and 1 m height (Benzaazoua et al., 2004; Bussière, 2007), and compacted to reach a porosity of 0.4. The base of the columns was equipped with a ceramic plate to control the water table level and inhibit air entry (Bussière et al., 2004). The columns were equipped with rubber joints, and column walls were covered with silicone grease to avoid preferential flow paths. Column C1 was filled with 16 cm of oxidized tailings from the southern zone and C3 contained 30 cm of oxidized tailings from the northern zone. C2 contained 16 cm of oxidized tailings over 35 cm of unweathered tailings from the southern zone, and C4 contained 30 cm of oxidized tailings over 40 cm of unweathered tailings from the northern zone. The column design was based on visual observations of vertical tailings profiles made during the sampling step. Each column was flushed monthly with 2 L of deionized water, which was left in contact with the tailings for four hours before the columns were allowed to drain. Leachates were collected and analyzed for their chemical composition. The columns were leached over 13 wetting-drainage cycles, lasting a total of 386 days. At the end, the four columns were dismantled using color and texture contrasts to separate layers. These solids were analyzed for inorganic C, total S, and paste pH.

Tank leaching tests (TLT) were designed to evaluate the contaminant diffusion potential through a solid matrix. The release of various chemical species from hardpan samples was assessed using tank leaching tests (Coussy et al., 2012; Nen, 2004; Taha et al., 2017). The TLT protocol consisted of leaching a monolithic block of hardpan with deionized water in a closed reactor with a total

renewal of leachates at predefined time intervals. Hardpan samples were carved into specimens with known external surface areas. The liquid/solid ratio was 10 cm3 for each exposed 1 cm² of sample. Leachates were collected and renewed after 6 hours, 1 day, 2.25 days, 4 days, 9 days, 16 days, 36 days, and 64 days. The leachates were analyzed for pH, EC, acidity/alkalinity, and chemical composition using ICP-AES..

5.5 Results

5.5.1 Physical properties

The physical properties of the samples were highly variable (Table 5.2). The northern zone showed a finer particle-size distribution compared to the southern zone. The D60, which corresponds to 60% passing on the cumulative particle-size distribution curve, was 16 μm for J2 NO and 88 μm and for J1-NO. The D60 was 11.71 μm for J2-Oxy and 13.2 μm for J1-Oxy. The D90, which corresponds to 90% passing on the cumulative particle-size distribution curve, was 32.54 μm for J2-NO and 163.57 μm for J1-NO. The D90 was 38.69 μm for J2-Oxy and 37.15 μm for J1-Oxy. Physical differences between the oxidized and unweathered samples were significant, but the most notable difference was in the SSA (Table 5.2). The SSA was 14.41 m2/g for J2-NO and 0.7 m2/g for J1-NO, while the SSA was 49.3 m2/g for J2-Oxy and 38.07 m2/g for J1-Oxy. The Gs values of oxidized samples were lower than those of the unweathered samples; 3.04 g/cm3 and 3.35 g/cm3 for J2-NO and J1-NO, respectively, and 2.97 g/cm3 and 2.83 g/cm3 for J2-Oxy and J1-Oxy, respectively.

Table 5.2 : Physical, chemical, mineralogical properties and static tests results of the studied samples

Physical characteristics			
D60 (µm)	D90 (µm)	SSA (m²/g)	Gs
J1-Oxy 13.2	37.15	38.07	2.83
J1-NO 87.6	163.57	0.7	3.35
J2-Oxy 11.71	38.69	49.3	2.97
J2-NO 15.57	32.54	14.41	3.04

Chemical composition (%)							
	Al	Ca	Mn	Mg	Fe	S	Zn	Cu
J1-Oxy	3.62	3.82	0.12	0.05	20.17	3.90	0.01	LD
Hardpan 1	2.61	3.26	0.39	0.47	25.39	5.42	0.011	0.003
J1-NO	1.50	3.53	0.74	1.75	25.78	6.39	0.011	LD
J2-Oxy	4.00	2.00	0.39	0.10	25.26	2.64	0.0096	LD
Hardpan 2	2.29	3.41	0.72	0.10	26.73	6.37	LD	LD
J2-NO	4.02	4.35	0.42	1.36	20.00	7.26	0.0161	LD

Mineralogical composition (%)				
	Sulphides	Carbonates	Fe-Oxides	Gypsum	Others
J1-Oxy	ND	1.76	23.74	19.30	55.20
Hardpan 1	3	19.60	9.70	14.90	52.80
J1-NO	7.4	42.15	ND	ND	50.45
J2-Oxy	0.33	1.07	24.80	20.50	53.30
Hardpan 2	5.5	24.2	18.20	10.40	41.70
J2-NO	7.26	19.8	ND	11.44	61.50

Static tests				
NP (titration) (Kg CaCO₃/t)	NP (carbonates) (Kg CaCO₃/t)	AP (Kg CaCO₃/t)	NNP (Kg CaCO₃/t)	NPR
J1-Oxy 3	20	5.5	-2.5	0.5
J1-NO 228	538	193.2	35.1	1.2
J2-Oxy 9	25	0.73	8.8	13.0
J2-NO 96	193	169	-73	0.6

5.5.2 Chemical and mineralogical properties

The chemical and mineralogical properties of oxidized, unweathered, and hardpan samples are summarized in Table 5.2. Chemical results revealed differences depending on sample location and depth within the TSFs. The Fe content in all samples exceeded 20 wt.%; it was approximately 25 wt.%, 27 wt.%, and 20 wt.% for the J2-Oxy, Hardpan 2, and J2-NO samples, respectively. In the southern zone samples, Fe concentrations were 20.17 wt.%, 25.50 wt.%, and 26 wt.% for the J1-Oxy, Hardpan 1, and J1-NO samples, respectively. Total sulfur was around 2.50 wt.%, 6.5 wt.%, and 7.50 wt.% for the J2-Oxy, Hardpan 2, and J2-NO samples, respectively. Similarly, total sulfur was around 4 wt.%, 5.50 wt.%, and 6.50 wt.% for the J1-Oxy, Hardpan 1, and J1-NO samples, respectively. The Ca content was between 2 wt.% and 4.50 wt.% for all samples.

The oxidized samples J1-oxy and J2-Oxy were, respectively, comprised of approximately 42 wt.% and 45 wt.% of secondary minerals (primarily, ferric oxyhydroxides and gypsum). Sulfides were below 0.5 wt.% in J2-Oxy and not detected in J1-Oxy. Carbonates (mainly siderite and ankerite) were detected in more significant concentrations than sulfides. Carbonate contents were around 1.7 wt.% and 1 wt.% for J1-Oxy and J2-Oxy, respectively.

Unweathered tailings had completely different mineralogical compositions. Sulfide contents (mainly pyrite) were 7.40 wt.% and 7.30 wt.% for J1-NO and J2-NO, respectively. Carbonate contents were 42 wt.% and 20 wt.% for J1-NO and J2-NO, respectively. Gypsum was detected in J2-NO at a concentration of about 11 wt.%.

The hardpan samples had mineralogical compositions between those observed in the oxidized and unweathered samples with respect to carbonates and sulfides. Sulfide contents (mainly pyrite) were about 3 wt.% and 5.50 wt.% for Hardpans 1 and 2, respectively. Carbonate contents were about 19.60 wt.% and 24.25 wt.% for Hardpans 1 and 2, respectively. Gypsum contents were 15 wt.% and 10.50 wt.% for Hardpans 1 and 2, respectively.

5.5.3 Porosity and hydrogeological properties

The two hardpan samples were analyzed using 3D X-ray imaging to estimate the samples' porosities. The results of these analyses are presented in Figure 2. The sample volumes for Hardpan 1 and Hardpan 2 were 829.7 mm^3 and 631.5 mm^3, respectively. Total porosity was similar for the two samples: ~ 9.1% for Hardpan 1 and 7.5% for Hardpan 2. Total porosity was similar to

connected porosity (7.3% for Hardpan 1 and 6.8% for Hardpan 2;Figure 5.2). The porosity of both hardpan samples was present as pores and linear cracks. Pore diameter sometimes exceed 200 μm (Figure 3S). The thickness of linear cracks varied between 80 and 220 μm. These linear cracks were generally discontinuous, and their lengths were variable.
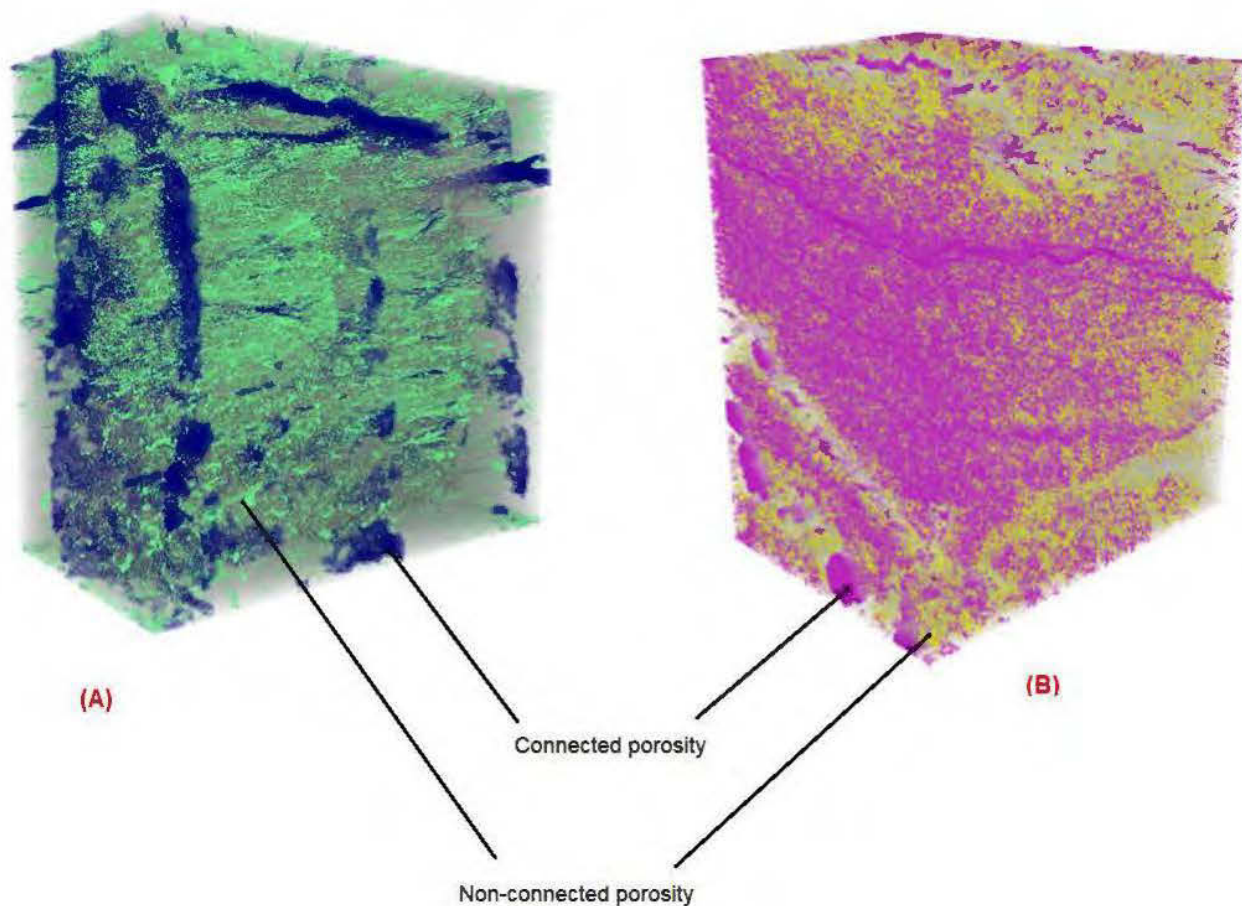
Figure 5.2 : Images showing segmentation of 3D connected and non-connected porosity for Hardpan 1 (B) and Hardpan 2 (A).

Predicted and measured ksat values and AEVs are presented in Table 3. These properties largely determine the hydrogeological behavior of the studied samples. The measured ksat values for J1-Oxy and J1-NO were 2.42E-05 cm/s and 3.06E-04 cm/s, respectively. The ksat values for J2-Oxy and J2-NO were 1E-04 cm/s and 5.65E-06 cm/s, respectively. The predicted ksat values were close to the measured values. Unweathered samples had smaller AEVs than the oxidized samples (Table 3). The AEVs estimated using the graphical method (Fredlund et al., 1994) were 75 KPa, 3.5 KPa, 80 KPa, and 25 KPa for J1-Oxy, J1-NO, J2-Oxy, and J2-NO, respectively.

Table 5.3: Measured and predicted saturated hydraulic conductivities

	Porosity	Predicted ksat (cm/s)	Measured Ksat (cm/s)
J1-Oxy	0.49	3.06E-04	2.16E-04
J1-NO	0.42	2.52E-05	2.42E-05
J2-Oxy	0.42	5.65E-06	3.68E-05
J2-NO	0.39	1.00E-04	6.04E-05

5.5.4 Determination of acid-generating potential

Static tests

The results of the static tests performed on the tailings from the two zones (Table 5.2) showed that the NP of the studied samples calculated based on the carbon content was higher than that analyzed using Sobek et al. (1978) method modified by Bouzahzah et al. (2015). The NNP was -2.5 kg $CaCO_3$/t, 35 kg $CaCO_3$/t respectively for J1-Oxy and J1-NO, while for J2-Oxy and J2-NO, the NNP was respectively 9 kg $CaCO_3$/t and -73 kg $CaCO_3$/t. Using NNP classification (Bouzahzah *et al.*, 2015a; Miller *et al.*, 1991b), J1-Oxy and J2-Oxy are classified as uncertain, J2-NO is classified as acid-generating and J1-NO is classified as non-acid-generating. The NPR were 0.5, 1.2, 13 and 0.6 respectively for J1-Oxy, J1-NO, J2-Oxy, and J2-NO. Consequently, the J1-Oxy, J1-NO, and J2-Oxy are classified as uncertain samples and J2-NO is classified as non-acid-generating.

Kinetic leaching tests

Results in terms of leachate chemical quality evolution (i.e. pH, EC and acidity/alkalinity) within the four columns are presented in Figure 5.3. Leachate pH corresponding to oxidized samples from the two zones (C1 and C3) remained acidic (pH ≈ 3) during the duration of the test, while pHs corresponding to the other scenarios (C2 and C4) start at neutral values (pH ≈ 7.5) and remain as until the end of testing.

Electrical conductivity (EC) of the leachates from the four columns was below 6 mS/cm. EC average values were 4.12 mS/cm, 5.10 mS/cm, 3.15 mS/cm and 3.56 mS/cm for the leachates from

C1, C2, C3, and C4 respectively. The electrical conductivity was higher when the unweathered samples are added to oxidized sample. The alkalinity of the leachates from columns C1 and C3 was equal to zero, while the alkalinity of the leachates from C2 was lower than 182 mg $CaCO_3$/L and lower than 324 mg $CaCO_3$/l for the leachates from the C4. Acidity of the leachates from columns C2 and C4 were below 100 mg $CaCO_3$/l during all the leaching test duration. However, the acidity of the leachates from the C1 was greater than 250 mg $CaCO_3$/l and greater than 346 mg $CaCO_3$/L for the leachates from the C3.

Results of leachate's chemical quality are presented in Figure 5.4 and Figure 5.5. The concentrations are normalized regarding the volume of the leachates and the weight of samples (mg/kg), which were different for the four columns. Calcium, magnesium, manganese, aluminum, and potassium are presented because they can indicate the reactivity of neutralizing minerals such as carbonates and silicates; iron and sulphur indicate in some case the reactivity of acidifying minerals, in particular for unweathered tailings and secondary minerals dissolution for oxidized samples (Benzaazoua et al., 2004c). Zinc is associated to sulphides or to secondary minerals as adsorbed or co-precipitated element. Other heavy metals such as cobalt and arsenic were below the detection limit of the ICP-AES, so they are not presented.

Sulphur and calcium are the most leachable element from the four columns. Maximum concentrations were leached during the beginning of the tests, which probably correspond to pre-oxidized and exchangeable species. The average concentrations of sulphur (most likely as sulphates) were 232 mg/kg, 138 mg/kg, 121 mg/kg and 53 mg/kg for the columns C1, C2, C3, and C4, respectively. The average concentrations of calcium leached from C1, C2, C3, and C4 were 169 mg/kg, 45 mg/kg, 82 mg/kg and 35 mg/kg, respectively. The average concentrations of magnesium leached form C1, C2, C3, and C4 were respectively 8 mg/kg, 69 mg/kg, 8 mg/kg, and 21 mg/kg. The manganese was leached at different concentrations from the four columns; it was about 3 mg/kg, 8 mg/kg, 24 mg/kg, and 2 mg/kg for the columns C1, C2, C3, and C4 respectively. Potassium leaching was very low from the four columns; its concentrations were below 1 mg/kg. Iron concentrations analyzed within the leachates from the four columns were important only for the column C1. Iron average concentrations were respectively 26 mg/kg, 6 mg/kg for C1 and C3 and below 0.5 mg/kg for columns C2, and C4 which probably due to iron precipitation within columns C2 and C4. The same tendency as iron was observed for aluminum, which was leached only from columns C1 and C3; aluminum average concentrations were respectively 7 mg/kg and

8 mg/kg for these two columns. Zinc average concentrations were respectively 3 mg/kg and 2 mg/kg for the leachates form C1 and C3.
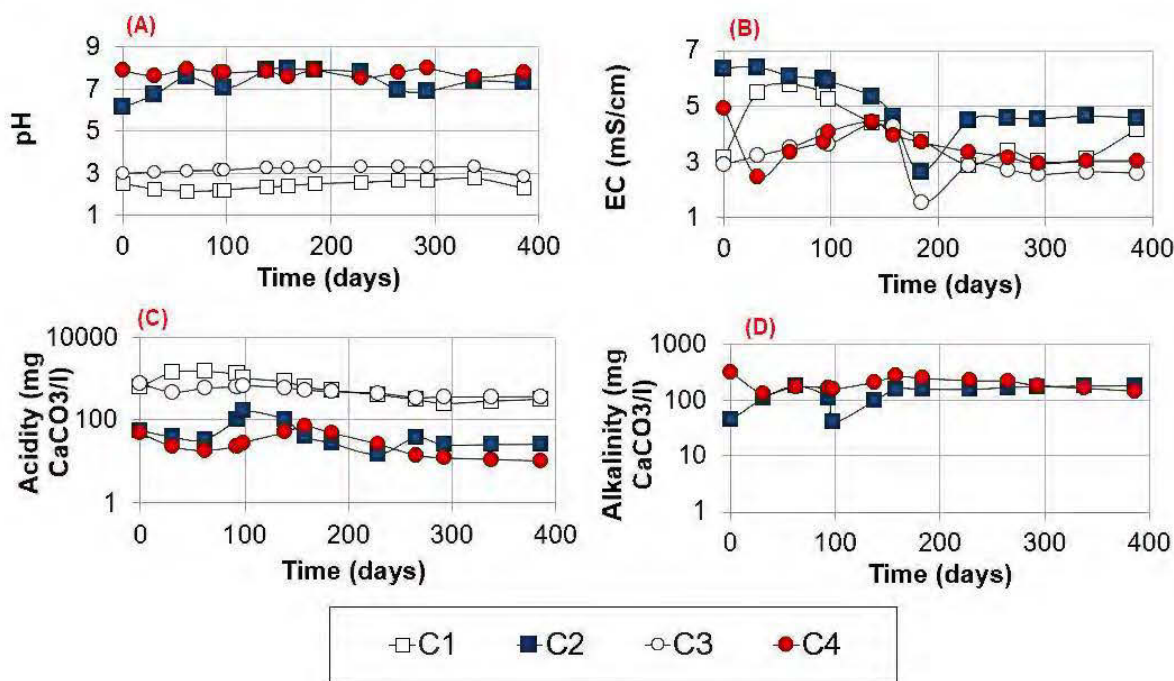
Figure 5.3: Graphs showing pH (A), EC (B), acidity (C) and alkalinity (D) evolution within the leachates if the four column leaching tests
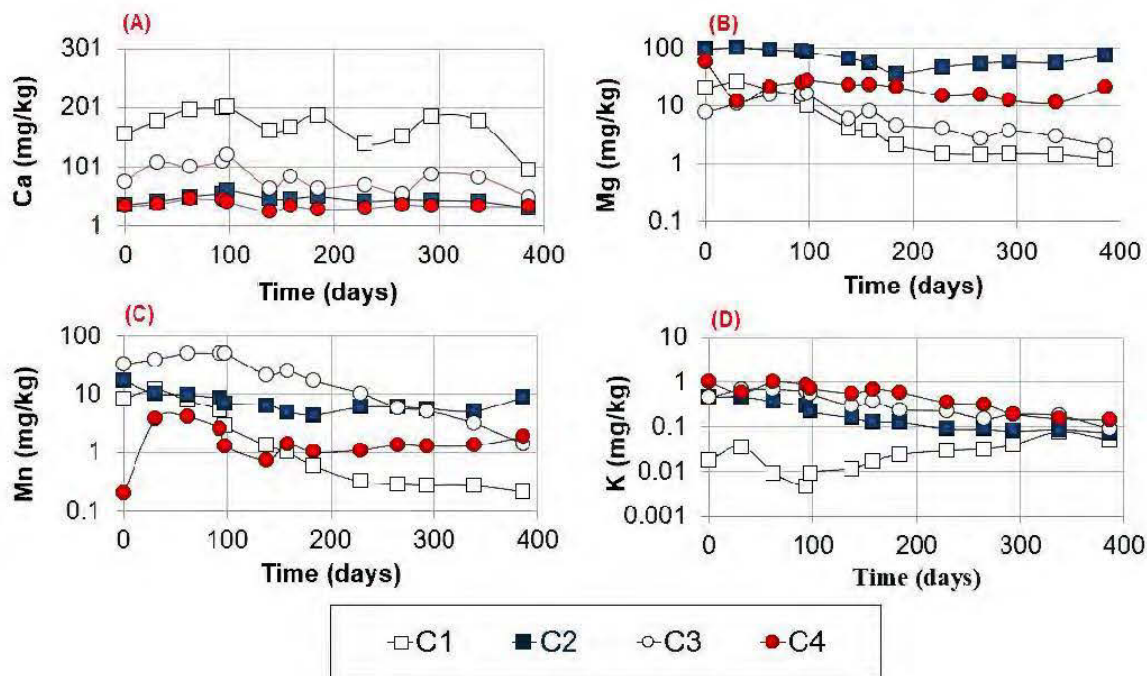
Figure 5.4: Chemical quality of leachates of the four column tests. A: Ca, B: Mg, C: Mn and D: K
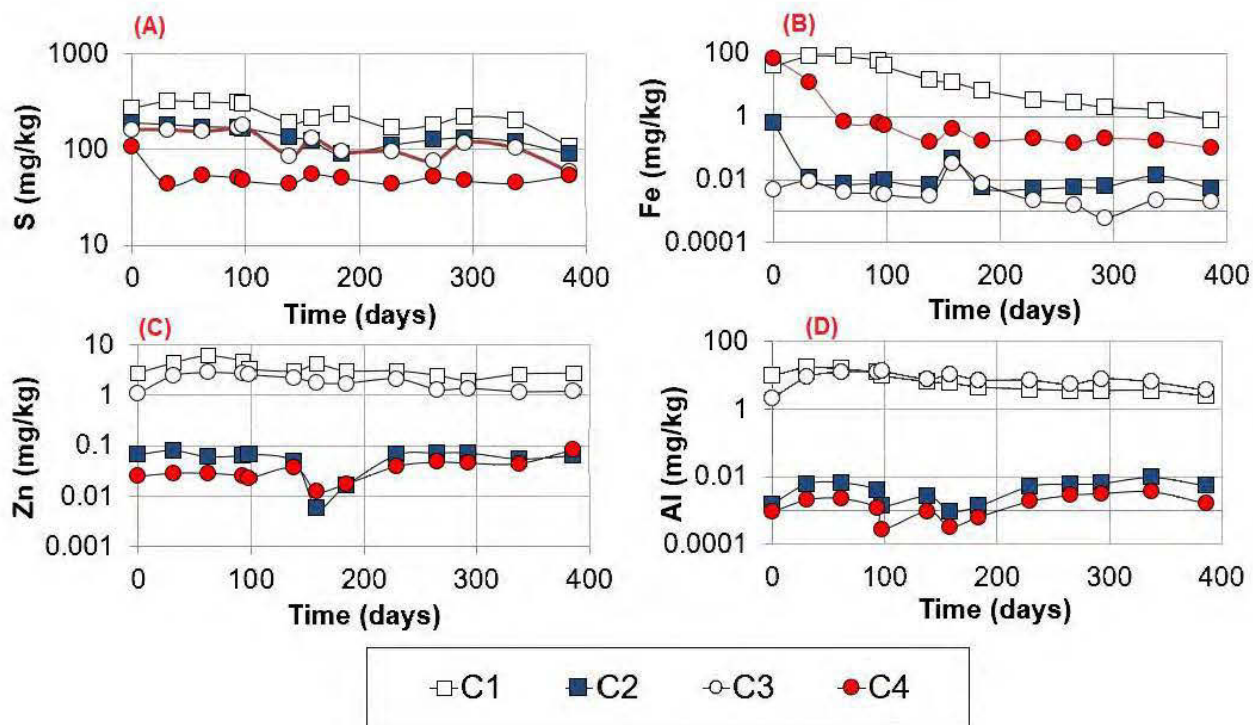
Figure 5.5: Graphs showing the chemical quality of leachates form the four columns. A: S, B: Fe, C: Zn and D: Al.

Post column-tests characterization

The four columns were dismantled and sub-samples were collected based on color and texture contrasts. Consequently, C1, C2, C3, and C4 were subdivided into 3, 7, 4, and 9 sections, respectively. Visual observations showed that a hardened and compacted layer appeared in C2 and C4 at the interface between the oxidized and unweathered tailings, as was seen during field observations. The thicknesses of the hardpans that formed in C2 and C4 were different; i.e., 3.5 cm in C2 (19 - 22.5 cm depth) and 6.5 cm in C4 (26 - 32.5 cm depth).

The results of paste pH, inorganic C, and total S analyses are presented as depth profiles in Figure 5.5. These parameters followed the same tendency regarding the depth. The paste pH of oxidized samples was < 3.5 for all columns. For unweathered tailings and hardpans, the paste pH was

circumneutral (> 5.2). Furthermore, S and C depth profiles (Figure 5A, B) showed depletions over the first 20 cm (oxidized tailings).
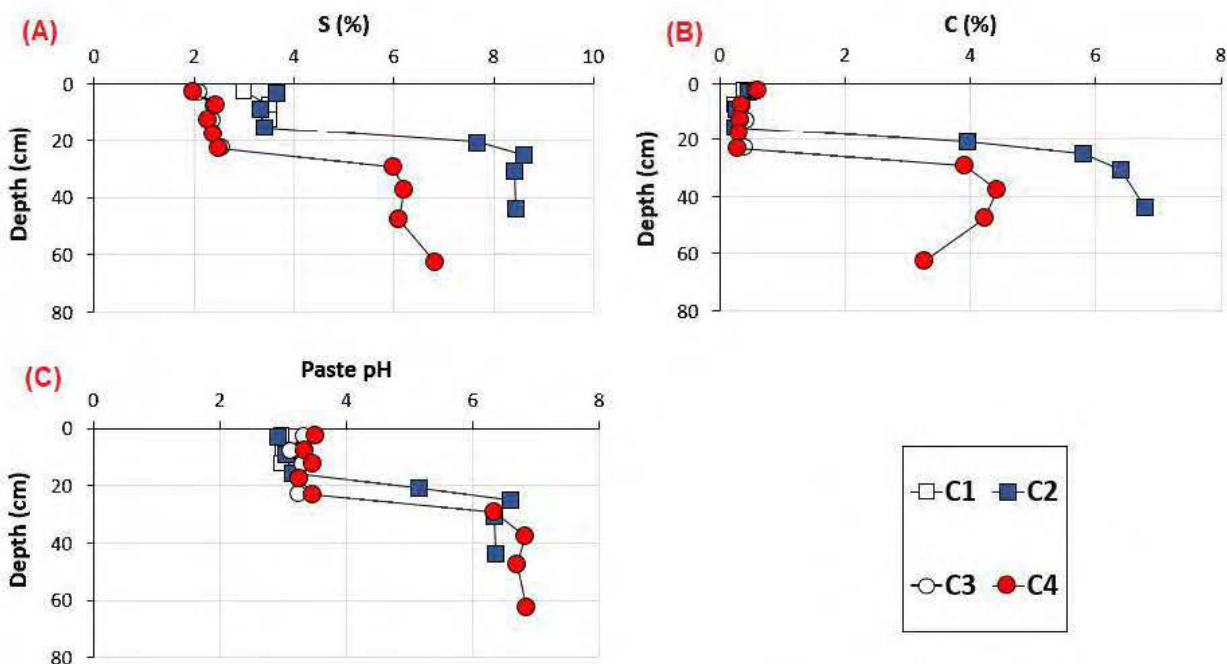
Figure 5.6: Graphs showing vertical profiles of inorganic carbon (A), total sulphur (B), paste pH (C) of samples post kinetic tests

Tank leaching tests (hardpan durability)

Results of tank leaching tests performed on the two hardpan samples are presented in Figure 5.7, Figure 5.8, and Figure 5.9. The two samples showed a similar tendency regarding the parameters analyzed at different levels. pH of the leachates from Hardpan 1 varied between 4.3 and 3.5 (Figure 5.7A), while pH of the leachates from Hardpan 2 was between 4.5 and 6 (Figure 5.7A). The average of Eh showed oxic conditions (Eh higher than 640 mV) (Figure 5.7B). Average EC of leachates of Hardpan 1 and Hardpan 2 was, respectively, 1.2 mS/cm and 1.3 mS/cm (Figure 5.7C). Acidity generated from the two samples was low and varied between 28 mg $CaCO_3$/l and 66 mg $CaCO3$/l for Hardpan 1 and between 8 mg $CaCO_3$/l and 19 mg $CaCO_3$/l for Hardpan 2 (Figure 5.7C).

Element diffusion from hardpan solids was evaluated for Al, Ca, Mg, Mn, Fe, K, Na, S, Si and Zn and the concentrations were normalized regarding the external surface of the samples. Calcium

concentrations varied between 3 g/m² and 17 g/m² for Hardpan 1 and between 16 g/m² and 103 g/m² for Hardpan 2. Sulphur is the most leachable element from the two samples (Figure 5.8A). The concentrations of sulphur leached from Hardpan 1 varied between 4 g/m² and 19 g/m² and between 20 g/m² and 99 g/m² for Hardpan 2. Ca and S showed similar behavior confirming gypsum dissolution and based on saturation index calculation for gypsum as calculated using Vminteq 3.1.

Magnesium concentrations varied between 0.5 g/m² and 1.8 g/m² for Hardpan 1 and between 1.4 g/m² and 5.1 g/m² for Hardpan 2. Manganese concentrations were between 0.1 g/m² and 0.45 g/m² for Hardpan 1 and between 0.30 g/m² and 1.50 g/m² for Hardpan 2. Iron concentrations were low, varying between 0.003 g/m² and 0.04 g/m² for Hardpan 1 and between 0.004 g/m² and 0.20 g/m² for Hardpan 2. Zinc concentrations and iron were low, demonstrating its stable state within the hardpan samples (Figure 5.9E). The maximum of iron leaching was analyzed at the beginning of the tests for the two samples, which correspond to surface reactivity. Then, iron concentrations decreased considerably to reach the steady state at nine days for the two samples. The evolution of K, Na, Al, and Si didn't reach the steady state after 64 days of the TLT, attesting to a weak silicates dissolution (Figure 5.9).
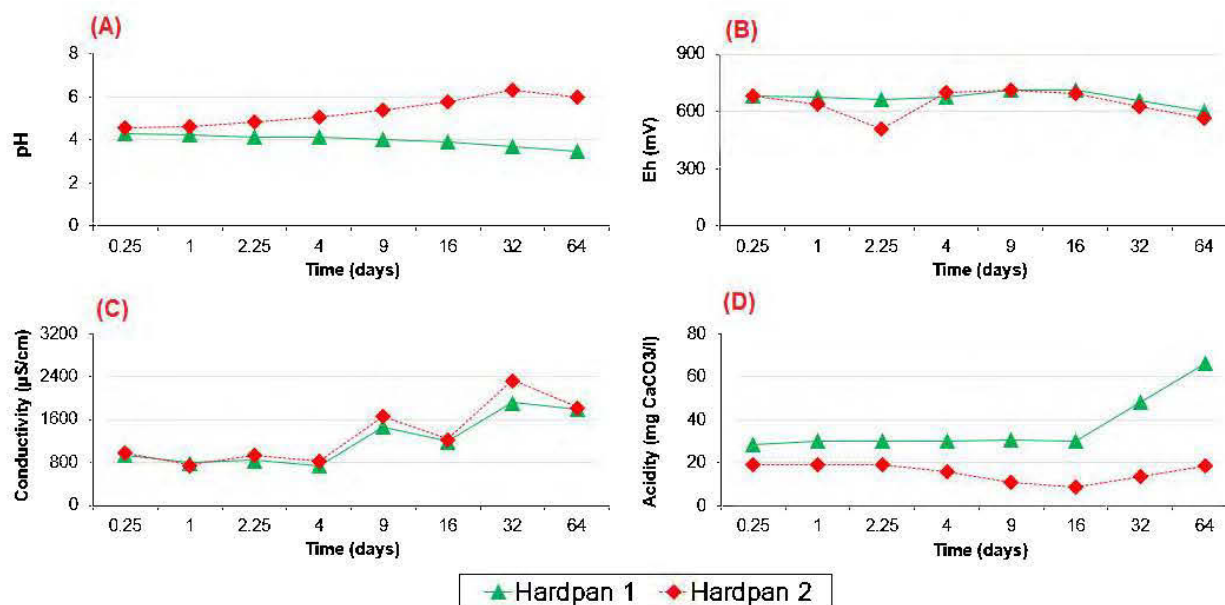
Figure 5.7: Graphs of pH (A), Eh (B), electrical conductivity (C) and acidity (D) results of TLT on the two-hardpan samples
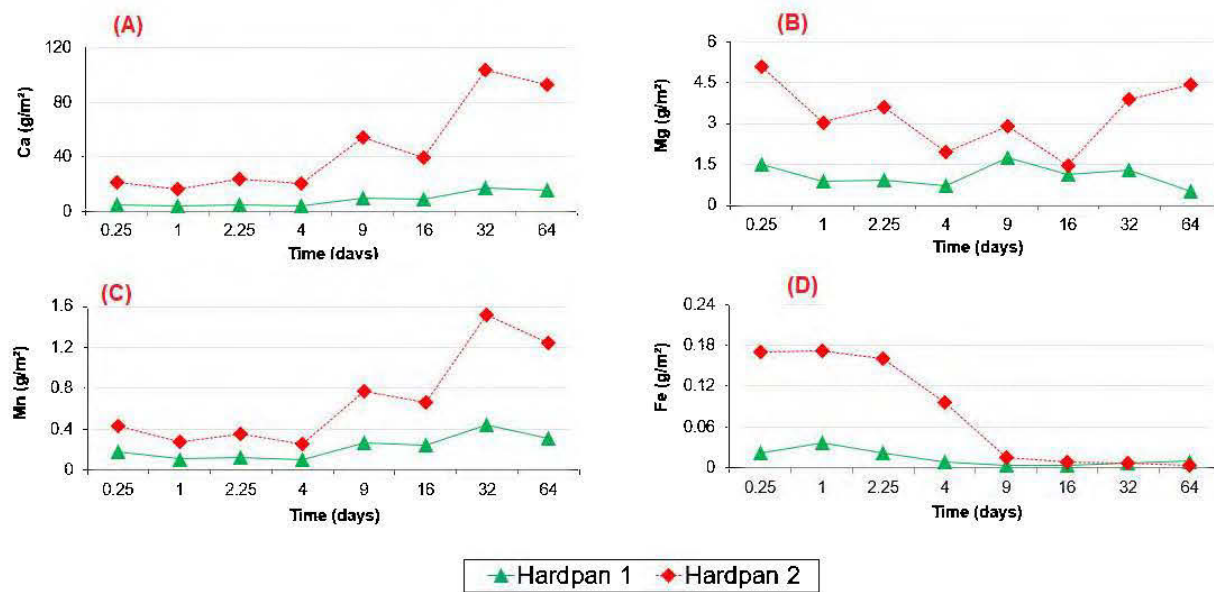
Figure 5.8 : Graphs of Al (A), Ca (B), Mg (C) and Mn (D) leaching during TLT on the two hardpan samples
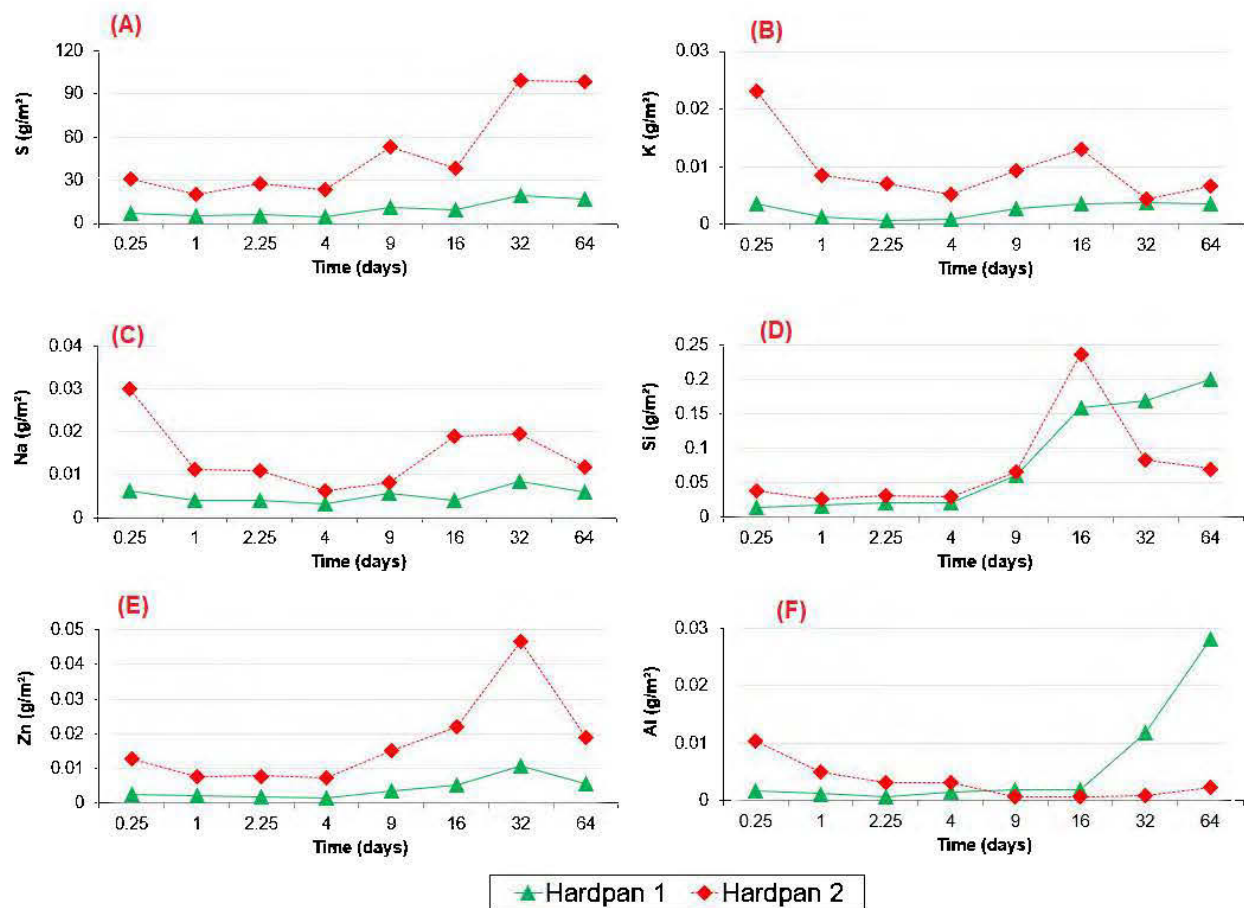
Figure 5.9 : Graphs showing results of S (A), K (B), Na (C), Si (D), Zn (E) and Al (F) leaching during TLT on the two hardpan samples

5.6 Discussion

Hereafter some important aspects will be discussed more thoroughly concerning the suggested hypothesis and conceptual model:

Hardpan is considered as low hydraulic conductivity layer (very low porosity). Precipitation of secondary minerals in general and especially ferric oxyhydroxides and gypsum, allow grains and minerals cementation, which reduces the porosity of the tailings on one hand and on the other hand may protect sulphides and carbonates against further oxidation/dissolution by limiting water infiltration and oxygen diffusion (DeSisto *et al.*, 2011). As observed in the field, hardpan occurrence is not a systematic phenomenon on the TSF; its formation depends on several

parameters such as the initial tailings chemistry and mineralogy, topography of the TSF, water table depth, and climatic conditions. Its formation requires water table fluctuation and an interface between two tailing horizons with significant geochemical contrast, as already stated in many previous works and as proposed in the conceptual model (Figure 5.1, stage 3) (Alakangas & Öhlander, 2006; Blowes *et al.*, 1991; Holmström *et al.*, 2001; Meima *et al.*, 2007). This has been demonstrated during column tests dismantling; mimicking what happened in Joutel TSF within columns C2 and C4, hardpans were formed at the neutralization interface between the oxidized tailings (acidic conditions) and unweathered tailings (neutral conditions as confirmed by paste pH) (Figure 5.1, stages 3 and 4). The geochemical contrast between the two tailings horizons favors secondary minerals precipitation. The porosity of hardpans is extremely low compared to that of tailings (0.3–0.45) and this was confirmed using 3D X-ray imaging results.

Moreover, considering mineralogical textures of the hardpan samples, it is considered as a durable and stable layer (for more information, see Elghali *et al.* 2017). In fact, TLT results showed a low leaching rate from the two hardpan samples. Hardpan reactivity is limited to surface reactivity, and diffusion phenomenon was limited; thus, sulphides and carbonates within hardpans are protected due to passivation/coating (Belzile *et al.*, 1997; Cai *et al.*, 2005; Harrison *et al.*, 2015; Kang *et al.*, 2016; Soler *et al.*, 2008). Sulphides coating within hardpan sample is illustrated in Fgure 5S. These tests correspond to the stage 3 of the proposed conceptual model (Figure 5.1). Moreover, contaminants could be immobilized due to iron oxides precipitation as it was confirmed using X-mapping for a coated pyrite. Consequently, hardpan formation reproduced first time in laboratory conditions suggests that there is an ongoing hardpan formation within Joutel TSF as suggested in stage 4 of the conceptual model (Figure 5.1).

5.7 Conclusion

The main conclusions drawn from this study are:

- The oxidized tailing showed an acidic behavior with charged leachates. However, when the fresh tailings are added below oxidized tailings, the acidity is buffered and consequently the hardpan is formed due to geochemical contrast between oxidized and unweathered horizons. Moreover, hardpan formation in laboratory conditions explain its formation in field conditions,

- The hardpan is characterized by low porosity compared to tailings and subsequent low hydraulic conductivity. Therefore, in Joutel TSF, surface and sub surface runoff are enhanced, and water vertical infiltration is limited which may enhance chemical species leaching and acidity generation within surface pore waters,

- Hardpan layer could be considered as low reactivity material due its compact and cementitious texture, which reduces oxygen diffusion to sulfide reactive core.

Acknowledgements

References

Acero, P., Ayora, C., Torrentó, C., & Nieto, J.-M. (2006). The behavior of trace elements during schwertmannite precipitation and subsequent transformation into goethite and jarosite. *Geochimica et Cosmochimica Acta, 70*(16), 4130-4139. doi:http://dx.doi.org/10.1016/j.gca.2006.06.1367

Ahn, J. S., Song, H., Yim, G.-J., Ji, S. W., & Kim, J.-G. (2011). An engineered cover system for mine tailings using a hardpan layer: A solidification/stabilization method for layer and field performance evaluation. *J Hazard Mater, 197*, 153-160. doi:http://dx.doi.org/10.1016/j.jhazmat.2011.09.069

Alakangas, L., & Öhlander, B. (2006). Formation and composition of cemented layers in low-sulphide mine tailings, Laver, northern Sweden. *Environmental Geology, 50*(6), 809-819. doi:10.1007/s00254-006-0253-x

Appleton Jr, A. R., Papelis, C., & Leckie, J. O. (1989). Adsorptive removal of trace elements from coal fly-ash wastewaters onto iron oxyhydroxide.

ASTM-D5856-95. (2002). standard test methods for measurement of hydraulic conductivity porous materials using a rigid-wall compaction-mold permeameter. Annu Book ASTM Stand. doi:10.1520/D5856-95R02E01.

ASTM-D-6836-02. (2008). Standard test methods for determination of the soil water characteristic curve for desorption using a hanging column, pressure extractor, chilled mirror hygrometer, and or centrifuge. . *Annual Book of ASTM Standards, 04.08.*

Astm, D. (2000). 5550 (2001) Standard test method for specific gravity of soil solids by gas pycnometer. *Annual Book of ASTM Standards, 4.*

Baker, B. J., & Banfield, J. F. (2003). Microbial communities in acid mine drainage. *FEMS microbiology ecology, 44*(2), 139-152.

Barnett, E., Hutchinson, R., Adamcik, A., & Barnett, R. (1982). Geology of the Agnico-Eagle gold deposit, Quebec. *Precambrian Sulphide Deposits. Geol. Assoc. Can. Spec. Pap, 25*, 403-426.

Belzile, N., Maki, S., Chen, Y.-W., & Goldsack, D. (1997). Inhibition of pyrite oxidation by surface treatment. *Science of The Total Environment, 196*(2), 177-186.

Benjamin, M. M., & Leckie, J. O. (1981a). Multiple-site adsorption of Cd, Cu, Zn, and Pb on amorphous iron oxyhydroxide. *Journal of Colloid and Interface Science, 79*(1), 209-221. doi:http://dx.doi.org/10.1016/0021-9797(81)90063-1

Benjamin, M. M., & Leckie, J. O. (1981b). Competitive adsorption of cd, cu, zn, and pb on amorphous iron oxyhydroxide. *Journal of Colloid and Interface Science, 83*(2), 410-419. doi:http://dx.doi.org/10.1016/0021-9797(81)90337-4

Benzaazoua, M., Bussière, B., Dagenais, A.-M., & Archambault, M. (2004). Kinetic tests comparison and interpretation for prediction of the Joutel tailings acid generation potential. *Environmental Geology, 46*(8), 1086-1101. doi:10.1007/s00254-004-1113-1

Blowes, D., Ptacek, C., Jambor, J., & Weisener, C. (2003). The geochemistry of acid mine drainage. *Treatise on geochemistry, 9*, 612.

Blowes, D., Ptacek, C., Jambor, J., Weisener, C., Paktunc, D., Gould, W., & Johnson, D. (2014). The geochemistry of acid mine drainage.

Blowes, D. W., Reardon, E. J., Jambor, J. L., & Cherry, J. A. (1991). The formation and potential importance of cemented layers in inactive sulfide mine tailings. *Geochimica et Cosmochimica Acta, 55*(4), 965-978. doi:http://dx.doi.org/10.1016/0016-7037(91)90155-X

Blowes, D. W., Jambor, J. L., Hanton-Fong, C. J., Lortie, L., & Gould, W. D. (1998). Geochemical, mineralogical and microbiological characterization of a sulphide-bearing carbonate-rich gold-mine tailings impoundment, Joutel, Québec. *Applied Geochemistry, 13*(6), 687-705. doi:http://dx.doi.org/10.1016/S0883-2927(98)00009-2

Bouzahzah, H., Benzaazoua, M., Plante, B., & Bussiere, B. (2015). A quantitative approach for the estimation of the "fizz rating" parameter in the acid-base accounting tests: a new adaptations of the Sobek test. *Journal of Geochemical Exploration, 153*, 53-65.

Bowell, R. J. (1994). Sorption of arsenic by iron oxides and oxyhydroxides in soils. *Applied Geochemistry, 9*(3), 279-286. doi:http://dx.doi.org/10.1016/0883-2927(94)90038-8

Bussière, B. (2007). Hydro-geotechnical properties of hard rock tailing from metal mines and emerging geo-environmental disposal approaches. *Canadian Geotechnical Journal, 44*(9), 1019-1052.

Bussière, B., Benzaazoua, M., Aubertin, M., & Mbonimpa, M. (2004). A laboratory study of covers made of low-sulphide tailings to prevent acid mine drainage. *Environmental Geology, 45*(5), 609-622.

Cai, M.-F., Dang, Z., Chen, Y.-W., & Belzile, N. (2005). The passivation of pyrrhotite by surface coating. *Chemosphere, 61*(5), 659-667.

Carbone, C., Dinelli, E., Marescotti, P., Gasparotto, G., & Lucchetti, G. (2013). The role of AMD secondary minerals in controlling environmental pollution: Indications from bulk leaching tests. *Journal of Geochemical Exploration, 132*(Supplement C), 188-200. doi:https://doi.org/10.1016/j.gexplo.2013.07.001

CEAEQ. (2006). Détermination du carbone et du soufre : méthode par combustion et dosage par spectrophotométrie infrarouge (MA. 310 – CS 1.0).

Coston, J. A., Fuller, C. C., & Davis, J. A. (1995). Pb2+ and Zn2+ adsorption by a natural aluminum- and iron-bearing surface coating on an aquifer sand. *Geochimica et Cosmochimica Acta, 59*(17), 3535-3547. doi:http://dx.doi.org/10.1016/0016-7037(95)00231-N

Coussy, S., Benzaazoua, M., Blanc, D., Moszkowicz, P., & Bussière, B. (2012). Assessment of arsenic immobilization in synthetically prepared cemented paste backfill specimens. *J Environ Manage, 93*(1), 10-21.

Cravotta III, C. (1994). *Secondary iron-sulfate minerals as sources of sulfate and acidity: Geochemical evolution of acidic ground water at a reclaimed surface coal mine in Pennsylvania.* Paper presented at the ACS Symposium Series. 1994.

Cravotta Iii, C. A. (2008). Dissolved metals and associated constituents in abandoned coal-mine discharges, Pennsylvania, USA. Part 2: Geochemical controls on constituent concentrations. *Applied Geochemistry, 23*(2), 203-226. doi:http://dx.doi.org/10.1016/j.apgeochem.2007.10.003

DeSisto, S. L., Jamieson, H. E., & Parsons, M. B. (2011). Influence of hardpan layers on arsenic mobility in historical gold mine tailings. *Applied Geochemistry, 26*(12), 2004-2018.

Dold, B. (2017). Acid rock drainage prediction: A critical review. *Journal of Geochemical Exploration, 172*, 120-132. doi:http://doi.org/10.1016/j.gexplo.2016.09.014

Elghali, A., Benzaazoua, M., Bussière, B., Schaumann, D., Graham, S., Genty, T., Noel, J., Kenedy, C., & Cayouette, J. (2017). *Investigation of the role of hardpans on the geochemical behavior of the Joutel mine tailings.* Paper presented at the the twenty-first international conference on Tailings and Mine Waste (TMW'17), Banff, Alberta, Canada.

Evangelou, V., & Zhang, Y. (1995). A review: pyrite oxidation mechanisms and acid mine drainage prevention. *Critical Reviews in Environmental Science and Technology, 25*(2), 141-199.

Fredlund, D. G., & Xing, A. (1994). Equations for the soil-water characteristic curve. *Canadian Geotechnical Journal, 31*(4), 521-532. Retrieved from http://www.nrcresearchpress.com.proxy.cegepat.qc.ca/doi/pdfplus/10.1139/t94-061

Gilbert, S., Cooke, D., & Hollings, P. (2003a). The effects of hardpan layers on the water chemistry from the leaching of pyrrhotite-rich tailings material. *Environmental Geology, 44*(6), 687-697.

Gilbert, S. E., Cooke, D. R., & Hollings, P. (2003b). The effects of hardpan layers on the water chemistry from the leaching of pyrrhotite-rich tailings material. *Environmental Geology, 44*(6), 687-697. doi:10.1007/s00254-003-0810-5

Graupner, T., Kassahun, A., Rammlmair, D., Meima, J. A., Kock, D., Furche, M., Fiege, A., Schippers, A., & Melcher, F. (2007). Formation of sequences of cemented layers and

hardpans within sulfide-bearing mine tailings (mine district Freiberg, Germany). *Applied Geochemistry, 22*(11), 2486-2508. doi:10.1016/j.apgeochem.2007.07.002

Hakkou, R., Benzaazoua, M., & Bussière, B. (2008). Acid mine drainage at the abandoned Kettara mine (Morocco): 1. Environmental characterization. *Mine Water and the Environment, 27*(3), 145-159.

Harrison, A. L., Dipple, G. M., Power, I. M., & Mayer, K. U. (2015). Influence of surface passivation and water content on mineral reactions in unsaturated porous media: implications for brucite carbonation and CO 2 sequestration. *Geochimica et Cosmochimica Acta, 148*, 477-495.

Holmström, H., & Öhlander, B. (2001). Layers rich in Fe- and Mn-oxyhydroxides formed at the tailings-pond water interface, a possible trap for trace metals in flooded mine tailings. *Journal of Geochemical Exploration, 74*(1–3), 189-203. doi:http://dx.doi.org/10.1016/S0375-6742(01)00184-4

Jönsson, J., Jönsson, J., & Lövgren, L. (2006). Precipitation of secondary Fe (III) minerals from acid mine drainage. *Applied Geochemistry, 21*(3), 437-445.

Kang, C.-U., Jeon, B.-H., Park, S.-S., Kang, J.-S., Kim, K.-H., Kim, D.-K., Choi, U.-K., & Kim, S.-J. (2016). Inhibition of pyrite oxidation by surface coating: a long-term field study. *Environ Geochem Health, 38*(5), 1137-1146.

Kohfahl, C., Graupner, T., Fetzer, C., Holzbecher, E., & Pekdeger, A. (2011). The impact of hardpans and cemented layers on oxygen diffusivity in mining waste heaps: diffusion experiments and modelling studies. *Sci Total Environ, 409*(17), 3197-3205. doi:10.1016/j.scitotenv.2011.04.055

Lapakko, K. (2002). Metal mine rock and waste characterization tools: an overview. *Mining, Minerals and Sustainable Development, 67*, 1-30.

Lawrence, R., & Wang, Y. (1996). Determination of neutralization potential for acid rock drainage prediction. *MEND project, 1*(3), 38.

Lottermoser, B. G., & Ashley, P. M. (2006). Mobility and retention of trace elements in hardpan-cemented cassiterite tailings, north Queensland, Australia. *Environmental Geology, 50*(6), 835-846.

Maest, A., & Nordstrom, D. K. (2017). A geochemical examination of humidity cell tests. *Applied Geochemistry*.

Mbonimpa, M., Aubertin, M., Chapuis, R. P., & Bussière, B. (2002). Practical pedotransfer functions for estimating the saturated hydraulic conductivity. *Geotechnical & Geological Engineering, 20*(3), 235-259. doi:10.1023/a:1016046214724

McGregor, R., & Blowes, D. (2002). The physical, chemical and mineralogical properties of three cemented layers within sulfide-bearing mine tailings. *Journal of Geochemical Exploration, 76*(3), 195-207.

McGregor, R., Blowes, D., Jambor, J., & Robertson, W. (1998). Mobilization and attenuation of heavy metals within a nickel mine tailings impoundment near Sudbury, Ontario, Canada. *Environmental Geology, 36*(3-4), 305-319.

Meima, J. A., Regenspurg, S., Kassahun, A., & Rammlmair, D. (2007). Geochemical modelling of hardpan formation in an iron slag dump. *Minerals Engineering, 20*(1), 16-25. doi:10.1016/j.mineng.2006.04.005

Miller, S., Jeffery, J., & Wong, J. (1991). *Use and misuse of the acid base account for "AMD" prediction.* Paper presented at the Proceedings of the 2nd International Conference on the Abatement of Acidic Drainage, Montréal, Que.

Nelsen, F., & Eggertsen, F. (1958). Determination of surface area. Adsorption measurements by continuous flow method. *Analytical Chemistry, 30*(8), 1387-1390.

Nen, E. (2004). 7375 (2004): Leaching characteristics of moulded or monolithic building and waste materials. *Determination of leaching of inorganic components with the diffusion test, NNIS (Netherlands Normalisation Institute Standard)*.

Nordstrom, D. K. (1982). *Aqueous pyrite oxidation and the consequent formation of secondary iron minerals*: Soil Science Society of America.

Nordstrom, D. K., & Southam, G. (1997). Geomicrobiology of sulfide mineral oxidation. *Reviews in mineralogy, 35*, 361-390.

Nordstrom, D. K., Blowes, D. W., & Ptacek, C. J. (2015). Hydrogeochemistry and microbiology of mine drainage: An update. *Applied Geochemistry, 57*, 3-16.

Paktunc, A. D. (1999). Characterization of mine wastes for prediction of acid mine drainage *Environmental impacts of mining activities* (pp. 19-40): Springer.

Quispe, D., Pérez-López, R., Acero, P., Ayora, C., Nieto, J. M., & Tucoulou, R. (2013). Formation of a hardpan in the co-disposal of fly ash and sulfide mine tailings and its influence on the generation of acid mine drainage. *Chemical Geology, 355*, 45-55. doi:10.1016/j.chemgeo.2013.07.005

Rietveld, H. (1969). A profile refinement method for nuclear and magnetic structures. *Journal of Applied Crystallography, 2*(2), 65-71.

Schroth, A. W., & Parnell Jr, R. A. (2005). Trace metal retention through the schwertmannite to goethite transformation as observed in a field setting, Alta Mine, MT. *Applied Geochemistry, 20*(5), 907-917. doi:http://dx.doi.org/10.1016/j.apgeochem.2004.09.020

Silverman, M. P. (1967). Mechanism of bacterial pyrite oxidation. *Journal of Bacteriology, 94*(4), 1046-1051.

Sobek, A. A., Schuller, W. A., & Freeman, J. R. (1978). Field and laboratory methods applicable to overburdens and minesoils *Field and laboratory methods applicable to overburdens and minesoils*: EPA.

Soler, J. M., Boi, M., Mogollón, J. L., Cama, J., Ayora, C., Nico, P. S., Tamura, N., & Kunz, M. (2008). The passivation of calcite by acid mine water. Column experiments with ferric sulfate and ferric chloride solutions at pH 2. *Applied Geochemistry, 23*(12), 3579-3588.

Taha, Y., Benzaazoua, M., Hakkou, R., & Mansori, M. (2017). Coal mine wastes recycling for coal recovery and eco-friendly bricks production. *Minerals Engineering, 107*, 123-138.

Van Genuchten, M. T. (1980). A closed-form equation for predicting the hydraulic conductivity of unsaturated soils. *Soil Science Society of America Journal, 44*(5), 892-898.

Webster, J. G., Swedlund, P. J., & Webster, K. S. (1998). Trace Metal Adsorption onto an Acid Mine Drainage Iron(III) Oxy Hydroxy Sulfate. *Environmental Science & Technology, 32*(10), 1361-1368. doi:10.1021/es9704390

Zhang, Y., Charlet, L., & Schindler, P. W. (1992). Adsorption of protons, Fe(II) and Al(III) on lepidocrocite (γ-FeOOH). *Colloids and Surfaces, 63*(3), 259-268. doi:http://dx.doi.org/10.1016/0166-6622(92)80247-Y

CHAPITRE 6   ARTICLE 4: SPATIAL MAPPING OF ACIDITY AND GEOCHEMICAL PROPERTIES OF OXIDIZED TAILINGS WITHIN THE FORMER EAGLE/TELBEL MINE SITE

Cet article est soumis à la revue Minerals

A. Elghali[1], M. Benzaazoua[1], B. Bussière[1], T. Genty[1]

[1] Université du Québec en Abitibi Témiscamingue, 445 Boul. Université, Rouyn-Noranda, QC, J9X 5E4, Canada

6.1 Abstract

Acid rock drainage (ARD) is often one of the most significant environmental challenges in mining operations. At some orphaned and abandoned mine sites, ARD can represent a complex challenge due to the advanced tailings oxidation state as well as a combination of other factors. At the field scale, a number of parameters control sulfides oxidation rates and, therefore, the generation of acidity. These factors include: i) the morphology (slope, flow direction and, water table level) of the tailings storage facility (TSF); ii) the chemical and mineralogical composition of the tailings and; iii) microbiological activity. Geographical information systems (GIS) were used as a decision-supporting tool in the design of reclamation scenarios considering the spatial distribution of the geochemical properties of the weathered tailings. Based on systematic sampling, various geochemical parameters were measured within the oxidized Joutel tailings, including the: neutralization potential, acid-generating potential, net neutralization potential, neutralization potential ratio, paste pH, thickness of oxidized, hardpan, and transition zones. GIS analyses allowed for quantification of the spatial variability of these parameters, and was used to establish correlations between the various parameters. The data showed high spatial variability in the

geochemical properties of oxidized tailings. Acidic zones, identified based on paste pH, were located in the eastern portion of the southern zone and at the northern tip of the northern zone.

Keywords: Acid rock drainage, geographical information systems, paste pH, siderite, multivariate analysis, spatial mapping.

6.2 Introduction

Mining operations generate large volumes of finely ground rock that is non-economic referred to as 'mine tailings'. They are characterized by fine particle size distribution compared to waste rocks (Bussière, 2007). Mine tailings often contain iron sulphide minerals (Blowes *et al.*, 2014). The most common sulphides are pyrite (FeS_2) and pyrrhotite ($Fe_{1-x}S$, x = 0 to 0.2). While some of the tailings at underground mine operations are used as backfill to support underground excavations (25% of total tailings produced) (Belem *et al.*, 2000; Benzaazoua *et al.*, 2002; Benzaazoua *et al.*, 2008), often they are stored on the surface in tailings storage facilities (TSFs).

In humid climates (such as Canada), TSFs usually have a water cover or the tailings are deposited in way to maintain tailings in high degree of saturation, which controls diffusion of oxygen into the tailings and reduces sulphide oxidation. However, if the water table drops and tailings desaturate, any iron-sulphides present in the tailings are exposed to atmospheric oxygen and can react and potentially produce acidity and leach metals (Nicholson *et al.*, 1988). When the tailings acidification potential is higher than their neutralization potential (Blowes *et al.*, 2003; Blowes *et al.*, 1998; Jambor, 1994; Jamieson *et al.*, 2015), the leachates resulting from sulphides oxidation become acidic. Therefore, high concentrations of sulphates, iron, and more or less significant concentrations of heavy metals (e.g. As, Co, Ni) are released (Benzaazoua *et al.*, 2004c; McGregor *et al.*, 1998a; Moncur *et al.*, 2005). This phenomenon is known as acid mine drainage (AMD) also called acid rock drainage (ARD). However, in some cases, the leachates can be near-neutral and still contain regulated elements of environmental concern that surpassing the environmental standards. This phenomenon is known as contaminated neutral drainage (CND) (Plante *et al.*, 2011b) or metal leaching (ML). Costs of mine site reclamation is influenced by the type of mine water drainage quality (Bussière *et al.*, 1999).

During sulphide oxidation, H^+ protons are produced to increase the acidity of pore water, which lead to subsequent carbonates dissolution for acidity buffering. Depending on the geochemical

conditions of the pore water, different reactions may occur such as hydrolysis, precipitation, co-precipitation, etc (Cornell *et al.*, 2004a; Cravotta III, 2008a, 2008b; Dold, 2017). During these reactions, the tailings mineralogical composition changes considerably depending on reaction rates (sulphides oxidation, carbonates and in lesser extent silicates dissolutions). During oxidation/neutralization and hydrolysis reactions, various newly formed phases are precipitated. The most common secondary phases are ferric oxyhydroxides (e.g. goethite, ferrihydrite, lepidocrocite), gypsum, and iron sulphates. These secondary phases affect the geochemical behavior of mine tailings considerably (Bowell, 1994; Bruemmer *et al.*, 1988; Burton *et al.*, 2009; Cornell *et al.*, 2004f, 2004a; Cornell & Schwertmann, 2004d; Cornell *et al.*, 2004b; Coston *et al.*, 1995; España *et al.*, 2006; Manceau *et al.*, 1992; Manceau & Combes, 1988; McKenzie, 1980).

Ferric oxyhydroxides are known for their high affinity to limit contaminant mobility due to various mechanisms (e.g. co-precipitation, adsorption, substitution). In some specific conditions, occurrence of secondary phases may also affect the hydrogeochemical behavior of the TSF by modifying the tailings hydrogeological properties (such as porosity). For example, hardpan formation within the TSF affects the water balance and flows (Blowes *et al.*, 1991; DeSisto *et al.*, 2011; Elghali *et al.*, 2017; Gilbert *et al.*, 2003; Graupner *et al.*, 2007; Lottermoser & Ashley, 2006; McGregor *et al.*, 2002). Hardpan formation is more likely in inactive mine sites, namely closed or abandoned sites.

Predicting and assessing the geochemical behavior of oxidized tailings involve challenges comparatively to unweathered, fresh tailings. Geochemical behavior of oxidized tailings is determined by the reactivity and nature of newly-formed secondary species and the residual phases. Moreover, in the case of an already closed mine site, the tailings top layer is generally oxidized, and the acidity is mainly already produced in some localized areas. Consequently, the acidic leachates, when they occur, result from two sources: the current sulphide oxidation and the latent acidity present in tailings pores. Within mine tailings, due to their low permeability and the area of the TSF, the hydraulic residence time of water is high. So, it may take some decades for the produced acidity to be flushed. This phenomenon of water transport can be more complex due to the presence of hardpan close to the surface that has different hydrogeological properties (Chermak & Runnells, 1996; Holmström *et al.*, 2001; Kohfahl *et al.*, 2011; McGregor *et al.*, 2002).

The Eagle and Telbel are closed mine sites located north of Abitibi-Témiscamingue (Québec). The mine was operated from 1974 to 1994. The gold was extracted from sulphide phases mostly as pyrite and pyrrhotite. The gold was extracted by bulk flotation and cyanidization (Blowes *et al.*, 1998). Tailings produced during ore processing were deposited in 120-ha tailings storage facility (TSF). The TSF was divided in two zones; the north zone, which was the first TSF from 1974 to 1986 and the south zone from 1986 to 1994. Since TSF closure, tailings were oxidized by oxygen, water, and bacterial activity (Barnett *et al.*, 1982; Benzaazoua *et al.*, 2004c; Blowes *et al.*, 1998; Elghali *et al.*, 2017).

In this study, a novel approach using geographical information systems (GIS) was suggested for environmental issues in the case of inactive mine sites based on a systematic sampling that covers the total area of Eagle/Telbel's TSF. The approach integrates different geochemical properties that could offer a decision-supporting tool for the design of the TSF reclamation scenario and a tool for an integral understanding of the geochemical processes within Eagle/Telbel's tailings. The main objective of this study is to map the spatial variability of the geochemical properties of the oxidized tailings that could be useful for the reclamation scenario. Consequently, a systematic sampling using a predefined grid. Then, the samples were analyzed for their geochemical properties. Analysis results were plotted using a geographical information system which allows to produce 2D maps of spatial distribution of each analyzed parameter.

6.3 Materials and methods

The methodology used in this study consisted of the combination of the geochemical, spatial, and statistical components for a better understanding of the geochemical processes within Joutel's TSF. The entire methodology used in this study is illustrated in Figure 6.1.
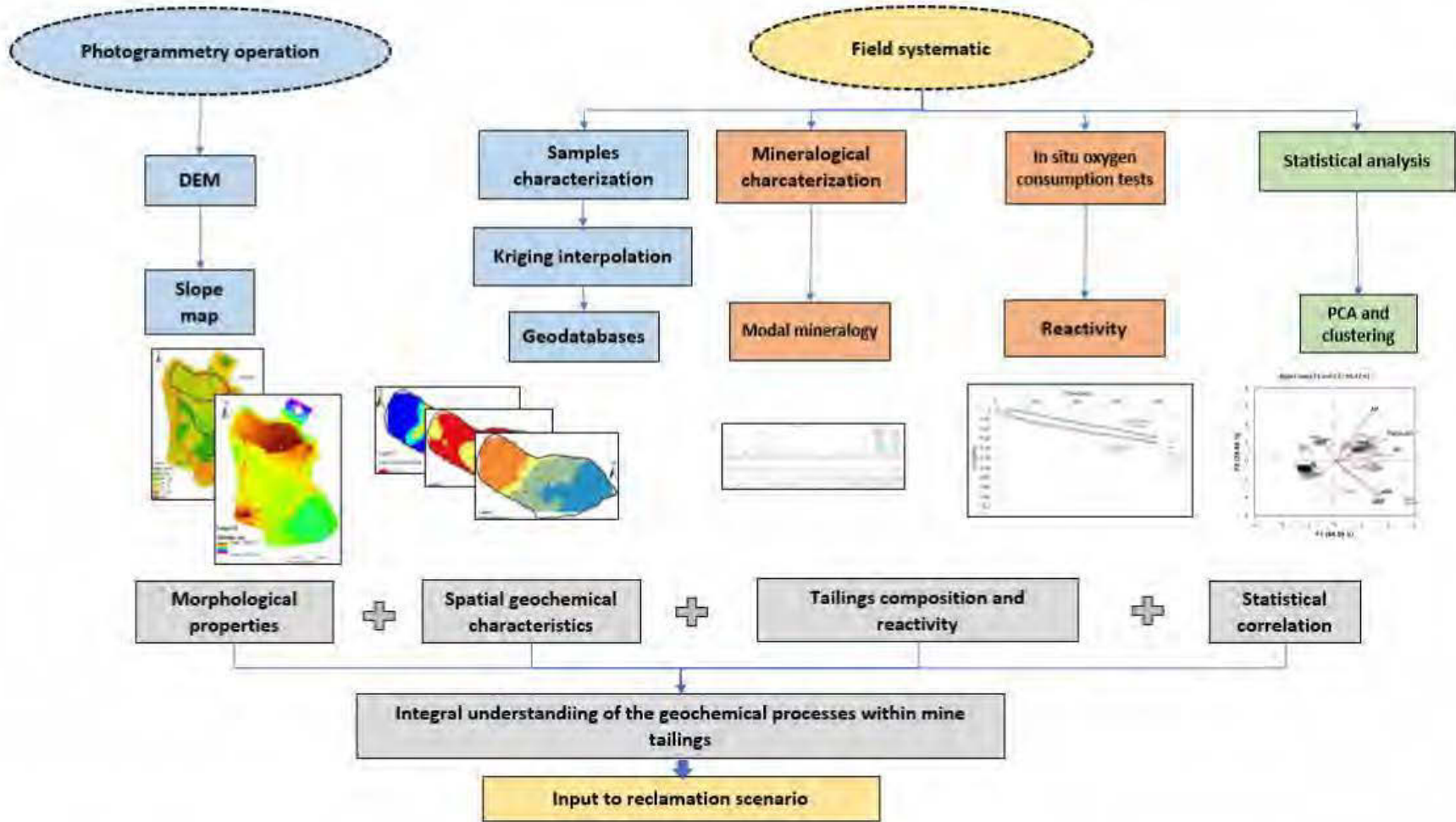
Figure 6.1: Image showing the methodological approach of this study

6.3.1 Materials sampling and methodology

Sampling is a sensitive step during prediction and assessment of acid potential (AP) of mine wastes. In general, the choice of sampling strategy and plan depend on the objectives of the study. This may justify the several sampling strategies used in different studies regarding AGP evaluation of mine wastes (Benzaazoua *et al.*, 2004c; Blowes *et al.*, 1998; Bussière *et al.*, 2004; Chopard *et al.*, 2015; Plante *et al.*, 2011b). Different strategies were also developed for soil and water pollution evaluation (Allen, 2003; Atkinson & Lloyd, 1998; Carter, 1993; Poduri & Rao, 2000; Popek, 2003) and could be used for AGP assessment of oxidized tailings considering that particle size of mine tailings is comparable to fine soil materials. The sampling strategy used for this study was systematic sampling (Carter, 1993; Poduri *et al.*, 2000; Sampath, 2001). The sampling grid was a square. Sampling lines were oriented east-west, sampling step and sampling lines spacing was about 100 m which worked well for both work/analysis expenses and sampling resolution (Figure 6.2). Depending on the field constraints (e.g. presence of vegetation, water streams), the predefined sampling point could be slightly moved. In each sampling point, oxidized tailings were sampled using a manual auger. Trenches were dug down to the unweathered tailings to allow measuring thickness of oxidation zone, hardpan, and transition zone. Each sample point was separately homogenized and submitted to different analysis. About 1 kg was collected from each point and each point was spatially referenced.
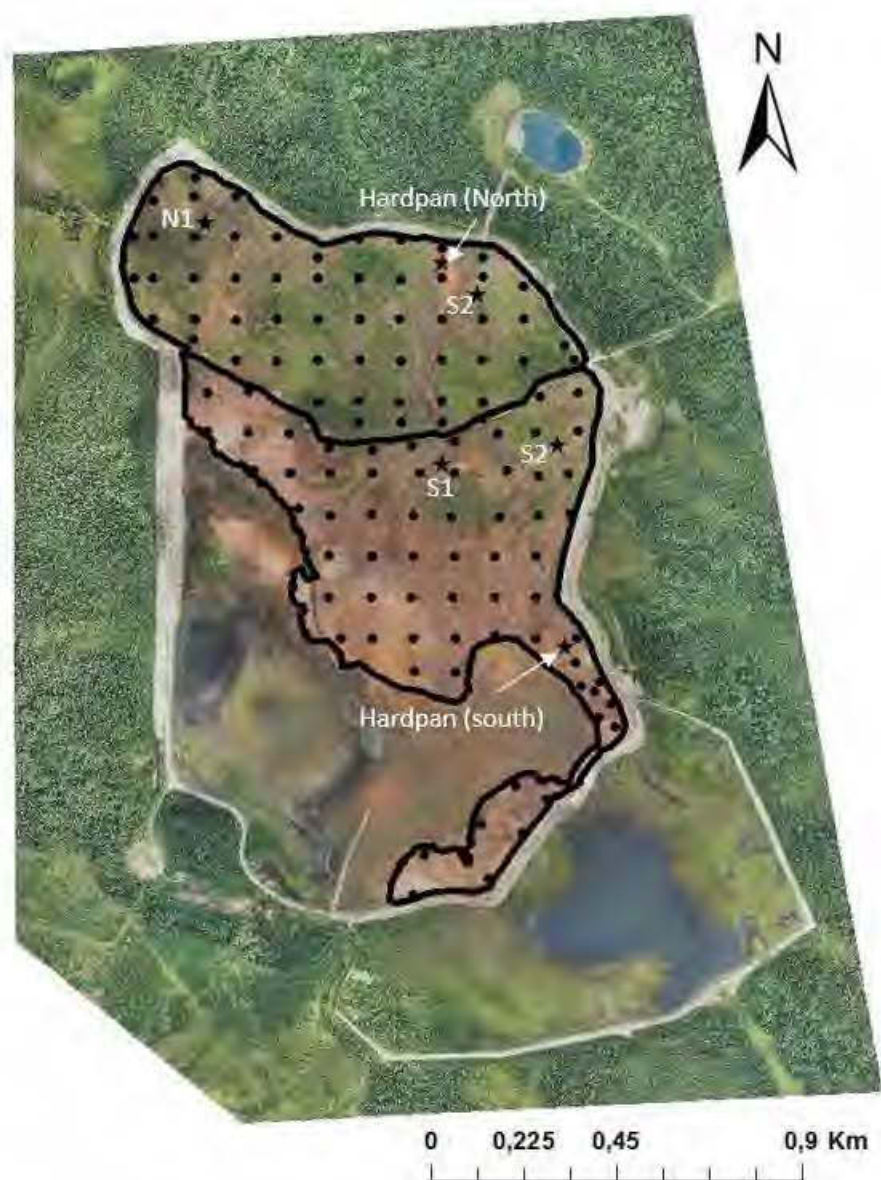
Figure 6.2: Map showing sampling grid at Joutel's mine site (stars correspond to oxygen

consumption tests localization; black circles correspond to tailings sampling)

6.3.2 Methods

6.3.2.1 Geochemical and mineralogical characterization

Total sulfur and inorganic carbon were analyzed using induction furnace (ELTRA CS-2000) with a detection limit of 0.09%. Sulphates were analyzed after solid digestion using 40% HCl.

Mineralogical composition of studied samples was studied by X-ray diffraction (XRD) using a Bruker AXS D8 Advance X-ray diffractometer equipped with a copper anticathode, scanning over a diffraction angle (2θ) range from $5°$ to $70°$. Scan settings were $0.005°$ 2θ step size and 4s counting time per step. The DiffracPlus EVA software (v.9.0 rel. 2003) was used to identify mineral species and the TOPAS software (v 2.2) implementing Rietveld refinement was used to quantify the abundance of all identified mineral species. The absolute precision of this quantification method is of the order of $\pm 0.5-1\%$.

Paste pH of solid samples was analyzed using a pH meter after adding 5 ml of deionized water to 2.5 g of solid sample with a precision of $\pm$ 0.02. Acidification potential (AP) was calculated using sulphide content (Bouzahzah *et al.*, 2015a; Sobek *et al.*, 1978b); the neutralization potential (NP) was calculated using carbon content and titrated using the Sobek method (Adam *et al.*, 1997; Chotpantarat, 2011; Jambor *et al.*, 2002b; Plante *et al.*, 2012; Sobek *et al.*, 1978b) and a correcting factor of 50% was applied due to presence of Fe-Mn carbonates that overestimate the NP calculated based on carbonates (Figure 6.5); this will be explained more in details in Section 3. The relative error related to NP titration is about $\pm$ 12 Kg $CaCO_3$/t (Paktunc *et al.*, 2001) and that related to AP calculation is about $\pm$ 3 Kg $CaCO_3$/t. The net neutralization potential (NNP) is defined as the difference between the NP and the AP. The neutralization potential ratio (NPR) is defined as the ratio between the NP and the AP. Net acid generation (NAG) tests were performed on 2.5 g of pulverized sample in 250 ml of 15% H_2O_2. The sample is allowed to react until effervescence ceases (Miller *et al.*, 1997; Price, 2009; Sapsford *et al.*, 2008). The pH of the liquor is the analyzed using a pH meter. The sample is considered acid-generating if the NAG pH is under 4.5 and non acid-generating if the NAG pH is higher than 4.5 (Smart *et al.*, 2002).

6.3.2.2 Field oxygen consumption tests

Oxygen consumption rates indicate tailings sulphides oxidation within mine tailings (Bussière *et al.*, 2004; Elberling *et al.*, 1996; Mbonimpa *et al.*, 2003; Mbonimpa *et al.*, 2011). In this study, six locations were chosen to evaluate oxygen consumption rates: four locations within oxidized tailings (two locations at the north zone and two locations at the south zone) and two locations within hardpan layers (Figure 6.2). The tests consisted of aluminum cylinders with known dimensions, which are manually embedded in the tailings to form a closed system (about 10 cm deep)

A). However, for hardpans (hard layers), the cylinder is embedded using a drill (Figure 6.3C). Then the cylinders are covered with a plastic cap which is equipped with an oxygen sensor (Elberling *et al.*, 1996) (Figure 6.3B). Oxygen concentrations were logged for five days using a data logger and the data was interpreted only for short duration (3h). Oxygen fluxes were calculated for a short time using the graphical method described in Mbonimpa et al. (2011).
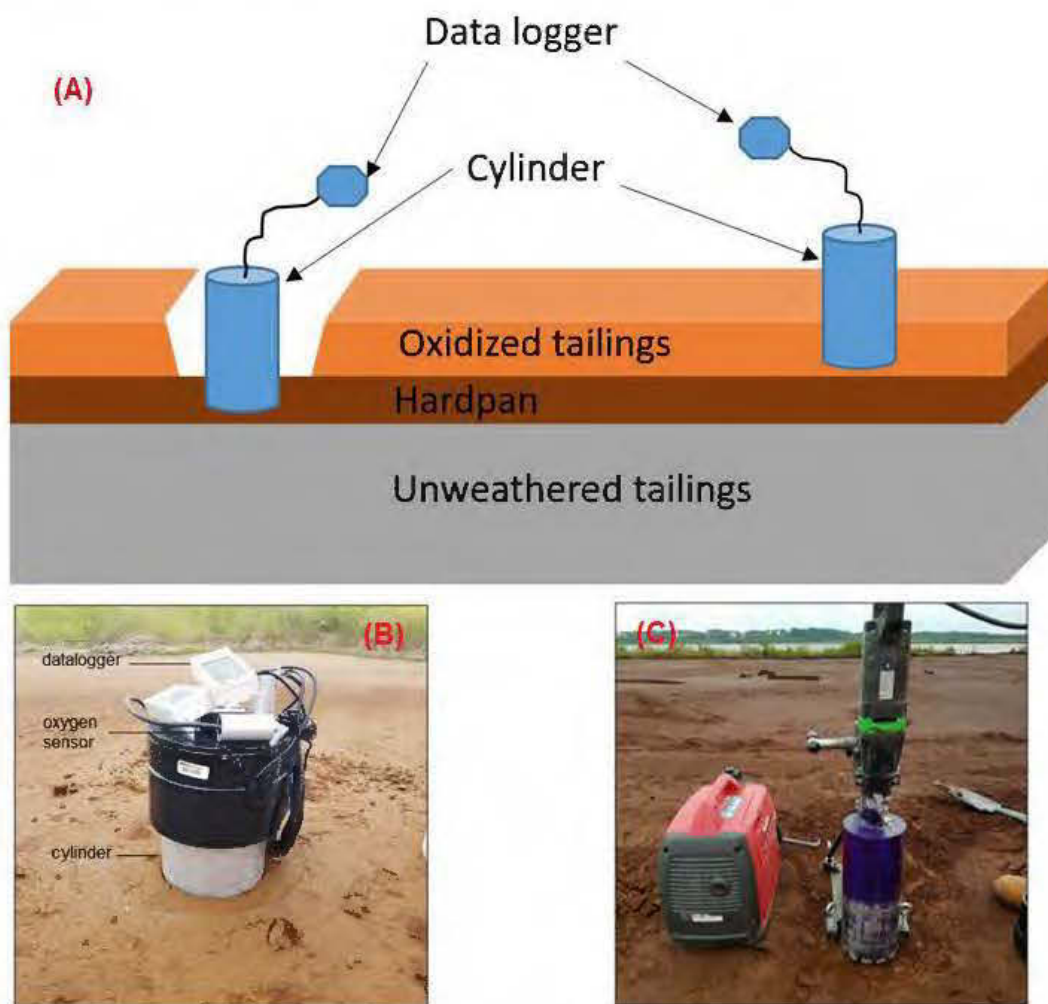
Figure 6.3: Images showing design of oxygen consumption tests.

6.3.3 Spatial mapping and statistical analysis

Due to the differences in terms of the tailings deposition age in the north and the south zone of Eagle/Telbel's TSF, each zone was interpolated separately based on the systematic sampling (cf 2.1). During this study, various data were analyzed and measured within oxidized tailings. A total

of 11 geodatabases were established using ArcGis 10.3.1. The geodatabases produced for each zone were: C wt.%, total S wt.%, S (sulphides) wt.%, paste pH, NP, AP, NNP, NPR, oxidized horizon thickness, transition zone thickness, and hardpan thickness. Other geodatabases such as the slope map and the flow accumulation map were produced for both zones using a digital elevation model of 21-cm pixel resolution produced using photogrammetry.

The analyzed and measured parameters were interpolated using kriging (Atkinson *et al.*, 1998; Cressie, 1988; Gratton, 2002; Oliver & Webster, 1990) with geostatistical wizard of ArcGis 10.3.1. Kriging, or interpolation method accuracy, was done using the validation technique. Random sampling was done after data interpolation. Data were plotted on the interpolated map, and then the estimated values by kriging were compared to those measured. Validation was done only for paste pH, being one of the most important parameters and the best reflection of the acidity of oxidized tailings. A total of 25 points were used to validate the interpolation method. Descriptive statistics and principal components analysis (PCA) were done using XL-stat extension of Microsoft Excel (Singh *et al.*, 2017). Results of kriging validation are presented in Figure 6.4, which confirmed reliable data interpolation. In fact, among 25 points, only one sample was considered an outlier and it is located outside of the confidence intervals ($\alpha=0.05$).
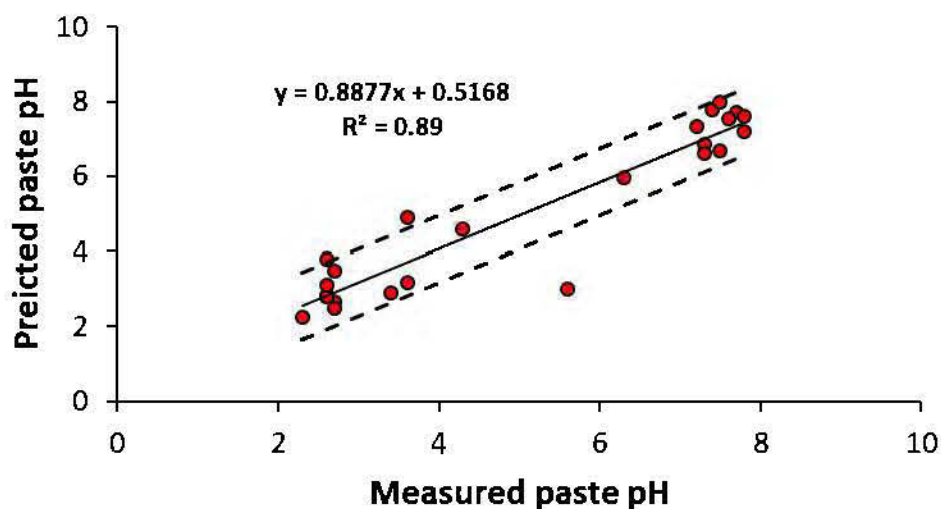
Figure 6.4: Results of kriging validation; measured paste pH vs predicted paste pH by kriging

6.4 Results and discussion

This section presents the main characterization results of Eagle/Telbel's tailings. First, the mineralogical composition will be discussed based on XRD analysis and effect of siderite on the available NP of the oxidized tailings. Then, the morphological component of the TSF (slope, digital elevation models (DEM)) and the geochemical characteristics of the oxidized tailings will be presented and discussed. The interrelationships of the geochemical characteristics of the field samples will be highlighted using statistical analysis (PCA). Then, the reactivity of some samples will be evaluated using field oxygen test consumption. At the end of this section, the results of NAG tests on some selected samples will be plotted versus paste pH to estimate the long-term behavior of the analyzed tailings samples according to previous studies (Weber *et al.*, 2006).

6.4.1 Mineralogical composition and effect of siderite on the tailings neutralization potential

Results of XRD characterization are shown in Table 6.1. The mineralogical composition of the studied samples showed a high spatial variability. Sulphide species detected within the different samples were pyrite, pyrrhotite, and chalcopyrite. Carbonates were represented mainly as siderite ($FeCO_3$) and ankerite ($Ca(Fe,Mg,Mn)(CO_3)_2$). Total carbonate contents were between 1 wt.% and 36 wt.% for south zone and between 0.5 wt.% and 36 wt.% for north zone. Total sulphides contents varied between 0.20 wt.% and 5 wt.% for south zone and between 1.30 wt.% and 4.80 wt.% for north zone. Secondary phases occurred as gypsum and ferric oxyhydroxides (hematite and goethite). Gypsum content ranged between 5 wt.% and 13 wt.% for south zone and up to 16.50 wt.% for north zone. Major mineralogical composition was represented as silicates (quartz, albite, biotite, chlorite, and muscovite). High variability of sulphide and carbonate contents within the analyzed samples is due to the variable oxidation and initial heterogeneities within the ore.

The presence of siderite leads to overestimation of the tailings NP when it is calculated based on carbonates content. This was confirmed comparing the calculated NP based on carbonate contents and analyzed using Sobek method (1978) modified by (Lawrence *et al.*, 1997b) (see Figure 6.5). The overestimation of NP based on carbonate content ranged between 10 and 54%. This difference is due to the presence of siderite and ankerite as major carbonates. Indeed, dissolution of Fe-Mn-bearing carbonates (siderite and ankerite) produces acidity due to oxidation of Fe^{2+} to Fe^{3+} and

subsequent precipitation of Fe^{3+} as ferric oxyhydroxide phases (Bouzahzah *et al.*, 2015a; Jambor *et al.*, 2003; Paktunc, 1999b; Weber *et al.*, 2004). Therefore, Fe-rich carbonates don't provide any additional buffering capacity (Bouzahzah *et al.*, 2015a; Jambor *et al.*, 2003). For this reason, the NP of Joutel's tailings was conservatively corrected by a factor of 50% for all samples used in this study (NP = 0.5 *NP(carbonates)).

Table 6.1: Mineralogical composition by XRD of selected samples from south and north zone

Zone	Sample	Quartz	Albite	Orthoclase	Biotite	Chlorite	Muscovite	Hematite	Goethite	Gypsum	Ankerite	Siderite	Pyrite	Chalcopyrite	Pyrrhotite
		SiO_2	$NaAlSi_3O_8$	$KAlSi_3O_8$	$K(Mg,Fe)_3[AlSi_3O_{10}(OH,F)_2$	$(Mg,Fe)_5Al(Si_3Al)O_{10}(OH)_8$	$KAl_2(Si_3Al)O_{10}(OH,F)_2$	Fe_2O_3	$FeO(OH)$	$CaSO_4·2H_2O$	$Ca(Fe,Mg,Mn)(CO_3)_2$	$FeCO_3$	FeS_2	$CuFeS_2$	$Fe_{(1-x)}S$
South	S1	21.39	24.82	3.8	4.03			1.21	29.99	12.63		1.89	0.23		
	S2	19.67	30.06	3.83	5.58	6.56		2.91	12.04	8.39		6.04	4.03	0.89	
	S3	17.94	18.73	3.26	3.78	3.06	10.61	5.12	15.24	5.58		12.07	2.63	1.97	
	S4	17.16	18.88	2.67	3.16	2.35	7.18	0.99	0.94	9.59	13.17	22.69	0.62	0.6	
North	N1	26.17	31.08		2.95				37.52	0.01		0.92	1.31		
	N2	26.14	30.07		4.19				4.49	2.86	12.53	14.94	4.77		
	N3	26.19	29.2		3.18				20.76	16.21		2.29	1.09		1.06
	N4	24.99	20.4		3.47		6.14		0.53	2.73	16.74	19.22	3.61		
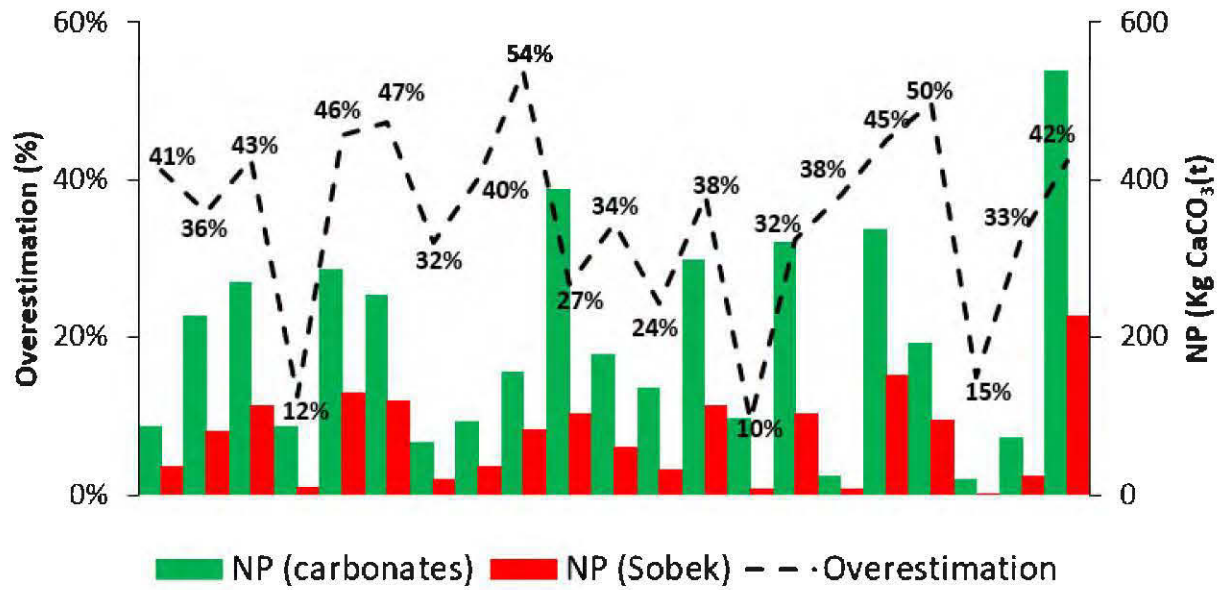
Figure 6.5: Graph showing comparison of NP calculated based on carbonates and NP analyzed using Sobek (1978) modified by (Lawrence *et al.*, 1997b)

6.4.2 Site topography and slopes

Results of DEM, slope map, and E-W/N-S elevation profiles are presented in Figure 6.6. The north zone is characterized by high elevation compared to the south zone (Figure 6.6A); the maximum elevation at the north zone and south zone is respectively about 306 m and 280 m. The elevation decreases from the north to the south and from the east to the west (Figure 6.6: Profile 1 and Profile 2). The slope within Joutel's TSF (Figure 6.6B) is weak and mostly lower than 8° except for some few areas where the slope values are higher than 80°. Therefore, water surface runoff is greatly influenced by the slope. These higher slope values correspond to water streams. Combining DEM and slope map, surface runoff flow directions are oriented NE-SW. Moreover, surface runoff is enhanced by the presence of some water streams.
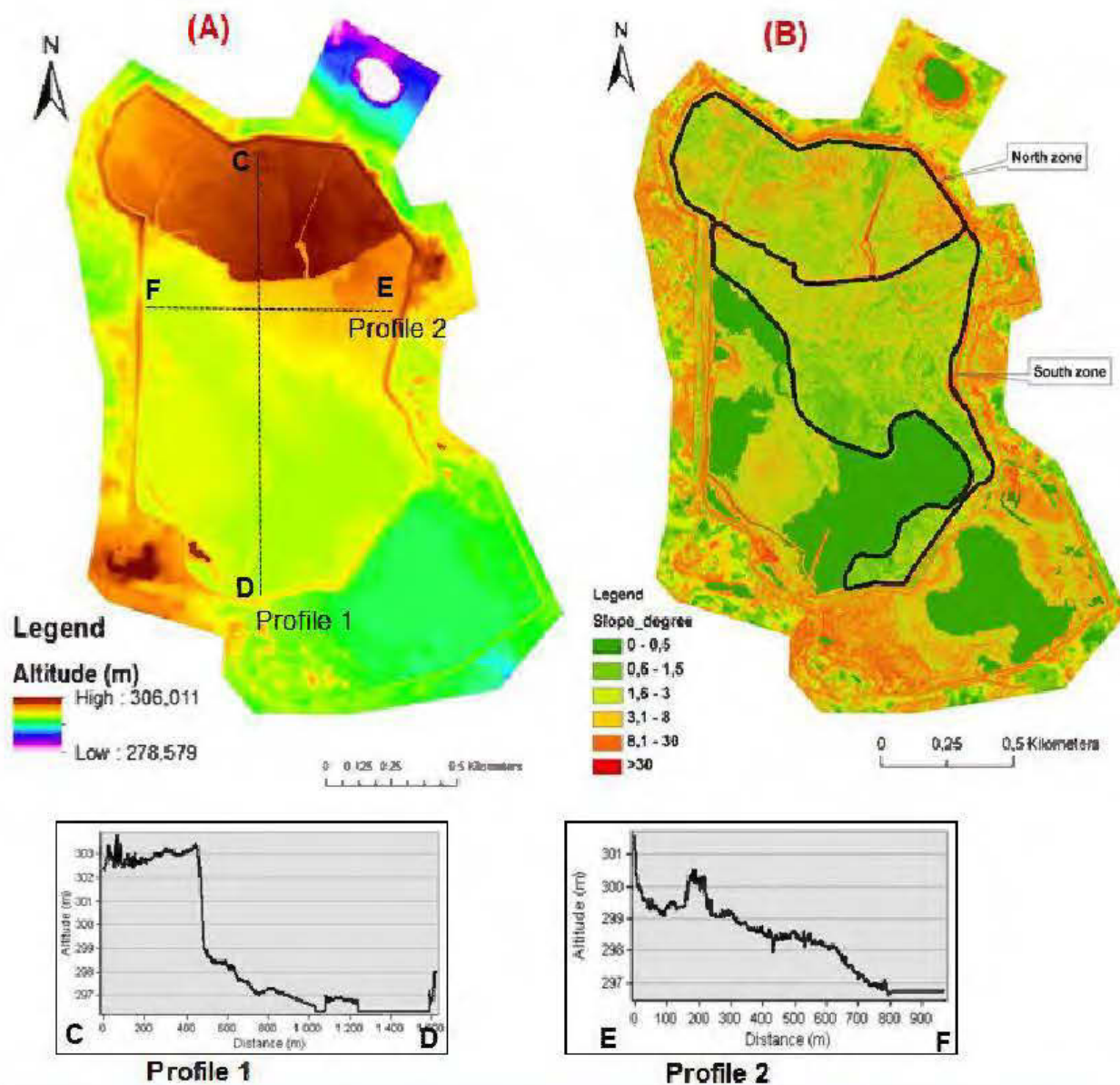
Figure 6.6: A: Digital elevation model (DEM) and B: slope map within Joutel TSF

6.4.3 Paste pH, oxidized horizon, hardpan and transition horizon thickness

The paste pH mapping, illustrated in Figure 6.7A, showed high spatial variability within oxidized tailings. For the north zone, only some localized areas are characterized by acidic paste pH values (<3.2). The majority of the north zone is characterized by neutral paste pH values (>6), while the south zone is characterized by acidic paste pH values located almost at the eastern part. In general, the extent of the acidity is much higher in the south zone than the north one.

Hardpan is formed at the interface between oxidized tailings and unweathered tailings. It is formed in the all of north zone and part of the south zone (Figure 6.7B). In the south zone, the hardpan appeared in the eastern part. The hardpan thickness was spatially variable and ranged between 1 and 15 cm. Hardpan occurrence seems to be associated to the elevation and especially to the water table level. Indeed, high topography elevation leads to deep water table level and unsaturated conditions, where sulphide oxidation is more active and consequently secondary phase precipitation (Elghali *et al.*, 2017). Consequently, the western part of the south zone is characterized by low elevation, and so near surface water table (being saturated) which delayed the process of hardpan formation.

The oxidized layer thickness ranged between some few centimeters to more than 25 cm (Figure 6.7C). The maximum of oxidized layer thickness was observed within the north zone in some locations at its western part. As a general observation, the north zone is characterized by high oxidation thickness compared to the south zone. This could be explained by two parameters, which are: i) tailings age deposit and ii) the thickness of the unsaturated zone which is influend by the topography elevation. The north zone is the older TSF and characterized by high elevation (Figure 6.6A) which favored unsaturated conditions and sulphide oxidation. The transition which corresponds to the unsaturated zone, the layer between oxidized and unweathered tailings, is also characterized by high variability (Figure 6.7D). The transition zone thickness ranged between 2 and more than 26 cm. The north zone is characterized by high thickness of this layer compared to south zone.
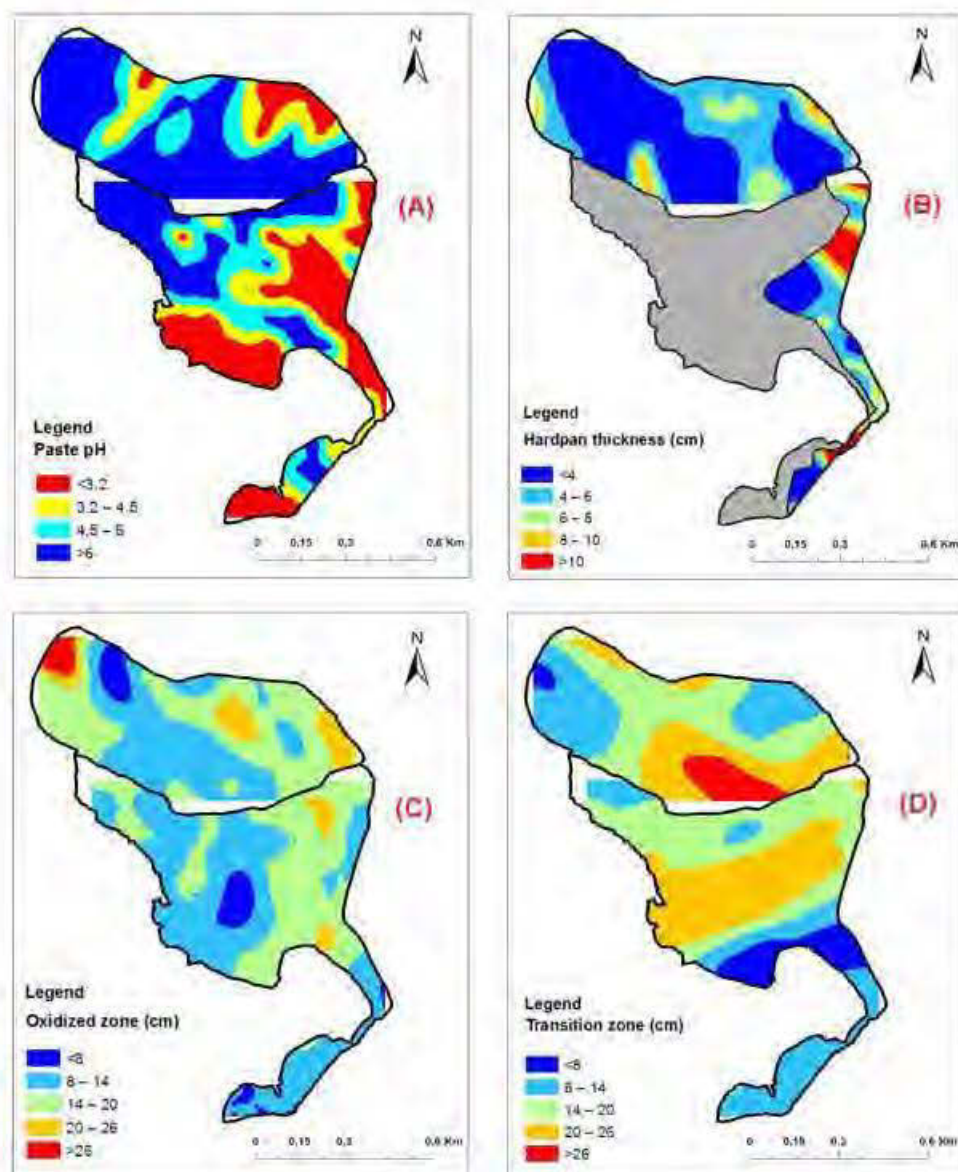
Figure 6.7: Results of mapping of paste pH (A), hardpan thickness (B), oxidized zone (C) and transition zone (D)

6.4.4 S(sulphides), %C, NNP, NPR

Results of total inorganic carbon and sulphur (sulphide) are illustrated in Figure 6.8A-B. Their distributions confirm the pattern of the oxidized layer. Indeed, carbon occurs as carbonates, which were locally almost depleted in the case of the eastern part of the south zone and the western part of north zone where the carbon content was less than 1 wt.%. Carbon content in the north zone decreases from the north to the south. This spatial distribution was not the same in the south zone;

carbon content decreases from the east to the west. Carbon (carbonates) depletion seems to be associated also the topography of the TSF (see profiles, Figure 6.6A). Carbon content ranged between 0.09 wt.% (detection limit of analysis method) and more than 4 wt.%.

Sulphide content distribution, which corresponds to residual acid potential of oxidized tailings, is illustrated in Figure 6.8B. This distribution could be compared to that of total inorganic carbon. Some locations are characterized by high sulphides depletion (<1 wt.%) such as that eastern part of south zone and the western part of north zone. In other locations, sulphur (sulphides, mainly pyrite) content was higher than 2 wt.%. In the south zone, sulphur (sulphides) content increases from east to west, while in the north zone it increases form north to south. As a general observation, sulphide oxidation seems to be faster and more effective within the eastern part of the south zone and extreme west of the north zone, which could be attributed to the tailings saturation degree due to the irregular topography of the TSF (Figure 6.6). High tailings saturation degree (> 85%) inhibits sulphide oxidation (Bussière et al., 2004; Ouangrawa et al., 2010).

The NNP and NPR criteria are used to classify Joutel's oxidized tailings regarding their acid generation potential. Mapping of NNP is illustrated in Figure 6.8C. In the south zone, almost all samples displayed NNP values ranging between -20 and 0 kg $CaCO_3$/t except some other few locations showing positive NNP. Using this criterion, samples from south zone could be classified as uncertain samples; only few locations could be classified as acid generating (NNP lower than -25 KgCaCO_3/t). The north zone showed higher NNP values; this zone could be divided into three parts from east to the west. The first part is located at the eastern part and characterized by positive NNP values ranging between 20 and 60 kg $CaCO_3$/t, the second one is localized at the central part and characterized by NNP values ranging between 0 and 20 kg $CaCO_3$/t, and the third is characterized by NNP values ranging between -20 and 0 kg $CaCO_3$/t. The criterion NPR mapping is illustrated in Figure 6.8D. The south zone showed NPR lower than 1 except for some few locations with NPR higher than 1. In general, tailings of the south zone could be classified as acid generating. The north zone is characterized by higher extent of zones with NPR values ranging between 1 and 2. The acid generating tailings are localized at the eastern part.
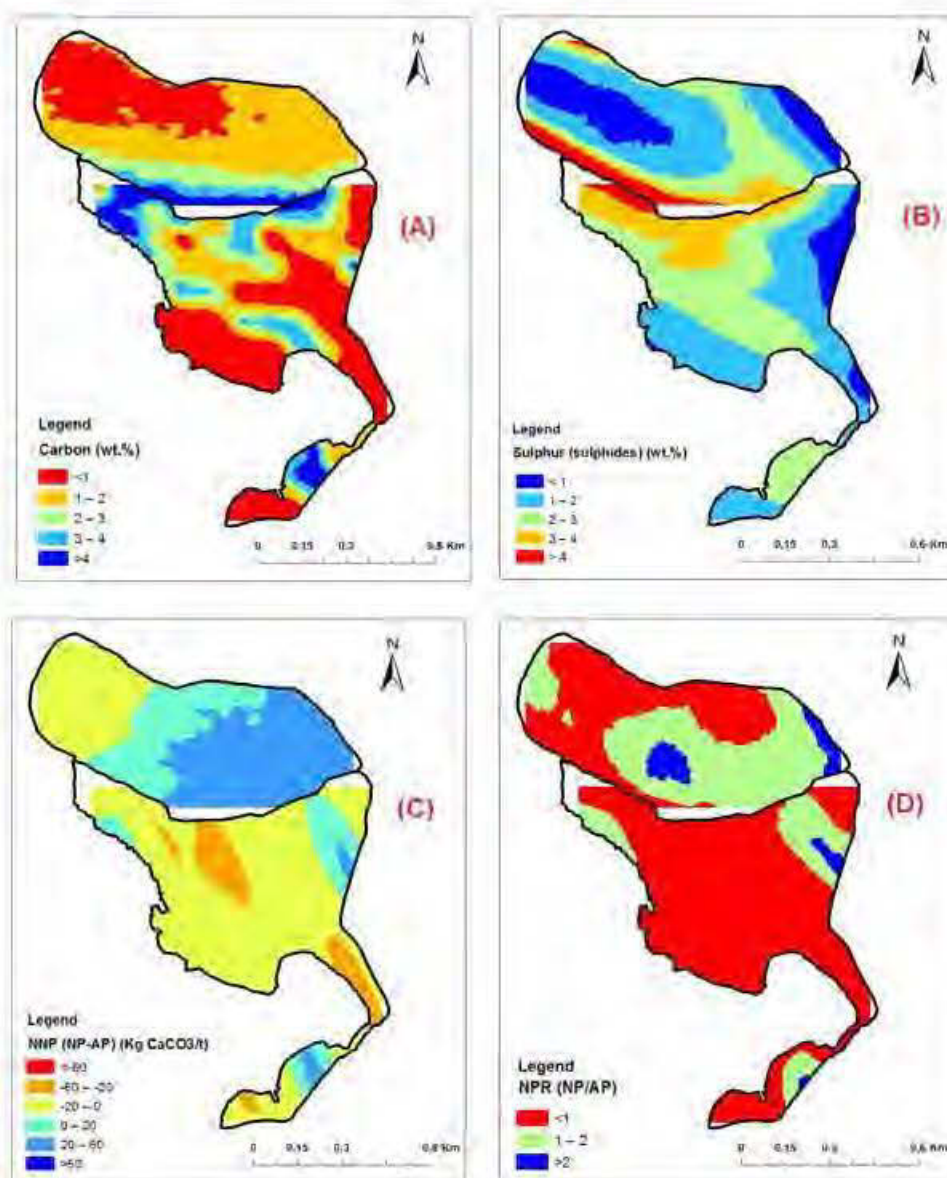
Figure 6.8: Results of mapping of carbon (A), sulphur (sulphides) (B), NNP (C) and NPR (D)

6.4.5 Oxygen consumption tests

Oxygen consumption is a parameter allowing the evaluation of the tailings reactivity (Bussière *et al.*, 2004). Calculation of oxygen fluxes consisted of oxygen consumption tests (Elberling *et al.*, 1994). The decrease of oxygen concentration could be converted to oxygen fluxes using the fundamental gas diffusion law (Fick law) (Bussière *et al.*, 2004; Elberling *et al.*, 1994; Elberling *et*

al., 1996; Mbonimpa et al., 2003). The relationship between decrease of oxygen concentration and oxygen flux is expressed as described in Elberling et al. (1994):

$$Fl = C0 * (Kr * De)^{0.5}$$

Where K_r is the first order reaction rate coefficient, D_e is the effective diffusion and C_0 is the initial concentration of oxygen for t=0. Solving the equation is expressed as followed:

$$Ln\left(\frac{C}{C0}\right) = -t(Kr * De)^{0.5} * \frac{A}{V}$$

Where A and V are respectively the area and volume of cylinder.

The slope of the plot Ln (C/C0) versus time is $(Kr * De)^{0.5}$. The interpretation of the test results is done for relatively short duration (about 180 min) as it is described in Mbonimpa et al. (2003). Results of oxygen flux calculation are shown in Table 6.2. Oxidized tailings from the south zone showed oxygen fluxes ranging between 83 and 162 mole/m^2/year; while oxidized tailings from north zone showed oxygen fluxes varying between 13 and 71 mole/m^2/year. Hardpan measurements showed oxygen fluxes of 63 and 42 mole/m^2/year for the south and north zone, respectively. The oxygen fluxes calculated for the six locations showed low values compared to other sulphidic tailings, which confirm the low reactivity of sulphide within the oxidized tailings of Joutel's TSF (Coulombe, 2012; Pabst et al., 2010; Tibble & Nicholson, 1997). These oxygen consumption rates are in accordance with the low sulphide content within the oxidized tailings (sulphide depletion). The hardpan presented low oxygen fluxes despite their high sulphides content (Elghali TMW and 2018) due to their microstructure (low porosity) and texture. Indeed, sulphides within hardpans are almost coated by ferric oxyhydroxides (Elghali et al., 2018b), which protect them from oxygen diffusion to the reactive core. The low reactivity of hardpans due its microstructure. Indeed, the hardpan is characterized by low porosity and a cementitious texture (Elghali et al., 2018b; Elghali et al., 2017).

Table 6.2: Results of field consumption tests on oxidized and hardpan samples

	Slope	R^2	A (m^2)	V(m^3)	$(Kr.De)^{1/2}$	Fs (mole/m^2/an)
S1	-8.00E-05	0.99	2.19E-02	4.89E-02	3.58E-05	162
S2	-7.00E-05	0.95	2.19E-02	8.28E-02	1.85E-05	83
N1	-1.00E-05	0.96	2.19E-02	7.64E-02	2.87E-06	13
N2	-5.00E-05	1.00	2.19E-02	6.99E-02	1.57E-05	71
Hardpan (south)	-6.00E-05	0.99	2.19E-02	9.37E-02	1.40E-05	63
Hardpan (north)	-4.00E-05	0.95	2.19E-02	9.37E-02	9.35E-06	42

6.4.6 Multivariate analysis

The paste pH in this study is used as a criterion indicating the instantaneous acidity within the upper oxidized tailings. To detect the key parameters that affect the paste pH and the interrelationships among the different geochemical parameters, PCA was conducted using four other parameters AP, NP, NNP, and NPR. Results of correlations within both zones of the TSF are shown in Table 6.3. Paste pH is positively correlated with AP and NP; the highest correlation was between NP and paste pH. Linear correlation values between NP and paste pH were 0.86 and 0.62 for the south and the north zone respectively. Despite the calculation of NNP and NPR based on NP and AP, their correlation values with paste pH are low (a maximum of 0.45). PCA was significant; using only the two first factors (F1 and F2), the cumulative variability was about 94.50% and 83.70% for south and north zone respectively. The factor F1 in the PCA explains 64.60% and 47.40% of total variance of data within south and north zone respectively, while factor F2 explains 29.90% and 36.30% of total variance of data within south and north zone respectively. Results of correlation values were more significant within PCA (Figure 6.9A-B). Paste pH, NP, and AP are in the same quadrant of the circle. There are high values of paste pH and NP in F1 and significant loading of AP, NNP, and NPR in F1 within data of the two zones, which is confirmed by the correlation matrix between factors and variables (Table 6.4). Concerning F2, there is a high value of AP in this component within the two zones and negative values of NNP and NPR in this component (Table 6.4). The high value of paste pH and NP in the F1 indicates as excepted that they are interdependent. High values of paste pH involve high values of NP and vice versa; acidic paste pH values are due to sulphide oxidation and subsequent carbonate dissolution. Consequently, the principal component F1 could be interpreted as the NP. The high loading of AP in the F2 and the negative loading of the NNP and NPR indicates that these parameters are negatively correlated.

This is explained by the initial calculation of NNP (NP-AP) and NPR (NP/AP). Consequently, the second principal component F2 could be interpreted as the AP.

Using the biplot showed in Figure 6.9C-D, which combines the graphical representation of variables versus observations, samples could be grouped into three groups for each zone. The differences between samples is due to their different compositions of F1 (NP) and F2 (AP). Some samples within north and south zone do not fit into the chosen groups and they could be considered outliers. The group 1 (Gr1) contains samples with AP more than 80 kg $CaCO_3$/t, NPR lower than 0.5, NNP lower than -65 kg $CaCO_3$/t and acidic paste pH. The group 2 (Gr2) is contains samples with AP lower than 30 kg $CaCO_3$/t, NPR lower than 0.45, NNP lower than -30 kg $CaCO_3$/t and paste pH lower than 3.30. The group 3 contains samples with paste pH greater than 6, AP greater than 90 kg $CaCO_3$/t, NNP ranging between -40 and 3 kg $CaCO_3$/t and average NPR of 1.

Table 6.3: Correlation matrix between paste pH and AP, NPR, NNP, and NP for south and north zone

	Paste pH (-)	AP (kg $CaCO_3$/t)	NPR (-)	NNP (kg $CaCO_3$/t)	NP (kg $CaCO_3$/t)
South zone (n=64)					
Paste pH (-)	1				
AP (kg $CaCO_3$/t)	**0.777**	1			
NPR (-)	0.457	0.025	1		
NNP (kg $CaCO_3$/t)	0.408	-0.056	0.868	1	
NP (kg $CaCO_3$/t)	**0.861**	0.681	0.655	0.693	1
North zone (n=54)					
Paste pH (-)	1				
AP (kg $CaCO_3$/t)	**0.517**	1			
NPR (-)	0.200	-0.495	1		
NNP (kg $CaCO_3$/t)	0.297	-0.200	0.531	1	
NP (kg $CaCO_3$/t)	**0.623**	0.539	0.105	0.717	1
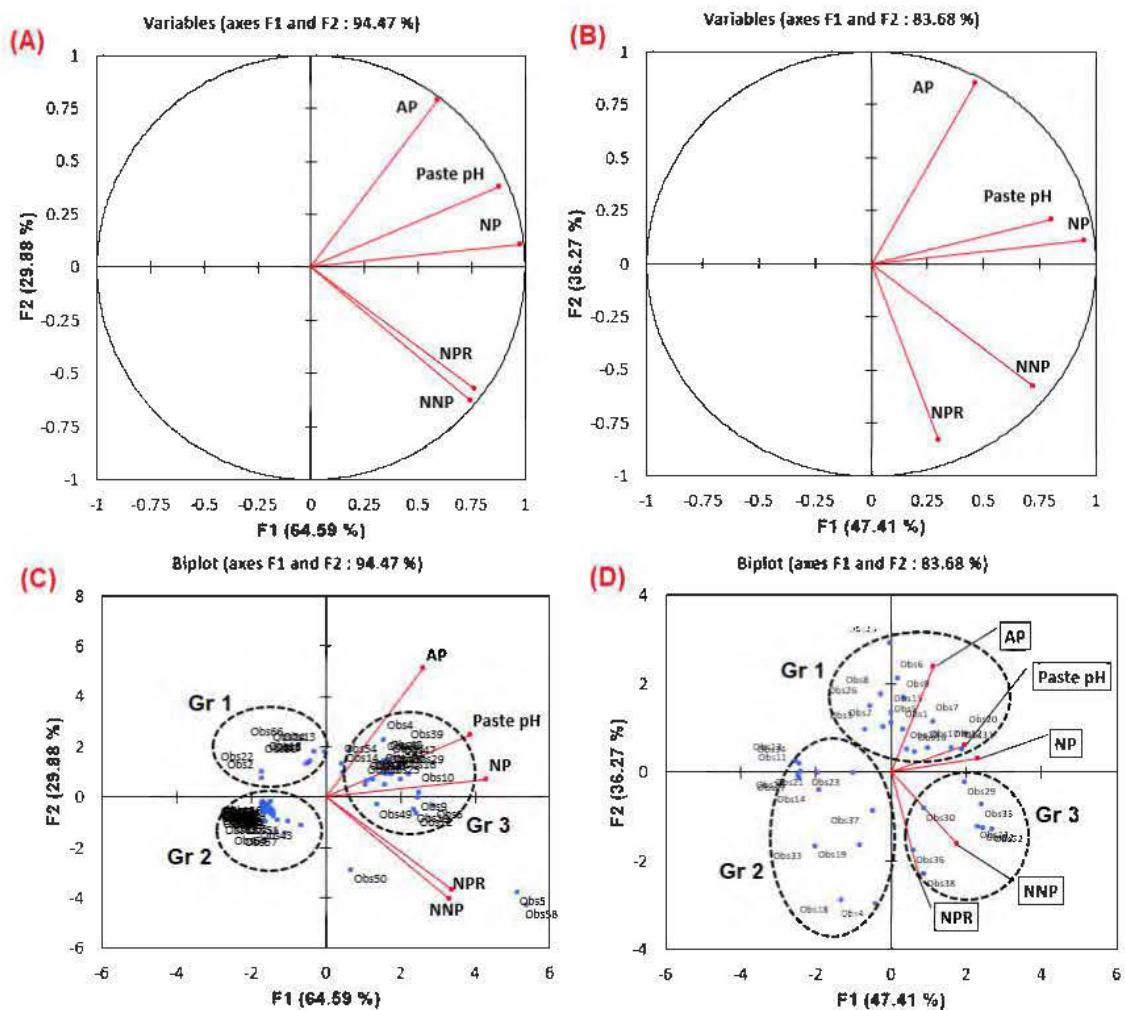
Figure 6.9: Images showing PCA (A for south zone and B for north zone) results and clustering of samples (C for south zone and D for north zone)

Table 6.4: Correlation between variables and factors for the south and the north zone

South zone (n=64)			
	F1	F2	F3	F4
Paste pH (-)	**0.879**	0.379	0.128	0.259
AP (kg CaCO₃/t)	0.595	**0.787**	-0.011	-0.163
NPR (-)	0.765	-0.571	0.268	-0.131
NNP (kg CaCO₃/t)	0.748	-0.628	-0.207	0.058
NP (kg CaCO₃/t)	**0.978**	0.107	-0.160	-0.075
North zone (n=S4)			
	F1	F2	F3	F4
Paste pH (-)	**0.805**	0.211	0.499	-0.242
AP (kg CaCO₃/t)	0.463	**0.854**	0.042	0.233
NPR (-)	0.302	-0.832	0.389	0.256
NNP (kg CaCO₃/t)	0.720	-0.580	-0.369	-0.096
NP (kg CaCO₃/t)	**0.948**	0.109	-0.288	0.083

6.4.7 Results interpretation regarding acid generation and mine site reclamation

pH paste is considered a static test for instantaneous acid-base reactivity and does not provide any indications about reaction kinetics for unweathered tailings (Weber *et al.*, 2006). To have an idea about the long-term behavior of oxidized samples, NAG pH was analyzed for some randomly selected samples (different paste pH values). Combination of paste pH and NAG pH could indicate the long-term behavior of these samples (Parbhakar-Fox *et al.*, 2017a; Weber *et al.*, 2006). Samples with extremely acidic paste pH (lower than 4) are classified as immediate acid generating. However, for some samples with neutral paste pH but acidic NAG pH are classified as potentially acid forming, which means that they will generate acidity after the lag time (Figure 6.10). The lag time within corresponds to the time where the Fe-Mn released by carbonate dissolutions are oxidized. As a conclusion, Joutel's tailings could be considered as potentially acid generating at the long-term.
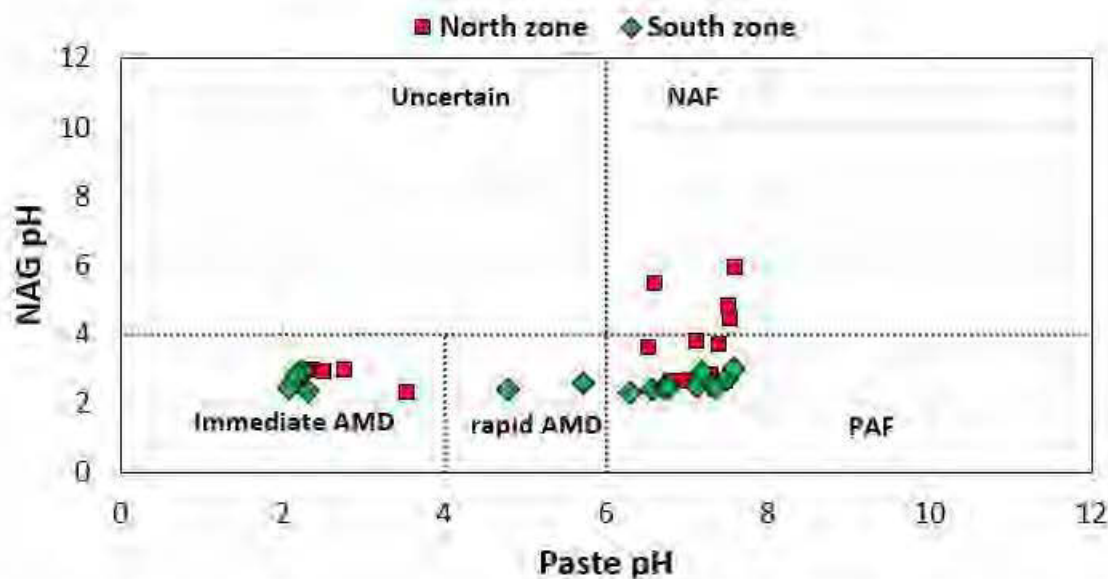
Figure 6.10: paste pH vs NAG pH for some selected samples for south and north zone

The use of the different georeferenced databases produced for the TSF could be helpful at two levels: i) the integral understanding of the different geochemical processes within the TSF and ii) the design for the site reclamation scenario. Based on the paste pH map, the TSF could be divided into two zones; zone of immediate acidity with paste pH lower than 6.5 and neutral zone with paste pH with paste pH values higher than 6.5. The acidic zones correspond to zones with almost completely depleted carbonates and which is confirmed by the high coefficient of correlation between the two parameters and similarly for sulphides. The neutral zones are characterized by non-negligible carbonate and sulphide contents. This means that not all the tailings are acid generating but only few locations are acidic. Consequently, before reclaiming the TSF, the acidic zones must be addressed separately. Knowing that the paste pH is correlated to %C, the option of alkaline amendment could be envisaged. This technique consists of adding alkaline materials for acidity buffering.

This methodology could be useful for other sites using amendments as mitigation scenario. The cost related to amendments is controlled by two parameters, which are the percentage of amendments and the thickness of tailings that must be amended. In this case, to reduce the cost of amendments, the oxidized layer thickness map could be helpful to optimize the amendment thickness regarding the spatial location as shown in Figure 6.7C. The amendment dosage must be

calculated depending on the residual sulphides based on the sulphur (sulphides) distribution (Figure 6.8B).

6.5 Conclusion

This study highlighted an approach for inactive TSF characterization for environmental issues using geographical information systems. The multi-technique characterization was exported to GIS based on a systematic sampling. This approach allowed producing a decision-supporting tool which was used for two main objectives: i) an integral understanding of the interrelationships between geochemical properties of the oxidized tailings and ii) helping to identify the most appropriate reclamation scenario of the TSF taking into account the spatial variabilities of these geochemical properties. It is a tool reducing cost related to TSF reclamation knowing the budget availability within inactive tailings. The GIS approach presents the advantage of adding a spatial component to the geochemical component, which is not possible within lab conditions (based on punctual sampling). Hardpan formation is a good example; it is formed partially within the south zone and covered the entire north zone. Moreover, its thickness may vary from a few millimetres to more than 20 cm. This means that its effect on the water balance changes depending on its properties. In addition, the acidified areas are located at the eastern part of the south zone and at the western part of the north zone. They seem to be within few locations where the carbonates are almost depleted as confirmed by the coefficient of correlation between paste pH and carbonates content.

References

Adam, K., Kourtis, A., Gazea, B., & Kontopoulos, A. (1997). Evaluation of static tests used to predict the potential for acid drainage generation at sulphide mine sites.

Allen, T. (2003). *Powder sampling and particle size determination*: Elsevier.

Atkinson, P. M., & Lloyd, C. D. (1998). Mapping precipitation in Switzerland with ordinary and indicator kriging. Special issue: Spatial Interpolation Comparison 97. *Journal of Geographic Information and Decision Analysis, 2*(1-2), 72-86.

Barnett, E., Hutchinson, R., Adamcik, A., & Barnett, R. (1982). Geology of the Agnico-Eagle gold deposit, Quebec. *Precambrian Sulphide Deposits. Geol. Assoc. Can. Spec. Pap, 25*, 403-426.

Belem, T., Benzaazoua, M., & Bussière, B. (2000). *Mechanical behaviour of cemented paste backfill.* Paper presented at the Proc. of 53rd Candadian Geotechnical Conference, Montreal.

Benzaazoua, M., Belem, T., & Bussiere, B. (2002). Chemical factors that influence the performance of mine sulphidic paste backfill. *Cement and Concrete Research, 32*(7), 1133-1144.

Benzaazoua, M., Bussière, B., Dagenais, A.-M., & Archambault, M. (2004). Kinetic tests comparison and interpretation for prediction of the Joutel tailings acid generation potential. *Environmental Geology, 46*(8), 1086-1101. doi:10.1007/s00254-004-1113-1

Benzaazoua, M., Bussière, B., Demers, I., Aubertin, M., Fried, É., & Blier, A. (2008). Integrated mine tailings management by combining environmental desulphurization and cemented paste backfill: Application to mine Doyon, Quebec, Canada. *Minerals Engineering, 21*(4), 330-340.

Blowes, D., Ptacek, C., Jambor, J., & Weisener, C. (2003). The geochemistry of acid mine drainage. *Treatise on geochemistry, 9*, 612.

Blowes, D., Ptacek, C., Jambor, J., Weisener, C., Paktunc, D., Gould, W., & Johnson, D. (2014). The geochemistry of acid mine drainage.

Blowes, D. W., Reardon, E. J., Jambor, J. L., & Cherry, J. A. (1991). The formation and potential importance of cemented layers in inactive sulfide mine tailings. *Geochimica et Cosmochimica Acta, 55*(4), 965-978. doi:http://dx.doi.org/10.1016/0016-7037(91)90155-X

Blowes, D. W., Jambor, J. L., Hanton-Fong, C. J., Lortie, L., & Gould, W. D. (1998). Geochemical, mineralogical and microbiological characterization of a sulphide-bearing carbonate-rich gold-mine tailings impoundment, Joutel, Québec. *Applied Geochemistry, 13*(6), 687-705. doi:http://dx.doi.org/10.1016/S0883-2927(98)00009-2

Bouzahzah, H., Benzaazoua, M., Plante, B., & Bussiere, B. (2015). A quantitative approach for the estimation of the "fizz rating" parameter in the acid-base accounting tests: A new adaptations of the Sobek test. *Journal of Geochemical Exploration, 153*, 53-65. doi:http://dx.doi.org/10.1016/j.gexplo.2015.03.003

Bowell, R. J. (1994). Sorption of arsenic by iron oxides and oxyhydroxides in soils. *Applied Geochemistry, 9*(3), 279-286. doi:http://dx.doi.org/10.1016/0883-2927(94)90038-8

Bruemmer, G. W., Gerth, J., & Tiller, K. G. (1988). Reaction kinetics of the adsorption and desorption of nickel, zinc and cadmium by goethite. I. Adsorption and diffusion of metals. *Journal of Soil Science, 39*(1), 37-52. doi:10.1111/j.1365-2389.1988.tb01192.x

Burton, E. D., Bush, R. T., Johnston, S. G., Watling, K. M., Hocking, R. K., Sullivan, L. A., & Parker, G. K. (2009). Sorption of Arsenic(V) and Arsenic(III) to Schwertmannite. *Environmental Science & Technology, 43*(24), 9202-9207. doi:10.1021/es902461x

Bussière, B., Aubertin, M., Benzaazoua, M., & Gagnon, D. (1999). Modèle d'estimation des coûts de restauration de sites miniers générateurs de DMA. *Séminaire Mines écologiques présentés dans le cadre du congrès APGGQ*.

Bussière, B., Benzaazoua, M., Aubertin, M., & Mbonimpa, M. (2004). A laboratory study of covers made of low-sulphide tailings to prevent acid mine drainage. *Environmental Geology, 45*(5), 609-622.

Carter, M. R. (1993). *Soil sampling and methods of analysis*: CRC Press.

Chermak, J. A., & Runnells, D. D. (1996). *Self-sealing hardpan barriers to minimize infiltration of water into sulfide-bearing overburden, ore, and tailings piles.* Paper presented at the Tailings and mine waste.

Chopard, A., Benzaazoua, M., Plante, B., Bouzahzah, H., & Marion, P. (2015). *Kinetic tests to evaluate the relative oxidation rates of various sulfides and sulfosalts.* Paper presented at the Proceedings of the 10th International Conference on Acid Rock Drainage and IMWA Annual Conference.

Chotpantarat, S. (2011). A review of static tests and recent studies. *American Journal of Applied Sciences, 8*(4), 400.

Cornell, R. M., & Schwertmann, U. (2004a). Environmental Significance *The Iron Oxides* (pp. 541-551): Wiley-VCH Verlag GmbH & Co. KGaA.

Cornell, R. M., & Schwertmann, U. (2004b). Cation Substitution *The Iron Oxides* (pp. 39-58): Wiley-VCH Verlag GmbH & Co. KGaA.

Cornell, R. M., & Schwertmann, U. (2004c). Adsorption of Ions and Molecules *The Iron Oxides* (pp. 253-296): Wiley-VCH Verlag GmbH & Co. KGaA.

Cornell, R. M., & Schwertmann, U. (2004d). Surface Chemistry and Colloidal Stability *The Iron Oxides* (pp. 221-252): Wiley-VCH Verlag GmbH & Co. KGaA.

Coston, J. A., Fuller, C. C., & Davis, J. A. (1995). Pb2+ and Zn2+ adsorption by a natural aluminum- and iron-bearing surface coating on an aquifer sand. *Geochimica et Cosmochimica Acta, 59*(17), 3535-3547. doi:http://dx.doi.org/10.1016/0016-7037(95)00231-N

Coulombe, V. (2012). *Performance de recouvrements isolants partiels pour contrôler l'oxydation de résidus miniers sulfureux.* Université du Québec en Abitibi-Témiscamingue.

Cravotta Iii, C. A. (2008a). Dissolved metals and associated constituents in abandoned coal-mine discharges, Pennsylvania, USA. Part 1: Constituent quantities and correlations. *Applied Geochemistry, 23*(2), 166-202. doi:http://dx.doi.org/10.1016/j.apgeochem.2007.10.011

Cravotta Iii, C. A. (2008b). Dissolved metals and associated constituents in abandoned coal-mine discharges, Pennsylvania, USA. Part 2: Geochemical controls on constituent concentrations. *Applied Geochemistry, 23*(2), 203-226. doi:http://dx.doi.org/10.1016/j.apgeochem.2007.10.003

Cressie, N. (1988). Spatial prediction and ordinary kriging. *Mathematical Geology, 20*(4), 405-421.

DeSisto, S. L., Jamieson, H. E., & Parsons, M. B. (2011). Influence of hardpan layers on arsenic mobility in historical gold mine tailings. *Applied Geochemistry, 26*(12), 2004-2018.

Dold, B. (2017). Acid rock drainage prediction: A critical review. *Journal of Geochemical Exploration, 172*, 120-132. doi:http://doi.org/10.1016/j.gexplo.2016.09.014

Elberling, B., & Nicholson, R. V. (1996). Field determination of sulphide oxidation rates in mine tailings. *Water Resources Research, 32*(6), 1773-1784.

Elberling, B., Nicholson, R., Reardon, E., & Tibble, R. (1994). Evaluation of sulphide oxidation rates: a laboratory study comparing oxygen fluxes and rates of oxidation product release. *Canadian Geotechnical Journal, 31*(3), 375-383.

Elghali, A., Benzaazoua, M., Bussière, B., Kennedy, C., Parawani, R., & Graham, S. (2018). The role of hardpan formation on the reactivity of sulphidic mine tailings: Joutel case study (submitted paper). *Science of The Total Environment.*

Elghali, A., Benzaazoua, M., Bussière, B., Schaumann, D., Graham, S., Genty, T., Noel, J., Kenedy, C., & Cayouette, J. (2017). *Investigation of the role of hardpans on the geochemical behavior of the Joutel mine tailings.* Paper presented at the the twenty-first international conference on Tailings and Mine Waste (TMW'17), Banff, Alberta, Canada.

España, J. S., Pamo, E. L., Pastor, E. S., Andrés, J. R., & Rubí, J. A. M. (2006). The Removal of Dissolved Metals by Hydroxysulphate Precipitates during Oxidation and Neutralization of Acid Mine Waters, Iberian Pyrite Belt. *Aquatic Geochemistry, 12*(3), 269-298. doi:10.1007/s10498-005-6246-7

Gilbert, S., Cooke, D., & Hollings, P. (2003). The effects of hardpan layers on the water chemistry from the leaching of pyrrhotite-rich tailings material. *Environmental Geology, 44*(6), 687-697.

Gratton, Y. (2002). Le krigeage: la méthode optimale d'interpolation spatiale. *Les articles de l'Institut d'Analyse Géographique, 1.*

Graupner, T., Kassahun, A., Rammlmair, D., Meima, J. A., Kock, D., Furche, M., Fiege, A., Schippers, A., & Melcher, F. (2007). Formation of sequences of cemented layers and hardpans within sulfide-bearing mine tailings (mine district Freiberg, Germany). *Applied Geochemistry, 22*(11), 2486-2508. doi:10.1016/j.apgeochem.2007.07.002

Holmström, H., & Öhlander, B. (2001). Layers rich in Fe- and Mn-oxyhydroxides formed at the tailings-pond water interface, a possible trap for trace metals in flooded mine tailings. *Journal of Geochemical Exploration, 74*(1–3), 189-203. doi:http://dx.doi.org/10.1016/S0375-6742(01)00184-4

Jambor, J. (1994). Mineralogy of sulfide-rich tailings and their oxidation products. *Environmental geochemistry of sulfide mine-wastes, 22*, 59-102.

Jambor, J., Dutrizac, J., Groat, L., & Raudsepp, M. (2002). Static tests of neutralization potentials of silicate and aluminosilicate minerals. *Environmental Geology, 43*(1), 1-17.

Jambor, J., Dutrizac, J., Raudsepp, M., & Groat, L. (2003). Effect of peroxide on neutralization-potential values of siderite and other carbonate minerals. *Journal of Environmental Quality, 32*(6), 2373-2378.

Jamieson, H. E., Walker, S. R., & Parsons, M. B. (2015). Mineralogical characterization of mine waste. *Applied Geochemistry, 57*, 85-105. doi:10.1016/j.apgeochem.2014.12.014

Kohfahl, C., Graupner, T., Fetzer, C., Holzbecher, E., & Pekdeger, A. (2011). The impact of hardpans and cemented layers on oxygen diffusivity in mining waste heaps: diffusion experiments and modelling studies. *Sci Total Environ, 409*(17), 3197-3205. doi:10.1016/j.scitotenv.2011.04.055

Lawrence, R. W., & Wang, Y. (1997). *Determination of neutralization potential in the prediction of acid rock drainage.* Paper presented at the Proceedings of the fourth international conference on acid rock drainage.

Lottermoser, B. G., & Ashley, P. M. (2006). Mobility and retention of trace elements in hardpan-cemented cassiterite tailings, north Queensland, Australia. *Environmental Geology, 50*(6), 835-846.

Manceau, A., & Combes, J. M. (1988). Structure of Mn and Fe oxides and oxyhydroxides: A topological approach by EXAFS. *Physics and Chemistry of Minerals, 15*(3), 283-295. doi:10.1007/bf00307518

Manceau, A., Charlet, L., Boisset, M. C., Didier, B., & Spadini, L. (1992). Sorption and speciation of heavy metals on hydrous Fe and Mn oxides. From microscopic to macroscopic. *Applied Clay Science, 7*(1), 201-223. doi:http://dx.doi.org/10.1016/0169-1317(92)90040-T

Mbonimpa, M., Aubertin, M., & Bussière, B. (2011). Oxygen consumption test to evaluate the diffusive flux into reactive tailings: interpretation and numerical assessment. *Canadian Geotechnical Journal, 48*(6), 878-890.

Mbonimpa, M., Aubertin, M., Aachib, M., & Bussière, B. (2003). Diffusion and consumption of oxygen in unsaturated cover materials. *Canadian Geotechnical Journal, 40*(5), 916-932.

McGregor, R., & Blowes, D. (2002). The physical, chemical and mineralogical properties of three cemented layers within sulfide-bearing mine tailings. *Journal of Geochemical Exploration, 76*(3), 195-207.

McGregor, R., Blowes, D., Jambor, J., & Robertson, W. (1998). Mobilization and attenuation of heavy metals within a nickel mine tailings impoundment near Sudbury, Ontario, Canada. *Environmental Geology, 36*(3-4), 305-319.

McKenzie, R. (1980). The adsorption of lead and other heavy metals on oxides of manganese and iron. *Soil Research, 18*(1), 61-73. doi:http://dx.doi.org/10.1071/SR9800061

Miller, S., Robertson, A., & Donahue, T. (1997). *Advances in acid drainage prediction using the net acid generation (NAG) test.* Paper presented at the Proc. 4th international conference on acid rock drainage, Vancouver, BC.

Moncur, M. C., Ptacek, C. J., Blowes, D. W., & Jambor, J. L. (2005). Release, transport and attenuation of metals from an old tailings impoundment. *Applied Geochemistry, 20*(3), 639-659. doi:10.1016/j.apgeochem.2004.09.019

Nicholson, R. V., Gillham, R. W., & Reardon, E. J. (1988). Pyrite oxidation in carbonate-buffered solution: 1. Experimental kinetics. *Geochimica et Cosmochimica Acta, 52*(5), 1077-1085. doi:http://dx.doi.org/10.1016/0016-7037(88)90262-1

Oliver, M. A., & Webster, R. (1990). Kriging: a method of interpolation for geographical information systems. *International Journal of Geographical Information Systems, 4*(3), 313-332. doi:10.1080/02693799008941549

Ouangrawa, M., Aubertin, M., Molson, J. W., Bussière, B., & Zagury, G. J. (2010). Preventing acid mine drainage with an elevated water table: Long-term column experiments and parameter analysis. *Water, Air, & Soil Pollution, 213*(1-4), 437-458.

Pabst, T., Aubertin, M., Bussière, B., & Molson, J. (2010). *Analysis of monolayer covers for the reclamation of acidgenerating tailings–Column testing and interpretation.* Paper presented at the Proceedings 63rd Canadian Geotechnical Conference and 1st Joint CGS/CNC-IPA Permafrost Specialty Conference, Calgary.

Paktunc, A., Leaver, M., Salley, J., & Wilson, J. (2001). *A new standard material for acid base accounting tests.* Paper presented at the Securing the Future. International conference on mining and the environment, Skelleftea, Sweden.

Paktunc, A. D. (1999). Characterization of Mine Wastes for Prediction of Acid Mine Drainage. In J. M. Azcue (Ed.), *Environmental Impacts of Mining Activities: Emphasis on Mitigation and Remedial Measures* (pp. 19-40). Berlin, Heidelberg: Springer Berlin Heidelberg.

Parbhakar-Fox, A., Fox, N., Hill, R., Ferguson, T., & Maynard, B. (2017). Improved mine waste characterisation through static blended test work. *Minerals Engineering.* doi:https://doi.org/10.1016/j.mineng.2017.09.011

Plante, B., Benzaazoua, M., & Bussière, B. (2011). Predicting geochemical behaviour of waste rock with low acid generating potential using laboratory kinetic tests. *Mine Water and the Environment, 30*(1), 2-21.

Plante, B., Bussière, B., & Benzaazoua, M. (2012). Static tests response on 5 Canadian hard rock mine tailings with low net acid-generating potentials. *Journal of Geochemical Exploration, 114*, 57-69.

Poduri, S., & Rao, R. (2000). Sampling methodology with applications: Chapman and Hall, New York.

Popek, E. P. (2003). *Sampling and analysis of environmental chemical pollutants: a complete guide*: Academic Press.

Price, W. A. (2009). Prediction manual for drainage chemistry from sulphidic geologic materials. *MEND report, 1*(1), 579.

Sampath, S. (2001). *Sampling theory and methods*: CRC press.

Sapsford, D., Bowell, R., Dey, M., Williams, C., & Williams, K. (2008). A comparison of kinetic NAG tests with static and humidity cell tests for the prediction of ARD. *Mine Water and the Environment, Ostrava*, 325-328.

Singh, C. K., Kumar, A., Shashtri, S., Kumar, A., Kumar, P., & Mallick, J. (2017). Multivariate statistical analysis and geochemical modeling for geochemical assessment of groundwater of Delhi, India. *Journal of Geochemical Exploration, 175*, 59-71.

Smart, R., Skinner, W., Levay, G., Gerson, A., Thomas, J., Sobieraj, H., Schumann, R., Weisener, C., Weber, P., & Miller, S. (2002). ARD test handbook: project P387A, prediction and kinetic control of acid mine drainage. *AMIRA International Ltd, Melbourne.*

Sobek, A. A., Schuller, W., Freeman, J., & Smith, R. (1978). Field and Laboratory Methods Applicable to Overburdens and Minesoils, 1978. *US Environmental Protection Agency, Cincinnati, Ohio, 45268*, 47-50.

Tibble, P., & Nicholson, R. (1997). *Oxygen consumption on sulphide tailings and tailings covers: measured rates and applications.* Paper presented at the Proceedings of the 4th International Conference on Acid Rock Drainage (ICARD), Vancouver, BC.

Weber, P. A., Thomas, J. E., Skinner, W. M., & Smart, R. S. C. (2004). Improved acid neutralisation capacity assessment of iron carbonates by titration and theoretical calculation. *Applied Geochemistry, 19*(5), 687-694. doi:http://dx.doi.org/10.1016/j.apgeochem.2003.09.002

Weber, P. A., Hughes, J. B., Conner, L. B., Lindsay, P., & Smart, R. (2006). *Short-Term Acid Rock Drainage Characteristics Determined by Paste pH and Kinetic NAG Testing: Cypress, Prospect, New Zealand.* ASMR.

CHAPITRE 7   ARTICLE 5:IN-SITU EFFECTIVENESS OF ALKALINE AND CEMENTITIOUS AMENDMENTS TO STABILIZE OXIDIZED ACID-GENERATING TAILINGS: SHORT-TERM INVESTIGATION

Cet article est soumis à la revue Waste Management

A. Elghali[1], M. Benzaazoua[1], B. Bussière[1], T. Genty[1]

[1] Université du Québec en Abitibi-Témiscamingue

7.1 Abstract

This paper presents a short-term investigation of the effectiveness of limestone and cementitious additives in the in-situ stabilization of localized acid generating tailings from a closed gold mine in Abitibi-Quebec (Eagle-Telbel mine site 'Joutel'). Five field cells (including control cell) were constructed and equipped with two different configurations of water collection; water vertical infiltration and surface runoff. The five filed cells consisted on: control cell, two cells with 5 wt.% (C2) and 10 wt.% (C3) limestone and two cemented cells with 5 wt.% ½ ordinary Portland cement - ½ fly ash (C4) and 5 wt.% ordinary Portland cement (C5). The control cell showed an acidic behavior with pH values less than 4.5 with variables chemical species such as Fe, Al, Zn and Cu. The amendments were used to neutralize the acidic leachates and decrease chemical species release from unamended mine tailings. Leachates from surface runoff were less loaded with chemical species compared to those from vertical infiltration. All amendment formulations increased pH of the leachates from approximately 4 to around neutrality interval. Furthermore, metal and metalloid release was greatly limited with amended tailings except for Zn and As for the carbonate-based amendments. The effectiveness order of the used amendments calculated based unamended cell, on metals/metalloids stabilization was: C2 = C3 = C4 = C5 for Fe, C4 > C5 > C2 > C3 for Al, C5 > C3 > C4 for Zn, C5 = C4 > C2 for As, C5 = C4 > C2 > C3 for Pb, C4 > C3 > C2 > C5 for Ni, C5 > C3 > C4 > C2 for Li and C4 > C5 > C2 > C3 for Cr.

Key words: Acid mine drainage, Joutel mine site, alkaline amendments, cementitious amendments, impermeabilization.

7.2 Introduction

Eagle-Telbel gold mine site (hereafter referred to as Joutel) is located at approximately 195 Km north of Val-d'Or (Quebec, Canada). The mine was in operation between 1974 and 1994. The ore belong to sulphide deposit type with pyrite and pyrrhotite as main sulphides (Barnett et al., 1982; Benzaazoua et al., 2004c; Blowes et al., 1998). Gold extraction generated large amounts of finely grinded tailings deposited in surface TSF of about 120-ha. The not reclaimed yet TSF is divided into two zones; the north zone which is the first TSF (1974 to 1986) and the south zone which is the recent one (1986-1994). The tailings exposition to atmospheric agents (water and oxygen) leads to sulphide oxidation above water table and subsequent acid generation in some located areas.

In Canada, environmental regulations require restoration and stabilization of tailings and effluent control before the final closing of mine sites. Stabilization of acidic tailings and contaminants released from oxidized tailings could be achieved using stabilization/solidification (S/S) technique. It consists on adding alkaline and/or cementitious materials or industrial sub-products, and it is referenced as mining amendments (Ahmaruzzaman, 2010; Alkattan et al., 1998; Chen et al., 2009; Doye et al., 2003; Falciglia et al., 2017; Fatahi et al., 2015; Fleri et al., 2007; Mitchell et al., 2018; Paradis et al., 2006; Pesonen et al., 2016; Rodríguez et al., 2018; Wang et al., 2018; Wang et al., 2015b; Yi et al., 2017). Mining amendments could be divided to two categories depending on the applications:

i)   alkaline amendments which are used for providing a supplementary neutralization potential to acidic tailings (Cravotta III & Trahan, 1999; de Andrade et al., 2008; Hakkou et al., 2009),

ii)   cementitious amendments which are used for either their neutralizing potential and impermeabilization/solidification against acidic tailings (Du et al., 2013; Gilles et al., 2014; Kogbara et al., 2011b; Li et al., 2001; Nehdi et al., 2007; Yilmaz et al., 2014).

Alkaline amendments were successfully used to control and neutralized acid mine drainage in laboratory conditions using kinetic tests (Alkattan et al., 1998; Doye et al., 2003; Duchesne et al., 1998; Holmström et al., 1999; Komnitsas et al., 2004; Mylona et al., 2000; Rodríguez et al., 2018). Limestone is one of the most used external materials as alkaline amendments. They aim to simply enhance the neutralization potential of tailings. Dissolution of alkaline amendments, in acidic

conditions, increases leachates pHs (alkalinity) and reduces contaminant mobility. Different mechanisms could be involved as:

i)   precipitation of low soluble iron oxy-hydroxides which co-precipitate and/or adsorb contaminants (Acero *et al.*, 2006; Asta *et al.*, 2010; Benjamin *et al.*, 1981b; Blowes *et al.*, 2014; Doye *et al.*, 2003),

ii)   ii) sulfide surface passivation which inhibits oxygen diffusion to and from sulfide reactive core (Belzile *et al.*, 1997; Cai *et al.*, 2005; Harrison *et al.*, 2015; Kang *et al.*, 2016),

iii)   iii) reduction of bacterial activity in neutral conditions (Evangelou *et al.*, 1995a; NEDEM, 1997; Nordstrom *et al.*, 1997). Other materials were successfully used as alkaline amendments such as red mud bauxite and cement kiln dust (Doye *et al.*, 2003; Lamontagne, 2001; Mackie & Walsh, 2015; Paradis *et al.*, 2006).

Cementitious amendments are commonly used for solidification of hazardous wastes and contaminated soils (Duchesne *et al.*, 2006; Ichrak *et al.*, 2016; Nehdi *et al.*, 2007; Wang *et al.*, 2015b). Compared to alkaline amendments, cementitious amendments reduce the contaminant mobility by the same mechanisms as the alkaline amendments. However, the application of this technique allows the solidification of the porous media, encapsulation of the reactive grains and physical trapping of contaminants (fixation). In fact, tailings cementation leads to:

i)   physical encapsulation of eventual mobile contaminants by increasing the cohesive properties of the mixture, and

ii)   ) improves the cohesion and the long-term impermeability of the tailings which reduce the available surface area of reactive particles (Benzaazoua *et al.*, 2004b; Deschamps *et al.*, 2009; Gilles *et al.*, 2014; Ichrak *et al.*, 2016; Nehdi *et al.*, 2007; Tariq *et al.*, 2013; Wang *et al.*, 2018; Wang *et al.*, 2015b; Yilmaz *et al.*, 2014).

Various materials were successfully used as cementitious additives for these purposes and ordinary cement Portland (OPC) also called general use (GU) is the most used additive. In cemented paste backfills industrial by-products, (such as fly ash, slags, lime and cement kiln dusts) were used to substitute partially the OPC (Benzaazoua *et al.*, 2004b; Chen *et al.*, 2009; Ciccu *et al.*, 2003; Coussy *et al.*, 2011; Criado *et al.*, 2007; Falciglia *et al.*, 2017; Kim *et al.*,

2011; Kumpiene *et al.*, 2008; Park, 2000; Peyronnard & Benzaazoua, 2012; Rodríguez *et al.*, 2018).

In this study, limestone, fly ash and ordinary cement Portland (OPC) were tested at Joutel mine site. The main objective of the work consisted in testing in-situ effectiveness of these materials to stabilize acidic tailings in real field conditions allowing cost-effective site mitigation. Each cell was equipped with two types of water collectors; water vertical infiltration and surface-runoff. This scheme allows to follow the chemical composition of the two main component of water balance which are the surface runoff and the vertical infiltration.

7.3 Materials and Methods

7.3.1 Materials

7.3.1.1 Joutel mine site

Eagle-Telbel mine site (hereafter referenced as Joutel) is a closed gold mine site located at the north of Abitibi-Témiscamingue (Canada). It was operated between 1974 and 1994. The gold was associated to a sulphidic deposit mainly as pyrite and traces of pyrrhotite, chalcopyrite, sphalerite and galena. The gold was extracted using sulphide bulk flotation followed by cyanidization. Ore treatment produced finely grinded tailings deposited in 120 ha of tailings storage facility (TSF). The TSF is divided into two zones; the north zone which the old and relatively elevated TSF and the south zone which is the recent one.

7.3.1.2 Amendments formulation

The two categories of mining amendments were tested within Joutel's oxidized tailings:

Alkaline amendments were applied using limestone. Two formulations were tested based on preliminary laboratory tests. 5 wt.% and 10 wt.% limestone was in-situ mixed with oxidized tailings and then filled in the field cells. The limestone used in this study had particle size under 6.25mm to ensure a mixture of fine and coarse particle size to ensure a mixture of fine reactive particles and long-term reactive coarse particles. Calculation of limestone needed to neutralize oxidized tailings was calculated based on NP and AP of limestone and the reactive tailings as expressed in equation 1 (Eq 15) :

$$\%R = 100 * \frac{\left(\text{NP tailings} - (f * \text{AP tailings})\right)}{(f * \sum_{i=1}^{n} Xi * \text{AP}i) - (\sum_{i=1}^{n} Xi * \text{NP}i)} \qquad \text{(Eq 15)}$$

Where

NP tailings : is the neutralization potential of the mine tailings,

AP tailings : is the acidification potential of the mine tailings,

f : is the ratio (NP/AP) target,

Xi : is proportion of each amendment material used (it equals 1 if only one amendment material is used),

APi : is the acidification potential of the amendment material,

NPi : is the neutralization potential of the amendment material.

For the studied mine tailings, the ratio calculated was about 5% for a ration (NP/AP) of 3.

The second type of the amendments used was cementitious additives which consisted on the integration of OPC and fly ashes. The two formulations used were OPC and ½ OPC- ½ FA at 5 % dosage regarding the total dry weight of the tailings.

7.3.1.3 Field cells construction

Field cells were constructed in an acidic area previously localized at Joutel TSF (Elghali *et al.*, 2018b). The cells were 4m in width, 4m in length and 30cm in depth. The cells were shaped as an inverted truncated pyramid. Only oxidized tailings were amended using the different formulations. Amendments mixing were achieved using the bucket of mechanical loader (Figure 7.1E, F, G, H). Then, the cells were excavated in the TSF and the linear low-density polyethylene geomembrane was installed in the bottom and the sides of each cell to control the exfiltration (Bussière *et al.*, 2007) (Figure 7.1B, F, D). Two systems of water collection were installed at each cell; collection of water vertical infiltration using 5cm PVC pipes and collection of surface and subsurface runoff was achieved using a combination of 5cm PVC pipes and a gutter (Figure 7.1C). Each collection system was connected to a separate external reservoir. Finally, only cemented cells (with binders) were covered with 20cm sand as a protection layer (Figure 7.1I). the drain for collection of water

vertical infiltration and the surface of each cell were installed with a slope of 2%. A schematic representation of the cells constructed is illustrated in the Figure 7.2.

Figure 7.1 : Images showing field cells construction and amendments mixing with oxidized tailings (A, B, C and D : cells excavation, geomembrane and drains installation, E, F, G, H, I: amendments mixing with oxidized tailings)
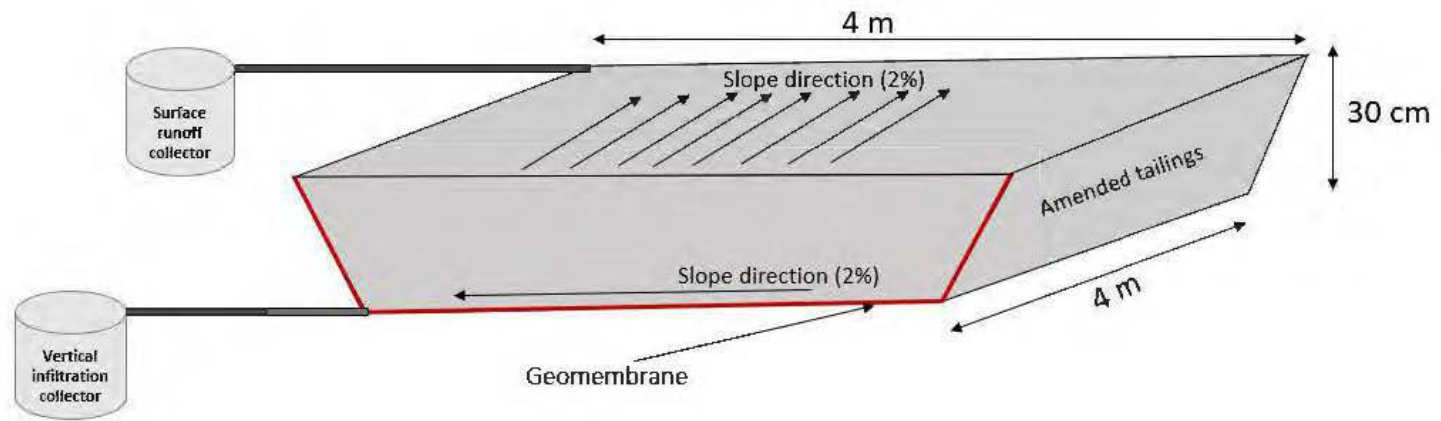
Figure 7.2: Schematic representation of the cells constructed in the TSF (image not to scale) illustrating the two water collectors

7.3.2 Methods

The grain size distribution of the studied samples was evaluated using a laser analyzer (Malvern Masetrsizer). The bulk chemical composition of the samples was analyzed using Perkin Elmer Optima 3100 RL ICP-AES following a total HNO3/Br2/HF/HCl digestion. Major minerals within oxidized and unweathered tailings were analyzed by X-ray diffraction (XRD; Brucker D8 Advance, with a detection limit and precision of approximately 1-5 %, operating with a copper cathode, $K\alpha$ radiation) using DIFFRACT.EVA software and quantified using TOPAS v4.2.

The collected leachates were analyzed for pH, Eh and electrical conductivity using a pH/Eh/conductivity meters and their chemical composition was analyzed using ICP-AES on acidified samples using 2% HNO_3. Iron pH-Eh diagrams were drawn for the control cell and the four cells with alkaline and cementitious amendments at 21 °C using Geochemist's workbench (GWB) database (student edition, version 12.0.1). Iron activities were calculated using Visual Minteq 3.1 based on average iron concentrations. Iron activities calculated were about $2.09E^{-03}$ and $1.8206E^{-06}$ for the control cell and the amended cells respectively. Then, results of pH and Eh were projected on the iron pH-Eh diagrams to visualize iron speciation.

7.4 Results

7.4.1 Chemical, mineralogical, AGP static tests and physical characterization of solid samples

Results of the chemical, mineralogical, static tests and physical characterizations of solid samples used in this study are summarized in Table 7.1. Particle size distribution of mine tailings (MT) were very fine compared to limestone. Ordinary Portland cement (OPC) and fly ash (FA) are also fine which may enhance their cementing potential. Indeed, D_{90} which corresponds to 90 wt.% passing on the cumulative grain size distribution curve, was about 30.5 µm for mine tailings sample, 4500 µm for limestone sample, 46.7 µm for OPC and 1500 for FA. The initial water content of studied samples was about 15 wt.% for mine tailings sample, 6.1 wt.% for limestone sample, Completely dry in the case of OPC sample and 3.5 wt.% for FA sample. Chemical characterization of studied samples showed that the mine tailings sample is iron-rich (19.30 %), its contains also sulfur (4.40 %) and calcium (3%) confirming the mineralogical composition. Limestone sample contained

mainly calcium (34%) and magnesium (2.50 %). OPC sample contained mostly calcium (49%), aluminum (2.75%) and iron (2.25%). The FA sample contained mainly calcium (7.50%), aluminum (4.75%) and iron (2.25%). Other elements were analyzed in trace concentrations within the four samples and the complete chemical composition of these sample is presented in Table 7.1. Mineralogical composition confirmed that mine tailings are highly oxidized; their composition contains many secondary minerals such as gypsum (14 wt.%) and goethite (36 wt.%). Carbonates and sulphides within mine tailings were below detection limit of XRD. Limestone sample was mostly based in calcite (76 wt.%) and dolomite (22 wt.%). Fly ash sample contained about 15 wt.% of calcite (carbonatation most probably), 28 wt.% of quartz and about 57 wt.% of various reactive silicate minerals. Neutralization potential as analyzed using sobek modified by Bouzahzah et *al.* (2015) was about 3 kg $CaCO_3$/t and 880 kg $CaCO_3$/t for mine tailings sample and limestone sample respectively. The low NP of the oxidized tailings is due to carbonate depletion.

Table 7.1: Physical, chemical, static tests and mineralogical characterization of studied samples

		Units	Mine tailings	Limestone	Ordinary cement Portland	Fly ash
Physical characteristics	D10	μm	1.8	50	4.2	82
	D30		4.7	250	11.3	180
	D90		30.4	4500	46.7	1500
	Initial water content	wt.%	15	6.1	dry	3.52
Chemical composition	Al	%	1.73	0.295	2.75	4.69
	Ca		3.00	33.82	49.07	7.58
	Mg		0.27	2.350	1.18	1.05
	Mn		0.23	0.031	0.06	0.42
	Na		0.97	0.125	0.16	1.96
	K		0.27	0.245	0.43	1.85
	Fe		19.30	0.483	2.23	2.24
	Li		0.42	≤0.0005	≤0.0005	0.002
	Pb		0.042	≤0.0005	≤0.0005	≤0.0005
	As		≤0.0005	≤0.0005	0.005	≤0.0005
	Cr		0.009	0.004	0.007	0.006
	Cu		0.001	≤0.0001	0.007	≤0.0001
	Zn		0.007	≤0.0055	0.05	0.07
	S (total)		4.36	0.93	1.74	0.43
	S (sulphates)		3.86	-	-	-
	C		0.23	-	-	-
Static tests	NP	Kg CaCO$_3$/t	3	880	-	-
	AP	Kg CaCO$_3$/t	15.60	-	-	-
Mineralogical composition	Quartz	wt.%	23.09	2.07	Not applicable	27.85
	Calcite		-	75.76		14.66
	Dolomite		-	22.17		≤DL
	Muscovite		5.56	-		7.83
	Labradorite		-	-		43.39
	Orthoclase		1.54	-		6.28
	Biotite		1.91	-		≤DL
	Albite		17.84	-		≤DL
	Gypsum		13.81	-		≤DL
	Goethite		36.25	-		≤DL
	Pyrite		-	-		≤DL

DL = detection limit

7.4.2 Field cells monitoring

The contact time between water and tailings is greater for vertical infiltration than the time required for surface and subsurface runoff. The leachates were collected periodically after each rainy event. The pH/Eh and electrical conductivity were in-situ analyzed.

7.4.2.1 Water vertical infiltration

Leachates from the different cells showed a different behavior regarding pH and electrical conductivity (Figure 7.3A, B). The control cell showed an acidic behavior with pH ranging between 1.7 and 4.3. However, the amended tailings showed a neutral pH values ranging between 6.65 and 7.9 for C2, between 7.15 and 8.15 for C3, between 6.6 and 8.56 for C4 and between 8.75 and 10.35 for C5 (Figure 7.3A). All amendment formulations allowed to buffer the acidity produced by the oxidized tailings. Indeed, acidic leachates reacts with limestone or binding phases, which neutralize leachates acidity through their partial dissolution (Blowes et al., 2003; Blowes et al., 2014; Blowes et al., 1994; Blowes et al., 2013; Doye et al., 2003; Hakkou et al., 2009; Holmström et al., 1999; Wang et al., 2015b). Eh values showed oxic conditions (Eh higher than 100 mV) within the five cells (Figure 7.3C). Electrical conductivity (EC) measures illustrates the chemical quality of leachates (Figure 7.3B); EC values showed that leachates from control cell are more loaded in term of chemical than leachates from amended cells. EC values corresponding to the control cell ranged between 8.8 and 13.40 mS/cm. Contrariwise, EC values from C2, C3, C4 and C5 were too much low; between 5 and 9 mS/cm, 6 and 12 mS/cm, 2 and 5 mS/cm and 2 and 5 mS/cm respectively. The cementitious amendments displayed the lowest EC values compared to control cell and limestone amendment. Hardening of tailings due to cementation processes reduces the available surface area, which reduces the chemical species leaching rates (Benzaazoua et al., 2002; Benzaazoua et al., 1999; Nehdi et al., 2007; Pesonen et al., 2016; Peyronnard et al., 2012; Tariq et al., 2013; Wang et al., 2018; Wang et al., 2015b).
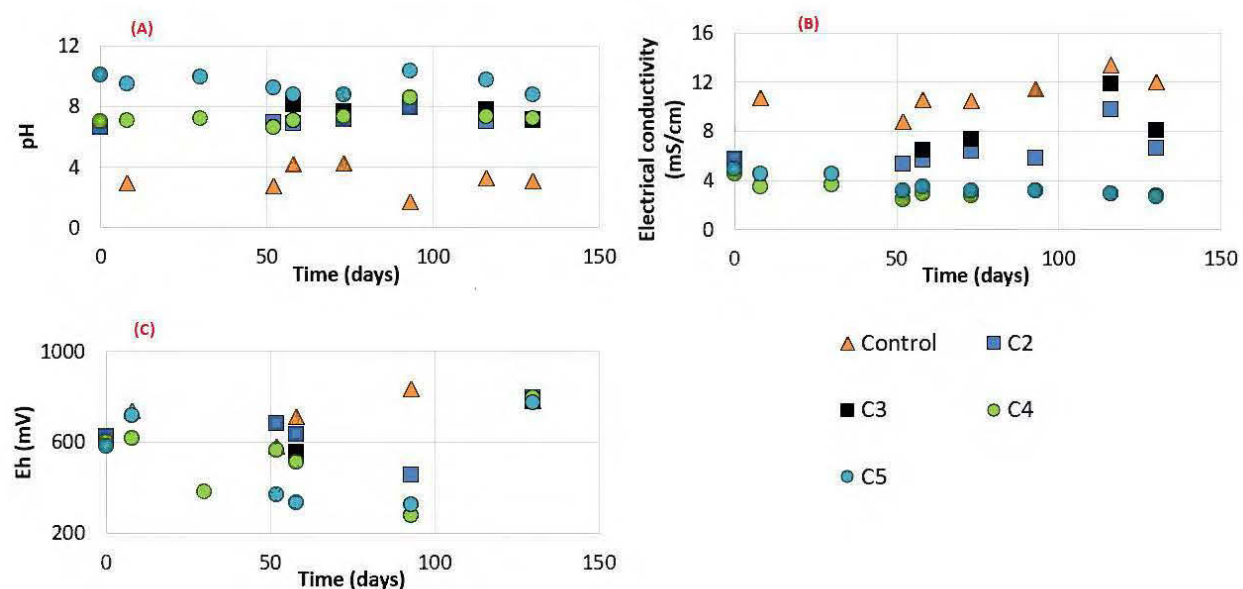
Figure 7.3 : Graphs showing pH (A), electrical conductivity (B) and Eh(C) evolution of vertical infiltrated water

Chemical quality of the leachates collected from the five cells were analyzed for Ca, Mg, Fe, S, Al, Zn, As, Pb, Ni, Li and Cr to evaluate eventual carbonate dissolution, sulphide oxidation and metals/metalloids release (Figure 7.4 and Figure 7.5). Calcium and magnesium concentrations were slightly different depending on the cell. Average Ca concentrations were about 406 mg/l, 478 mg/l, 443 mg/l, 470 mg/l, 543 mg/l for C1, C2, C3, C4 and C5 respectively. Average magnesium concentrations were about 2900 mg/l, 1660 mg/l, 2550 mg/l, 26 mg/l and 2.50 mg/l for control cell, C2, C3, C4 and C5 respectively (Figure 7.4A). Average iron concentrations were about 161.5 mg/l, 0.12 mg/l, 0.12 mg/l, 0.08 mg/l and 0.10 mg/l for control cell, C2, C3, C4 and C5 respectively (Figure 7.4C). The control cell displayed the highest iron concentrations compared to amended cells (Figure 7.4C). Average sulphur concentrations were about 4822 mg/l, 2510 mg/l, 3590 mg/l, 742 mg/l and 978 mg/l for control cell, C2, C3, C4 and C5 respectively (Figure 7.4D).

Regarding aluminum leaching, the control cell and the amended cells released showed the smallest Al concentration. Indeed, average Al concentrations were about 3 mg/l, 0.08 mg/l, 0.09 mg/l, 0.03 mg/l and 0.30 mg/l for control cell, C2, C3, C4 and C5 respectively (Figure 7.4E). Zinc concentrations (Figure 7.5A) were around 0.62 mg/l, 0.90 mg/l, 0.20 mg/l, 0.26 mg/l and 0.12 mg/l for control cell, C2, C3, C4 and C5 respectively. Arsenic was more released within control cell and cells within carbonates amendments (C2 and C3) compared to cells with cementitious amendments

(C4 and C5). Average As concentrations were about 0.18 mg/l, 0.15 mg/l and 0.20 mg/l for control cell, C2 and C3; however, for C4 and C5, no As was detected (Figure 7.5B). Lead average concentrations (mg/l) were about 0.12, 0.012, 0.024 for control cell, C2 and C3 respectively and under detection limit of ICP-AES for C4 and C5 respectively (Figure 7.5C). Nickel average concentrations (mg/l) were about 0.46, 0.026, 0.018, 0.01 and 0.175 for control cell, C2, C3, C4 and C5 respectively (Figure 7.5D). Lithium average concentrations (mg/l) were about 0.08, 0.024, 0.015, 0.02 and 0.007 for control cell, C2, C3, C4 and C5 respectively (Figure 7.5E). Finally, chromium average concentrations (mg/l) were about 0.42, 0.028, 0.029, 0.001 and 0.015 for control cell, C2, C3, C4 and C5 respectively (Figure 7.5F). Comparison of average chemical concentrations of Fe, As, Zn, Ni and Pb with those allowed by the D019 of Quebec province (Ministère du développement durable, 2012), Fe is the only element that exceed the threshold limited by the directive 019 (D019) being around 3 mg/l.
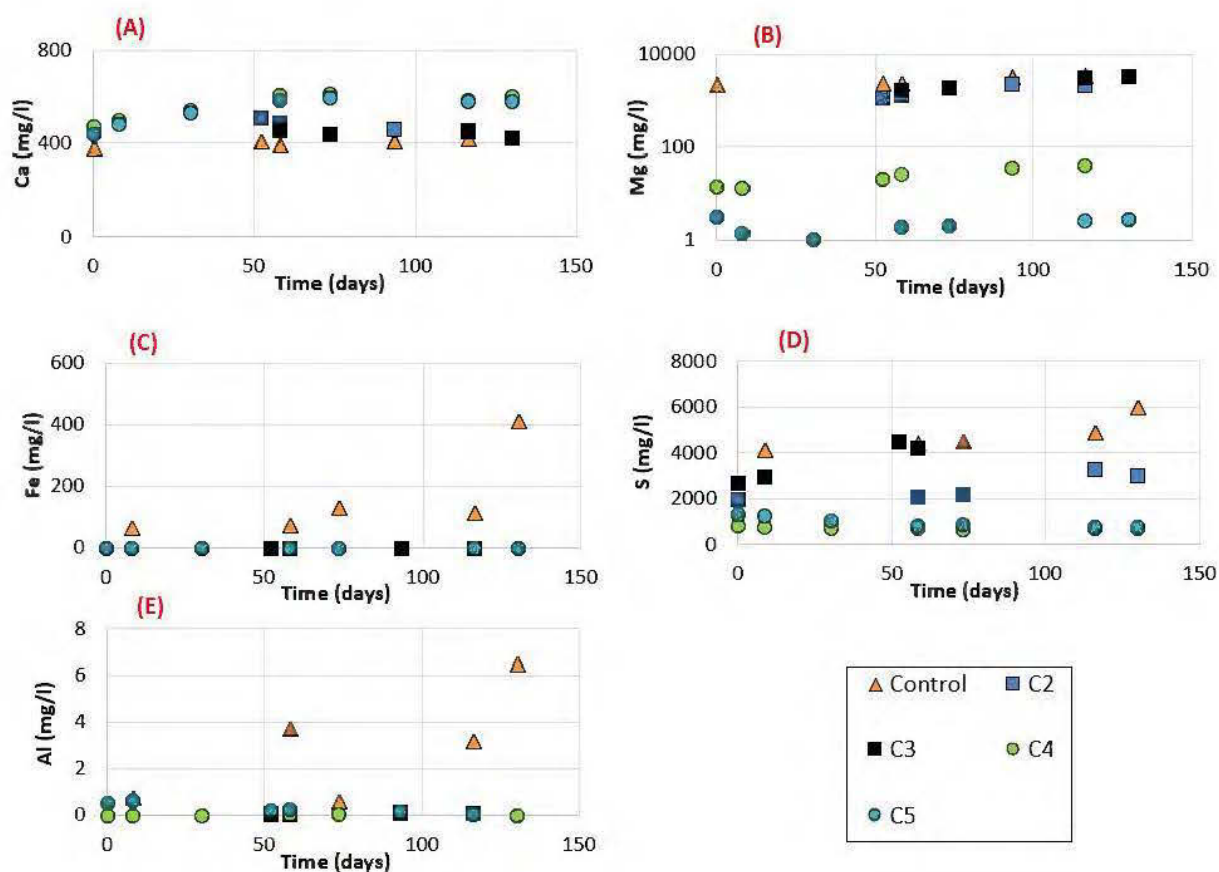
Figure 7.4: Graphs showing punctual concentrations of Ca (A), Mg (B), Fe (C), S (D) and Al (E) of water vertical infiltration
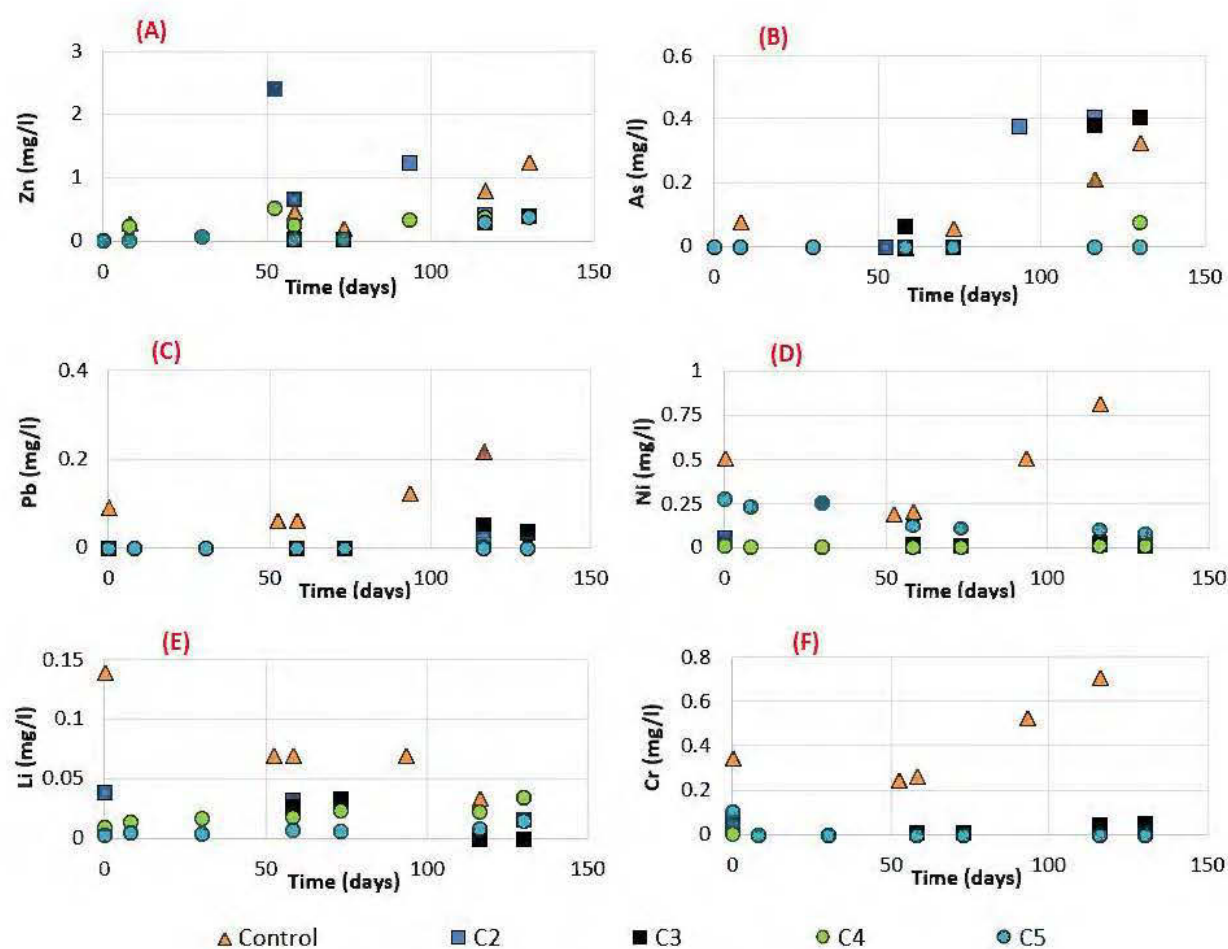
Figure 7.5 : Graphs showing evolution of punctual concentrations of Zn (A), As (B), Pb (C), Ni (D), Li (E) and Cr (F) of water vertical infiltration

7.4.2.2   Surface and subsurface runoff

Leachates collected from surface and subsurface runoff within the five cells were analyzed for the same parameters as the leachates from water vertical infiltration. During the monitoring, no leachates were collected from cemented cell C4 (OPC/FA) suggesting that all water serves to saturate the material. Surface runoff from control cell displayed an acidic behavior with pH values less than 4 (Figure 7.6A) compared to the amended cells which presented pH values higher than 6. Consequently, the different amendment formulations neutralized successfully the acidity produced by the oxidized tailings. EC values for all cells were between 1 and 3 mS/cm (Figure 7.6B) and Eh values were higher than 300 mV indicating oxic conditions (Figure 7.6C).

Average calcium concentrations were about 381 mg/l, 419 mg/l, 451 mg/l and 452 mg/l for control cell, C2, C3 and C5 respectively (Figure 7.7A). Average magnesium concentrations were about 88 mg/l, 172.5 mg/l, 86.4 mg/l and 34.4 mg/l for control cell, C2, C3 and C5 respectively (Figure 7.7B). Average iron concentrations were about 1.50 mg/l, 0.04 mg/l, 0.03 mg/l and 0.04 mg/l for control cell, C2, C3 and C5 respectively (Figure 7.7C). Sulphur leaching were about 514 mg/l, 579 mg/l, 545 mg/l and 510 mg/l for control cell, C2, C3 and C5 respectively (Figure 7.7D). Metals detected within leachates from the five cells were only Al and Zn. Average aluminium concentrations were about 0.26 mg/l and 0.03 mg/l for the control cell and C5 respectively, and for cells C2 and C3 aluminium was only released during 6th sampling period (0.065 mg/l for C2 and 0.06 mg/l for C3) (Figure 7.7E). Average zinc concentrations were 0.20 mg/l, 0.06 mg/l, 0.04 mg/l and 0.26 mg/l for control cell, C2, C3 and C5 respectively (Figure 7.7F). During surface runoff, all chemical species analyzed within the different cells didn't exceed the threshold allowed by the D019. So, reducing contact and time contact between water and the oxidized tailings is an interesting option to reduce chemical species release.
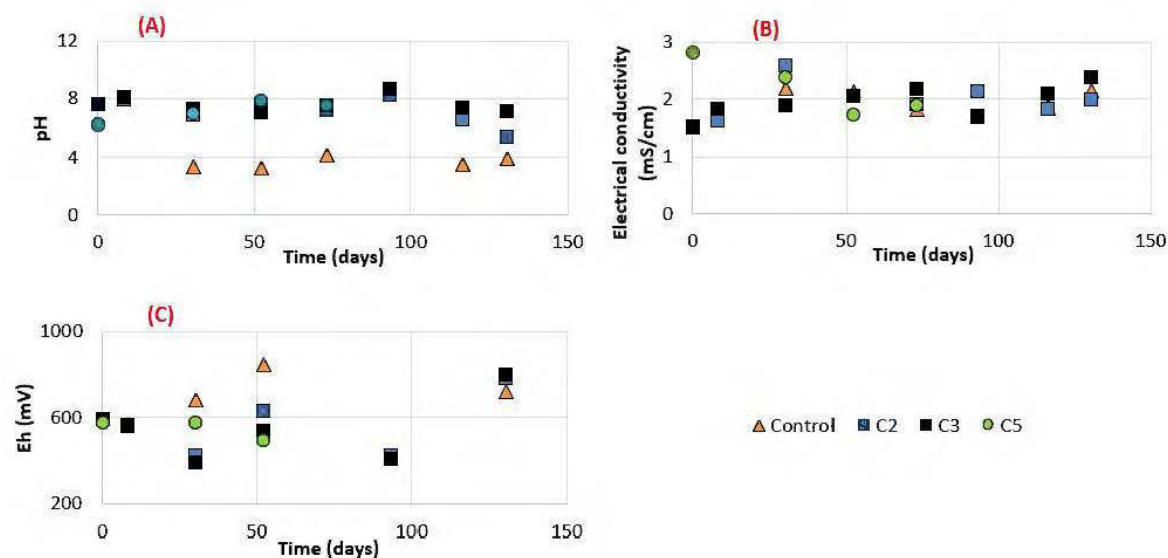
Figure 7.6: Graphs showing the evolution of pH (A), electrical conductivity (B) and Eh(C) within surface and subsurface runoff
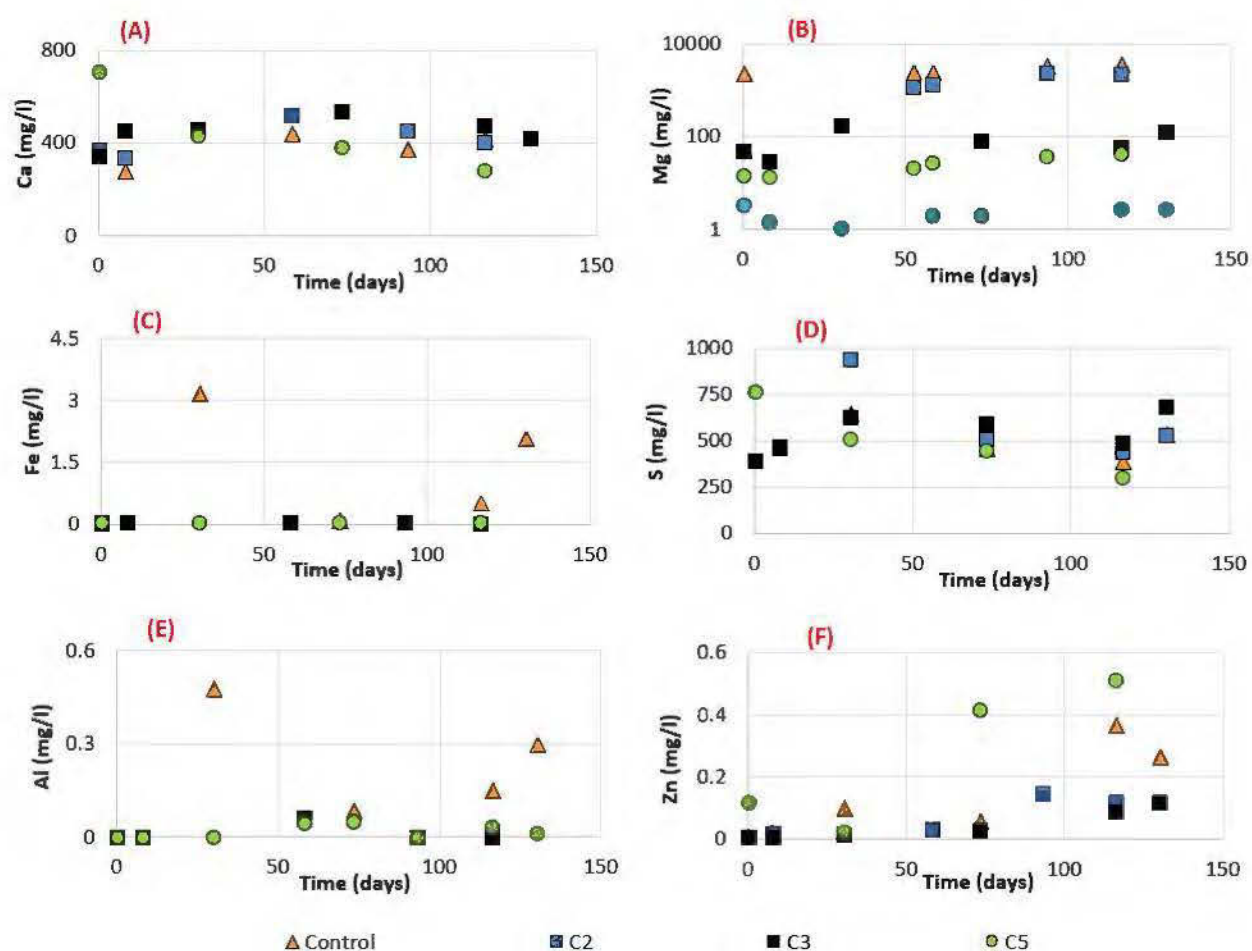
Figure 7.7: Graphs showing the punctual concentrations of Ca (A), Mg (B), Fe (C), S (D), Al (E) and Zn (F) of surface and subsurface runoff

7.5 Discussion

Oxidized tailings showed acidic behavior with pH values less than 4. It seems that the type of water pathways influences considerably the water quality. Indeed, during water vertical infiltration the leachates are more acidic and more loaded in chemical species because they remain for a long time in contact with the reactive minerals. Water vertical infiltration rate depends on the physical, and hydrogeological properties of the tailings (Bear, 2012; Beven & Germann, 1982; Bussière *et al.*, 2001; Childs & Bybordi, 1969; Whitaker, 1986). However, surface runoff rate is greatly controlled by the morphological properties of the tailings storage facility (slope gradient, slope length), the hydrogeological properties (hydraulic conductivity), and the precipitation intensity (Dunne *et al.*, 1991; Getter *et al.*, 2007; Vermang *et al.*, 2015).

During the monitoring period, the behavior of amended tailings showed that alkaline and cementitious amendments are a promising technique that could be used for at least local stabilization and neutralization of acid-generating tailings. The leachates from the different amended cells (C2, C3, C4, C5) were characterized by neutral pH values and were less loaded in terms of chemical species compared to control cell except for calcium which more released within C5 (5 wt.% OPC). In fact, dissolution of carbonates and cement binders produce alkalinity and buffer leachates pH. pH buffering by carbonate dissolution is a well described mechanism (Benzaazoua *et al.*, 2004c; Benzaazoua *et al.*, 2001; Blowes *et al.*, 2003; Blowes *et al.*, 2014; Blowes *et al.*, 1994; Blowes *et al.*, 1998; Blowes *et al.*, 2013; Bussière *et al.*, 2004; Caldeira *et al.*, 2010; Cravotta III *et al.*, 1999; Doye *et al.*, 2003; Jambor, 1994; Jambor *et al.*, 2002b; Jamieson *et al.*, 2015; Lapakko, 1994; Nicholson *et al.*, 1988; Nordstrom *et al.*, 1997). The levels of pH were established early due to high dissolution rates of limestone and cement in acidic medias. Dissolution of carbonates (calcite) could be expressed by the reactions (eq 2 and eq 3) depending on the pH value:

$$CaCO_{3(s)} + 2H^+_{(aq)} \rightarrow H_2CO_{3(aq)} + Ca^{2+} \qquad \text{(Eq 2)}$$

$$CaCO_3(s) + H^+_{(aq)} \rightarrow HCO_3^- + Ca^{2+} \qquad \text{(Eq 3)}$$
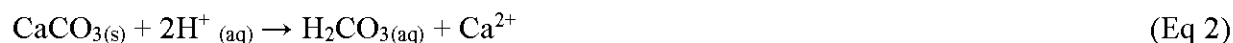
Ca leaching was higher within C5 which contains OPC as binder. In fact, dissolution of tricalcium silicate (C3S) contained in OPC according to the following reaction (Eq 4):

$$2Ca_3SiO_5 + 6H_2O \rightarrow 6Ca^{2+} + 8OH^- + 2H_2SiO_4^{2-} \qquad \text{(Eq 4)}$$
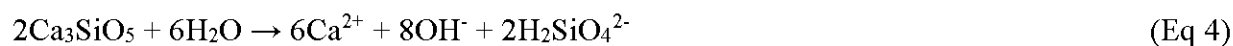
Otherwise, Ca is released by gypsum and in less extent by carbonate dissolution for the control cell. Furthermore, other chemical species (As, Fe, Al, Li, Pb, Cr, Li and Zn) seems to be immobilized within the amended cells. The mechanism responsible for the attenuation is the precipitation, co-precipitation and sorption mechanisms related to secondary iron oxy-hydroxides at neutral pH values (Doye *et al.*, 2003; Komnitsas *et al.*, 2004; Manceau *et al.*, 1992; Yi *et al.*, 2017). In deed, iron Eh-pH diagram presented in Figure 7.8 showed that in iron will precipitate as iron oxides. However, for cementitious amendments (C4 and C5), in addition to iron secondary phases precipitation, two other mechanisms are responsible for chemical species attenuation: i) physical trapping and ii) diminution of water/tailings contact surface and time. Application of

cementitious additives enhances the mechanical resistance of tailings and consequently increases their long-term impermeability (Benzaazoua et al., 2002; Benzaazoua et al., 2004b; Benzaazoua et al., 1999; Nehdi et al., 2007; Wang et al., 2015a). As it can be seen in Figure 7.9, all amendments used in this study were greatly capable to decrease the mobility of the analyzed element compared the control cell except for zinc and arsenic for the C2 and the C3 respectively which referred to 5 wt.% and 10 wt.% limestone. The reduction factor is calculated as illustrated in eq 5:

$$RF = 100 * (1 - \frac{Ca}{C0})$$ (Eq 5)

Where:

RF is reduction factor,

C_a is the concentration of element in the amended cell,

C_0 is the concentration of element in the control cell.

Iron was almost completely immobilized within the different amendment formulations; its reduction factor was about 100%. Aluminium concentrations were reduced of more than 90% with a maximum of reduction factor of 99% calculated for C3. Zinc mobility is greatly reduced within C4 with a reduction factor of 81% and a minimum of 58% for the C4, however for the C2 (5% limestone), Zn zinc concentrations were enhanced with a factor of 45%. Arsenic release was completely inhibited for cementitious formulations (C4 and C5) with a reduction factor of 100% and weakly reduced for C2 with only 17% reduction factor and more released from the C3 displaying a negative rate (-13%). Lead was successfully immobilized within the different amendment formulations but different reduction factor; lead reduction factor was 100% for cementitious amendments and more than 80% for alkaline amendments. Nickel concentrations were greatly reduced within C2, C3 and C4 with a reduction factor about 96% and 62% for C4. Lithium concentrations were reduced within all amendment formulations of a maximum of reduction within C4. Finally, chromium was successfully stabilized within the four amended cells (more than 93%). The order of effectiveness of the different amendment was: C2 = C3 = C4 = C5 for Fe, C4 > C5 > C2 > C3 for Al, C5 > C3 > C4 for Zn, C5 = C4 > C2 for As, C5 = C4 > C2 > C3 for Pb, C4 > C3 > C2 > C5 for Ni, C5 > C3 > C4 > C2 for Li and C4 > C5 > C2 > C3 for Cr. As it could be seen when comparing the efficiency order, cementitious amendments showed high

capacity to immobilization of chemical species and relatively less efficiency of limestone because it fails to stabilize zinc (C2, Figure 7.9) and arsenic (C3, Figure 7.9).
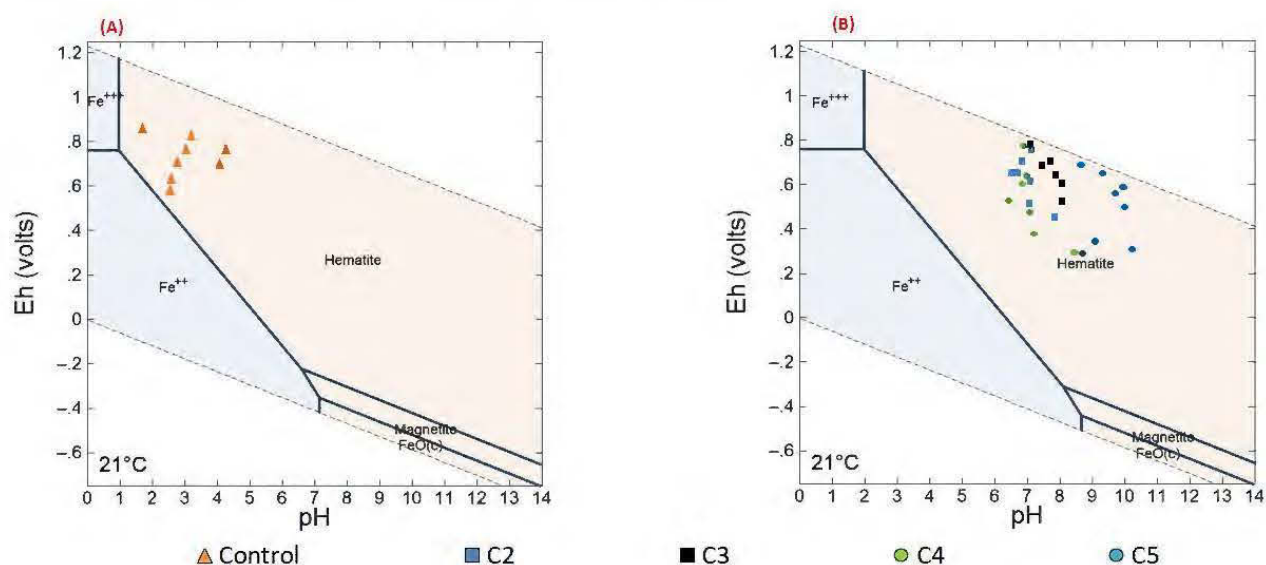
Figure 7.8: Leachate pH and Eh projection into Fe-species pH-Eh for the 5 field cells (A : control cell calculated for an iron-activity of 2.09E-03; B : cells with amendments calculated for an iron-activity of 1.82E-06).
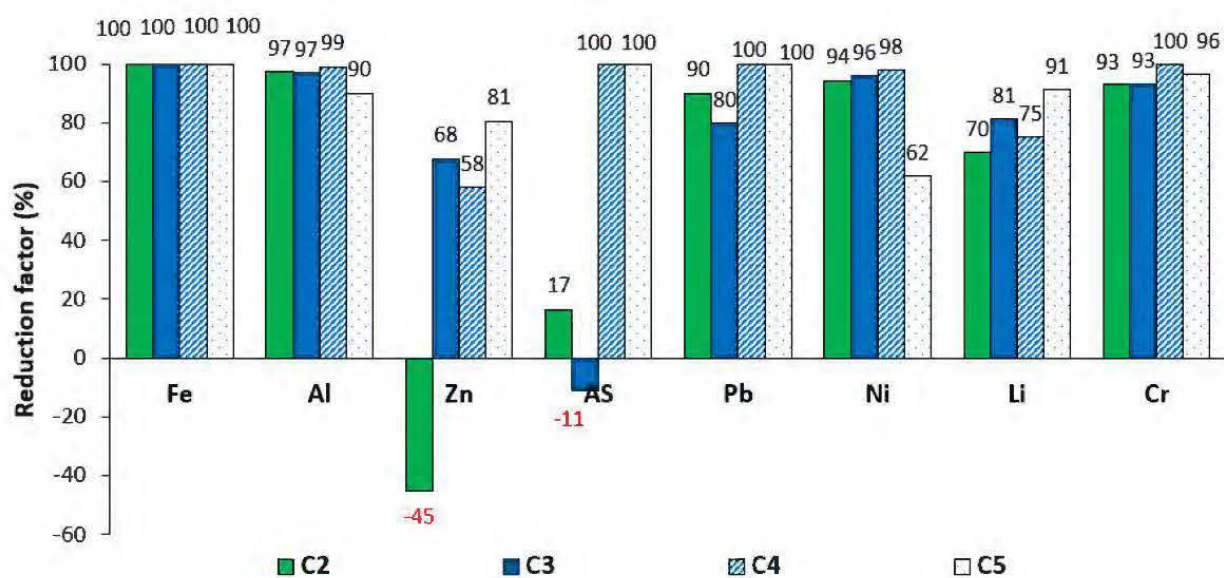
Figure 7.9: Reduction factors of Fe, Al, Zn, As, Pb, Ni, Li and Cr release by the different amendment formulations within vertical infiltrations

7.6 Conclusion

Reducing risks such as acidity generation and contaminant release from mine tailings is a serious challenge facing mining industries that requires cost-effective techniques and practices. Limestone as alkaline amendment and ordinary cement and fly ash as cementitious amendment was tested for the control of local acid generating oxidized tailings in Joutel closed mine TSF. The field tests provided promising results in terms of acidity neutralization and contaminant release capacities from amended tailings based on the early stages of the testing. Furthermore, ordinary Portland cement was successfully substituted by fly ash which may reduce costs of this category of amendment. The cementitious amendment showed a high efficiency compared to limestone. In fact, within cementitious amendment, all the metal and metalloid concentrations were reduced compared to limestone formulation which failed regarding zinc and arsenic stabilization for 5% and 10% limestone respectively. However, the applicability of mining amendments as reclamation technique is decided considering two major points which are i) the long-term behavior of amended tailings and how much time the contaminant will be immobilized and ii) the cost related to this technique. The economical factor will be greatly affected by the availability or not of the materials (amendment) at the proximity of the mine site. The ongoing works consisted of measuring the water flows within surface runoff and water vertical infiltration collectors. Also, the effectiveness of these amendment formulations will be monitored for additional years.

Acknowledgment

References

Acero, P., Ayora, C., Torrentó, C., & Nieto, J.-M. (2006). The behavior of trace elements during schwertmannite precipitation and subsequent transformation into goethite and jarosite. *Geochimica et Cosmochimica Acta, 70*(16), 4130-4139. doi:http://dx.doi.org/10.1016/j.gca.2006.06.1367

Ahmaruzzaman, M. (2010). A review on the utilization of fly ash. *Progress in Energy and Combustion Science, 36*(3), 327-363. doi:10.1016/j.pecs.2009.11.003

Alkattan, M., Oelkers, E. H., Dandurand, J.-L., & Schott, J. (1998). An experimental study of calcite and limestone dissolution rates as a function of pH from− 1 to 3 and temperature from 25 to 80 C. *Chemical Geology, 151*(1), 199-214.

Asta, M. P., Ayora, C., Román-Ross, G., Cama, J., Acero, P., Gault, A. G., Charnock, J. M., & Bardelli, F. (2010). Natural attenuation of arsenic in the Tinto Santa Rosa acid stream (Iberian Pyritic Belt, SW Spain): The role of iron precipitates. *Chemical Geology, 271*(1–2), 1-12. doi:http://dx.doi.org/10.1016/j.chemgeo.2009.12.005

Barnett, E., Hutchinson, R., Adamcik, A., & Barnett, R. (1982). Geology of the Agnico-Eagle gold deposit, Quebec. *Precambrian Sulphide Deposits. Geol. Assoc. Can. Spec. Pap, 25*, 403-426.

Bear, J. (2012). *Hydraulics of groundwater*: Courier Corporation.

Belzile, N., Maki, S., Chen, Y.-W., & Goldsack, D. (1997). Inhibition of pyrite oxidation by surface treatment. *Science of The Total Environment, 196*(2), 177-186.

Benjamin, M. M., & Leckie, J. O. (1981). Competitive adsorption of cd, cu, zn, and pb on amorphous iron oxyhydroxide. *Journal of Colloid and Interface Science, 83*(2), 410-419. doi:http://dx.doi.org/10.1016/0021-9797(81)90337-4

Benzaazoua, M., Bussière, B., & Dagenais, A. (2001). Comparison of kinetic tests for sulfide mine tailings. *Proceedings of tailings and mine waste '01, Balkema, Fort Collins*, 263-272.

Benzaazoua, M., Belem, T., & Bussiere, B. (2002). Chemical factors that influence the performance of mine sulphidic paste backfill. *Cement and Concrete Research, 32*(7), 1133-1144.

Benzaazoua, M., Bussière, B., Dagenais, A.-M., & Archambault, M. (2004a). Kinetic tests comparison and interpretation for prediction of the Joutel tailings acid generation potential. *Environmental Geology, 46*(8), 1086-1101. doi:10.1007/s00254-004-1113-1

Benzaazoua, M., Marion, P., Picquet, I., & Bussière, B. (2004b). The use of pastefill as a solidification and stabilization process for the control of acid mine drainage. *Minerals Engineering, 17*(2), 233-243. doi:http://dx.doi.org/10.1016/j.mineng.2003.10.027

Benzaazoua, M., Ouellet, J., Servant, S., Newman, P., & Verburg, R. (1999). Cementitious backfill with high sulfur content Physical, chemical, and mineralogical characterization. *Cement and Concrete Research, 29*(5), 719-725. doi:https://doi.org/10.1016/S0008-8846(99)00023-X

Beven, K., & Germann, P. (1982). Macropores and water flow in soils. *Water Resources Research, 18*(5), 1311-1325.

Blowes, D., Ptacek, C., Jambor, J., & Weisener, C. (2003). The geochemistry of acid mine drainage. *Treatise on geochemistry, 9*, 612.

Blowes, D., Ptacek, C., Jambor, J., Weisener, C., Paktunc, D., Gould, W., & Johnson, D. (2014). The geochemistry of acid mine drainage.

Blowes, D. W., Jambor, J. L., & Alpers, C. N. (1994). *The environmental geochemistry of sulfide mine-wastes* (Vol. 22): Mineralogical Association of Canada.

Blowes, D. W., Ptacek, C. J., & Jambor, J. (2013). Mineralogy of mine wastes and strategies for remediation. *Environmental Mineralogy II: Vaughan, Wogelius (Eds), Europ. Mineral. Union Notes in Mineral, 13*, 295-338.

Blowes, D. W., Jambor, J. L., Hanton-Fong, C. J., Lortie, L., & Gould, W. D. (1998). Geochemical, mineralogical and microbiological characterization of a sulphide-bearing carbonate-rich gold-mine tailings impoundment, Joutel, Québec. *Applied Geochemistry, 13*(6), 687-705.

Bussière, B., Aubertin, M., & Julien, M. (2001). Couvertures avec effets de barrière capillaire pour limiter le drainage minier acide: aspects théoriques et pratiques. *Vecteur environnement, 34*(3), 37-50.

Bussière, B., Benzaazoua, M., Aubertin, M., & Mbonimpa, M. (2004). A laboratory study of covers made of low-sulphide tailings to prevent acid mine drainage. *Environmental Geology, 45*(5), 609-622.

Bussière, B., Aubertin, M., Mbonimpa, M., Molson, J. W., & Chapuis, R. P. (2007). Field experimental cells to evaluate the hydrogeological behaviour of oxygen barriers made of silty materials. *Canadian Geotechnical Journal, 44*(3), 245-265.

Cai, M.-F., Dang, Z., Chen, Y.-W., & Belzile, N. (2005). The passivation of pyrrhotite by surface coating. *Chemosphere, 61*(5), 659-667.

Caldeira, C. L., Ciminelli, V. S. T., & Osseo-Asare, K. (2010). The role of carbonate ions in pyrite oxidation in aqueous systems. *Geochimica et Cosmochimica Acta, 74*(6), 1777-1789. doi:http://dx.doi.org/10.1016/j.gca.2009.12.014

Chen, Q., Tyrer, M., Hills, C. D., Yang, X., & Carey, P. (2009). Immobilisation of heavy metal in cement-based solidification/stabilisation: a review. *Waste Management, 29*(1), 390-403.

Childs, E., & Bybordi, M. (1969). The vertical movement water in stratified porous material: 1. Infiltration. *Water Resources Research, 5*(2), 446-459.

Ciccu, R., Ghiani, M., Serci, A., Fadda, S., Peretti, R., & Zucca, A. (2003). Heavy metal immobilization in the mining-contaminated soils using various industrial wastes. *Minerals Engineering, 16*(3), 187-192. doi:10.1016/s0892-6875(03)00003-7

Coussy, S., Benzaazoua, M., Blanc, D., Moszkowicz, P., & Bussière, B. (2011). Arsenic stability in arsenopyrite-rich cemented paste backfills: A leaching test-based assessment. *J Hazard Mater, 185*(2–3), 1467-1476. doi:http://dx.doi.org/10.1016/j.jhazmat.2010.10.070

Cravotta Iii, C. A., & Trahan, M. K. (1999). Limestone drains to increase pH and remove dissolved metals from acidic mine drainage. *Applied Geochemistry, 14*(5), 581-606. doi:https://doi.org/10.1016/S0883-2927(98)00066-3

Criado, M., Fernández-Jiménez, A., & Palomo, A. (2007). Alkali activation of fly ash: Effect of the SiO2/Na2O ratio. *Microporous and Mesoporous Materials, 106*(1-3), 180-191. doi:10.1016/j.micromeso.2007.02.055

de Andrade, R. P., Figueiredo, B. R., de Mello, J. W. V., Santos, J. C. Z., & Zandonadi, L. U. (2008). Control of geochemical mobility of arsenic by liming in materials subjected to acid mine drainage. *Journal of Soils and Sediments, 8*(2), 123-129. doi:10.1065/jss2008.03.283

Deschamps, T., Benzaazoua, M., Bussière, B., Aubertin, M., Bouzahzah, H., & Martin, V. (2009). Les effets d'amendements alcalins sur des résidus miniers sulfureux entreposés en surface: Cas des dépôts en pâte. *DÉCHE TS, 19*.

Doye, I., & Duchesne, J. (2003). Neutralisation of acid mine drainage with alkaline industrial residues: laboratory investigation using batch-leaching tests. *Applied Geochemistry, 18*(8), 1197-1213. doi:10.1016/s0883-2927(02)00246-9

Du, Y.-J., Jiang, N.-J., Liu, S.-Y., Jin, F., Singh, D. N., & Puppala, A. J. (2013). Engineering properties and microstructural characteristics of cement-stabilized zinc-contaminated kaolin. *Canadian Geotechnical Journal, 51*(3), 289-302.

Duchesne, J., & Reardon, E. (1998). Determining controls on element concentrations in cement kiln dust leachate. *Waste Management, 18*(5), 339-350.

Duchesne, J., & Laforest, G. (2006). Remediation of electric arc furnace dust leachate by the use of cementitious materials: A column-leaching test. *Chinese Journal of Geochemistry, 25*, 99-99.

Dunne, T., Zhang, W., & Aubry, B. F. (1991). Effects of rainfall, vegetation, and microtopography on infiltration and runoff. *Water Resources Research, 27*(9), 2271-2285.

Elghali, A., Benzaazoua, M., Bussière, B., Kennedy, C., Parawani, R., & Graham, S. (2018). The role of hardpan formation on the reactivity of sulphidic mine tailings: Joutel case study (submitted paper). *Science of The Total Environment*.

Evangelou, V., & Zhang, Y. (1995). A review: pyrite oxidation mechanisms and acid mine drainage prevention. *Critical Reviews in Environmental Science and Technology, 25*(2), 141-199.

Falciglia, P. P., Romano, S., & Vagliasindi, F. G. (2017). Stabilisation/Solidification of soils contaminated by mining activities: Influence of barite powder and grout content on γ-radiation shielding, unconfined compressive strength and 232Th immobilisation. *Journal of Geochemical Exploration, 174*, 140-147.

Fatahi, B., & Khabbaz, H. (2015). Influence of Chemical Stabilisation on Permeability of Municipal Solid Wastes. *Geotechnical and Geological Engineering, 33*(3), 455-466. doi:10.1007/s10706-014-9831-y

Fleri, M. A., & Whetstone, G. T. (2007). In situ stabilisation/solidification: Project lifecycle. *J Hazard Mater, 141*(2), 441-456. doi:http://dx.doi.org/10.1016/j.jhazmat.2006.05.096

Getter, K. L., Rowe, D. B., & Andresen, J. A. (2007). Quantifying the effect of slope on extensive green roof stormwater retention. *Ecological engineering, 31*(4), 225-231.

Gilles, B., Mostafa, B., Abdelkabir, M., & Bruno, B. (2014). Long term hydro-geochemical behaviour of surface paste disposal in field experimental cells. *In: Proceedings of the Conference Canadienne de Géotechnique, GeoRegina, CD-Rom, 1*(1), 19.

Hakkou, R., Benzaazoua, M., & Bussière, B. (2009). Laboratory evaluation of the use of alkaline phosphate wastes for the control of acidic mine drainage. *Mine Water and the Environment, 28*(3), 206.

Harrison, A. L., Dipple, G. M., Power, I. M., & Mayer, K. U. (2015). Influence of surface passivation and water content on mineral reactions in unsaturated porous media:

implications for brucite carbonation and CO 2 sequestration. *Geochimica et Cosmochimica Acta, 148*, 477-495.

Holmström, H., Ljungberg, J., & Öhlander, B. (1999). Role of carbonates in mitigation of metal release from mining waste. Evidence from humidity cells tests. *Environmental Geology, 37*(4), 267-280. doi:10.1007/s002540050384

Ichrak, H., Mostafa, B., Abdelkabir, M., & Bruno, B. (2016). Effect of cementitious amendment on the hydrogeological behavior of a surface paste tailings' disposal. *Innovative Infrastructure Solutions, 1*(1), 19.

Jambor, J. (1994). Mineralogy of sulfide-rich tailings and their oxidation products. *Environmental geochemistry of sulfide mine-wastes, 22*, 59-102.

Jambor, J., Dutrizac, J., Groat, L., & Raudsepp, M. (2002). Static tests of neutralization potentials of silicate and aluminosilicate minerals. *Environmental Geology, 43*(1), 1-17.

Jamieson, H. E., Walker, S. R., & Parsons, M. B. (2015). Mineralogical characterization of mine waste. *Applied Geochemistry, 57*, 85-105. doi:10.1016/j.apgeochem.2014.12.014

Kang, C.-U., Jeon, B.-H., Park, S.-S., Kang, J.-S., Kim, K.-H., Kim, D.-K., Choi, U.-K., & Kim, S.-J. (2016). Inhibition of pyrite oxidation by surface coating: a long-term field study. *Environ Geochem Health, 38*(5), 1137-1146.

Kim, J. W., & Jung, M. C. (2011). Solidification of arsenic and heavy metal containing tailings using cement and blast furnace slag. *Environ Geochem Health, 33 Suppl 1*, 151-158. doi:10.1007/s10653-010-9354-2

Kogbara, R. B., Yi, Y., & Al-Tabbaa, A. (2011). Process envelopes for stabilisation/solidification of contaminated soil using lime–slag blend. *Environmental Science and Pollution Research, 18*(8), 1286-1296. doi:10.1007/s11356-011-0480-x

Komnitsas, K., Bartzas, G., & Paspaliaris, I. (2004). Efficiency of limestone and red mud barriers: laboratory column studies. *Minerals Engineering, 17*(2), 183-194. doi:10.1016/j.mineng.2003.11.006

Kumpiene, J., Lagerkvist, A., & Maurice, C. (2008). Stabilization of As, Cr, Cu, Pb and Zn in soil using amendments – A review. *Waste Management, 28*(1), 215-225. doi:http://dx.doi.org/10.1016/j.wasman.2006.12.012

Lamontagne, A. (2001). *Étude de la méthode d'empilement des stériles par entremêlement par couches pour contrôler le drainage minier acide.* Université Laval.

Lapakko, K. A. (1994). *Evaluation of neutralization potential determinations for metal mine waste and a proposed alternative.* Paper presented at the Proceeding: of the Third International Conference on the Abatement of Acidic Drainage, April.

Li, X. D., Poon, C. S., Sun, H., Lo, I. M. C., & Kirk, D. W. (2001). Heavy metal speciation and leaching behaviors in cement based solidified/stabilized waste materials. *J Hazard Mater, 82*(3), 215-230. doi:http://dx.doi.org/10.1016/S0304-3894(00)00360-5

Mackie, A. L., & Walsh, M. E. (2015). Investigation into the use of cement kiln dust in high density sludge (HDS) treatment of acid mine water. *Water Res, 85*, 443-450. doi:10.1016/j.watres.2015.08.056

Manceau, A., Charlet, L., Boisset, M. C., Didier, B., & Spadini, L. (1992). Sorption and speciation of heavy metals on hydrous Fe and Mn oxides. From microscopic to macroscopic. *Applied Clay Science, 7*(1), 201-223. doi:http://dx.doi.org/10.1016/0169-1317(92)90040-T

Ministère du développement durable, e. e. p., Gouvernement du Québec. (2012). Directive 019 sur l'industrie minière. 105.

Mitchell, K., Trakal, L., Sillerova, H., Avelar-González, F. J., Guerrero-Barrera, A. L., Hough, R., & Beesley, L. (2018). Mobility of As, Cr and Cu in a contaminated grassland soil in response to diverse organic amendments; a sequential column leaching experiment. *Applied Geochemistry, 88*, 95-102.

Mylona, E., Xenidis, A., & Paspaliaris, I. (2000). Inhibition of acid generation from sulphidic wastes by the addition of small amounts of limestone. *Minerals Engineering, 13*(10), 1161-1175. doi:http://dx.doi.org/10.1016/S0892-6875(00)00099-6

NEDEM. (1997). DIVERSITÉ MICROBIOLOGIQUE DANS LA PRODUCTION DE DRAINAGE MINIER ACIDE À LA HALDE SUD DE LA MINE DOYON

Nehdi, M., & Tariq, A. (2007). Stabilization of sulphidic mine tailings for prevention of metal release and acid drainage using cementitious materials: a review. *Journal of Environmental Engineering and Science, 6*(4), 423-436.

Nicholson, R. V., Gillham, R. W., & Reardon, E. J. (1988). Pyrite oxidation in carbonate-buffered solution: 1. Experimental kinetics. *Geochimica et Cosmochimica Acta, 52*(5), 1077-1085. doi:http://dx.doi.org/10.1016/0016-7037(88)90262-1

Nordstrom, D. K., & Southam, G. (1997). Geomicrobiology of sulfide mineral oxidation. *Reviews in mineralogy, 35*, 361-390.

Paradis, M., Duchesne, J., Lamontagne, A., & Isabel, D. (2006). Using red mud bauxite for the neutralization of acid mine tailings: a column leaching test. *Canadian Geotechnical Journal, 43*(11), 1167-1179. doi:10.1139/t06-071

Park, C.-K. (2000). Hydration and solidification of hazardous wastes containing heavy metals using modified cementitious materials. *Cement and Concrete Research, 30*(3), 429-435. doi:http://dx.doi.org/10.1016/S0008-8846(99)00272-0

Pesonen, J., Yliniemi, J., Illikainen, M., Kuokkanen, T., & Lassi, U. (2016). Stabilization/solidification of fly ash from fluidized bed combustion of recovered fuel and biofuel using alkali activation and cement addition. *Journal of Environmental Chemical Engineering, 4*(2), 1759-1768. doi:http://dx.doi.org/10.1016/j.jece.2016.03.005

Peyronnard, O., & Benzaazoua, M. (2012). Alternative by-product based binders for cemented mine backfill: Recipes optimisation using Taguchi method. *Minerals Engineering, 29*, 28-38. doi:10.1016/j.mineng.2011.12.010

Rodríguez, L., Gómez, R., Sánchez, V., Villaseñor, J., & Alonso-Azcárate, J. (2018). Performance of waste-based amendments to reduce metal release from mine tailings: One-year leaching behaviour. *J Environ Manage, 209*, 1-8.

Tariq, A., & Yanful, E. K. (2013). A review of binders used in cemented paste tailings for underground and surface disposal practices. *J Environ Manage, 131*, 138-149. doi:10.1016/j.jenvman.2013.09.039

Vermang, J., Norton, L., Huang, C., Cornelis, W., Da Silva, A., & Gabriels, D. (2015). Characterization of soil surface roughness effects on runoff and soil erosion rates under simulated rainfall. *Soil Science Society of America Journal, 79*(3), 903-916.

Wang, F., Shen, Z., & Al-Tabbaa, A. (2018). PC-based and MgO-based binders stabilised/solidified heavy metal-contaminated model soil: strength and heavy metal speciation in early stage. *Géotechnique*, 1-6.

Wang, F., Wang, H., Jin, F., & Al-Tabbaa, A. (2015a). The performance of blended conventional and novel binders in the in-situ stabilisation/solidification of a contaminated site soil. *J Hazard Mater, 285*, 46-52.

Wang, F., Wang, H., Jin, F., & Al-Tabbaa, A. (2015b). The performance of blended conventional and novel binders in the in-situ stabilisation/solidification of a contaminated site soil. *J Hazard Mater, 285*, 46-52. doi:10.1016/j.jhazmat.2014.11.002

Whitaker, S. (1986). Flow in porous media I: A theoretical derivation of Darcy's law. *Transport in porous media, 1*(1), 3-25.

Yi, Y., Wen, J., Zeng, G., Zhang, T., Huang, F., Qin, H., & Tian, S. (2017). A comparative study for the stabilisation of heavy metal contaminated sediment by limestone, MnO 2 and natural zeolite. *Environmental Science and Pollution Research, 24*(1), 795-804.

Yilmaz, E., Benzaazoua, M., Bussière, B., & Pouliot, S. (2014). Influence of disposal configurations on hydrogeological behaviour of sulphidic paste tailings: A field experimental study. *International Journal of Mineral Processing, 131*, 12-25. doi:10.1016/j.minpro.2014.08.004

CHAPITRE 8   DISCUSSION GÉNÉRALE

Les différentes caractérisations et essais de prédiction environnementaux réalisés sur des stériles et résidus miniers, dans le cadre de ce doctorat, ont permis d'obtenir des données qualitatives et quantitatives sur : i) l'effet de la libération des sulfures et des carbonates sur le comportement géochimique des stériles miniers, ii) l'effet des oxy-hydroxydes de fer et du hardpan sur le comportement géochimique des résidus miniers oxydés et enfin iii) l'efficacité de divers amendements pour le contrôle du DMA dans des parcs à résidus. Parmi les contributions de cette thèse, on souligne la proposition d'une nouvelle méthodologie pour la caractérisation des stériles miniers pour une gestion optimale des rejets : une approche de caractérisation basée sur l'intégration de la minéralogie automatisée en considérant des échantillons qui assurent une représentativité de la distribution granulométrique des stériles tels qu'ils sont produits lors de l'opération minière. La finalité est de gérer séparément les stériles dépendamment de la distribution granulométrique et texturale des sulfures et des carbonates. Ensuite, cette thèse a permis de montrer que, dans certains cas, les essais cinétiques au laboratoire ne sont pas capables de reproduire le comportement géochimique du terrain. C'est le cas des résidus miniers riches en carbonates de fer et manganèse. Classés comme incertains, ils ont montré un comportement acidogène plus ou moins localisé sur le terrain, d'où la nécessité, dans ces cas, d'interpréter les essais cinétiques de laboratoire avec une grande précaution. Finalement, pour ces résidus acidogènes des techniques de mitigation ont été testées sur le terrain, consistant à évaluer l'efficacité de divers amendements. Ce chapitre traitera des principaux résultats de cette étude et tentera d'en discuter certains aspects.

8.1 Importance de la procédure d'échantillonnage pour l'étude du comportement géochimique des rejets miniers

L'objectif principal de l'échantillonnage est de sélectionner des échantillons ayant les mêmes caractéristiques que les lithologies échantillonnées (EPA, 1994). Différents plans d'échantillonnage ont été développés pour différentes thématiques (Carter, 1993). L'étape de l'échantillonnage est reconnue une étape clé pour bien mener des études dans différents domaines (Esbensen & Heydorn, 2004; Møller, 2004). L'échantillonnage des rejets est encore plus complexe à cause de l'hétérogénéité de leurs propriétés physiques suite à leur déposition ; (surtout dans le

cas des stériles) et minéralogiques (particulièrement le cas des résidus miniers oxydés). La difficulté d'échantillonnage diffère selon le type de rejets (stériles ou résidus).

En effet, les stériles miniers étant caractérisés par un étalement de la distribution granulométrique, présentent la complexité de la taille maximale à considérer lors de l'échantillonnage et le protocole d'échantillonnage (Lapakko *et al.*, 2006; Smith *et al.*, 2000). Différents auteurs ont suggéré la taille maximale des particules à considérer ; Smith *et al.*, (2000) ont suggéré 2 mm comme taille des particules pour avoir le maximum de minéraux disponibles alors que Lapakko *et al.*, (2006) suggèrent 6.3 mm. Notons la diffulté d'obtenir un échantillon représentatitf à partir d'une halde à stériles qui présente des hétérogénéités lithologiques et granulométriques bien établies. Durant ce projet, cette problématique a été évitée en échantillant en amont juste après un dynamitage sur le site. L'étude sur les stériles présentée dans cette thèse a montré qu'à partir de 2.4 mm, les sulfures, pour ces matériaux, sont très faiblement disponibles aux réactions d'oxydation, sachant que 2.4 mm est un paramètre spécicifique aux échantillons et au site étudiés, ce qui est en concordance avec les travaux de Smith *et al.*, (2000). Etant donné la grande variabilité des propriétés métalogéniques des gisements au travers le monde, la taille maximale à considérer lors de l'échantillonnage doit être choisie en fonction du degré de libération des sulfures suite à un dynamitage donné. Le choix de ce paramètre est fait en considérant que l'oxydation des sulfures est la première réaction du drainage minier et peut être responsable de l'acidité. De plus, l'échantillonnage doit être réailisé après dynamitage des stériles pour l'unique raison de considérer la même distribution granulométrique des stériles tels que produits lors de des opérations d'extraction. En conséquence, le choix des carottes, qui s'imposent dans le cas d'un projet minier dans ses phases de faisabilités, doit se faire avec une grande précaution. Lors du concassage de ces carottes, il faut générer suffisamment de fines pour simuler un stérile issu du dynamitage. Par ailleurs, dans le cas de stériles préalablement altérés, la notion de passivation (coating) des sulfures est un aspect à considérer en sachant qu'il peut être quantifié à l'aide de la minéralogie appliquée.

Pour le cas des parcs à résidus fermés ou abondonnés, l'oxydation des résidus est très variable dépendamment de la localisation sur le parc à résidus et surtout de la topgraphie du site (profondeur de la nappe, proximité des digues, etc.). En considérant que les résidus suite à leur déposition sont hétérogènes des points de vue de la composition minéralogique et de la distribution granulométrique, la procédure d'échantillonnage proposée pour des fins de restauration est basée sur une cartographie spatiale des propriétés géochimiques des résidus oxydés en utilisant un

échantillonnage systématique. C'est une technique largement développée et recommandée pour la caractérisation des sols et pour les besoins de l'exploration géochimique (Bellhouse, 2005; Buckland *et al.*, 2005; Carter, 1993; Cruz-Orive, 1989; Gilbert, 1987). Cette procédure est généralement plus fastidieuse et couteuse qu'un échantillonnage ponctuel aléatoire, mais elle représente beaucoup d'avantages : elle permet de quantifier la variablité spatiale des propriétés environnementales des résidus oxydés, de quantifier les correlations spatiales entre les différents paramètres analysés et de fournir la possibilité de dévisier le parc à résidus en différentes zones homogènes de point du vu degré de contamination. En effet, c'est une méthodologie qui rajoute la composante spatiale aux autres composantes relatives aux résidus (minéralogie, morphologie, etc.). L'intégration des SIG à ce niveau permet de produire un outil d'aide à la décision pour orienter les travaux de mitigation/restauration des parcs à résidus inactifs. Les zones à neutraliser avant le scénario de restauration global seront délimitées basé sur le SIG produit. La difficulté de cette technique se situe au niveau du choix du pas d'échantillonnage. En effet, il n'existe pas de moyen statistique qui permet de définir le pas d'échantillonnage, mais il peut être estimé par l'opérateur en fonction de différentes contraintes à savoir : i) les objectifs de l'étude, ii) le niveau de connaissance du site d'étude et de la problématique et enfin, iii) le budget alloué pour l'étude.

8.2 Importance de la caractérisation minéralogique et effet de la libération minérale sur le comportement géochimique des rejets miniers

La caractérisation minéralogique est considérée parmi les étapes clés d'une bonne prédiction et compréhension du comportement géochimique des rejets miniers. Certains auteurs ont suggéré l'utilisation de la minéralogie dès l'étape de l'exploration pour bien planifier le mode de traitement du minerai et aussi prédire les problèmes environnementaux liés à l'exploitation du minerai en question (Bouzahzah *et al.*, 2014a; Chopard, 2017; Chopard *et al.*, 2015; Jamieson *et al.*, 2015). La minéralogie multi-technique a été utilisée comme moyen d'explication et de prédiction des phénomènes géochimiques qui peuvent avoir lieu lors du processus d'oxydation des rejets miniers (Blowes *et al.*, 2003; Dong, 2015; Goodall, 2008; Gottlieb *et al.*, 2000; Jambor, 1994; Mukherjee, 2012; Paktunc *et al.*, 2000a; Petruk, 2000). La caractérisation minéralogique peut varier selon l'objectif de l'étude ; elle peut commencer par des observations sous microscopie optique et se

terminer par des méthodes plus poussées comme les systèmes de minéralogie automatisés permettant de quantifier divers paramètres minéralogiques (e.g. QEMSCAN, MLA, *Mineralogic Mining*, TIMA). Cette thèse a mis en évidence l'importance de la minéralogie automatisée comme technique d'identification et de quantification des paramètres texturaux d'un rejet minier qui peuvent être d'une grande importance lors de la gestion des rejets ou encore lors du traitement minerai.

En effet malgré son coût, la minéralogie automatisée permet de quantifier le degré de libération minérale, les associations minéralogiques, la composition minéralogique modale, la granulo-minéralogie, la distribution élémentaire, etc. Le degré de libération minérale décrit le taux d'exposition d'un minéral. En effet, un minéral est qualifié par un degré de libération de 100% s'il n'a aucun contour partagé avec un autre minéral. Un minéral est dit encapsulé à 100% si ses contours sont complètement partagés avec d'autres minéraux. Il est admis que les surfaces minérales relevées sur les analyses microscopiques (sections polies) sont représentatives des textures volumiques et que la réactivité d'un minéral dépend de son taux d'exposition. Le chapitre 3 et 4 de cette thèse ont montré un exemple concret de l'utilisation de la minéralogie automatisée pour la prédiction environnementale et du potentiel polluant des stériles miniers tenant en compte de leur granulo-minéralogie. C'est une approche qui propose la séparation d'un stérile minier selon un paramètre appelé ici diamètre d'encapsulation physique des sulfures (DPLS, *diameter of physical locking of sulphides*); il définit la taille minimale des particules au-dessus de laquelle les sulfures sont presque complètement encapsulés dans une matrice de gangue silicatée. De ce fait, la fraction +DPLS est caractérisée par une réactivité négligeable en comparaison à la réactivité de la fraction -DPLS. Généralement la réactivité de l'échantillon total est déterminée par la réactivité de la fraction -DPLS. Malgré que ce DPLS ne peut pas être généralisé pour tous les types de stériles et pour tous les sites miniers, la méthodologie proposée est valable indépendamment de la géologie des lithologies en question moyennant des modifications qui peuvent avoir lieu sur le nombre de fractions à analyser. Le nombre de fractions granulométriques à analyser dépend de la taille maximale des particules (Dmax) de l'échantillon étudié. En règle générale, plus Dmax est grand plus qu'il faut augmenter le nombre de fractions à analyser.

L'objectif ultime de définir ce DPLS est de suggérer une nouvelle façon pour la gestion des stériles. Cette méthodologie présente théoriquement un grand intérêt économique pour l'industrie minière qui produit des stériles ayant une granulométrie étalée. Sachant que la fraction grossière présente

une proportion importante de l'échantillon total, le DPLS va réduire la quantité de stériles à gérer et les haldes à restaurer.

L'influence du degré de libération a été étudiée indirectement en étudiant l'effet de la granulométrie sur le comportement géochimique des rejets miniers (Erguler *et al.*, 2015; Kalyoncu Erguler *et al.*, 2014; Lapakko *et al.*, 2006; Paktunc *et al.*, 2000a). Dans cette thèse, l'effet du degré de libération des sulfures sur le comportement géochimique des stériles a été intégrée à une prédiction du PGA de type statique et cinétique en colonnes monitorées sur 543 jours. Le taux d'oxydation de la pyrite pour les trois lithologies en question a montré que la fraction -DPLS présente un taux d'oxydation six fois plus important que celui de l'oxydation de la pyrite pour l'échantillon total et encore dix fois plus important que celui de l'oxydation de la pyrite pour la fraction +DPLS. De plus, la réalisation des essais statiques sur un stériles miniers nécessite sa pulvérisation pour qu'il soit conforme aux protocoles et méthodes développées dans la littérature (Bouzahzah *et al.*, 2015a; Jambor *et al.*, 2002a; Lawrence *et al.*, 1997b; NEDEM, 2008; Plante *et al.*, 2012). La pulvérisation de l'échantillon est une étape qui détruit la texture initiale de l'échantillon indépendamment de sa granulométrie initiale. L'analyse ou le calcul du NP à partir d'un échantillon pulvérisé suppose que tous les minéraux présents dans l'échantillon vont réagir ce qui n'est pas vrai et démontré par des essais cinétiques dont les résultats sont illustrés au chapitre 4 de ce mémoire (Blowes *et al.*, 2003; Blowes *et al.*, 1994; Blowes *et al.*, 2013). De ce fait, introduire un facteur de correction de la valeur du soufre et le carbone inorganique utilisés dans les tests de prédiction du PGA, qui prend en considération la texture initiale de l'échantillon, est nécessaire. Cette correction consiste à multiplier le PA par le degré de libération des minéraux acidifiants et le PN par le degré de libération des minéraux neutralisants comme analysés par le système de minéralogie automatisé. Mais dans les cas où les minéraux neutralisants (ou minéraux acidifiants) sont multiples, il faut corriger le PN (ou PA) par rapport au degré de libération de chaque minéral en considérant sa participation à la neutralisation globale (ou acidification) de l'échantillon. Le PN des stériles étudiés ici a été corrigé seulement par rapport au degré de libération des carbonates parce qu'ils sont les principaux minéraux qui participent à la neutralisation. Cette conclusion a été justifiée en comparant le PN calculé par les carbonates et le PN analysé selon la méthode de Sobek modifiée par Bouzahzah *et al.* (2015). Par ailleurs, plusieurs auteurs ont étudié l'apport des silicates au PN des rejets miniers et ont démontré qu'ils ne participent pas d'une manière significative en plus de leurs cinétiques de dissolution lentes (Jambor *et al.*, 2002a). Par conséquent, le DPLS est un

paramètre intrinsèque à chaque type de lithologie et spécifique à chaque site. Il peut être intégré lors de la gestion des stériles pour réduire les coûts liés aux éventuelles opérations de réhabilitation. Cette approche suggère la séparation des stériles miniers en fonction du DPLS spécifique avant la mise en place de la halde à stérile. L'objectif ultime de l'utilisation du DPLS est d'isoler la fraction -DPLS qui présente une réactivité importante et un volume faible pour ne pas contaminer le comportement géochimique global de la halde à stériles. C'est une approche qui nécessite une étude de faisabilité technique et économique. Un principe similaire est utilisé en Australie par le CRC ore appelé *'grade engineering'* qui vise à maximiser la récupération du minerai dès la première étape du sautage en se basant sur une séparation granulométrique in-situ. Ce principe est illustré dans la Figure 8.1.
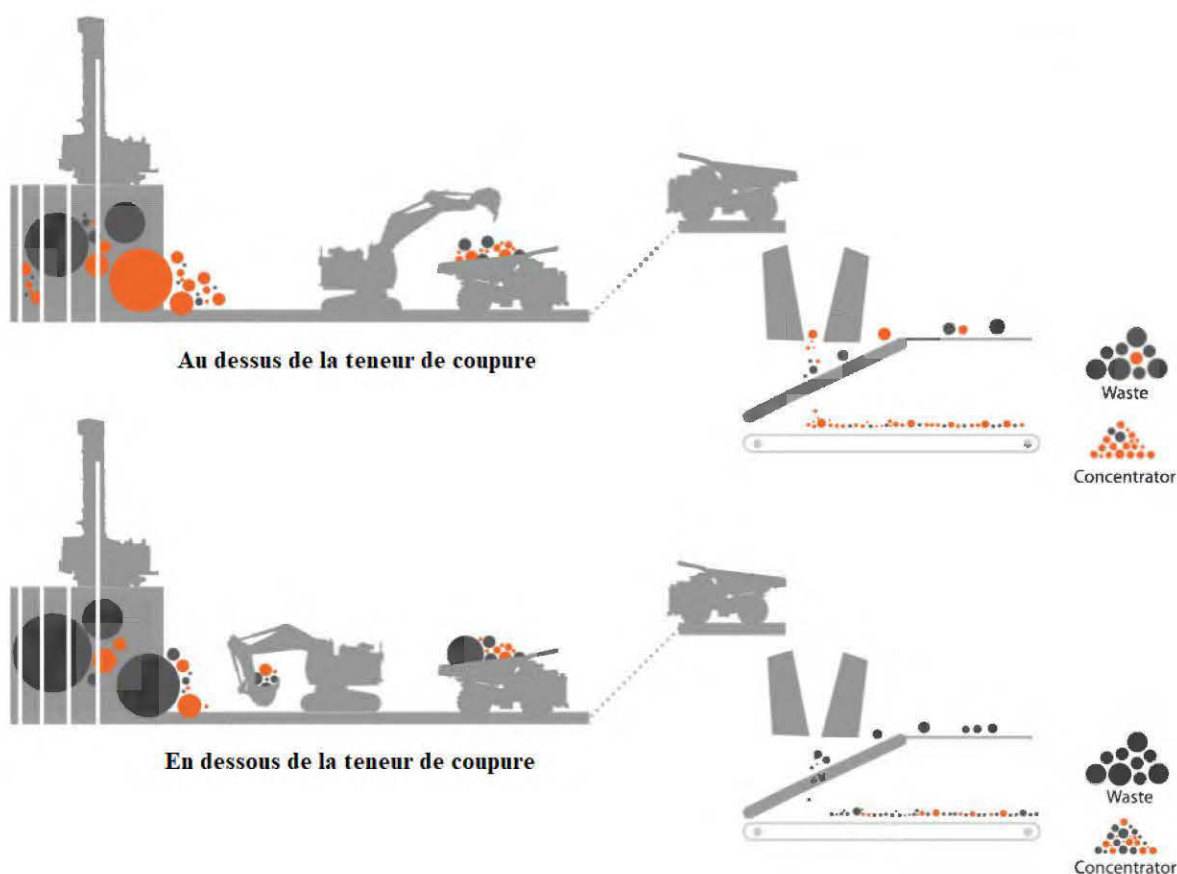
Figure 8.1: Principe du *'grade engineerin'g* développé par le CRC ore (tiré de https://www.crcore.org.au/grade-engineering consulté le 2018-03-15)

Par analogie à ce principe, le schéma proposé pour la gestion des stériles en intégrant la notion du DPLS est illustré à la Figure 8.2. Cette approche suggérée peut être appliquée, si elle est faisable

techniquement et économiquement, avant la mise en place de la halde à stérile. Elle consiste à un criblage des stériles selon le DPLS qui doit être défini par une caractérisation minéralogique automatisée. L'ouverture du crible doit être égale au DPLS. Le passant du crible devrait être la fraction réactive et le refus du crible est la fraction non-réactive. De plus, la définition du DPLS pour un gisement doit être fait sur un grand nombre d'échantillons pour être représentatif par rapport à la totalité des lithologies présentes en utilisant la caractérisation minéralogique et, pour plus de sécurité, il doit être confirmé par le biais des essais cinétiques.
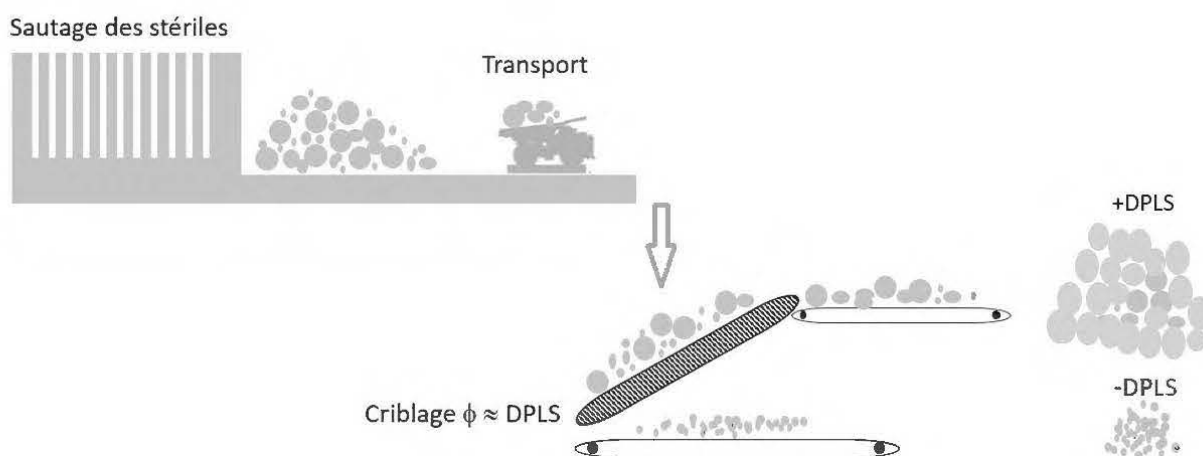
Figure 8.2: Schéma simplifié de la gestion des stériles proposée

Pour le cas des résidus miniers, l'effet de la libération minérale n'est pas aussi remarquable que pour les stériles à cause de la différence de granulométrie entre les deux matériaux (Bussière, 2007). Ceci n'empêche pas que la notion de libération des minéraux peut aussi influencer le comportement géochimique des résidus miniers. Un exemple concret est celui de la passivation des sulfures et/ou des carbonates au niveau des résidus miniers par précipitation des minéraux secondaires comme les oxy-hydroxydes de fer (Belzile *et al.*, 1997; Cai *et al.*, 2005; Cravotta III, 2008a; Kang *et al.*, 2016; Soler *et al.*, 2008). D'une façon générale, la caractérisation minéralogique des rejets miniers est la première étape d'une bonne prédiction de leur comportement environnemental. Elle permet de : i) identifier la composition minéralogique de l'échantillon pour anticiper les minéraux problématiques et les éventuels métaux qui peuvent être lixiviés suite à une oxydation, ii) quantifier les minéraux présents pour un bilan entre les minéraux acidifiants et ceux neutralisants et iii) surtout quantifier la texture de l'échantillon qui est un paramètre reconnu déterminant de la réactivité globale de l'échantillon (libération et passivation). La caractérisation

minéralogique seule combinée aux tests statiques ne peut en pasquantifier les cinétiques de réaction, les taux de relargage des éléments et la prédiction du comportement à long terme des rejets, d'où la nécessité de réaliser des essais cinétiques sur les rejets pour évaluer leur comportement environnemental. La section suivante décrit les limites et les enjeux des essais de prédiction du comportement géochimique des rejets miniers.

8.3 Limites et enjeux des essais de prédiction du comportement géochimique des rejets miniers incertains

Les essais cinétiques ont été désignés dans l'objectif de simuler l'oxydation naturelle des rejets miniers. C'est un outil qui permet de quantifier les cinétiques de réaction, les taux de réactions, le *lag time* s'il existe et prédire le comportement environnemental à long terme de l'échantillon testé (Benzaazoua *et al.*, 2017b; Benzaazoua *et al.*, 2004c; Bouzahzah *et al.*, 2014a; Brough *et al.*, 2017; Chopard *et al.*, 2015; Erguler *et al.*, 2015; Maest *et al.*, 2017; Morin *et al.*, 1994, 2001; Price, 2009). Les essais cinétiques au laboratoire les plus utilisés sont les mini-cellules d'altération, les cellules humides et les colonnes. Le choix de l'un ou l'autre des essais cinétiques dépend de plusieurs paramètres comme la masse d'échantillon disponible, l'objectif du test et la durée prévue pour le test (Bouzahzah *et al.*, 2014b). La durée du test est variable; généralement un essai cinétique est arrêté lorsqu'un état stationnaire est atteint. Plusieurs auteurs ont noté que les résultats des essais cinétiques au laboratoire sont différents de ceux observés in-situ ; il s'agit de l'effet d'échelle et des conditions du milieu (Banwart *et al.*, 2002; Malmström *et al.*, 2000; Miller *et al.*, 2003; Plante *et al.*, 2014; Strömberg *et al.*, 1999). Plante *et al.* (2014) ont suggéré que la différence des taux de réactions entre le laboratoire et le terrain est due au changement des conditions des tetst entre le laboratoire et le terrain. En effet, le ratio liquide/solide, les conditions climatiques, la surface de contact, la masse d'échantillon en plus des facteurs biologiques sont différents entre le terrain et le laboratoire. En plus de ces aspects, la formation des oxy-hydroxydes de fer, du hardpan et la présnece de carbonates de Fe-Mn sont des facteurs qui peuvent mener à ces différences de résultats entre les travaux de laboratoire et ceux du terrain. C'est le cas du parc à résidus de Joutel qui consititue un bel exemple.

Les résidus de Joutel ont été étudiés initialement par Blowes *et al.* (1998) et Benzaazoua *et al.* (2004). Les résultats de ces travaux ont montré que les résidus de Joutel peuvent être classés

grossièrement comme incertains par rapport à leur potentiel de génération d'acidité et quelques échantillons sont non générateurs d'acidité à long terme. La cartographie spatiale du parc à résidus réalisés plus récemment a montré que ces derniers ont une tendance à générer de l'acidité. Ceci peut être expliqué partiellement par la formation du hardpan (ce qui n'était pas le cas lors des études antérieures) et son effet sur le bilan hydrique sur le site. En effet, les résultats de la micro-tomographie ont montré que la porosité des hardpan est très faible (0.07%) comparé aux résidus miniers (0.3-0.45). Ceci induit une faible perméabilité de cette couche (Blowes *et al.*, 1991; Gilbert *et al.*, 2003; McGregor *et al.*, 2002). De ce fait, le bilan d'eau sur le parc à résidus de Joutel est différent de celui d'un parc à résidus où il n'y pas de hardpan. La présence du hardpan diminue les infiltrations verticales d'eau, au dépend des ruissellements de surface et de subsurface. Par conséquence, les lixiviats réagissent avec la couche oxydée de surface, s'acidifient et ruissellent en surface à cause de la présence du hardpan qui constitue une barrière à cet écoulement d'eau. Cependant, dans des conditions de laboratoire et même si les conditions géochimiques sont favorables pour la formation du hardpan, son effet sur les écoulements d'eau est minime. En effet, les essais en colonnes par principe simulent un écoulement vertical en 1D ce qui peut se traduire par deux aspects : i) altération des propriétés du hardpan par solubilisation des phases secondaires et/ou ii) percolation de l'eau à travers les parois de la colonne. Par conséquent, les eaux acidifiées et chargées en éléments chimiques, après contact avec les résidus oxydés, entrent en réaction avec les résidus frais en profondeur et se neutralisent par dissolution des carbonates de ces résidus. En conclusion, l'utilisation des colonnes (écoulement vertical 1D) ne peut pas produire le même comportement géochimique observé sur le terrain indépendamment de l'effet d'échelle. De plus, le rôle des oxy-hydroxydes de fer dans un rejet minier complique la tâche de la prédiction environnementale. Dans la littérature, ces phases secondaires sont généralement étudiées pour leurs rôles à sorber une large gamme de contaminants (Acero *et al.*, 2006; Asta *et al.*, 2010; Asta *et al.*, 2009; Benjamin & Leckie, 1981a; Benjamin *et al.*, 1981b; Coston *et al.*, 1995; España *et al.*, 2006; Lin & Herbert Jr., 1997; McGregor *et al.*, 1998a). Il a été démontré que grâce aux différents mécanismes de sorption, les oxy-hydroxydes de fer sont capables d'immobiliser une large gamme de métaux dépendamment de leurs affinités avec ces phases selon un mécanisme compétitif. D'autres auteurs ont signalé que ces mécanismes de sorption sont réversibles sous certaines conditions (changement de pH/Eh) (Davranche *et al.*, 2000). Le relargage des métaux des oxy-hydroxydes de fer dépend de plusieurs paramètres comme : les conditions géochimiques du milieu

(dissolution réductive), le mécanisme de sorption et la cristallinité du minéral. En effet, d'une part le métal lourd est facilement relargué s'il est adsorbé par une phase amorphe par comparaison au même élément en substitution dans une phase minérale cristallisée et, d'autre part, certains auteurs ont discuté quelques réactions des oxy-hydroxydes de fer qui peuvent générer de l'acidité (Cornell et al., 2004a, 2004b). L'adsorption cationique est un mécanisme qui génère de l'acidité selon la réaction suivante (Eq 16):

$$\equiv FeOH + Me^{z+} \leftrightarrow \equiv FeOM^{(z-1)+} + H^+ \hspace{3cm} \text{(Eq 16)}$$

Les deux mécanismes de la réversibilité des réactions de sorption et de la génération d'acidité par adsorption cationique sont difficiles à quantifier à cause de la complexité des réactions qui peuvent avoir lieu lors de l'oxydation d'un rejet minier. Cependant, dans le cas des résidus complètement oxydés, les oxy-hydroxydes de fer sont les phases minérales prépondérantes, en plus des silicates, et qui contrôlent la géochimie globale du parc à résidus.

8.4 Efficacité des amendements miniers comme technique de stabilisation/solidification des résidus miniers générateurs d'acide

Les résidus oxydés de Joutel ont présenté un comportement générateur d'acide par endroit sur le parc à résidus. Les zones acides ont été cartographiées à l'aide d'un échantillonnage systématique en utilisant le pH de pâte comme indicateur de l'acidité instantanée. L'approche d'ajout d'amendements miniers a été testée comme approche pour stabiliser ces résidus problématiques. Il s'agit de 5 cellules de terrain avec une largeur et une longueur de 4m et une profondeur de 30 cm. Les amendements miniers peuvent être classés en deux catégories dépendamment de l'objectif de la technique. Il s'agit d'amendement alcalin lorsque l'objectif est l'ajout simple de l'alcalinité pour augmenter le pouvoir de neutralisation des résidus en question. Avec les amendements alcalins, les processus de stabilisation des contaminants sont liés à la dissolution des phases carbonatées (alcalins). En effet, la dissolution des carbonates tamponne le pH et neutralise l'acidité du milieu, ce qui favorise la précipitation des phases secondaires comme le gypse et les oxy-hydroxydes de fer dans des conditions proches de la neutralité (Blowes et al., 2003; Blowes et al., 2014; Cravotta III, 2008b; Cravotta III et al., 1999). La précipitation des oxy-hydroxydes de fer diminue la

mobilité des métaux et métalloïdes par différents mécanismes comme la précipitation, co-précipitation et la sorption (Bowell, 1994; Coston *et al.*, 1995; Fukushi *et al.*, 2003; Giménez *et al.*, 2007; Gledhill *et al.*, 1994). L'utilisation du calcaire comme amendement alcalin dans des conditions de terrain a montré des résultats prometteurs pour la stabilisation de lixiviats des résidus oxydés de Joutel. En effet, l'utilisation de 5% et 10% du calcaire a permis la neutralisation des lixiviats dès les premiers jours de lixiviation. De plus, les concentrations en éléments chimiques ont été réduites à la suite de la précipitation des oxy-hydroxydes de fer. Ce mécanisme n'a pas pu être prouvé par observation minéralogique vu que le suivi des cellules de terrain est actuellement prolongé. Cependant, les diagrammes Eh-pH construits pour le fer ont montré que dans les conditions analysées des lixiviats, le fer précipitera sous forme d'oxyde de fer, ce qui favorisera l'atténuation de ces éléments chimiques (e.g. Fe, Al, Pb, As). En effet, la comparaison de la cellule témoin (résidus Joutel non amendés) avec les deux cellules amendées avec du calcaire a montré son efficacité à stabiliser la plupart des éléments chimiques à l'exception de l'As dans le cas de 10% calcaire et le Zn dans le cas de 5% calcaire. Généralement, l'As et le Zn sont des éléments très mobiles dans des conditions proches de la neutralité.

L'autre catégorie des amendements miniers est l'utilisation des liants appelée amendement cimentaire. Les cendres volantes (FA) et le ciment d'usage général (OPC) ont été testés comme matériaux à Joutel pour vérifier leurs efficacités à stabiliser les résidus miniers oxydés problématiques. Les deux formulations testées sont 5% ciment et 5% (1/2OPC-1/2FA). Les résultats du suivi des lixiviats ont montré que ces deux formulations permettent de neutraliser le pH dès les premiers jours de lixiviation. Par comparaison aux amendements alcalins, les amendements cimentaires ont permis l'atténuation totale ou partielle des éléments chimiques analysés sans exception. Le minimum de réduction des concentrations des éléments chimiques a été calculé pour le zinc pour la formulation qui contient des FA et était de l'ordre 58%. Généralement, basé sur les résultats de la première saison de suivi des cellules de terrain, les amendements cimentaires peuvent être considérés comme les meilleurs. De plus, l'incorporation des FA (sous-produit sans valeur) au niveau de la formulation cimentaire permettra de réduire les coûts liés au ciment en plus de présenter un avantage concernant l'atténuation des contaminants. En effet, la dissolution du ciment permet une neutralisation et, par conséquent, une stabilisation à la suite de la précipitation des oxy-hydroxydes de fer en plus du phénomène du piégeage physique des éléments chimiques. L'ajout des liants aux résidus miniers permet l'augmentation de leur

résistance mécanique et ainsi le développement d'une imperméabilité à long-terme. De ce fait, la surface de contact eau/résidus est réduite considérablement ce qui peut expliquer majoritairement l'atténuation des concentrations des métaux et métalloïdes (Benzaazoua *et al.*, 2004b; Falciglia *et al.*, 2017; Nehdi *et al.*, 2007; Rodríguez *et al.*, 2018; Tariq *et al.*, 2013).

CHAPITRE 9   CONCLUSION ET RECOMMANDATIONS

L'industrie minière, tout en étant primordiale pour beaucoup de pays à travers le monde dont le Canada, génère d'importantes quantités de rejets miniers qu'il convient de gérer adéquatement encadrée d'un important et croissant arsenal règlementaire. Cette gestion ne peut être efficace et optimale que si la prédiction du potentiel contaminant, et en particulier du potentiel de génération d'acidité (PGA), est précise. Les méthodes de prédiction existantes, quoiqu'elles aient connu beaucoup de développement ces deux dernières décennies, continuent de souffrir de certaines limites les rendant imprécises et inadaptées dans certains cas. C'est dans ce cadre que cette thèse de doctorat se donnait comme objectif général l'amélioration des outils de prédiction du potentiel de génération d'acidité de rejets miniers. La première partie de cette étude consistait en l'introduction de la notion du degré de libération des minéraux acidifiants et neutralisants (sulfures et carbonates principalement) pour mieux prédire le potentiel de génération d'acidité et définir une taille des particules au-dessus de laquelle la réactivité des stériles miniers est négligeable. Par conséquent, ce paramètre, appelé DPLS, peut être utilisé pour une gestion intégrée des rejets miniers et la réduction des coûts liés à la gestion et à la restauration des haldes à stériles. La deuxième partie du doctorat était de démystifier l'effet des oxy-hydroxydes de fer sur le comportement géochimique des résidus miniers classifiés comme incertains en termes de PGA et de tester l'efficacité des amendements alcalins et cimentaires à stabiliser certaines parties localisées acidifiées du parc au laboratoire et dans des conditions de terrain. Les objectifs doctorat ont été atteints et la méthodologie qui y a été développée en se basant sur une revue de littérature ainsi que les conclusions sont résumées ci-après.

9.1 Effet de la libération minérale sur le comportement géochimique des stériles miniers

Les stériles miniers sont principalement caractérisés par un étalement de leur distribution granulométrique. Une granulométrie qui peut varier de quelques microns à une échelle métrique; en faisant un mélange d'argile, sable et graviers d'un point de vue géotechnique. En conséquence, le taux d'exposition minérale ou encore la surface spécifique est très étalée en allant des fractions fines vers les fractions plus grossières. De ce fait, la réactivité des stériles va être hétérogène et étalée dépendamment de la distribution granulométrique et de la texture minérale ne mettant en jeu

qu'une fraction des stériles. Les trois lithologies échantillonnées ont subi un protocole de caractérisation rigoureux et original; les trois lithologies ont été séparées en sept fraction granulométriques Chaque fraction a été caractérisée des points de vue chimique, statique et minéralogique avec l'apport, notamment, de la minéralogie automatisée. Les principaux résultats de ces caractérisations ont montré un enrichissement en sulfures (principalement sous forme de pyrite) des fractions fines par rapport aux fractions grossières. Les carbonates ont été présentes à des teneurs plus importantes que les sulfures et ne semblaient pas montrer un enrichissement selon la granulométrie. Par la suite, la technique QEMSCAN^{TM} a été utilisée pour quantifier les paramètres minéralogiques et texturaux d'un échantillon, à savoir le degré de libération des minéraux, les associations minéralogiques, la granulo-minéralogie et la distribution élémentaire. La réinterprétation des données brutes de la quantification du degré de libération des carbonates et des sulfures des trois échantillons a permis de conclure que le degré de libération des sulfures devient négligeable à partir d'une taille de particule de 2,4mm. De ce fait, 2,4mm a été défini comme le DPLS de ces échantillons. Par ailleurs, la quantification du degré de libération des sulfures et des carbonates a été utilisé pour corriger les résultats des tests statiques (tests ABA) pour considérer la texture initiale (telle qu'imposée par le dynamitage) de l'échantillon. Ces corrections permettent d'éliminer toute la fraction grossière (≥DPLS) lors de l'interprétation des tests vu que le degré de libération des sulfures pour ces fractions était négligeable et ainsi leurs PA est considéré nul aussi. Une classification basée sur le seul test statique, même incluant la minéralogie, a besoin d'être justifiée en vue de consolider la conclusion concernant une DPLS de 2,4mm . Pour cette raison, des essais cinétiques en colonnes ont été montés et monitorés pour une durée de 543 jours pour confirmer la taille de particules de stériles de 2,4mm comme DPLS. Les colonnes qui contenaient l'échantillon +DPLS ont montré des réactivités négligeables en comparaison à l'échantillon total et l'échantillon -DPLS. Le calcul du taux d'oxydation des sulfures pour les trois échantillons montre clairement la forte réactivité de la fraction -DPLS et la réactivité négligeable de la fraction +DPLS. En effet, le taux d'oxydation de la pyrite au niveau de l'échantillon +DPLS était de l'ordre de 0,26 µmol/Kg/jour, 0,27 µmol/Kg/jour et 0,30 µmol/Kg/jour pour les lithologies A, B et C, respectivement. La réactivité de l'échantillon -DPLS était de l'ordre de 4,84 µmol/Kg/jour, 12,46 µmol/Kg/jour et 9,41 µmol/Kg/jour pour les lithologies A, B et C, respectivement. La réactivité de l'échantillon total était de l'ordre de 2,50 µmol/Kg/jour, 2,43 µmol/Kg/jour et 2,45 µmol/Kg/jour pour les lithologies A, B et C,

respectivement. La faible réactivité de l'échantillon grossier est due seulement à la faible quantité de sulfures qui affleurent au niveau des grains; c'est une réactivité de surface qui tend en général à s'estomper naturellement. Finalement, il est important de signaler que cette étude a été faite sur des échantillons sélectionnés sur la base de la connaissance géologique du gisement et, donc, les données recueillies auront une portée géométallurgique importante. Pour généraliser ces résultats, il faudrait les valider en appliquant la même méthodologie sur d'autres échantillons basé sur la géologie actualisée du gisement. La définition du DPLS pour un stérile minier permettra de suggérer une nouvelle méthode de gestion des stériles. En effet, au lieu de gérer tout les stériles comme une seule entité et le déposer dans une seule halde à stérile, on propose leur fractionnement selon le DPLS à l'aide d'un simple procédé de criblage. De ce fait, les stériles peuvent être séparés en deux fractions à gérer séparément. La fraction réactive (-DPLS), puisqu'elle constitue une faible proportion de l'échantillon total, peut être gérée différemment. Concernant la fraction +DPLS, les matériaux sont non-réactifs et peuvent être entreposés dans une halde non-problématique ou bien valorisés. L'applicabilité de cette approche doit faire l'objet d'une étude de faisabilité technico-économique.

9.2 Comportement géochimique des résidus et efficacité des amendements miniers pour le contrôle du DMA dans le parc à résidus de Joutel

9.2.1 Effet des oxy-hydroxydes de fer sur le comportement hydrogéochimique des résidus miniers incertains du site Joutel

Les oxy-hydroxydes de fer sont des phases néoformées lors des réactions d'oxydation des sulfures et la dissolution des carbonates. Ces phases minérales souvent mal ou finement cristallisées jouent un rôle important dans la géochimie globale des résidus miniers. Les oxy-hydroxydes de fer sont reconnus pour leur rôle à atténuer et diminuer la mobilité des contaminants. En effet, lors de la précipitation de ces phases secondaires, plusieurs contaminants peuvent être fixés grâce à une multitude de mécanismes groupés sous le nom de sorption. Il peut s'agir de l'adsorption, complexation et/ou encore la substitution. En revanche, les oxy-hydroxydes pourraient participer à la génération d'acide par le biais de deux mécanismes qui sont la formation du hardpan (couche

indurée) et l'échange cationique. Le hardpan est défini comme une couche indurée qui se frome suite à la précipitation et l'accumulation massive des oxy-hydroxydes de fer au niveau de la zone de transition entre les résidus oxydés et les résidus non-oxydés. Cette zone correspond à une zone de contraste géochimique important (pH, Eh, concentrations en éléments dissous) ce qui favorise la précipitation des phases secondaires. Quant à l'échange cationique, il s'agit d'un mécanisme difficile à quantifier à cause de la complexité de la composition chimique et minéralogique des résidus miniers oxydés. De plus, l'activité biologique (non investiguée dans cette étude) joue certainement un rôle très important à ce registre.

Les résidus miniers oxydés de Joutel sont un exemple concret illustrant l'influence de l'occurrence des oxy-hydroxydes de fer sur la géochimie des résidus miniers et la prédiction environnementale. En effet, des essais cinétiques en colonnes et en cellules humides réalisés sur des résidus frais de Joutel par Benzaazoua *et al.*, (2004) ont montré un comportement environnemental incertain et des essais en minicellules d'altération ont montré un comportement non-générateur d'acide. Cependant, après 25 ans d'exposition, les résidus oxydés de Joutel ont montré un comportement générateur d'acide par endroits dans le parc à résidus. Des investigations sur le terrain ainsi que l'échantillonnage systématique du parc à résidus de Joutel ont permis de cartographier l'extension spatiale de l'acidité et du hardpan. L'hypothèse de base, qui a été formulée pour expliquer ce changement de comportement environnemental des résidus oxydés de Joutel, était basée sur la présence du hardpan et certains carbonates de fer et de manganèse; deux éléments hydrolysables. En effet, les résultats de la micro-tomographie de deux échantillons du hardpan ont montré une faible porosité de cette couche qui induit sa faible perméabilité comme il a été reporté dans plusieurs papiers dans la littérature. Le hardpan à Joutel joue le rôle d'un écran contre les écoulements d'eau verticaux et aussi empêche la diffusion de l'oxygène. En conséquence, l'occurrence du hardpan modifie considérablement le bilan d'eau dans le parc à résidus; la composante du ruissellement de surface est favorisée aux dépends de l'infiltration verticale. C'est pour cette raison que les lixiviats acides provenant de la couche oxydée n'ont pas la chance de s'infiltrer pour se neutraliser en profondeur. Ceci a été démontré par des essais cinétiques en colonnes qui contenaient un échantillon oxydé au-dessus d'un échantillon frais; les lixiviats étaient caractérisés par un pH neutre comparé à des lixiviats provenant d'un échantillon oxydé qui ont montré un pH acide. Ce constat complique la tâche de prédiction du comportement géochimique des résidus de Joutel au laboratoire. En effet, le rôle du hardpan sera difficilement simulé lors des

essais conventionnels en colonnes. Lors des essais en colonnes, l'écoulement est supposé être en 1D. Donc, même si le hardpan se forme, il ne jouera pas le rôle d'un écran contre les écoulements d'eau à cause des chemins préférentiels. L'acidité générée par les résidus de Joutel n'est pas généralisée sur la totalité du parc à résidus, mais elle est limitée dans quelques zones, comme il a été démontré par l'échantillonnage systématique réalisé. La cartographie spatiale démontre l'hétérogénéité de l'oxydation au niveau du parc à résidus. Ceci est dû probablement à l'irrégularité de niveau de la nappe ce qui cause une saturation des résidus dans certaines zones et la non-saturation dans d'autres zones, ce qui influence la réactivité des résidus miniers. Finalement, considérer le terrain est primordiale pour bien comprendre le comportement géochimique des résidus miniers car les essais de laboratoire pourraient ne pas prédire adéquatement ce qui est le vrai devenir des résidus miniers in-situ.

9.2.2 Efficacité des amendements alcalins et cimentaires à stabiliser les résidus miniers oxydés acidogènes du site Joutel

Les amendements testés dans cette étude ont montré des résultats prometteurs à stabiliser les résidus miniers oxydés générateurs d'acide. L'avantage de cette étude est la réalisation des essais expérimentaux (cellules de terrain) dans des conditions réalistes au point de vue climat (température, précipitation, effet du gel dégel), des conditions bactériologiques, etc. Les formulations testées étaient 5% et 10% calcaire pour la catégorie des amendements alcalins et 5% ciment et 5% 50:50 ciment - cendres volantes pour la catégorie des amendements cimentaires. La première année de suivi a montré que les quatre formulations ont été capables de neutraliser l'acidité produite et tamponner le pH à des valeurs proches de la neutralité dès le début de lixiviation des résidus. L'efficacité de ces amendements à réduire le relargage des contaminants était différente dépendamment du type d'amendement. Les facteurs de réduction calculés à partir des concentrations moyennes sur la première année de suivi ont montré que :

- Les deux formulations alcalines ont stabilisé la plupart des éléments chimiques à l'exception du zinc pour la formulation 5% calcaire (C2) et l'arsenic pour la formulation 10% calcaire (C3) à cause de la mobilité importante de ces éléments dans les conditions de neutralité.

■ Les deux formulations cimentaires ont réussi à stabiliser tous les éléments chimiques analysés avec un léger avantage pour la formulation qui contient des cendres volantes (C4) par comparaison à la formulation qui contient uniquement du ciment ordinaire (C5).

En effet, les facteurs de réduction sont présentés au chapitre IIX. De manière générale, la formulation C4 présente la meilleure efficacité car elle a permis la stabilisation de tous les éléments chimiques et a permis la substitution de 50 % du ciment, d'une part, et, d'autre part, la valorisation d'un déchet d'une centrale de combustion de la biomasse. Cependant, l'efficacité de ces amendements à long terme est primordiale, d'où la nécessité de continuer le suivi de ces cellules de terrain à plus long terme. Finalement, une évaluation technico-économique constitue une étape importante à prendre en considération lors de la comparaison de l'efficacité de ces formulations.

9.3 Perspectives du travail

En premier lieu, la quantification du degré de libération est un paramètre très important pour caractériser la réactivité d'un stérile minier. Ce paramètre est généralement estimé pour un minéral cible et est calculé indépendamment des minéraux voisins. Le calcul du degré de libération minéral devrait être interprété dépendamment des associations minéralogiques. En effet, la méthode actuelle de calcul de libération minérale pour des objectifs environnementaux doit tenir compte des assemblages minéralogiques dans le cas d'un rejet minier qui contient plusieurs minéraux sulfureux. Le cas suivant est à considérer :

-Sulfure #1 vs sulfures #2 : dans ce cas, deux sulfures à différent potentiel électrochimique vont s'oxyder par voie galvanique, d'où la nécessité de corriger la libération d'un sulfure par rapport à ces contours partagés avec d'autres sulfures voisins.

En deuxième lieu, l'intégration du degré de libération minérale dans les codes numériques lors des modélisations géochimiques est un outil qui pourra améliorer les prédictions à long terme. Par ailleurs, il est suggéré dans ce doctorat, de corriger le PA et le PN d'un rejet minier par rapport au degré de libération minéral. Ensuite, pour pouvoir généraliser l'approche de caractérisation des stériles miniers en intégrant la notion de libération minérale, il sera intéressant de tester cette approche sur d'autres types de stériles et minéralisations. Finalement, la séparation des stériles dépendamment du diamètre d'encapsulation physique des sulfures est une option qui nécessite une

étude de faisabilité technique et économique, actuellement en cours dans le cadre d'un projet de maitrise (H. Amar).

Concernant l'effet des oxy-hydroxydes, il a été démontré, durant ce doctorat, l'importance de considérer le terrain lors des essais de prédiction du comportement géochimique des résidus miniers. En effet, les colonnes en 1D sont parfois incapables de simuler les mêmes phénomènes observés sur le terrain. Les réactions de précipitations des minéraux secondaires changent considérablement les propriétés hydrogéochimiques des résidus miniers (à l'échelle du grain et à l'échelle du parc), ce qui peut influencer la réactivité et les mouvements d'eau dans les parcs à résidus. Les essais cinétiques au laboratoire ont mis en évidence des caractéristiques cimentaires et imperméables du hardpan. Par ailleurs, la perméabilité du hardpan a été évaluée qualitativement en prenant en référence sa faible porosité, mais il sera intéressant d'évaluer quantitativement sa perméabilité in-situ. De plus, l'évaluation spatiale de sa perméabilité sur le parc à résidus de Joutel est un aspect qui va permettre de mieux comprendre les écoulements d'eau sur l'ensemble du parc à résidus. Considérant le hardpan et les propriétés minéralogiques des résidus de Joutel, leur géochimie a été évaluée indépendamment du facteur bactériologique. Cet aspect peut jouer un rôle important dans cette génération localisée d'acidité, d'où l'importance d'effectuer une caractérisation bactériologique dans les différentes zones de Joutel, à savoir les zones acides et neutres.

Concernant l'efficacité des amendements alcalins et cimentaires à stabiliser les résidus oxydés générateurs d'acide, il est important de poursuivre les cellules de terrain afin permettre d'évaluer leurs efficacités à long terme. De plus, la quantification de la passivation des carbonates par la précipitation des oxy-hydroxydes de fer est un aspect qui va permettre de quantifier la réactivité du calcaire à long terme. Par ailleurs, quantifier les débits d'eau des ruissellements de surface et de l'infiltration verticale au niveau des cellules de terrain est une donnée qui permettra de mieux interpréter les résultats du suivi géochimique de ces cellules

BIBLIOGRAPHIE

Acero, P., Ayora, C., Torrentó, C., & Nieto, J.-M. (2006). The behavior of trace elements during schwertmannite precipitation and subsequent transformation into goethite and jarosite. *Geochimica et Cosmochimica Acta, 70*(16), 4130-4139. doi:http://dx.doi.org/10.1016/j.gca.2006.06.1367

Adam, K., Kourtis, A., Gazea, B., & Kontopoulos, A. (1997). Evaluation of static tests used to predict the potential for acid drainage generation at sulphide mine sites.

Ahmaruzzaman, M. (2010). A review on the utilization of fly ash. *Progress in Energy and Combustion Science, 36*(3), 327-363. doi:10.1016/j.pecs.2009.11.003

Alakangas, L., & Öhlander, B. (2006). Formation and composition of cemented layers in low-sulphide mine tailings, Laver, northern Sweden. *Environmental Geology, 50*(6), 809-819. doi:10.1007/s00254-006-0253-x

Alkattan, M., Oelkers, E. H., Dandurand, J.-L., & Schott, J. (1998). An experimental study of calcite and limestone dissolution rates as a function of pH from− 1 to 3 and temperature from 25 to 80 C. *Chemical Geology, 151*(1), 199-214.

Allen, T. (2003). *Powder sampling and particle size determination*: Elsevier.

Amos, R. T., Blowes, D. W., Bailey, B. L., Sego, D. C., Smith, L., & Ritchie, A. I. M. (2015). Waste-rock hydrogeology and geochemistry. *Applied Geochemistry, 57*, 140-156. doi:10.1016/j.apgeochem.2014.06.020

Appelo, C., Van der Weiden, M., Tournassat, C., & Charlet, L. (2002). Surface complexation of ferrous iron and carbonate on ferrihydrite and the mobilization of arsenic. *Environmental Science & Technology, 36*(14), 3096-3103.

Asta, M. P., Cama, J., Martínez, M., & Giménez, J. (2009). Arsenic removal by goethite and jarosite in acidic conditions and its environmental implications. *J Hazard Mater, 171*(1–3), 965-972. doi:http://dx.doi.org/10.1016/j.jhazmat.2009.06.097

Asta, M. P., Ayora, C., Román-Ross, G., Cama, J., Acero, P., Gault, A. G., Charnock, J. M., & Bardelli, F. (2010). Natural attenuation of arsenic in the Tinto Santa Rosa acid stream (Iberian Pyritic Belt, SW Spain): The role of iron precipitates. *Chemical Geology, 271*(1–2), 1-12. doi:http://dx.doi.org/10.1016/j.chemgeo.2009.12.005

ASTM-D5744-96. (2007). Standard Test Method for Accelerated Weathering of Solid Materials Using a Humidity Cell. *Annual Book of ASTM Standards*

ASTM-D5856-95. (2002). Standard test methods for measurement of hydraulic conductivity porous materials using a rigid-wall compaction-mold permeameter. Annu Book ASTM Stand. doi:10.1520/D5856-95R02E01. *Standard test method for measurement of hydraulic conductivity of porous material using a rigid-wall, compaction-mold permeameter.*

ASTM-D-6836-02. (2008). Standard test methods for determination of the soil water characteristic curve for desorption using a hanging column, pressure extractor, chilled mirror hygrometer, and or centrifuge. . *Annual Book of ASTM Standards, 04.08.*

ASTM, A. (2014). C136/C136M–14, Standard Test Method for Sieve Analysis of Fine and Coarse Aggregates, ASTM International, West Conshohocken, PA, 2014.

Astm, D. (2000). 5550 (2001) Standard test method for specific gravity of soil solids by gas pycnometer. *Annual Book of ASTM Standards, 4*.

Atkinson, P. M., & Lloyd, C. D. (1998). Mapping precipitation in Switzerland with ordinary and indicator kriging. Special issue: Spatial Interpolation Comparison 97. *Journal of Geographic Information and Decision Analysis, 2*(1-2), 72-86.

Aubertin, M., Bussière, B., & Bernier, L. (2002). Environnement et gestion des résidus miniers. *Presses Internationales de Polytechnique, Corporation de l'École Polytechnique de Montréal, Montréal, Canada.*

Aubertin, M., Fala, O., Molson, J., Chouteau, M., Anterrieu, O., Hernandez, M. A., Chapuis, R. P., Bussière, B., Lahmira, B., & Lefebvre, R. (2008). *Caractérisation du comportement hydrogéologique et géochimique des haldes à stériles.* Paper presented at the Proceedings: Symposium.

Ayling, B., Rose, P., Petty, S., Zemach, E., & Drakos, P. (2012). *QEMSCAN (Quantitative evaluation of minerals by scanning electron microscopy): capability and application to fracture characterization in geothermal systems.* Paper presented at the Proc, Thirty-Seventh Workshop on Geotherm Reserv Eng. Stanford, California: Stanford University.

Bailey, B. L., Blowes, D. W., Smith, L., & Sego, D. C. (2016). The Diavik Waste Rock Project: Geochemical and microbiological characterization of low sulfide content large-scale waste rock test piles. *Applied Geochemistry, 65,* 54-72. doi:http://dx.doi.org/10.1016/j.apgeochem.2015.10.010

Baker, B. J., & Banfield, J. F. (2003). Microbial communities in acid mine drainage. *FEMS microbiology ecology, 44*(2), 139-152.

Banwart, S. A., Evans, K. A., & Croxford, S. (2002). Predicting mineral weathering rates at field scale for mine water risk assessment. *Geological Society, London, Special Publications, 198*(1), 137-157.

Barnett, E., Hutchinson, R., Adamcik, A., & Barnett, R. (1982). Geology of the Agnico-Eagle gold deposit, Quebec. *Precambrian Sulphide Deposits. Geol. Assoc. Can. Spec. Pap, 25,* 403-426.

Bear, J. (2012). *Hydraulics of groundwater*: Courier Corporation.

Belem, T., Benzaazoua, M., & Bussière, B. (2000). *Mechanical behaviour of cemented paste backfill.* Paper presented at the Proc. of 53rd Candadian Geotechnical Conference, Montreal.

Bellhouse, D. (2005). Systematic sampling methods. *Encyclopedia of Biostatistics.*

Belzile, N., Maki, S., Chen, Y.-W., & Goldsack, D. (1997). Inhibition of pyrite oxidation by surface treatment. *Science of The Total Environment, 196*(2), 177-186.

Benjamin, M. M., & Leckie, J. O. (1981a). Multiple-site adsorption of Cd, Cu, Zn, and Pb on amorphous iron oxyhydroxide. *Journal of Colloid and Interface Science, 79*(1), 209-221. doi:http://dx.doi.org/10.1016/0021-9797(81)90063-1

Benjamin, M. M., & Leckie, J. O. (1981b). Competitive adsorption of cd, cu, zn, and pb on amorphous iron oxyhydroxide. *Journal of Colloid and Interface Science, 83*(2), 410-419. doi:http://dx.doi.org/10.1016/0021-9797(81)90337-4

Benzaazoua, M., Bussière, B., & Dagenais, A. (2001). Comparison of kinetic tests for sulfide mine tailings. *Proceedings of tailings and mine waste '01, Balkema, Fort Collins*, 263-272.

Benzaazoua, M., Belem, T., & Bussière, B. (2002). Chemical factors that influence the performance of mine sulphidic paste backfill. *Cement and Concrete Research, 32*(7), 1133-1144. doi:http://dx.doi.org/10.1016/S0008-8846(02)00752-4

Benzaazoua, M., Bussière, B., Dagenais, A. M., & Archambault, M. (2004a). Kinetic tests comparison and interpretation for prediction of the Joutel tailings acid generation potential. *Environmental Geology, 46*(8), 1086-1101. doi:10.1007/s00254-004-1113-1

Benzaazoua, M., Marion, P., Picquet, I., & Bussière, B. (2004b). The use of pastefill as a solidification and stabilization process for the control of acid mine drainage. *Minerals Engineering, 17*(2), 233-243. doi:http://dx.doi.org/10.1016/j.mineng.2003.10.027

Benzaazoua, M., Bussière, B., Dagenais, A.-M., & Archambault, M. (2004c). Kinetic tests comparison and interpretation for prediction of the Joutel tailings acid generation potential. *Environmental Geology, 46*(8), 1086-1101. doi:10.1007/s00254-004-1113-1

Benzaazoua, M., Ouellet, J., Servant, S., Newman, P., & Verburg, R. (1999). Cementitious backfill with high sulfur content Physical, chemical, and mineralogical characterization. *Cement and Concrete Research, 29*(5), 719-725. doi:https://doi.org/10.1016/S0008-8846(99)00023-X

Benzaazoua, M., Bussière, B., Demers, I., Aubertin, M., Fried, É., & Blier, A. (2008). Integrated mine tailings management by combining environmental desulphurization and cemented paste backfill: Application to mine Doyon, Quebec, Canada. *Minerals Engineering, 21*(4), 330-340.

Benzaazoua, M., Bouzahzah, H., Taha, Y., Kormos, L., Kabombo, D., Lessard, F., Bussière, B., Demers, I., & Kongolo, M. (2017a). Integrated environmental management of pyrrhotite tailings at Raglan Mine: Part 1 challenges of desulphurization process and reactivity prediction. *Journal of Cleaner Production, 162*, 86-95. doi:https://doi.org/10.1016/j.jclepro.2017.05.161

Benzaazoua, M., Bouzahzah, H., Taha, Y., Kormos, L., Kabombo, D., Lessard, F., Bussière, B., Demers, I., & Kongolo, M. (2017b). Integrated environmental management of pyrrhotite tailings at Raglan Mine: Part 1 challenges of desulphurization process and reactivity prediction. *Journal of Cleaner Production*.

Beven, K., & Germann, P. (1982). Macropores and water flow in soils. *Water Resources Research, 18*(5), 1311-1325.

Bigham, J., Golden, D., Bowen, L., Buol, S., & Weed, S. (1978). Iron oxide mineralogy of well-drained Ultisols and Oxisols: I. Characterization of iron oxides in soil clays by Mössbauer spectroscopy, X-ray diffractometry, and selected chemical techniques. *Soil Science Society of America Journal, 42*(5), 816-825.

Blesa, M., & Maroto, A. (1986). Dissolution of metal oxides. *Journal de chimie physique, 83*(11-12), 757-764.

Blesa, M. A., & Matijević, E. (1989). Phase transformations of iron oxides, oxohydroxides, and hydrous oxides in aqueous media. *Adv Colloid Interface Sci, 29*(3-4), 173-221.

Bligh, M. W., & Waite, T. D. (2010). Formation, aggregation and reactivity of amorphous ferric oxyhydroxides on dissociation of Fe(III)–organic complexes in dilute aqueous suspensions. *Geochimica et Cosmochimica Acta, 74*(20), 5746-5762. doi:http://dx.doi.org/10.1016/j.gca.2010.07.008

Bloom, P. R., & Nater, E. A. (1991). Kinetics of Dissoluton of Oxide and Primary Silicate Minerals. *Rates of soil chemical processes*(ratesofsoilchem), 151-189.

Blowes, D., Ptacek, C., Jambor, J., & Weisener, C. (2003). The geochemistry of acid mine drainage. *Treatise on geochemistry, 9*, 612.

Blowes, D., Ptacek, C., Jambor, J., Weisener, C., Paktunc, D., Gould, W., & Johnson, D. (2014). The geochemistry of acid mine drainage.

Blowes, D. W., Jambor, J. L., & Alpers, C. N. (1994). *The environmental geochemistry of sulfide mine-wastes* (Vol. 22): Mineralogical Association of Canada.

Blowes, D. W., Ptacek, C. J., & Jambor, J. (2013). Mineralogy of mine wastes and strategies for remediation. *Environmental Mineralogy II: Vaughan, Wogelius (Eds), Europ. Mineral. Union Notes in Mineral, 13*, 295-338.

Blowes, D. W., Reardon, E. J., Jambor, J. L., & Cherry, J. A. (1991). The formation and potential importance of cemented layers in inactive sulfide mine tailings. *Geochimica et Cosmochimica Acta, 55*(4), 965-978. doi:http://dx.doi.org/10.1016/0016-7037(91)90155-X

Blowes, D. W., Jambor, J. L., Hanton-Fong, C. J., Lortie, L., & Gould, W. D. (1998). Geochemical, mineralogical and microbiological characterization of a sulphide-bearing carbonate-rich gold-mine tailings impoundment, Joutel, Québec. *Applied Geochemistry, 13*(6), 687-705. doi:http://dx.doi.org/10.1016/S0883-2927(98)00009-2

Bouzahzah, H. (2013). *Modification et amélioration des tests statiques et cinétiques pour une prédiction fiable du drainage minier acide.* Université du Québec en Abitibi-Témiscamingue.

Bouzahzah, H., Benzaazoua, M., & Bussière, B. (2010). A modified protocol of the ASTM normalized humidity cell test as laboratory weathering method of concentrator tailings. *Proceedings of international mine water and the environment (IMWA), mine water and innovative thinking, Sydney, NS, Canada*, 15-18.

Bouzahzah, H., Benzaazoua, M., Bussiere, B., & Plante, B. (2014a). Prediction of Acid Mine Drainage: Importance of Mineralogy and the Test Protocols for Static and Kinetic Tests. *Mine Water and the Environment, 33*(1), 54-65. doi:10.1007/s10230-013-0249-1

Bouzahzah, H., Benzaazoua, M., Bussière, B., & Plante, B. (2014b). Revue de littérature détaillée sur les tests statiques et les essais cinétiques comme outils de prédiction du drainage minier acide. *Déchets Sciences et Techniques Techniques, 66*, 14-31.

Bouzahzah, H., Benzaazoua, M., Plante, B., & Bussiere, B. (2015a). A quantitative approach for the estimation of the "fizz rating" parameter in the acid-base accounting tests: A new adaptations of the Sobek test. *Journal of Geochemical Exploration, 153*, 53-65. doi:http://dx.doi.org/10.1016/j.gexplo.2015.03.003

Bouzahzah, H., Benzaazoua, M., Bussière, B., & Plante, B. (2015b). ASTM Normalized Humidity Cell Kinetic Test: Protocol Improvements for Optimal Sulfide Tailings Reactivity. *Mine Water and the Environment, 34*(3), 242-257. doi:10.1007/s10230-014-0307-3

Bowell, R. J. (1994). Sorption of arsenic by iron oxides and oxyhydroxides in soils. *Applied Geochemistry, 9*(3), 279-286. doi:http://dx.doi.org/10.1016/0883-2927(94)90038-8

Bracewell, R. N. (2003). *Fourier Analysis and Imaging.* New York, NY (USA): Kluwer Academic.

Brough, C., Strongman, J., Bowell, R., Warrender, R., Prestia, A., Barnes, A., & Fletcher, J. (2017). Automated environmental mineralogy; the use of liberation analysis in humidity cell testwork. *Minerals Engineering, 107*, 112-122.

Brown, J. B. (1971). Jarosite-geoethite stabilities at 25 °C, 1 ATM. *Mineralium Deposita, 6*(3), 245-252. doi:10.1007/bf00208032

Brown, J. G., & Glynn, P. D. (2003). Kinetic dissolution of carbonates and Mn oxides in acidic water: measurement of in situ field rates and reactive transport modeling. *Applied Geochemistry, 18*(8), 1225-1239. doi:http://dx.doi.org/10.1016/S0883-2927(03)00010-6

Bruemmer, G. W., Gerth, J., & Tiller, K. G. (1988). Reaction kinetics of the adsorption and desorption of nickel, zinc and cadmium by goethite. I. Adsorption and diffusion of metals. *Journal of Soil Science, 39*(1), 37-52. doi:10.1111/j.1365-2389.1988.tb01192.x

Buckland, S. T., Anderson, D. R., Burnham, K. P., & Laake, J. L. (2005). *Distance sampling*: Wiley Online Library.

Burke, S. P., & Banwart, S. A. (2002). A geochemical model for removal of iron(II)(aq) from mine water discharges. *Applied Geochemistry, 17*(4), 431-443. doi:http://dx.doi.org/10.1016/S0883-2927(01)00092-0

Burton, E. D., Bush, R. T., Johnston, S. G., Watling, K. M., Hocking, R. K., Sullivan, L. A., & Parker, G. K. (2009). Sorption of Arsenic(V) and Arsenic(III) to Schwertmannite. *Environmental Science & Technology, 43*(24), 9202-9207. doi:10.1021/es902461x

Bussière, B. (2007). Hydro-geotechnical properties of hard rock tailing from metal mines and emerging geo-environmental disposal approaches. *Canadian Geotechnical Journal, 44*(9), 1019-1052.

Bussière, B., Aubertin, M., & Julien, M. (2001). Couvertures avec effets de barrière capillaire pour limiter le drainage minier acide: aspects théoriques et pratiques. *Vecteur environnement, 34*(3), 37-50.

Bussière, B., Aubertin, M., Benzaazoua, M., & Gagnon, D. (1999). Modèle d'estimation des coûts de restauration de sites miniers générateurs de DMA. *Séminaire Mines écologiques présentés dans le cadre du congrès APGGQ.*

Bussière, B., Benzaazoua, M., Aubertin, M., & Mbonimpa, M. (2004). A laboratory study of covers made of low-sulphide tailings to prevent acid mine drainage. *Environmental Geology, 45*(5), 609-622.

Bussière, B., Aubertin, M., Zagury, G. J., Potvin, R., & Benzaazoua, M. (2005). *Principaux défis et pistes de solution pour la restauration des aires d'entreposage de rejets miniers abandonnées.* Paper presented at the Symposium 2005 sur l'environnement et les mines.

Bussière, B., Aubertin, M., Mbonimpa, M., Molson, J. W., & Chapuis, R. P. (2007). Field experimental cells to evaluate the hydrogeological behaviour of oxygen barriers made of silty materials. *Canadian Geotechnical Journal, 44*(3), 245-265.

Butcher, A., Helms, T., Gottlieb, P., Bateman, R., Ellis, S., & Johnson, N. (2000). *Advances in the quantification of gold deportment by QemSCAN.* Paper presented at the Seventh Mill Operators Conference, Kalgoorlie, WA, AusIMM.

Buzug, T. M. (2010). *Computed Tomography: From Photon Statistics to Modern Cone-Beam CT.* Leipzig, Germany: Springer-Verlag Berlin Heidelberg.

Cai, M.-F., Dang, Z., Chen, Y.-W., & Belzile, N. (2005). The passivation of pyrrhotite by surface coating. *Chemosphere, 61*(5), 659-667.

Caldeira, C. L., Ciminelli, V. S. T., & Osseo-Asare, K. (2010). The role of carbonate ions in pyrite oxidation in aqueous systems. *Geochimica et Cosmochimica Acta, 74*(6), 1777-1789. doi:http://dx.doi.org/10.1016/j.gca.2009.12.014

Caldeira, C. L., Ciminelli, V. S. T., Dias, A., & Osseo-Asare, K. (2003). Pyrite oxidation in alkaline solutions: nature of the product layer. *International Journal of Mineral Processing, 72*(1–4), 373-386. doi:http://dx.doi.org/10.1016/S0301-7516(03)00112-1

Carrasco, C., Keeney, L., Scott, M., & Napier-Munn, T. J. (2016). Value driven methodology to assess risk and operating robustness for grade engineering strategies by means of stochastic optimisation. *Minerals Engineering, 99,* 76-88. doi:https://doi.org/10.1016/j.mineng.2016.09.029

Carter, M. R. (1993). *Soil sampling and methods of analysis*: CRC Press.

Casey, W. (1995). Surface chemistry during the dissolution of oxide and silicate minerals. *Mineral surfaces, 5,* 185-217.

CEAEQ. (2006). Détermination du carbone et du soufre : méthode par combustion et dosage par spectrophotométrie infrarouge (MA. 310 – CS 1.0).

Chen, Q., Tyrer, M., Hills, C. D., Yang, X., & Carey, P. (2009). Immobilisation of heavy metal in cement-based solidification/stabilisation: a review. *Waste Management, 29*(1), 390-403.

Chermak, J. A., & Runnells, D. D. (1996). *Self-sealing hardpan barriers to minimize infiltration of water into sulfide-bearing overburden, ore, and tailings piles.* Paper presented at the Tailings and mine waste.

Childs, E., & Bybordi, M. (1969). The vertical movement water in stratified porous material: 1. Infiltration. *Water Resources Research, 5*(2), 446-459.

Chopard, A. (2017). *Évaluation environnementale de minerais sulfurés polymétalliques basée sur une approche minéralogique pluridisciplinaire.* Université du Québec en Abitibi-Témiscamingue.

Chopard, A., Benzaazoua, M., Plante, B., Bouzahzah, H., & Marion, P. (2015). *Kinetic tests to evaluate the relative oxidation rates of various sulfides and sulfosalts.* Paper presented at

the Proceedings of the 10th International Conference on Acid Rock Drainage and IMWA Annual Conference.

Chopard, A., Benzaazoua, M., Bouzahzah, H., Plante, B., & Marion, P. (2017a). A contribution to improve the calculation of the acid generating potential of mining wastes. *Chemosphere, 175*, 97-107.

Chopard, A., Plante, B., Benzaazoua, M., Bouzahzah, H., & Marion, P. (2017b). Geochemical investigation of the galvanic effects during oxidation of pyrite and base-metals sulfides. *Chemosphere, 166*, 281-291. doi:https://doi.org/10.1016/j.chemosphere.2016.09.129

Chotpantarat, S. (2011). A review of static tests and recent studies. *American Journal of Applied Sciences, 8*(4), 400.

Ciccu, R., Ghiani, M., Serci, A., Fadda, S., Peretti, R., & Zucca, A. (2003). Heavy metal immobilization in the mining-contaminated soils using various industrial wastes. *Minerals Engineering, 16*(3), 187-192. doi:10.1016/s0892-6875(03)00003-7

Cnudde, V., Masschaele, B., Dierick, M., Vlassenbroeck, J., Van Hoorebeke, L., & Jacobs, P. (2006). Recent progress in X-ray CT as a geosciences tool. *Applied Geochemistry, 21*(5), 826-832. Retrieved from http://ac.els-cdn.com/S0883292706000503/1-s2.0-S0883292706000503-main.pdf?_tid=d7fb19ce-8288-11e7-bc58-00000aacb362&acdnat=1502891171_a2fab75a5ca25a85e33eb507cc2367fc

Cornell, R., & Schindler, P. (1987). Photochemical dissolution of goethite in acid/oxalate solution. *Clays Clay Miner, 35*(5), 347-352.

Cornell, R. M., & Schwertmann, U. (2004a). Environmental Significance *The Iron Oxides* (pp. 541-551): Wiley-VCH Verlag GmbH & Co. KGaA.

Cornell, R. M., & Schwertmann, U. (2004b). Cation Substitution *The Iron Oxides* (pp. 39-58): Wiley-VCH Verlag GmbH & Co. KGaA.

Cornell, R. M., & Schwertmann, U. (2004c). Dissolution *The Iron Oxides* (pp. 297-344): Wiley-VCH Verlag GmbH & Co. KGaA.

Cornell, R. M., & Schwertmann, U. (2004d). Surface Chemistry and Colloidal Stability *The Iron Oxides* (pp. 221-252): Wiley-VCH Verlag GmbH & Co. KGaA.

Cornell, R. M., & Schwertmann, U. (2004e). Solubility *The Iron Oxides* (pp. 201-220): Wiley-VCH Verlag GmbH & Co. KGaA.

Cornell, R. M., & Schwertmann, U. (2004f). Adsorption of Ions and Molecules *The Iron Oxides* (pp. 253-296): Wiley-VCH Verlag GmbH & Co. KGaA.

Coston, J. A., Fuller, C. C., & Davis, J. A. (1995). Pb2+ and Zn2+ adsorption by a natural aluminum- and iron-bearing surface coating on an aquifer sand. *Geochimica et Cosmochimica Acta, 59*(17), 3535-3547. doi:http://dx.doi.org/10.1016/0016-7037(95)00231-N

Coulombe, V. (2012). *Performance de recouvrements isolants partiels pour contrôler l'oxydation de résidus miniers sulfureux*. Université du Québec en Abitibi-Témiscamingue.

Coussy, S., Benzaazoua, M., Blanc, D., Moszkowicz, P., & Bussière, B. (2011). Arsenic stability in arsenopyrite-rich cemented paste backfills: A leaching test-based assessment. *J Hazard Mater, 185*(2–3), 1467-1476. doi:http://dx.doi.org/10.1016/j.jhazmat.2010.10.070

Cravotta III, C. (1994). *Secondary iron-sulfate minerals as sources of sulfate and acidity: Geochemical evolution of acidic ground water at a reclaimed surface coal mine in Pennsylvania.* Paper presented at the ACS Symposium Series. 1994.

Cravotta III, C. A. (2008a). Dissolved metals and associated constituents in abandoned coal-mine discharges, Pennsylvania, USA. Part 1: Constituent quantities and correlations. *Applied Geochemistry, 23*(2), 166-202. doi:http://dx.doi.org/10.1016/j.apgeochem.2007.10.011

Cravotta III, C. A. (2008b). Dissolved metals and associated constituents in abandoned coal-mine discharges, Pennsylvania, USA. Part 2: Geochemical controls on constituent concentrations. *Applied Geochemistry, 23*(2), 203-226. doi:http://dx.doi.org/10.1016/j.apgeochem.2007.10.003

Cravotta III, C. A., & Trahan, M. K. (1999). Limestone drains to increase pH and remove dissolved metals from acidic mine drainage. *Applied Geochemistry, 14*(5), 581-606. doi:https://doi.org/10.1016/S0883-2927(98)00066-3

Cressie, N. (1988). Spatial prediction and ordinary kriging. *Mathematical Geology, 20*(4), 405-421.

Criado, M., Fernández-Jiménez, A., & Palomo, A. (2007). Alkali activation of fly ash: Effect of the SiO2/Na2O ratio. *Microporous and Mesoporous Materials, 106*(1-3), 180-191. doi:10.1016/j.micromeso.2007.02.055

Cruz-Orive, L. M. (1989). On the precision of systematic sampling: a review of Matheron's transitive methods. *Journal of Microscopy, 153*(3), 315-333.

Cruz, R., Bertrand, V., Monroy, M., & González, I. (2001). Effect of sulfide impurities on the reactivity of pyrite and pyritic concentrates: a multi-tool approach. *Applied Geochemistry, 16*(7), 803-819.

Davis, J. A., & Leckie, J. O. (1978). Effect of adsorbed complexing ligands on trace metal uptake by hydrous oxides. *Environmental Science & Technology, 12*(12), 1309-1315.

Davranche, M., & Bollinger, J.-C. (2000). Release of Metals from Iron Oxyhydroxides under Reductive Conditions: Effect of Metal/Solid Interactions. *Journal of Colloid and Interface Science, 232*(1), 165-173. doi:http://dx.doi.org/10.1006/jcis.2000.7177

de Andrade, R. P., Figueiredo, B. R., de Mello, J. W. V., Santos, J. C. Z., & Zandonadi, L. U. (2008). Control of geochemical mobility of arsenic by liming in materials subjected to acid mine drainage. *Journal of Soils and Sediments, 8*(2), 123-129. doi:10.1065/jss2008.03.283

Deans, S. R. (2007). *The Radon Transform and Some of its Applications.* Mineloa, New York, NY (USA): Dover Publications, Inc.

Deschamps, T., Benzaazoua, M., Bussière, B., Aubertin, M., Bouzahzah, H., & Martin, V. (2009). Les effets d'amendements alcalins sur des résidus miniers sulfureux entreposés en surface: Cas des dépôts en pâte. *DÉCHE TS, 19.*

DeSisto, S. L., Jamieson, H. E., & Parsons, M. B. (2011). Influence of hardpan layers on arsenic mobility in historical gold mine tailings. *Applied Geochemistry, 26*(12), 2004-2018.

Dold, B. (2017). Acid rock drainage prediction: A critical review. *Journal of Geochemical Exploration, 172*, 120-132. doi:http://doi.org/10.1016/j.gexplo.2016.09.014

Dong, F. (2015). *Proceedings of the 11th International Congress for Applied Mineralogy (ICAM)*: Springer.

Doye, I., & Duchesne, J. (2003). Neutralisation of acid mine drainage with alkaline industrial residues: laboratory investigation using batch-leaching tests. *Applied Geochemistry, 18*(8), 1197-1213. doi:10.1016/s0883-2927(02)00246-9

Du, Y.-J., Jiang, N.-J., Liu, S.-Y., Jin, F., Singh, D. N., & Puppala, A. J. (2013). Engineering properties and microstructural characteristics of cement-stabilized zinc-contaminated kaolin. *Canadian Geotechnical Journal, 51*(3), 289-302.

Duchesne, J., & Reardon, E. (1998). Determining controls on element concentrations in cement kiln dust leachate. *Waste Management, 18*(5), 339-350.

Duchesne, J., & Laforest, G. (2006). Remediation of electric arc furnace dust leachate by the use of cementitious materials: A column-leaching test. *Chinese Journal of Geochemistry, 25*, 99-99.

Dunne, T., Zhang, W., & Aubry, B. F. (1991). Effects of rainfall, vegetation, and microtopography on infiltration and runoff. *Water Resources Research, 27*(9), 2271-2285.

Edwards, K. J., Schrenk, M. O., Hamers, R., & Banfield, J. F. (1998). Microbial oxidation of pyrite: experiments using microorganisms from an extreme acidic environment. *American Mineralogist, 83*(11), 1444-1453.

Egal, M., Elbaz-Poulichet, F., Casiot, C., Motelica-Heino, M., Négrel, P., Bruneel, O., Sarmiento, A. M., & Nieto, J. M. (2008). Iron isotopes in acid mine waters and iron-rich solids from the Tinto–Odiel Basin (Iberian Pyrite Belt, Southwest Spain). *Chemical Geology, 253*(3–4), 162-171. doi:http://dx.doi.org/10.1016/j.chemgeo.2008.05.006

Egiebor, N. O., & Oni, B. (2007). Acid rock drainage formation and treatment: a review. *Asia-Pacific Journal of Chemical Engineering, 2*(1), 47-62.

El Adnani, M., Plante, B., Benzaazoua, M., Hakkou, R., & Bouzahzah, H. (2016). Tailings Weathering and Arsenic Mobility at the Abandoned Zgounder Silver Mine, Morocco. *Mine Water and the Environment, 35*(4), 508-524. doi:10.1007/s10230-015-0370-4

Elberling, B., & Nicholson, R. V. (1996). Field determination of sulphide oxidation rates in mine tailings. *Water Resources Research, 32*(6), 1773-1784.

Elberling, B., Nicholson, R., Reardon, E., & Tibble, R. (1994). Evaluation of sulphide oxidation rates: a laboratory study comparing oxygen fluxes and rates of oxidation product release. *Canadian Geotechnical Journal, 31*(3), 375-383.

Elghali, A., Benzaazoua, M., Bouzahzah, H., Bussière, B., & Herminso, G. (2018a). Determination of the absolute acid generation potential of waste rocks, part I: Mineralogical approach (submitted paper). *Applied Geochemistry*.

Elghali, A., Benzaazoua, M., Bussière, B., Kennedy, C., Parawani, R., & Graham, S. (2018b). The role of hardpan formation on the reactivity of sulphidic mine tailings: Joutel case study (submitted paper). *Science of The Total Environment*.

Elghali, A., Benzaazoua, M., Bussière, B., Schaumann, D., Graham, S., Genty, T., Noel, J., Kenedy, C., & Cayouette, J. (2017). *Investigation of the role of hardpans on the geochemical behavior of the Joutel mine tailings.* Paper presented at the the twenty-first international conference on Tailings and Mine Waste (TMW'17), Banff, Alberta, Canada.

EPA, U. S. (1994). Technical Document: Acid Mine Drainage Prediction, EPA 530-R-94-036. *Office of Solid Waste, Special Waste Branch.*

Erguler, Z. A., & Kalyoncu Erguler, G. (2015). The effect of particle size on acid mine drainage generation: Kinetic column tests. *Minerals Engineering, 76,* 154-167. doi:10.1016/j.mineng.2014.10.002

Esbensen, K. H., & Heydorn, K. (2004). Metrology in sampling—a first foray (biological materials). *Chemometrics and Intelligent Laboratory Systems, 74*(1), 115-120. doi:https://doi.org/10.1016/j.chemolab.2004.04.010

España, J. S., Pamo, E. L., Pastor, E. S., Andrés, J. R., & Rubí, J. A. M. (2006). The Removal of Dissolved Metals by Hydroxysulphate Precipitates during Oxidation and Neutralization of Acid Mine Waters, Iberian Pyrite Belt. *Aquatic Geochemistry, 12*(3), 269-298. doi:10.1007/s10498-005-6246-7

Evangelou, V., & Zhang, Y. (1995a). A review: pyrite oxidation mechanisms and acid mine drainage prevention. *Critical Reviews in Environmental Science and Technology, 25*(2), 141-199.

Evangelou, V. P., & Zhang, Y. L. (1995b). A review: Pyrite oxidation mechanisms and acid mine drainage prevention. *Critical Reviews in Environmental Science and Technology, 25*(2), 141-199. doi:10.1080/10643389509388477

Falciglia, P. P., Romano, S., & Vagliasindi, F. G. (2017). Stabilisation/Solidification of soils contaminated by mining activities: Influence of barite powder and grout content on γ-radiation shielding, unconfined compressive strength and 232Th immobilisation. *Journal of Geochemical Exploration, 174,* 140-147.

Fatahi, B., & Khabbaz, H. (2015). Influence of Chemical Stabilisation on Permeability of Municipal Solid Wastes. *Geotechnical and Geological Engineering, 33*(3), 455-466. doi:10.1007/s10706-014-9831-y

Feldkamp, L. A., Davis, L. C., & Kress, J. W. (1984). Practical cone-beam algorithm. *J. Opt. Soc. Am. A, 1*(6), 612-619.

Fendorf, S., & Fendorf, M. (1996). Sorption mechanisms of lanthanum on oxide minerals. *Clays and Clay Minerals, 44*(2), 220-227.

Fleri, M. A., & Whetstone, G. T. (2007). In situ stabilisation/solidification: Project lifecycle. *J Hazard Mater, 141*(2), 441-456. doi:http://dx.doi.org/10.1016/j.jhazmat.2006.05.096

Forján, R., Asensio, V., Rodríguez-Vila, A., & Covelo, E. F. (2014). Effect of amendments made of waste materials in the physical and chemical recovery of mine soil. *Journal of Geochemical Exploration, 147,* 91-97. doi:10.1016/j.gexplo.2014.10.004

Fredlund, D. G., & Xing, A. (1994). Equations for the soil-water characteristic curve. *Canadian Geotechnical Journal, 31*(4), 521-532. Retrieved from http://www.nrcresearchpress.com.proxy.cegepat.qc.ca/doi/pdfplus/10.1139/t94-061

Frostad, S., Klein, B., & Lawrence, R. W. (2002). Evaluation of laboratory kinetic test methods for measuring rates of weathering. *Mine Water and the Environment, 21*(4), 183-192. Retrieved from https://link.springer.com/content/pdf/10.1007%2Fs102300200042.pdf

Fukushi, K., Sasaki, M., Sato, T., Yanase, N., Amano, H., & Ikeda, H. (2003). A natural attenuation of arsenic in drainage from an abandoned arsenic mine dump. *Applied Geochemistry, 18*(8), 1267-1278. doi:http://dx.doi.org/10.1016/S0883-2927(03)00011-8

Getter, K. L., Rowe, D. B., & Andresen, J. A. (2007). Quantifying the effect of slope on extensive green roof stormwater retention. *Ecological engineering, 31*(4), 225-231.

Gilbert, R. O. (1987). *Statistical methods for environmental pollution monitoring*: John Wiley & Sons.

Gilbert, S., Cooke, D., & Hollings, P. (2003). The effects of hardpan layers on the water chemistry from the leaching of pyrrhotite-rich tailings material. *Environmental Geology, 44*(6), 687-697.

Gilles, B., Mostafa, B., Abdelkabir, M., & Bruno, B. (2014). Long term hydro-geochemical behaviour of surface paste disposal in field experimental cells. *In: Proceedings of the Conference Canadienne de Geotechnique, GeoRegina, CD-Rom, 1*(1), 19.

Giménez, J., Martínez, M., de Pablo, J., Rovira, M., & Duro, L. (2007). Arsenic sorption onto natural hematite, magnetite, and goethite. *J Hazard Mater, 141*(3), 575-580. doi:http://dx.doi.org/10.1016/j.jhazmat.2006.07.020

Gledhill, M., & van den Berg, C. M. G. (1994). Determination of complexation of iron(III) with natural organic complexing ligands in seawater using cathodic stripping voltammetry. *Marine Chemistry, 47*(1), 41-54. doi:http://dx.doi.org/10.1016/0304-4203(94)90012-4

Goodall, W. R. (2008). Characterisation of mineralogy and gold deportment for complex tailings deposits using QEMSCAN®. *Minerals Engineering, 21*(6), 518-523.

Goodall, W. R., Scales, P. J., & Butcher, A. R. (2005). The use of QEMSCAN and diagnostic leaching in the characterisation of visible gold in complex ores. *Minerals Engineering, 18*(8), 877-886.

Gottlieb, P., Wilkie, G., Sutherland, D., Ho-Tun, E., Suthers, S., Perera, K., Jenkins, B., Spencer, S., Butcher, A., & Rayner, J. (2000). Using quantitative electron microscopy for process mineralogy applications. *JoM, 52*(4), 24-25.

Grangeat, P. (1991). Mathematical framework of cone beam 3D reconstruction via the first derivative of the Radon transform *Lecture Notes in Mathematics: Mathematical Methods in Tomography. Herman G T, Louis A K, and Natterer F. (Editors)* (pp. 66-97). Berlin (Germany): Springer.

Gratton, Y. (2002). Le krigeage: la méthode optimale d'interpolation spatiale. *Les articles de l'Institut d'Analyse Géographique, 1*.

Graupner, T., Kassahun, A., Rammlmair, D., Meima, J. A., Kock, D., Furche, M., Fiege, A., Schippers, A., & Melcher, F. (2007). Formation of sequences of cemented layers and hardpans within sulfide-bearing mine tailings (mine district Freiberg, Germany). *Applied Geochemistry, 22*(11), 2486-2508. doi:10.1016/j.apgeochem.2007.07.002

Gu, Y. (2003). Automated scanning electron microscope based mineral liberation analysis an introduction to JKMRC/FEI mineral liberation analyser. *Journal of Minerals and Materials Characterization and Engineering, 2*(01), 33.

Hakkou, R., Benzaazoua, M., & Bussière, B. (2009). Laboratory evaluation of the use of alkaline phosphate wastes for the control of acidic mine drainage. *Mine Water and the Environment, 28*(3), 206.

Harrison, A. L., Dipple, G. M., Power, I. M., & Mayer, K. U. (2015). Influence of surface passivation and water content on mineral reactions in unsaturated porous media: implications for brucite carbonation and CO 2 sequestration. *Geochimica et Cosmochimica Acta, 148*, 477-495.

Helt, K. M., Williams-Jones, A. E., Clark, J. R., Wing, B. A., & Wares, R. P. (2014). Constraints on the genesis of the Archean oxidized, intrusion-related Canadian Malartic gold deposit, Quebec, Canada. *Economic Geology, 109*(3), 713-735.

Herman, G. T. (2009). *Fundamentals of Computerized Tomography: Image Reconstruction from Projections, 2nd Ed.* London, UK: Springer.

Hingston, F., Posner, A., & Quirk, J. (1971). Competitive adsorption of negatively charged ligands on oxide surfaces. *Discussions of the Faraday Society, 52*, 334-342.

Holmes, P. R., & Crundwell, F. K. (1995). Kinetic aspects of galvanic interactions between minerals during dissolution. *Hydrometallurgy, 39*(1), 353-375. doi:http://dx.doi.org/10.1016/0304-386X(95)00041-E

Holmström, H., & Öhlander, B. (2001). Layers rich in Fe- and Mn-oxyhydroxides formed at the tailings-pond water interface, a possible trap for trace metals in flooded mine tailings. *Journal of Geochemical Exploration, 74*(1–3), 189-203. doi:http://dx.doi.org/10.1016/S0375-6742(01)00184-4

Holmström, H., Ljungberg, J., & Öhlander, B. (1999). Role of carbonates in mitigation of metal release from mining waste. Evidence from humidity cells tests. *Environmental Geology, 37*(4), 267-280. doi:10.1007/s002540050384

Hsieh, J. (2015). *Computed Tomography: Principles, Design, Artifacts, and Recent Advances, 3rd Ed.* Bellingham, WA (USA): SPIE – The International Society for Optical Engineering.

Ichrak, H., Mostafa, B., Abdelkabir, M., & Bruno, B. (2016). Effect of cementitious amendment on the hydrogeological behavior of a surface paste tailings' disposal. *Innovative Infrastructure Solutions, 1*(1), 19.

Jambor, J. (1994). Mineralogy of sulfide-rich tailings and their oxidation products. *Environmental geochemistry of sulfide mine-wastes, 22*, 59-102.

Jambor, J., Dutrizac, J., Groat, L., & Raudsepp, M. (2002a). Static tests of neutralization potentials of silicate and aluminosilicate minerals. *Environmental Geology, 43*(1-2), 1-17.

Jambor, J., Dutrizac, J., Groat, L., & Raudsepp, M. (2002b). Static tests of neutralization potentials of silicate and aluminosilicate minerals. *Environmental Geology, 43*(1), 1-17.

Jambor, J., Dutrizac, J., Raudsepp, M., & Groat, L. (2003). Effect of peroxide on neutralization-potential values of siderite and other carbonate minerals. *Journal of Environmental Quality, 32*(6), 2373-2378.

Jamieson, H. E., Walker, S. R., & Parsons, M. B. (2015). Mineralogical characterization of mine waste. *Applied Geochemistry, 57*, 85-105. doi:10.1016/j.apgeochem.2014.12.014

Jones, A. M., Griffin, P. J., Collins, R. N., & Waite, T. D. (2014). Ferrous iron oxidation under acidic conditions – The effect of ferric oxide surfaces. *Geochimica et Cosmochimica Acta, 145*, 1-12. doi:http://dx.doi.org/10.1016/j.gca.2014.09.020

Jönsson, J., Persson, P., Sjöberg, S., & Lövgren, L. (2005). Schwertmannite precipitated from acid mine drainage: phase transformation, sulphate release and surface properties. *Applied Geochemistry, 20*(1), 179-191. doi:http://dx.doi.org/10.1016/j.apgeochem.2004.04.008

Kak, A. C., & Slaney, M. (1988). *Principles of Computerized Tomographic Imaging*. New York, NY (USA): IEEE Press.

Kalyoncu Erguler, G., Erguler, Z. A., Akcakoca, H., & Ucar, A. (2014). The effect of column dimensions and particle size on the results of kinetic column test used for acid mine drainage (AMD) prediction. *Minerals Engineering, 55*, 18-29. doi:10.1016/j.mineng.2013.09.008

Kang, C.-U., Jeon, B.-H., Park, S.-S., Kang, J.-S., Kim, K.-H., Kim, D.-K., Choi, U.-K., & Kim, S.-J. (2016). Inhibition of pyrite oxidation by surface coating: a long-term field study. *Environ Geochem Health, 38*(5), 1137-1146.

Katsevich, A. (2002). Theoretically exact filtered backprojection-type inversion algorithm for spiral cone-beam. *SIAM J. Appl. Math., 62*(6), 2012–2026.

Katsevich, A. (2003). U.S. Patent No. 6,574,299.

Kim, J. W., & Jung, M. C. (2011). Solidification of arsenic and heavy metal containing tailings using cement and blast furnace slag. *Environ Geochem Health, 33 Suppl 1*, 151-158. doi:10.1007/s10653-010-9354-2

Kogbara, R. B., & Al-Tabbaa, A. (2011a). Mechanical and leaching behaviour of slag-cement and lime-activated slag stabilised/solidified contaminated soil. *Sci Total Environ, 409*(11), 2325-2335. doi:10.1016/j.scitotenv.2011.02.037

Kogbara, R. B., Yi, Y., & Al-Tabbaa, A. (2011b). Process envelopes for stabilisation/solidification of contaminated soil using lime–slag blend. *Environmental Science and Pollution Research, 18*(8), 1286-1296. doi:10.1007/s11356-011-0480-x

Kohfahl, C., Graupner, T., Fetzer, C., Holzbecher, E., & Pekdeger, A. (2011). The impact of hardpans and cemented layers on oxygen diffusivity in mining waste heaps: diffusion experiments and modelling studies. *Sci Total Environ, 409*(17), 3197-3205. doi:10.1016/j.scitotenv.2011.04.055

Komnitsas, K., Bartzas, G., & Paspaliaris, I. (2004). Efficiency of limestone and red mud barriers: laboratory column studies. *Minerals Engineering, 17*(2), 183-194. doi:10.1016/j.mineng.2003.11.006

Kooner, Z. S. (1993). Comparative study of adsorption behavior of copper, lead, and zinc onto goethite in aqueous systems. *Environmental Geology, 21*(4), 242-250. doi:10.1007/bf00775914

Kumpiene, J., Lagerkvist, A., & Maurice, C. (2008). Stabilization of As, Cr, Cu, Pb and Zn in soil using amendments – A review. *Waste Management, 28*(1), 215-225. doi:http://dx.doi.org/10.1016/j.wasman.2006.12.012

Kwong, Y.-T. J. (1993). *Prediction and prevention of acid rock drainage from a geological and mineralogical perspective*: MEND.

Kwong, Y. J., & Ferguson, K. D. (1997). *Mineralogical changes during NP determinations and their implications.* Paper presented at the Proc. 4th International Conference on Acid Rock Drainage, Vancouver, BC.

Lamontagne, A. (2001). *Étude de la méthode d'empilement des stériles par entremêlement par couches pour contrôler le drainage minier acide.* Université Laval.

Langmuir, D. (1971). Particle size effect on the reaction goethite= hematite+ water. *American Journal of Science, 271*(2), 147-156.

Lapakko, K. (2002). Metal mine rock and waste characterization tools: an overview. *Mining, Minerals and Sustainable Development, 67*, 1-30.

Lapakko, K. (2003). Developments in humidity-cell tests and their application. *Environmental Aspects of Mine Wastes. Mineralogical Assoc. Canada, Short Course, 31*, 147-164.

Lapakko, K., & Lawrence, R. W. (2009). Modification of the net acid production (NAP) test.

Lapakko, K. A. (1994). *Evaluation of neutralization potential determinations for metal mine waste and a proposed alternative.* Paper presented at the Proceeding: of the Third International Conference on the Abatement of Acidic Drainage, April.

Lapakko, K. A., Engstrom, J. N., & Antonson, D. A. (2006). *Effects of particle size on drainage quality from three lithologies.* Paper presented at the Poster paper presented at the 7th International Conference on Acid Rock Drainage (ICARD).

Lasdon, L. S., Fox, R. L., & Ratner, M. W. (1974). Nonlinear optimization using the generalized reduced gradient method. *Revue française d'automatique, informatique, recherche opérationnelle. Recherche opérationnelle, 8*(V3), 73-103.

Lastra, R., & Paktunc, D. (2016). An estimation of the variability in automated quantitative mineralogy measurements through inter-laboratory testing. *Minerals Engineering, 95*, 138-145. doi:https://doi.org/10.1016/j.mineng.2016.06.025

Lastra, R., Petruk, W., & Wilson, J. (1998). Image analysis techniques and applications to mineral processing. *Modern Approaches to Ore and Environmental Mineralogy, 27*, 327-366.

Lawrence, R., & Wang, Y. (1996). Determination of neutralization potential for acid rock drainage prediction. *MEND project, 1*(3), 38.

Lawrence, R. W., & Scheske, M. (1997a). A method to calculate the neutralization potential of mining wastes. *Environmental Geology, 32*(2), 100-106. Retrieved from https://link.springer.com/article/10.1007%2Fs002540050198

Lawrence, R. W., & Wang, Y. (1997b). *Determination of neutralization potential in the prediction of acid rock drainage.* Paper presented at the Proceedings of the fourth international conference on acid rock drainage.

Ledin, M., & Pedersen, K. (1996). The environmental impact of mine wastes—roles of microorganisms and their significance in treatment of mine wastes. *Earth-Science Reviews, 41*(1-2), 67-108.

Li, X. D., Poon, C. S., Sun, H., Lo, I. M. C., & Kirk, D. W. (2001). Heavy metal speciation and leaching behaviors in cement based solidified/stabilized waste materials. *J Hazard Mater, 82*(3), 215-230. doi:http://dx.doi.org/10.1016/S0304-3894(00)00360-5

Lin, Z., & Herbert Jr., R. B. (1997). Heavy metal retention in secondary precipitates from a mine rock dump and underlying soil, Dalarna, Sweden. *Environmental Geology, 33*(1), 1-12. doi:10.1007/s002540050220

Liu, X., & Millero, F. J. (1999). The solubility of iron hydroxide in sodium chloride solutions. *Geochimica et Cosmochimica Acta, 63*(19–20), 3487-3497. doi:http://dx.doi.org/10.1016/S0016-7037(99)00270-7

Lottermoser, B. G., & Ashley, P. M. (2006). Mobility and retention of trace elements in hardpan-cemented cassiterite tailings, north Queensland, Australia. *Environmental Geology, 50*(6), 835-846.

Lowson, R. T. (1982). Aqueous oxidation of pyrite by molecular oxygen. *Chemical Reviews, 82*(5), 461-497. doi:10.1021/cr00051a001

Mackay, D., Simandl, G., Ma, W., Redfearn, M., & Gravel, J. (2016). Indicator mineral-based exploration for carbonatites and related specialty metal deposits—A QEMSCAN® orientation survey, British Columbia, Canada. *Journal of Geochemical Exploration, 165*, 159-173.

Mackie, A. L., & Walsh, M. E. (2015). Investigation into the use of cement kiln dust in high density sludge (HDS) treatment of acid mine water. *Water Res, 85*, 443-450. doi:10.1016/j.watres.2015.08.056

Maest, A., & Nordstrom, D. K. (2017). A geochemical examination of humidity cell tests. *Applied Geochemistry*.

Maire, E., & Withers, P. J. (2014). Quantitative X-ray tomography. *International materials reviews, 59*(1), 1-43.

Majima, H., & Peter, E. (1968). *Electrochemistry of sulphide dissolution in hydrometallurgical systems.* Paper presented at the Leningrad: International Mineral Processing Congress.

Malmström, M. E., Destouni, G., Banwart, S. A., & Strömberg, B. H. (2000). Resolving the scale-dependence of mineral weathering rates. *Environmental Science & Technology, 34*(7), 1375-1378.

Manceau, A. (1995). The mechanism of anion adsorption on iron oxides: Evidence for the bonding of arsenate tetrahedra on free Fe (O, OH) 6 edges. *Geochimica et Cosmochimica Acta, 59*(17), 3647-3653.

Manceau, A., & Combes, J. M. (1988). Structure of Mn and Fe oxides and oxyhydroxides: A topological approach by EXAFS. *Physics and Chemistry of Minerals, 15*(3), 283-295. doi:10.1007/bf00307518

Manceau, A., Charlet, L., Boisset, M. C., Didier, B., & Spadini, L. (1992). Sorption and speciation of heavy metals on hydrous Fe and Mn oxides. From microscopic to macroscopic. *Applied Clay Science, 7*(1), 201-223. doi:http://dx.doi.org/10.1016/0169-1317(92)90040-T

Mbonimpa, M., Aubertin, M., & Bussière, B. (2011). Oxygen consumption test to evaluate the diffusive flux into reactive tailings: interpretation and numerical assessment. *Canadian Geotechnical Journal, 48*(6), 878-890.

Mbonimpa, M., Aubertin, M., Chapuis, R. P., & Bussière, B. (2002). Practical pedotransfer functions for estimating the saturated hydraulic conductivity. *Geotechnical & Geological Engineering, 20*(3), 235-259. doi:10.1023/a:1016046214724

Mbonimpa, M., Aubertin, M., Aachib, M., & Bussière, B. (2003). Diffusion and consumption of oxygen in unsaturated cover materials. *Canadian Geotechnical Journal, 40*(5), 916-932.

MbonimpaA, M., Aubertin, M., Chapuis, R., Maqsoud, A., & Bussière, B. (2009). Estimation of specific surface areas of coarse-grained materials with grain-size curves represented by two-parameter lognormal distributions. *Proceedings of the GeoHalifax*, 1607-1614.

McGregor, R., & Blowes, D. (2002). The physical, chemical and mineralogical properties of three cemented layers within sulfide-bearing mine tailings. *Journal of Geochemical Exploration, 76*(3), 195-207.

McGregor, R., Blowes, D., Jambor, J., & Robertson, W. (1998a). Mobilization and attenuation of heavy metals within a nickel mine tailings impoundment near Sudbury, Ontario, Canada. *Environmental Geology, 36*(3-4), 305-319.

McGregor, R., Blowes, D., Jambor, J., & Robertson, W. (1998b). The solid-phase controls on the mobility of heavy metals at the Copper Cliff tailings area, Sudbury, Ontario, Canada. *Journal of Contaminant Hydrology, 33*(3), 247-271.

McKenzie, R. (1980). The adsorption of lead and other heavy metals on oxides of manganese and iron. *Soil Research, 18*(1), 61-73. doi:http://dx.doi.org/10.1071/SR9800061

Mees, F., Swennen, R., Van Geet, M., & Jacobs, P. (2003a). Applications of X-ray computed tomography in the geosciences. *Geological Society, London, Special Publications, 215*(1), 1-6.

Mees, F., Swennen, R., Van Geet, M., & Jacobs, P. (2003b). Applications of X-ray computed tomography in the geosciences. *Geological Society, London, Special Publications, 215*, 1-6.

Mehta, A., & Murr, L. (1983). Fundamental studies of the contribution of galvanic interaction to acid-bacterial leaching of mixed metal sulfides. *Hydrometallurgy, 9*(3), 235-256.

Meima, J. A., Regenspurg, S., Kassahun, A., & Rammlmair, D. (2007). Geochemical modelling of hardpan formation in an iron slag dump. *Minerals Engineering, 20*(1), 16-25. doi:10.1016/j.mineng.2006.04.005

Miller, S., Jeffery, J., & Wong, J. (1991a). *In-pit identification and management of acid forming waste rock at the Golden Cross Gold Mine, New Zealand.* Paper presented at the Proceedings of the Second International Conference on the Abatement of Acidic Drainage Montreal, Quebec September.

Miller, S., Jeffery, J., & Wong, J. (1991b). *Use and misuse of the acid base account for "AMD" prediction*. Paper presented at the Proceedings of the 2nd International Conference on the Abatement of Acidic Drainage, Montréal, Que.

Miller, S., Robertson, A., & Donahue, T. (1997). *Advances in acid drainage prediction using the net acid generation (NAG) test*. Paper presented at the Proc. 4th International Conference on Acid Rock Drainage, Vancouver, BC.

Miller, S., Andrina, J., & Richards, D. (2003). Overburden geochemistry and acid rock drainage scale-up investigations at the grasberg mine, Papua province, Indonesia. *Proceedings of the 6th ICARD, Cairns, Australia*, 12-18.

Miller, S. D., Stewart, W. S., Rusdinar, Y., Schumann, R. E., Ciccarelli, J. M., Li, J., & Smart, R. S. C. (2010). Methods for estimation of long-term non-carbonate neutralisation of acid rock drainage. *Science of The Total Environment, 408*(9), 2129-2135. Retrieved from http://ac.els-cdn.com/S0048969710000136/1-s2.0-S0048969710000136-main.pdf?_tid=9d6d9dd8-28fe-11e7-b5b9-00000aab0f6c&acdnat=1493046148_4f58f45cfebd25644de2ca63e2d94c97

Ministère du développement durable, e. e. p., Gouvernement du Québec. (2012). Directive 019 sur l'industrie minière. 105.

Mitchell, K., Trakal, L., Sillerova, H., Avelar-González, F. J., Guerrero-Barrera, A. L., Hough, R., & Beesley, L. (2018). Mobility of As, Cr and Cu in a contaminated grassland soil in response to diverse organic amendments; a sequential column leaching experiment. *Applied Geochemistry, 88*, 95-102.

Møller, H. (2004). Sampling of heterogeneous bottom ash from municipal waste-incineration plants. *Chemometrics and Intelligent Laboratory Systems, 74*(1), 171-176. doi:https://doi.org/10.1016/j.chemolab.2004.03.016

Moncur, M., Jambor, J., Ptacek, C., & Blowes, D. (2009). Mine drainage from the weathering of sulfide minerals and magnetite. *Applied Geochemistry, 24*(12), 2362-2373.

Moncur, M. C., Ptacek, C. J., Blowes, D. W., & Jambor, J. L. (2005). Release, transport and attenuation of metals from an old tailings impoundment. *Applied Geochemistry, 20*(3), 639-659. doi:https://doi.org/10.1016/j.apgeochem.2004.09.019

Moon, J., Wang, Z., Kim, M. O., & Chun, S.-C. (2016). Strength enhancement of alkaline activated fly ash cured at ambient temperature by delayed activation of substituted OPC. *Construction and Building Materials, 122*, 659-666. doi:http://dx.doi.org/10.1016/j.conbuildmat.2016.06.111

Morin, K. A., & Hutt, N. M. (1994). *Observed preferential depletion of neutralization potential over sulfide minerals in kinetic tests: site-specific criteria for safe NP/AP ratios*. Paper presented at the Proceedings of the Third International Conference on the Abatement of Acidic Drainage, Pittsburgh, USA.

Morin, K. A., & Hutt, N. M. (1998). *Kinetic tests and risk assessment for ARD*. Paper presented at the Fifth Annual British Columbia Metal Leaching and ARD Workshop.

Morin, K. A., & Hutt, N. M. (2001). *Environmental geochemistry of minesite drainage: Practical theory and case studies, Digital Edition*: MDAG Publishing (www. mdag. com), Surrey, British Columbia. ISBN: 0-9682039-1-4.

Mukherjee, S. (2012). *Applied mineralogy: applications in industry and environment*: Springer Science & Business Media.

Murad, E., Schwertmann, U., Bigham, J. M., & Carlson, L. (1994). *Mineralogical characteristics of poorly crystallized precipitates formed by oxidation of Fe super (2+) in acid sulfate waters.* Paper presented at the A. C. S. Symposium Series.

Mylona, E., Xenidis, A., & Paspaliaris, I. (2000). Inhibition of acid generation from sulphidic wastes by the addition of small amounts of limestone. *Minerals Engineering, 13*(10), 1161-1175. doi:http://dx.doi.org/10.1016/S0892-6875(00)00099-6

Natterer, F., & Wübbeling, F. (2001). *Mathematical Methods in Image Reconstruction.* Philadelphia, PA (USA): SIAM.

Natterer, F., & Ritman, E. L. (2002). Past and future directions in x-ray computed tomography (CT). *International Journal of Imaging Systems and Technology, 12*(4), 175-187.

NEDEM. (1995). *Evaluation of static and kinetic prediction test data and comparison with field monitoring data.*

NEDEM. (1997). DIVERSITÉ MICROBIOLOGIQUE DANS LA PRODUCTION DE DRAINAGE MINIER ACIDE À LA HALDE SUD DE LA MINE DOYON

NEDEM. (2008). Acid rock drainage prediction manual

Nehdi, M., & Tariq, A. (2007). Stabilization of sulphidic mine tailings for prevention of metal release and acid drainage using cementitious materials: a review. *Journal of Environmental Engineering and Science, 6*(4), 423-436.

Nelsen, F., & Eggertsen, F. (1958). Determination of surface area. Adsorption measurements by continuous flow method. *Analytical Chemistry, 30*(8), 1387-1390.

Nicholson, R. V., Gillham, R. W., & Reardon, E. J. (1988). Pyrite oxidation in carbonate-buffered solution: 1. Experimental kinetics. *Geochimica et Cosmochimica Acta, 52*(5), 1077-1085. doi:http://dx.doi.org/10.1016/0016-7037(88)90262-1

Nordstrom, D. K. (1982). *Aqueous pyrite oxidation and the consequent formation of secondary iron minerals*: Soil Science Society of America.

Nordstrom, D. K. (2000). Advances in the hydrogeochemistry and microbiology of acid mine waters. *International Geology Review, 42*(6), 499-515.

Nordstrom, D. K. (2009). Acid rock drainage and climate change. *Journal of Geochemical Exploration, 100*(2–3), 97-104. doi:http://dx.doi.org/10.1016/j.gexplo.2008.08.002

Nordstrom, D. K., & Southam, G. (1997). Geomicrobiology of sulfide mineral oxidation. *Reviews in mineralogy, 35*, 361-390.

Nordstrom, D. K., Blowes, D. W., & Ptacek, C. J. (2015). Hydrogeochemistry and microbiology of mine drainage: An update. *Applied Geochemistry, 57*, 3-16.

Oliver, M. A., & Webster, R. (1990). Kriging: a method of interpolation for geographical information systems. *International Journal of Geographical Information Systems, 4*(3), 313-332. doi:10.1080/02693799008941549

Ouangrawa, M., Molson, J., Aubertin, M., Bussière, B., & Zagury, G. (2009). Reactive transport modelling of mine tailings columns with capillarity-induced high water saturation for preventing sulfide oxidation. *Applied Geochemistry, 24*(7), 1312-1323.

Ouangrawa, M., Aubertin, M., Molson, J. W., Bussière, B., & Zagury, G. J. (2010). Preventing acid mine drainage with an elevated water table: Long-term column experiments and parameter analysis. *Water, Air, & Soil Pollution, 213*(1-4), 437-458.

Pabst, T., Aubertin, M., Bussière, B., & Molson, J. (2010). *Analysis of monolayer covers for the reclamation of acidgenerating tailings–Column testing and interpretation.* Paper presented at the Proceedings 63rd Canadian Geotechnical Conference and 1st Joint CGS/CNC-IPA Permafrost Specialty Conference, Calgary.

Paktunc, A. (1999a). Mineralogical constraints on the determination of neutralization potential and prediction of acid mine drainage. *Environmental Geology, 39*(2), 103-112.

Paktunc, A., & Davé, N. (2000a). *Mineralogy of pyritic waste rock leached by column experiments and prediction of acid mine drainage.* Paper presented at the In: Rammlmair D (ed.) Applied Mineralogy, pp. 621–623. Balkema.

Paktunc, A., Leaver, M., Salley, J., & Wilson, J. (2001). *A new standard material for acid base accounting tests.* Paper presented at the Securing the Future. International conference on mining and the environment, Skelleftea, Sweden.

Paktunc, A. D. (1999b). Characterization of Mine Wastes for Prediction of Acid Mine Drainage. In J. M. Azcue (Ed.), *Environmental Impacts of Mining Activities: Emphasis on Mitigation and Remedial Measures* (pp. 19-40). Berlin, Heidelberg: Springer Berlin Heidelberg.

Paktunc, A. D., & Dave, N. K. (2000b). *Prediction of Acidic Drainage and Accompanying Metal Releases from Unsegregated Pyritic Uranium Mill Tailings Based on Effluent Chemistry and Post Leaching Sample Mineralogy.* Paper presented at the Proceedings of the Fifth International Conference on Acid Rock Drainage. Society for Mining, Metallurgy, and Exploration, Inc.(SME), Denver.

Paradis, M., Duchesne, J., Lamontagne, A., & Isabel, D. (2006). Using red mud bauxite for the neutralization of acid mine tailings: a column leaching test. *Canadian Geotechnical Journal, 43*(11), 1167-1179. doi:10.1139/t06-071

Parbhakar-Fox, A., Fox, N., Hill, R., Ferguson, T., & Maynard, B. (2017a). Improved mine waste characterisation through static blended test work. *Minerals Engineering.* doi:https://doi.org/10.1016/j.mineng.2017.09.011

Parbhakar-Fox, A., Lottermoser, B., Hartner, R., Berry, R. F., & Noble, T. L. (2017b). Prediction of Acid Rock Drainage from Automated Mineralogy *Environmental Indicators in Metal Mining* (pp. 139-156): Springer.

Park, C.-K. (2000). Hydration and solidification of hazardous wastes containing heavy metals using modified cementitious materials. *Cement and Concrete Research, 30*(3), 429-435. doi:http://dx.doi.org/10.1016/S0008-8846(99)00272-0

Pérez-López, R., Nieto, J. M., Álvarez-Valero, A. M., & Ruiz de Almodóvar, G. (2007). Mineralogy of the hardpan formation processes in the interface between sulfide-rich sludge and fly ash: Applications for acid mine drainage mitigation. *American Mineralogist, 92*(11-12), 1966-1977.

Pesonen, J., Yliniemi, J., Illikainen, M., Kuokkanen, T., & Lassi, U. (2016). Stabilization/solidification of fly ash from fluidized bed combustion of recovered fuel and biofuel using alkali activation and cement addition. *Journal of Environmental Chemical Engineering, 4*(2), 1759-1768. doi:http://dx.doi.org/10.1016/j.jece.2016.03.005

Petruk, W. (2000). Applied mineralogy to tailings and waste rock pile-sulfide oxidation reactions and remediation of acidic water drainage. *Applied mineralogy in the mining industry*, 201-225.

Petruk, W., & Lastra, R. (1993). Evaluation of the recovery of liberated and unliberated chalcopyrite by flotation columns in a copper cleaner circuit. *International Journal of Mineral Processing, 40*(1), 137-149. doi:https://doi.org/10.1016/0301-7516(93)90046-D

Peyronnard, O., & Benzaazoua, M. (2012). Alternative by-product based binders for cemented mine backfill: Recipes optimisation using Taguchi method. *Minerals Engineering, 29*, 28-38. doi:10.1016/j.mineng.2011.12.010

Pirrie, D., Butcher, A. R., Power, M. R., Gottlieb, P., & Miller, G. L. (2004). Rapid quantitative mineral and phase analysis using automated scanning electron microscopy (QemSCAN); potential applications in forensic geoscience. *Geological Society, London, Special Publications, 232*(1), 123-136.

Plante, B., Benzaazoua, M., & Bussière, B. (2011a). Kinetic testing and sorption studies by modified weathering cells to characterize the potential to generate contaminated neutral drainage. *Mine Water and the Environment, 30*(1), 22-37.

Plante, B., Benzaazoua, M., & Bussière, B. (2011b). Predicting geochemical behaviour of waste rock with low acid generating potential using laboratory kinetic tests. *Mine Water and the Environment, 30*(1), 2-21.

Plante, B., Bussière, B., & Benzaazoua, M. (2012). Static tests response on 5 Canadian hard rock mine tailings with low net acid-generating potentials. *Journal of Geochemical Exploration, 114*, 57-69.

Plante, B., Bussière, B., & Benzaazoua, M. (2014). Lab to field scale effects on contaminated neutral drainage prediction from the Tio mine waste rocks. *Journal of Geochemical Exploration, 137*, 37-47. doi:http://dx.doi.org/10.1016/j.gexplo.2013.11.004

Poduri, S., & Rao, R. (2000). Sampling methodology with applications: Chapman and Hall, New York.

Popek, E. P. (2003). *Sampling and analysis of environmental chemical pollutants: a complete guide*: Academic Press.

Price, W. A. (2009). Prediction manual for drainage chemistry from sulphidic geologic materials. *MEND report, 1*(1), 579.

Price, W. A., & Kwong, Y. J. (1997a). *Waste rock weathering, sampling and analysis: Observations from the British Columbia Ministry of Employment and Investment database.*

Paper presented at the Proceedings of 4th International Conference on Acid Rock Drainage (ICARD), Vancouver.

Price, W. A., Morin, K., & Hutt, N. (1997b). *Guidelines for the prediction of acid rock drainage and metal leaching for mines in British Columbia: Part II. Recommended procedures for static and kinetic testing.* Paper presented at the Proceedings of the Fourth International Conference on Acid Rock Drainage.

Quispe, D., Pérez-López, R., Acero, P., Ayora, C., Nieto, J. M., & Tucoulou, R. (2013). Formation of a hardpan in the co-disposal of fly ash and sulfide mine tailings and its influence on the generation of acid mine drainage. *Chemical Geology, 355,* 45-55. doi:10.1016/j.chemgeo.2013.07.005

Rammlmair, D. (2002). Hard pan formation on mining residuals *Uranium in the Aquatic Environment* (pp. 173-182): Springer.

Regenspurg, S., Brand, A., & Peiffer, S. (2004). Formation and stability of schwertmannite in acidic mining lakes 1. *Geochimica et Cosmochimica Acta, 68*(6), 1185-1197. doi:http://dx.doi.org/10.1016/j.gca.2003.07.015

Rietveld, H. (1969). A profile refinement method for nuclear and magnetic structures. *Journal of Applied Crystallography, 2*(2), 65-71.

Rimstidt, J. D., & Vaughan, D. J. (2003). Pyrite oxidation: a state-of-the-art assessment of the reaction mechanism. *Geochimica et Cosmochimica Acta, 67*(5), 873-880. doi:http://dx.doi.org/10.1016/S0016-7037(02)01165-1

Rodríguez, L., Gómez, R., Sánchez, V., Villaseñor, J., & Alonso-Azcárate, J. (2018). Performance of waste-based amendments to reduce metal release from mine tailings: One-year leaching behaviour. *J Environ Manage, 209,* 1-8.

Rohwerder, T., Gehrke, T., Kinzler, K., & Sand, W. (2003). Bioleaching review part A. *Applied Microbiology and Biotechnology, 63*(3), 239-248. doi:10.1007/s00253-003-1448-7

Rue, E. L., & Bruland, K. W. (1995). Complexation of iron(III) by natural organic ligands in the Central North Pacific as determined by a new competitive ligand equilibration/adsorptive cathodic stripping voltammetric method. *Marine Chemistry, 50*(1), 117-138. doi:http://dx.doi.org/10.1016/0304-4203(95)00031-L

Sampath, S. (2001). *Sampling theory and methods*: CRC press.

Sapsford, D., Bowell, R., Dey, M., Williams, C., & Williams, K. (2008). A comparison of kinetic NAG tests with static and humidity cell tests for the prediction of ARD. *Mine Water and the Environment, Ostrava,* 325-328.

Sapsford, D. J., Bowell, R. J., Dey, M., & Williams, K. P. (2009). Humidity cell tests for the prediction of acid rock drainage. *Minerals Engineering, 22*(1), 25-36. doi:10.1016/j.mineng.2008.03.008

Schroth, A. W., & Parnell Jr, R. A. (2005). Trace metal retention through the schwertmannite to goethite transformation as observed in a field setting, Alta Mine, MT. *Applied Geochemistry, 20*(5), 907-917. doi:http://dx.doi.org/10.1016/j.apgeochem.2004.09.020

Schwertmann, U., & Cornell, R. M. (2007). The Iron Oxides *Iron Oxides in the Laboratory* (pp. 5-18): Wiley-VCH Verlag GmbH.

Sheoran, A. S., & Sheoran, V. (2006). Heavy metal removal mechanism of acid mine drainage in wetlands: A critical review. *Minerals Engineering, 19*(2), 105-116. doi:http://dx.doi.org/10.1016/j.mineng.2005.08.006

Sherlock, E., Lawrence, R., & Poulin, R. (1995). On the neutralization of acid rock drainage by carbonate and silicate minerals. *Environmental Geology, 25*(1), 43-54. Retrieved from http://download.springer.com/static/pdf/361/art%253A10.1007%252FBF01061829.pdf?originUrl=http%3A%2F%2Flink.springer.com%2Farticle%2F10.1007%2FBF01061829&token2=exp=1493047298~acl=%2Fstatic%2Fpdf%2F361%2Fart%25253A10.1007%25252FBF01061829.pdf%3ForiginUrl%3Dhttp%253A%252F%252Flink.springer.com%252Farticle%252F10.1007%252FBF01061829*~hmac=d4d14c9b0b08e400f6433fc1508d9d3147534f81a6f876c33b6e71d0af5b2572

Sherman, D. M., & Randall, S. R. (2003). Surface complexation of arsenic(V) to iron(III) (hydr)oxides: structural mechanism from ab initio molecular geometries and EXAFS spectroscopy. *Geochimica et Cosmochimica Acta, 67*(22), 4223-4230. doi:http://dx.doi.org/10.1016/S0016-7037(03)00237-0

Silverman, M. P. (1967). Mechanism of bacterial pyrite oxidation. *Journal of Bacteriology, 94*(4), 1046-1051.

Singh, C. K., Kumar, A., Shashtri, S., Kumar, A., Kumar, P., & Mallick, J. (2017). Multivariate statistical analysis and geochemical modeling for geochemical assessment of groundwater of Delhi, India. *Journal of Geochemical Exploration, 175*, 59-71.

Smart, R., Skinner, W., Levay, G., Gerson, A., Thomas, J., Sobieraj, H., Schumann, R., Weisener, C., Weber, P., & Miller, S. (2002). ARD test handbook: project P387A, prediction and kinetic control of acid mine drainage. *AMIRA International Ltd, Melbourne.*

Smith, K., & Huyck, H. (1999). The Environmental Geochemistry of Mineral Deposits, Part A. Processes, Techniques, and Health Issues.

Smith, K. S., Ramsey, C. A., & Hageman, P. L. (2000). *Sampling strategy for the rapid screening of mine-waste dumps on abandoned mine lands*: US Department of the Interior, US Geological Survey.

Sobek, A. A., Schuller, W. A., & Freeman, J. R. (1978a). Field and laboratory methods applicable to overburdens and minesoils *Field and laboratory methods applicable to overburdens and minesoils*: EPA.

Sobek, A. A., Schuller, W., Freeman, J., & Smith, R. (1978b). Field and Laboratory Methods Applicable to Overburdens and Minesoils, 1978. *US Environmental Protection Agency, Cincinnati, Ohio, 45268*, 47-50.

Soler, J. M., Boi, M., Mogollón, J. L., Cama, J., Ayora, C., Nico, P. S., Tamura, N., & Kunz, M. (2008). The passivation of calcite by acid mine water. Column experiments with ferric sulfate and ferric chloride solutions at pH 2. *Applied Geochemistry, 23*(12), 3579-3588.

Stewart, W. A., Miller, S. D., & Smart, R. (2006). *Advances in acid rock drainage (ARD) characterisation of mine wastes.* Asmr.

Stock, S. (2008a). Recent advances in X-ray microtomography applied to materials. *International Materials Reviews, 53*(3), 129-181.

Stock, S. R. (2008b). Recent advances in X-ray microtomography applied to materials. *International Materials Reviews, 53*(3), 129-181.

Strömberg, B., & Banwart, S. (1999). Weathering kinetics of waste rock from the Aitik copper mine, Sweden: scale dependent rate factors and pH controls in large column experiments. *Journal of Contaminant Hydrology, 39*(1), 59-89. doi:https://doi.org/10.1016/S0169-7722(99)00031-5

Sutherland, D., & Gottlieb, P. (1991). Application of automated quantitative mineralogy in mineral processing. *Minerals Engineering, 4*(7-11), 753-762.

Sverdrup, H. U. (1990). *The kinetics of base cation release due to chemical weathering*: Krieger Publishing Company.

Tariq, A., & Yanful, E. K. (2013). A review of binders used in cemented paste tailings for underground and surface disposal practices. *J Environ Manage, 131*, 138-149. doi:10.1016/j.jenvman.2013.09.039

Tibble, P., & Nicholson, R. (1997). *Oxygen consumption on sulphide tailings and tailings covers: measured rates and applications.* Paper presented at the Proceedings of the 4th International Conference on Acid Rock Drainage (ICARD), Vancouver, BC.

Tributsch, H. (2001). Direct versus indirect bioleaching. *Hydrometallurgy, 59*(2), 177-185. doi:https://doi.org/10.1016/S0304-386X(00)00181-X

Van Genuchten, M. T. (1980). A closed-form equation for predicting the hydraulic conductivity of unsaturated soils. *Soil Science Society of America Journal, 44*(5), 892-898.

Vermang, J., Norton, L., Huang, C., Cornelis, W., Da Silva, A., & Gabriels, D. (2015). Characterization of soil surface roughness effects on runoff and soil erosion rates under simulated rainfall. *Soil Science Society of America Journal, 79*(3), 903-916.

Villeneuve, M. (2006). *Évaluation du comportement géochimique à long terme de rejets miniers à faible potentiel de génération d'acide à l'aide d'essais cinétiques.*

Wang, F., Shen, Z., & Al-Tabbaa, A. (2018). PC-based and MgO-based binders stabilised/solidified heavy metal-contaminated model soil: strength and heavy metal speciation in early stage. *Géotechnique*, 1-6.

Wang, F., Wang, H., Jin, F., & Al-Tabbaa, A. (2015a). The performance of blended conventional and novel binders in the in-situ stabilisation/solidification of a contaminated site soil. *J Hazard Mater, 285*, 46-52. doi:10.1016/j.jhazmat.2014.11.002

Wang, F., Wang, H., Jin, F., & Al-Tabbaa, A. (2015b). The performance of blended conventional and novel binders in the in-situ stabilisation/solidification of a contaminated site soil. *J Hazard Mater, 285*, 46-52.

Waychunas, G. A., Rea, B. A., Fuller, C. C., & Davis, J. A. (1993). Surface chemistry of ferrihydrite: Part 1. EXAFS studies of the geometry of coprecipitated and adsorbed arsenate. *Geochimica et Cosmochimica Acta, 57*(10), 2251-2269. doi:http://dx.doi.org/10.1016/0016-7037(93)90567-G

Weber, P. A., Thomas, J. E., Skinner, W. M., & Smart, R. S. C. (2004). Improved acid neutralisation capacity assessment of iron carbonates by titration and theoretical

calculation. *Applied Geochemistry, 19*(5), 687-694. doi:http://dx.doi.org/10.1016/j.apgeochem.2003.09.002

Weber, P. A., Hughes, J. B., Conner, L. B., Lindsay, P., & Smart, R. (2006). *Short-Term Acid Rock Drainage Characteristics Determined by Paste pH and Kinetic NAG Testing: Cypress, Prospect, New Zealand.* ASMR.

Webster, J. G., Swedlund, P. J., & Webster, K. S. (1998). Trace Metal Adsorption onto an Acid Mine Drainage Iron(III) Oxy Hydroxy Sulfate. *Environmental Science & Technology, 32*(10), 1361-1368. doi:10.1021/es9704390

Whitaker, S. (1986). Flow in porous media I: A theoretical derivation of Darcy's law. *Transport in porous media, 1*(1), 3-25.

Yeniay, O. (2005). A comparative study on optimization methods for the constrained nonlinear programming problems. *Mathematical Problems in Engineering, 2005*(2), 165-173.

Yi, Y., Wen, J., Zeng, G., Zhang, T., Huang, F., Qin, H., & Tian, S. (2017). A comparative study for the stabilisation of heavy metal contaminated sediment by limestone, MnO 2 and natural zeolite. *Environmental Science and Pollution Research, 24*(1), 795-804.

Yilmaz, E., Benzaazoua, M., Bussière, B., & Pouliot, S. (2014). Influence of disposal configurations on hydrogeological behaviour of sulphidic paste tailings: A field experimental study. *International Journal of Mineral Processing, 131*, 12-25. doi:10.1016/j.minpro.2014.08.004

ANNEXE A – COMPUTED TOMOGRAPHY PROCESS

Samples of waste rocks collected at Canadian Malartic mine were scanned by the X-ray computed tomography (CT) technique using an XTH 225 ST system, produced by Nikon Metrology. X-ray CT is a non-destructive technique with wide applications in geological disciplines and materials science(Cnudde *et al.*, 2006; Maire *et al.*, 2014; Mees *et al.*, 2003b; Stock, 2008b) given its ability to provide the internal view of objects based on variations of density, and therefore dependent of their material composition. X-ray CT can be used for qualitative and quantitative analysis of internal structures of geological materials as long as those structures are sufficiently marked by differences in atomic composition and/or material density. The schematic workflow chart for the full CT process is shown in Figure A.1. The basics X-ray CT setup consists of an X-ray source tube, a detector, and a rotary table. The object or sample to be studied is positioned on the rotary table in between an X-ray source and an X-ray detector, and then it rotates 360 degrees while the detector acquires two-dimensional radiographs for different positions during step-wise rotation around a central axis. The radiographs are produced when the X-rays pass through the object along several different paths and several different directions. The contrast in the projected X-ray images is generated by differences in X-ray attenuation that arise principally from differences in density within the sample's material. As a rule of thumb, more energetic X-rays would be able to penetrate denser materials and larger (or thicker) samples, so the contrast in the images is material and energy-dependent. Thanks to the continuous improvements of scanning resolutions, CT systems for material research include the possibility of using higher X-ray intensities and the possibility of using microfocus X-ray sources to obtain higher resolutions in the order of a few micrometers. The generation of three-dimensional (3D) data from the two-dimensional X-ray CT images, is achieved using reconstruction software. The most important algorithms for reconstruction are Fourier-based methods, and algebraic and statistical approaches(Buzug, 2010; Herman, 2009; Hsieh, 2015; Kak & Slaney, 1988; Natterer & Ritman, 2002; Natterer & Wübbeling, 2001). However, two-dimensional Fourier-based reconstruction methods are the most computationally efficient, and therefore more widely used. They are based on the Radon Transform and Fourier Slice Theorem(Bracewell, 2003; Buzug, 2010; Deans, 2007; Herman, 2009; Kak *et al.*, 1988). In most cone-beam setups, as shown in Figure A.2, the CT reconstruction is generally based on the FDK (Feldkamp-Davis-Kress) algorithm(Feldkamp *et al.*, 1984; Grangeat, 1991). However, more

recently, Katsevich's algorithms(Katsevich, 2002, 2003) ,which require a helical path for the CT scan acquisition, have been used. After the 3D reconstruction, the 3D data offers the possibility of qualitative inspection and quantitative measurements in both the interior and exterior of the specimen under investigation. The 3D image in gray values represents a 3D volumetric density map of the X-ray absorptions' coefficients for the specimen along the crossing paths of the X-rays. Each gray level offers information about what the X-rays have encountered in their paths and their spatial location, thus revealing external and internal structures of the specimen that has been scanned. Quantitative analysis can be obtained as well as localization of structural material inclusion and identification of pores not usually visible through traditional methods of nondestructive testing. CT analysis can thus provide size and morphology determination, voids/porosity distribution, and location of the waste rocks inclusions.

The scan protocol included securing the sample with synthetic foam transparent to the X-rays, X-ray setting standardized to a cone-beam generated by a tube voltage of 170 kV and tube current of 192 μA, and collecting up to 2880 radiographs over 360 degrees' rotation with an integration time of 708 ms per image. After scanning, the reconstruction was performed with a FDK (Feldkamp-Davis-Kress) type commercial algorithm to produce a 3D image as well as serial cross-sectional images of the rock sample. These consisted of matrices of 2000 $\times$ 2000 pixels which collective composed a volume of isotropic 70 μm^3 voxel size for each of the waste rocks samples (UQAT Stones AGR, UQAT Stones CPO, and UQAT Stones EGR). Once the 3D reconstruction was complete a local adaptive or dynamic gradient threshold was applied for surface determination and material segmentation. This was performed with the software package VGStudio Max 2.2 from Volume Graphics, GmbH. The insight gained from imaging the specimen's internal structure is quite valuable.
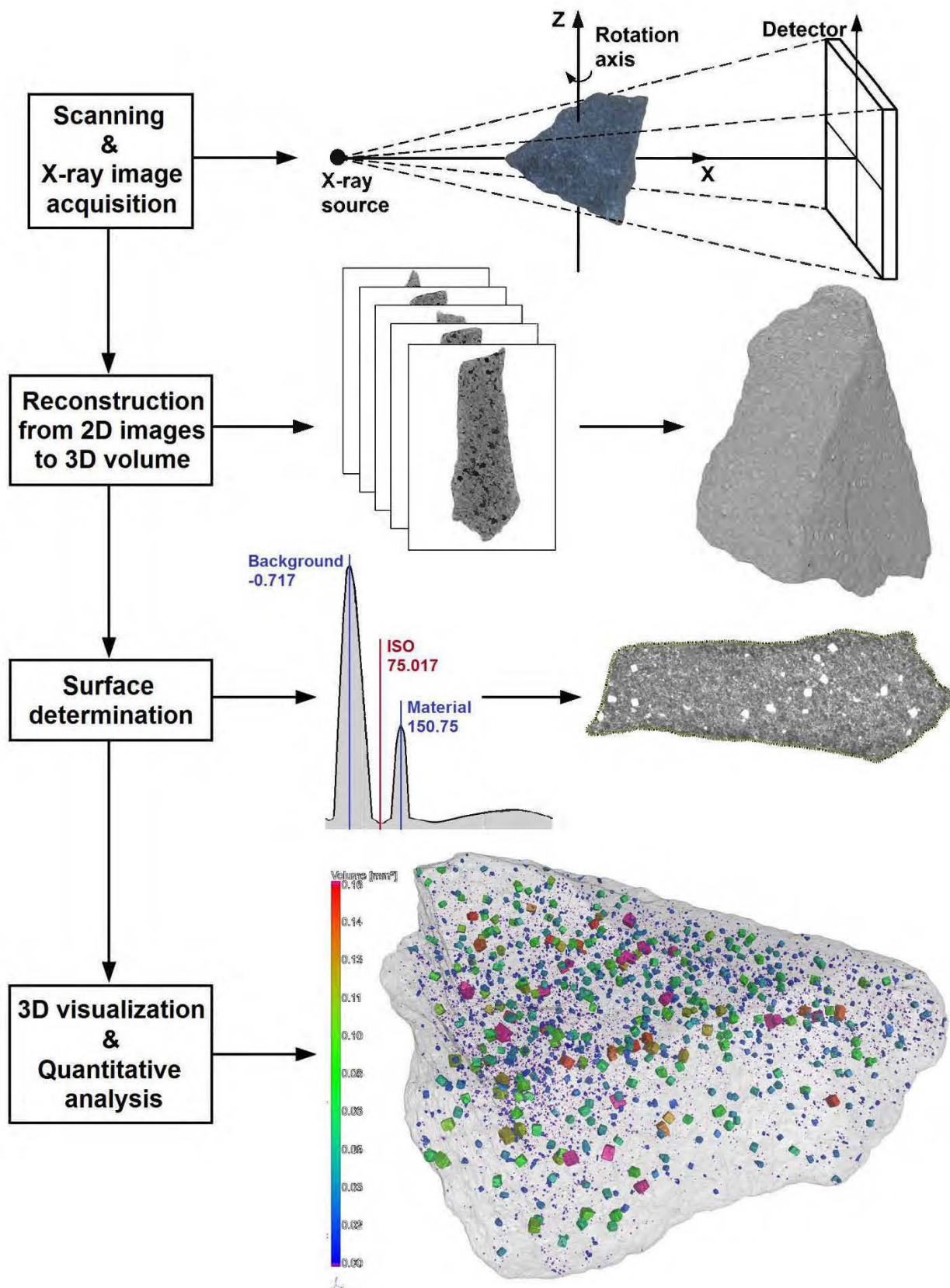
Figure A.3 : Workflow chart for the full process of X-ray CT in the analysis of waste rocks

ANNEXE B – ARTICLE 6: INVESTIGATION OF THE ROLE OF HARDPANS ON THE GEOCHEMICAL BEHAVIOR OF THE JOUTEL MINE TAILINGS

Abdellatif Elghali
Université du Québec en Abitibi-Témiscamingue (UQAT), 445 boul de l'Université, Rouyn-Noranda J9X 5E4, QC, Canada
Mostafa Benzaazoua
Université du Québec en Abitibi-Témiscamingue (UQAT), 445 boul de l'Université, Rouyn-Noranda J9X 5E4, QC, Canada
Bruno Bussière
Université du Québec en Abitibi-Témiscamingue (UQAT), 445 boul de l'Université, Rouyn-Noranda J9X 5E4, QC, Canada
Dirk Schaumann
Fibics Incorporated, Ottawa, Ontario, Canada
Shaun Graham
ZEISS Natural Resources Lab, 509 Coldhams Lane, Cambridge, CB1 3JS
Thomas Genty
Agnico Eagle Mines Limited 10 200, route de Preissac, Rouyn-Noranda J0Y 1C0, QC, Canada
Josée Noel
Agnico Eagle Mines Limited 10 200, route de Preissac, Rouyn-Noranda J0Y 1C0, QC, Canada
Chris Kenedy
Agnico Eagle Mines Limited 10 200, route de Preissac, Rouyn-Noranda J0Y 1C0, QC, Canada
Jean Cayouette
Agnico Eagle Mines Limited 10 200, route de Preissac, Rouyn-Noranda J0Y 1C0, QC, Canada

ABSTRACT

This paper focuses on the mineralogical and geochemical characterization of oxidized, unweathered tailings and hardpans formed in the Joutel Eagle-Telbel mine tailings impoundment (Québec). To highlight geochemical behavior of oxidized and unweathered tailings, oxidized and non-oxidized tailings were sampled, analyzed and subjected to kinetic testing. Two scenarios were tested: oxidized tailings alone to simulate surface runoff due to presence of hardpans, and oxidized tailings above unweathered tailings to simulate vertical infiltration. The mineralogical characterization of hardpan samples revealed a composition of 46% iron oxy-hydroxides, 19% siderite, 4% pyrite and non-sulphide gangue minerals. The 11-months column test results showed that the leachate from the oxidized sample were consistently acidic (pH 2.44); the average concentrations were 781 mg/l S, 550 mg/l Ca, 31 mg/l Mg, 106 mg/l Fe and 11 mg/l Zn. However, the leachates provided by vertical infiltration scenario were consistently neutral (pH = 7.3), with average species concentrations of 1653 mg/l S, 523 mg/l Ca, 817 mg/l Mg, 0.88 mg/l Fe and 0.67 mg/l Zn.

Introduction

Sulphides within mine tailings can oxidize and generate acidity, sulphates and metals leaching. When carbonates are also present in the tailings, they neutralize, through dissolution reactions, the acidic tailings pore water. These oxidation/neutralization and hydrolysis mechanisms cause the precipitation of various secondary phases. In some specific cases, massive precipitation of secondary phases leads to the formation of "cemented" layers of precipitated minerals called hardpans (Blowes *et al.*, 1998; Blowes *et al.*, 1991; McGregor *et al.*, 2002; Pérez-López *et al.*, 2007).

Hardpans are naturally formed beneath tailings surface and their mineralogy is variable depending on the initial chemical and mineralogical composition of tailings. Hardpans may occur as continuous or discontinued layers in tailings storage areas, typically contained primary minerals, poorly crystalized phases, amorphous ferric oxides, metal sulphates, etc. (Lottermoser *et al.*, 2006). Hardpans are usually formed in the vadose zone where there is a geochemical contrast of pH, Eh and chemical concentrations between oxidized and unweathered tailings. Hardpans formation may be accelerated using alkaline amendments to reactive tailings (Pérez-López *et al.*, 2007). Precipitation of secondary minerals reduces the porosity of the initial tailings. These cemented layers are compact and impermeable compared to the initial tailings materials, which influences water and oxygen fluxes (Blowes *et al.*, 1991). The geochemical behavior of tailings impoundments is then influenced by various mechanisms related to the hardpans: i) precipitation of secondary phases decrease contaminant concentrations by co-precipitation and adsorption mechanisms, ii) protection of the underlying tailings by inhibiting oxygen diffusion, and iii) deviation of water fluxes. Deflecting the vertical infiltration water flow to surface runoff isolates the unweathered tailings.

Joutel Eagle-Telbel is a closed mine site located north of Abitibi-Témiscamingue (Québec). Joutel's tailings were characterized as "uncertain" regarding potential for acid generation. Results of kinetic tests on unweathered and oxidized tailings confirmed that their long-term environmental behavior is uncertain for most samples, and acid generating for some others (Benzaazoua *et al.*, 2004a). The results confirm a high spatial variability of chemical and mineralogical tailings characteristics. Recently and in some specific zones of the impoundment, acidity has been observed

in the supernatant waters. However, the final effluent shows a neutral behavior. To explain this phenomenon, various materials consisting of oxidized and unweathered were sampled, characterized and submitted to laboratory kinetic leaching tests. Leaching tests consisted on two scenarios: i) a column with only the oxidized tailings to simulate surface and sub-surface runoff due to presence of hardpan and ii) a column with oxidized tailings above unweathered tailings to simulate vertical infiltration. The project hypothesis is that the hardpan when it exists deflects the water vertical infiltration to surface runoff.

Materials and methods

Materials sampling

Samples used in this project were collected in acidic zones based on previously determined paste pH. Samples were collected from different vertical horizons (i.e. oxidized, hardpan and unweathered tailings) in a trench dug out in the selected zones (Figure B.4). A composite sample was made for each horizon based on samples collected on different locations. The samples were homogenized in the laboratory using quartering.
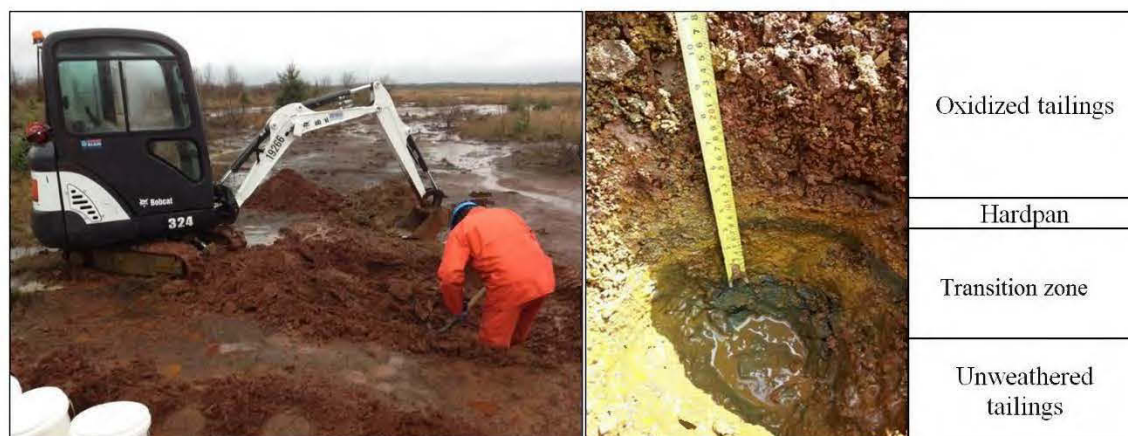

Figure B.5 : Tailings sampling and horizons

Physical, chemical and mineralogical analysis

The tailings grain size distribution was evaluated using a laser analyzer (Malvern Masetrsizer S). Specific gravity (Gs) was determined using micromeritics Helium Pycnometer, and the specific surface area (SSA) was evaluated with a micromeritics analyzer using B.E.T method.

The bulk chemical composition of the samples was analyzed using Perkin Elmer Optima 3100 RL ICP-AES following a total HNO3/Br2/HF/HCl digestion. The total sulfur and inorganic carbon contents were determined by using induction furnace (ELTRA CS-2000). The chemical analysis of the leachates samples from column leaching tests were done using pH, Eh and conductivity meter. The elemental composition was determined using ICP-AES on acidified samples (2% HNO_3). The acidity and alkalinity were evaluated using automatic titror.

Major minerals within oxidized and unweathered tailings were analyzed by X-ray diffraction (XRD; Brucker D8 Advance, with a detection limit and precision of approximately 0.5 %, operating with a copper cathode, $K\alpha$ radiation) using DIFFRACT.EVA software and quantified using TOPAS v4.2.

Hardpan samples were analyzed using automated mineralogy system and light microscopy. The objectives of this characterization were to determine the mineralogical composition, mineralogical association and stoichiometry of minerals forming hardpan sample.

A large-area light-microscopy image mosaic of one hardpan sample was acquired with coaxial reflected light using a Zeiss AXIO Zoom.V16. Large-area SEM image mosaics of a polished 30 mm diameter epoxy mount of a hardpan sample was acquired with the ZEISS Atlas 5 software by using a ZEISS EVO MA 15 tungsten filament SEM at Fibics Incorporated (Ottawa, Canada). The light-microscopy image mosaic was imported in the Atlas 5 correlative workspace and aligned with the sample in the SEM chamber. The data set was exported to an autonomous series of files called the Browser-Based Viewer. The Browser-Based Viewer dataset of the hardpan sample can be viewed at the following link:

http://www.petapixelproject.com/mosaics/UQAT/Hardpan-03-BBV-Export-LM-BSD/Hardpan-03-BBV-Export-LM-BSD/index.html.

Element distribution maps and point analyses of several regions of interest were acquired with the Bruker Esprit 1.9 software on the Zeiss EVO MA 15 SEM at 8.5 mm working distance and an acceleration voltage of 20 kV. The acquired element maps and point analyses were exported from the Bruker Esprit software.

The automated mineralogy analysis was carried out at Fibics Incorporated (Ottawa, Canada) using Zeiss Mineralogic Mining on a ZEISS EVO MA 15 tungsten filament SEM equipped with two Bruker 6│30 Xflash energy dispersive x-ray spectrometers (EDS). Mineralogic Mining version

1.02 was used for this analysis with its fully quantitative EDS mineral classification protocol, where minerals are classified based on the weight percent contribution of elements present, and thus the mineral's stoichiometry. The full mapping analysis mode was used with an EDS analysis carried out every 4 µm of the sample surface with approximately 4000 counts per EDS spectrum for quantification with an electron beam dwell time of 0.07 seconds. The automated mineralogy analysis was acquired at 8.5 mm working distance, an acceleration voltage of 20 kV, and a probe current of 2.0 nA.

Static and kinetic leaching tests

Acid potential (AP) of oxidized and unweathered samples was calculated using sulfur sulphides which is the difference between total sulfur and sulphates. Neutralization potential (NP) was analyzed using titration method as described in (Bouzahzah *et al.*, 2015a). The net neutralization potential (NNP) was defined as the difference between NP and AP; the neutralization potential ratio (NPR) as the ratio between NP and AP (Miller *et al.*, 1991b).

Kinetic tests were done using Plexiglas columns of 14-cm diameter and 1-m height. Two scenarios were tested: the first consisted only of the oxidized sample, and the second consisted of an oxidized sample above unweathered sample. The column with only oxidized tailings was mounted to simulate surface runoff due to the presence of hardpans. The column with oxidized sample above unweathered sample was used to simulate vertical water infiltration in the absence of hardpans. These scenarios were chosen due to the difficulty to generate a hardpan artificially at the laboratory scale. The columns were monthly flushed with 2 L of deionized water and columns were allowed to dry under ambient air between two flushes. The leachate waters were collected and analyzed after 4 hours of contact with the samples.

Results and discussion

RESULTS

Physical characterization

The physical characteristics of the samples studied were very variable (Table B.1). The D60 and D90 represent the grain size for 60 and 90%, respectively, passing on the cumulative grain size distribution curve. The oxidized sample had a finer particle size compared to unweathered sample.

The D60 and D90 for the oxidized and unweathered samples are respectively 13 µm, 88µm, 37 µm and 163 µm.

The specific surface area of oxidized sample was of about 38 g/m² while of only 0.7 g/m² for unweathered sample. High specific surface area lead to high exposure rate of minerals. The specific gravity (Gs) of unweathered sample (Gs=3.35) was greater than that of oxidized sample (Gs=2.83). The variation of physical parameters between oxidized and unweathered samples is mainly due to oxidation. In fact, oxidation when occurring reduces de particle size of minerals (sulphides, carbonates) and decreases the specific gravity of sample by depleting sulphides.

Chemical and mineralogical characterization

Chemical and mineralogical compositions are summarized in Table 1. The chemical composition of the solids was different for the three samples due to their different mineralogical composition. The concentration of sulfur increases from oxidized tailings (%S=3.9) to unweathered tailings (%S=6.39). The hardpan sample presents an intermediary concentration of sulfur (%S=5.42). This is explained by sulphides oxidation process. Sulfur from oxidized sample is oxidized and leached, and then precipitated as iron oxy-hydroxide and gypsum in the hardpan's zone. Hardpan's sulphides are coated and passivated by precipitation of these secondary minerals. Generally, coating of sulphides (Figure B.6) reduces significantly oxygen diffusion (Blowes *et al.*, 1991).

Concentrations of magnesium in oxidized sample, hardpan and unweathered sample are respectively 0.045, 0.47 and 1.75%. This element is mostly linked to carbonates (dolomite, ankerite). Iron is slightly enriched in unweathered sample (25.78%) and hardpan (25.39%) comparatively to oxidized sample (20.17%). The oxidized sample is more enriched in Al (3.62%) followed by hardpan sample (2.61%) and then unweathered sample (1.5%). Calcium concentrations are similar in three horizons.

Mineralogical characterization of oxidized and unweathered samples was performed using X-ray diffraction and hardpan was characterized using Mineralogical Mining. Sulphides distribution presents an increasing of concentrations as a function of depth. The sulphides are mostly a reflection of pyrite content. Sulphides in the oxidized horizon are almost depleted due to 25 years of oxidation and the sulphides in the unweathered horizon are protected against oxidation by the water table.

Oxidation of sulphides within upper surface tailings favors carbonates dissolution. Therefore, carbonates distribution follows the same trend than sulphides distribution. Carbonates are thus almost depleted in the oxidized horizon while they are preserved in the unweathered horizon. In general, carbonates and sulphides in the hardpan are protected due to massive precipitation of secondary iron oxy-hydroxides (Figure B.7).

Table B.2: Physical, chemical and mineralogical compositions of studied samples

Physical characteristics			
	D60 (μm)	D90 (μm)	SSA (m²/g)	Gs
Oxidized	13.2	37.15	0.7	2.83
Unweathered	87.6	163.57	38.07	3.35

Chemical composition (%)								
	Al	Ca	Mn	Mg	Fe	S	Zn	Cu
Oxidized	3.62	3.82	0.12	0.045	20.17	3.90	0.010	<ND
Hardpan	2.61	3.26	0.39	0.47	25.39	5.42	0.011	0.003
Unweathered	1.5	3.53	0.74	1.75	25.78	6.39	0.011	<ND

Mineralogical composition (%)					
	Sulphides	Carbonates	Fe-oxi-hydroxides	Gypsum	Others
Oxidized	ND	1.76	23.74	19.3	55.2
Hardpan	4.51	19.65	45.78	0.26	29.8
Unweathered	7.40	42.15	<ND	<ND	50.45

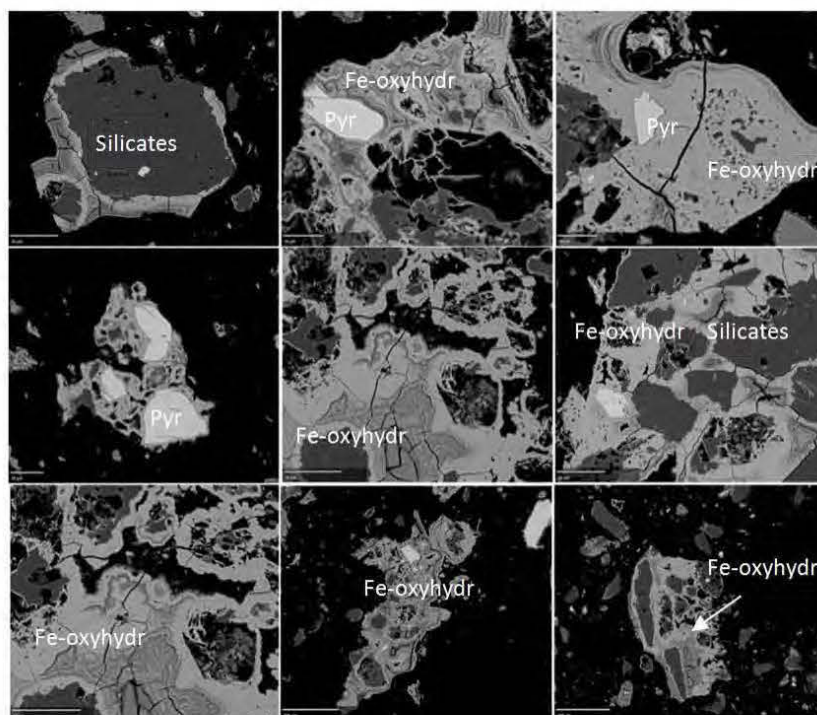| Static tests				
	NP (titration)	NP (carbonates)	AP	NNP	NPR
Oxidized	3	20	5.5	-2.5	0.5
Unweatherd	228	538	193	35	1.2

ND: detection limit

Figure B.8 : BSE images showing textures of secondary iron oxy-hydroxides within the hardpan sample (Fe-oxyhydr = iron oxy-hydroxide, pyr = pyrite)

Hardpans are formed in the tailings impoundment due to oxidation/neutralization and hydrolysis reactions. This layer is characterized by its low saturated hydraulic conductivity (McGregor *et al.*, 2002) due to the cementation of particles through the precipitation of secondary minerals reduces tailings porosity and the permeability. Therefore, the mineralogic characterization is crucial to understand hardpan formation and its effect on the geochemical and hydrogeological behaviour of tailings impoundments. The detailed mineralogical characterization of hardpan is presented in Table B.3 based on the analysis of more than 70,000 particles.

Table B.4: Mineralogical characterization of hardpan using Mineralogic Mining

Mineral	Formula	Weight %	Wt% Average Composition
Hematite	Fe_2O_3	32.23	Fe 68.54; O 31.46;
Goethite	FeOOH	2.97	Fe 60.17; O 39.83;
Goethite-Silicate	-	2.22	O 36.64; Fe 28.85; Si 21.23; Al 7.74; Na 4.96; K 0.31; Mg 0.26;
Other iron oxide	-	8.36	Fe 79.9; O 20.1;
Pyrite	FeS_2	3.97	Fe 51.02; S 48.98;
Pyrrhotite	FeS	0.54	Fe 77.82; S 22.18;
Dolomite	$CaMg(CO_3)_2$	0.09	O 50.8; Ca 29.82; Mg 11.69; Fe 7.67; Al 0.02;
Calcite	$CaCO_3$	0.01	Ca 50.81; O 47.59; Fe 1.6;
Ankerite	$Ca(Fe,Mg,Mn)(CO_3)_2$	0.52	O 44.36; Ca 26.52; Fe 20.05; Mg 6.19; Mn 2.88;
Siderite	$FeCO_3$	19.03	Fe 56.35; O 36.19; Mg 3.96; Mn 3.22; Al 0.28;
Gypsum	$CaSO_4.2(H_2O)$	0.26	O 39.41; Ca 37.87; S 22.72;
Quartz	SiO_2	12.45	Si 51.75; O 45.76; Fe 1.69; Al 0.75; K 0.05;
Albite	$NaAlSiO_3$	11.75	O 42.67; Si 33.37; Al 12.6; Na 9.55; Fe 1.75; K 0.04; Ca 0.02
Illite	$(K,H_3O)(Al,Mg,Fe)_2(Si,Al)_4O_{10}[(OH)_2,(H_2O)]$	1.62	O 44.69; Si 34.39; Al 14.09; Fe 3.82; K 2.96; Mg 0.03;
Orthoclase	$KAlSi_3O_8$	1.57	O 42.81; Si 29.35; Al 17.87; K 4.86; Na 2.95; Fe 2.17;
Biotite	$K(Mg,Fe)_3[AlSi_3O_{10}(OH,F)_2$	1.49	O 39.38; Si 18.76; Al 18.24; Fe 17.62; K 5.77; Mg 0.23;
Muscovite	$KAl2(Si_3Al)O_{10}(OH,F)_2$	0.51	O 42.97; Al 24.24; Si 23.53; K 7.27; Fe 1.68; Mg 0.31;
Chamosite	$(Fe^{2+},Mg,Fe^{3+})_5Al(Si_3Al)O_{10}(OH,O)_8$	0.31	O 39.1; Fe 32.85; Si 14.28; Al 10.23; Mg 3.24; K 0.3;
Rutile	TiO_2	0.10	O 51.72; Ti 48.28;

Iron oxy-hydroxides (Figure B.9) are precipitated and form the cement matrix surrounding the grains. Most of the secondary iron phases present is hematite (Table 2). The mineralogical associations of iron oxy-hydroxides are presented in Figure B.10. Hardpan iron oxy-hydroxides

are present as liberated and mostly as binary association to other iron oxy-hydroxides. They are more associated to carbonates (8%) than sulphides (2%). This leads to passivation of sulphides and carbonates. Sulphides within hardpan sample are almost all associated with iron oxy-hydroxides (47%pyrite and 33% pyrrhotite). Generally, association of iron oxy-hydroxides with sulphides is known as sulphide's coating.

The results of the static tests on oxidized and unweathered samples are presented in Table 1. Neutralization potential (NP), AP and NNP are presented in kg of CaCO₃/t. Neutralization potential analyzed by titration is smaller than the value calculated by total inorganic carbon concentration. This is due to the presence of iron carbonates which reduces the real NP of tailings (Bouzahzah *et al.*, 2015a). Neutralization potential of oxidized sample is lower than its AP which may lead to an acidic behavior of this sample. The unweathered tailings have 35 kg CaCO₃/t of difference between its NP and AP. This sample is uncertain regarding acid generation (Miller *et al.*, 1991b) .
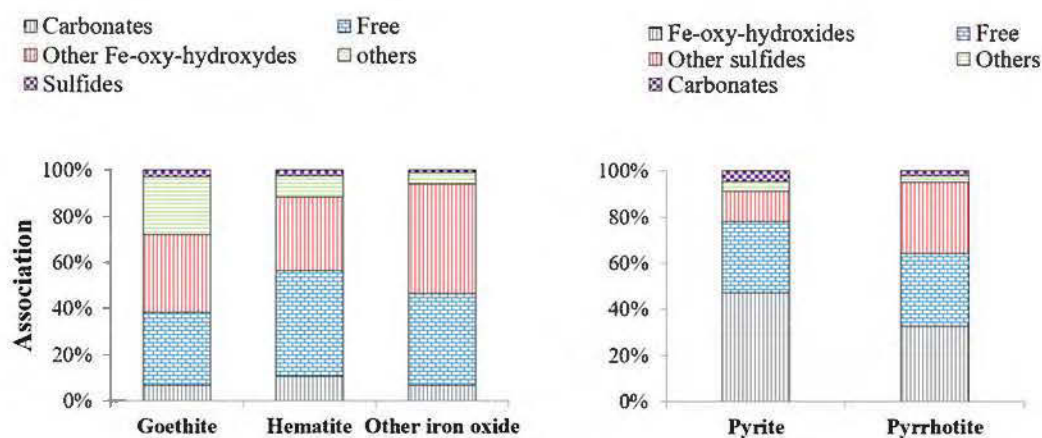

Figure B.11 : Mineralogical associations of secondary iron phases and sulfides

Leaching tests

Results of the geochemical quality of column tests leachates are shown in Figure B.12 . The columns leaching tests were run for 11 months. The preliminary results showed an acidic behavior for the oxidized tailings: pH of oxidized tailings leachates was between 2.15 and 2.77 with a tendency of slight increase. However, when leachate water from oxidized sample is allowed to infiltrate vertically into unweathered sample, the acidic leachates are neutralized by carbonates dissolution within unweathered tailings. pH of column leachates stayed neutral between 6 and 8.

The electrical conductivity of the leachates from the oxidized tailings is slightly lower than that from oxidized tailings above the unweathered tailings. It varies between 2.89 mS/cm and 5.79 mS/cm while that from vertical infiltration varies between 2.65 mS/cm and 6.4 mS/cm. This may be explained by more extensive dissolution and oxidation reactions due to presence of unweathered tailings.

Acidity and alkalinity are two parameters that describe the capacity of a solution to acidify and neutralize a solution. The acidity measurement obtained from the surface runoff leachates is higher than that measured for leachates from vertical infiltration. Acidity of surface runoff leachates varies between 250 mg $CaCO_3$/l and 1550 mg $CaCO_3$/l. The acidity of vertical infiltration leachates is low and varies between 15 mg $CaCO_3$ and 168 mg $CaCO_3$. During the vertical infiltration, the acidity produced in the oxidized tailing is neutralized by carbonates within the unweathered tailings. The alkalinity of surface runoff was zero during the entire column test duration. The alkalinity of vertical infiltrated water was between 40 mg $CaCO_3$ and 179 mg $CaCO_3$.

The leachates chemical compositions for the two scenarios were different. Leachates from surface runoff scenario are characterized by high concentrations of Ca, Al, Fe and Zn while the leachates from vertical infiltration contain more S and Mg. The concentration of S leached from the oxidized sample ranged between 735 mg/l and 1112 mg/l and that from the scenario of vertical infiltration was between 926 mg/l and 2200 mg/l. The calcium concentrations from the surface runoff scenario varied between 619 mg/l and 894 mg/l and those from vertical infiltration scenario ranged between 423 mg/l and 638 mg/l. The average concentration of Fe leached from the oxidized sample was about 106 mg/l and that leached from vertical infiltration scenario was about 0.88 mg/l. The average concentration of Mg leached from the oxidized sample was low and equalled to 31.4 mg/l, while the leachates form vertical infiltration through the unweathered sample contained high concentrations of Mg and varied between 372 mg/l and 1110 mg/l. A higher concentration of Zn was leached during the surface runoff scenario than during the vertical infiltration scenario with average concentration of 11.13 mg/l and 0.67 mg/l, respectively. Similar results were obtained for Al. The concentration of Al was higher in the leachate from surface runoff scenario (10 mg/l and 50 mg/l) than that measured in the leachate from the vertical infiltration scenario (0.014 mg/l and 0.072 mg/l).

DISCUSSION AND ON-GOING WORKS

The oxidized tailings contain mainly secondary phases while most of sulphides and carbonates were dissolved. The unweathered sample showed high concentrations of carbonates (mainly siderite) and sulphides (pyrite). The hardpan sample showed a mineralogical composition formed by a mixture of oxidized and unweathered tailings minerals. It is formed through the precipitation of secondary phases forming crusts around grains and ultimately forming a cement matrix around them which reduces the porosity of these horizons. The formation of hardpan and the reduction of the porosity influence considerably the hydrogeological properties of these tailings' horizons. As a result, the hydraulic conductivity of this tailings horizons decreases leading to a change of the local water flow at the Joutel tailing impoundments which in turn influences the geochemical behavior of tailings (McGregor *et al.*, 2002).

The oxidized sample which was run to simulate surface runoff due to presence of hardpans generated leachates with high concentrations of Ca, Fe, Al and Zn. These elements are associated with secondary minerals. In general, Ca and S originate from the dissolution of gypsum. The mineralogical characterization of oxidized sample showed 19.3% gypsum. Fe and Zn are related to secondary iron oxy-hydroxides. Precipitation of secondary iron phases leads to trapping of wide range of contaminants (Fukushi *et al.*, 2003; McGregor *et al.*, 1998a; McKenzie, 1980). These elements are released during iron oxy-hydroxides dissolution (Sheoran *et al.*, 2006).

The acid generation in the oxidized sample is mainly related to secondary iron phases (El Adnani *et al.*, 2016). The acidity is maintained during all kinetic tests because of the absence of neutralizing minerals which is confirmed by absence of alkalinity in the leachates from oxidized sample. The neutralization potential of oxidized tailings is depleted after more than 25 years of field exposure and the same tendency for sulphides.

The oxidized sample above unweathered sample was run to simulate vertical infiltration of water flows due to absence of hardpans. The geochemical monitoring of this column test showed a non-acid generating behavior. The acidity generated by the oxidized tailings is neutralized by unweathered tailings carbonates. Carbonates dissolution is the main pH buffering within the unweathered tailings. This is confirmed by Ca and Mg leaching during this scenario. During surface runoff scenario, there are some contaminants leached such as Al and Zn. These contaminants are present in very small concentrations during vertical infiltration scenario. It may be that, during pH

buffering by carbonates dissolution, these elements are co-precipitated or adsorbed by the new formed iron secondary phases.

Evaluation of hydrogeological properties of oxidized, unweathered and hardpan samples is ongoing to demonstrate the variation of permeability and water retention curves. Hydrogeological modelling using Hydrus 1D is ongoing to evaluate the water content and water flow in the tailings impoundment in presence and absence of hardpans.
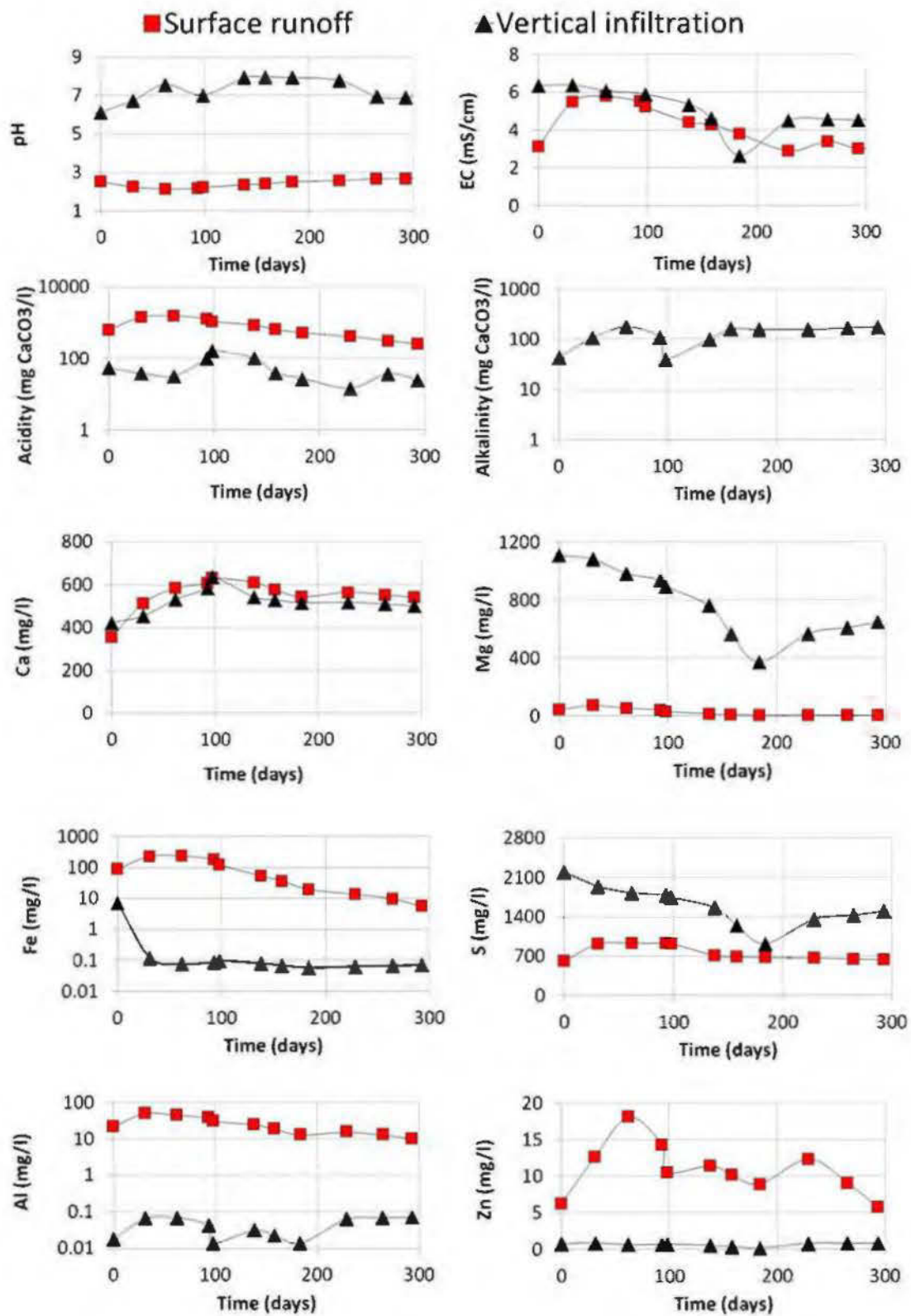
Figure B.13: Geochemical monitoring of column tests